DAO ATBD Version 1.01

Richard B. Rood, Head
Data Assimilation Office
Goddard Space Flight Center
Greenbelt, Maryland 20771

Phone (301) 286-8203
FAX (301) 286-1754
rood@dao.gsfc.nasa.gov
http://dao.gsfc.nasa.gov

Algorithm Theoretical Basis Document for Goddard Earth Observing System Data Assimilation System (GEOS DAS) With a Focus on Version 2

Staff*
Data Assimilation Office, Goddard Laboratory for Atmospheres
Goddard Space Flight Center, Greenbelt, Maryland

* *Refer to this document as:*
DAO, 1996: Algorithm Theoretical Basis Document Version 1.01, Data Assimilation Office, NASA's Goddard Space Flight Center.

Goddard Space Flight Center
Greenbelt, Maryland 20771
November 1996

Preface

The development of the Goddard Earth Observing System (GEOS) Data Assimilation System (DAS) has been a learning process for us all. When the effort was started the scope was not well understood by any of the principal people involved. It was deemed as something important for the Earth Observing System (EOS), and the expectations were very high.

The Data Assimilation Office (DAO) was formed in February 1992 at Goddard Space Flight Center to develop a data assimilation capability for EOS and the broader NASA mission. In the following four or so years the progress has been tremendous and hard fought. The effort extends far beyond scientific and involves many logistical aspects of developing a routine production capability. In many ways, we are just getting to the starting line.

The GEOS DAS is a computing effort as large, or larger, than any in the world. An effort that is coming on line when the traditional supercomputing paradigm is, by many counts, collapsing. The computing is characterized by high levels of processor communications which eliminates any easy solution to the problem. Therefore a tremendous scientific challenge has been compounded by an immense computational challenge. A challenge to be achieved with about half the historical budget available to comparable efforts.

This document describes the algorithms proposed by the DAO to be at the basis of the 1998 system provided to coincide with the launch of the AM-1 Platform. It is intended to be an integrated document. However, the chapters are also designed to stand alone if necessary. References and acronyms for each chapter are compiled individually. Detailed contents are given at the beginning of each chapter. Occasionally there is a comment intended to address the difficulty of writing an interesting algorithm theoretical basis document. You will have to read it carefully to find them

Greenbelt, Maryland *R. Rood*
November 1996

Outline

Chapter 1
Scope of Algorithm Theoretical Basis Document

What is and is not in this document.

Chapter 2
Background

The role of data assimilation in the MTPE enterprise. The DAO Advisory Panels and their advice. How does the GEOS DAS relate to efforts at NWP centers. How are requirements defined and linked to MTPE priorities. How to confront the computer problem. What are the limitations of data assimilation.

Chapter 3
Supporting Documentation

A list of DAO publications that provide more details on the algorithm and algorithm performance.

Chapter 4
GEOS-1 Data Assimilation System

Our first data assimilation system. The baseline on which progress is measured.

Chapter 5
The Goddard Earth Observing System - Version 2
Data Assimilation System

It is the system we are validating right now. It is a major development over GEOS-1 and provides the infrastructure to address the future mission. When you think of reviewing the algorithm, this is the main course.

Chapter 6
Quality Control of Input Data Sets

This is how we manage the input data sets in the current system.

Chapter 7
New Data Types

How will new data types be incorporated into the GEOS DAS. What are the priorities, and how are these decisions made. What is the link to MTPE Earth science priorities. This chapter is at the basis of what needs to be done over the next few years.

Chapter 8
Quality Assessment/Validation of
the GEOS Data Assimilation System

How do we decide when to declare a new version of the assimilation system. It is not easy; nothing is.

Chapter 9
Evolution from GEOS-2 DAS to GEOS-3 DAS

What will be added to GEOS-2 for the 1998 mission. Improvements to all aspects of the data assimilation system.

Chapter 10
Summarizing Remarks

Wrapping it up, and what are the risks.

The People in the DAO

The list below includes visitors, part time, and administrative staff.

NAME	*TELEPHONE*	*E-MAIL ADDRESS*
Almeida, Manina (GSC)	(301) 805-7950	almeida@dao.gsfc.nasa.gov
Alpert, Pinhas (Tel Aviv U)	(301) 805-8334	pinhas@dao.gsfc.nasa.gov
Ardizzone, Joe (GSC)	(301) 286-3109	ardizone@iris611.gsfc.nasa.gov
Atlas, R. (Bob) (GSFC)	(301) 286-3604	atlas@dao.gsfc.nasa.gov
Bloom, Steve (GSC)	(301) 286-7349	bloom@dystopia.gsfc.nasa.gov
Brin, Genia (GSC)	(301) 286-5182	genia@genia.gsfc.nasa.gov
Bungato, Dennis (GSC)	(301) 286-2705	ctdrb@iris611.gsfc.nasa.gov
Chang, L. P. (GSC)	(301) 805-6998	lpchang@dao.gsfc.nasa.gov
Chang, Yehui (GSC)	(301) 286-2511	chang@dao.gsfc.nasa.gov
Chen, Minghang (ARC)	(301) 805-6997	mchen@dao.gsfc.nasa.gov
Cohn, Steve (GSFC)	(301) 805-7951	cohn@dao.gsfc.nasa.gov
Conaty, Austin (GSC)	(301) 286-3745	conaty@dao.gsfc.nasa.gov
Dee, Dick (GSC)	(301) 805-7963	dee@dao.gsfc.nasa.gov
DelSole, Timothy (NRC)	(301) 286-8128	delsole@dao.gsfc.nasa.gov
Ekers, Ken (GSC)	(301) 805-8336	ekers@dao.gsfc.nasa.gov
Elengical, George (HITC)	(301) 286-3790	elengical@dao.gsfc.nasa.gov
Fox-Rabinovitz, Michael (JCESS)	(301) 805-7953	foxrab@dao.gsfc.nasa.gov
Gaspari, Greg (USRA)	(301) 805-8754	gaspari@dao.gsfc.nasa.gov
Govindaraju, Ravi (GSC)	(301) 805-7962	ravi@dao.gsfc.nasa.gov
Guo, Jing (GSC)	(301) 805-8333	guo@dao.gsfc.nasa.gov
Hall, Monique (GSC)	(301) 805-8440	hall@dao.gsfc.nasa.gov
Helfand, Mark (GSFC)	(301) 286-7509	hmh@dao.gsfc.nasa.gov
Hou, Arthur (GSFC)	(301) 286-3594	hou@dao.gsfc.nasa.gov
Joiner, Joanna (GSFC)	(301) 805-8442	joiner@dao.gsfc.nasa.gov
Jusem, Juan Carlos (GSC)	(301) 286-4086	carlos@gmsb02.gsfc.nasa.gov
Karki, Mahendra (GSC)	(301) 805-6105	karki@dao.gsfc.nasa.gov
Kondratyeva, Yelena (GSC)	(301) 805-7952	yelena@tyler.gsfc.nasa.gov
Lamich, Dave (GSC)	(301) 805-7954	lamich@dao.gsfc.nasa.gov
Larson, Jay (JCESS)	(301) 805-8334	larson@dao.gsfc.nasa.gov
Ledvina, Dave (GSC)	(301) 805-7955	ledvina@dao.gsfc.nasa.gov
Li, Yong (GSC)	(301) 262-0191	lyong@dao.gsfc.nasa.gov
Lin, Shian-Jiann (GSC)	(301) 286-9540	lin@dao.gsfc.nasa.gov
Lou, Guang Ping (GSC)	(301) 805-6996	glou@dao.gsfc.nasa.gov
Lucchesi, Rob (GSC)	(301) 286-9084	rob@dao.gsfc.nasa.gov
Lyster, Peter (JCESS)	(301) 805-6960	lys@dao.gsfc.nasa.gov
Menard, Richard (USRA)	(301) 805-7958	menard@dao.gsfc.nasa.gov
Min, Wei (USRA)	(301) 286-4630	min@dao.gsfc.nasa.gov
Molod, Andrea (GSC)	(301) 286-3908	molod@dao.gsfc.nasa.gov

NAME	*TELEPHONE*	*E-MAIL ADDRESS*
Nebuda, Sharon (GSC)	(301) 286-6543	nebuda@dao.gsfc.nasa.gov
Omidvar, Kazem (GSFC)	(301) 805-6930	omidvar@dao.gsfc.nasa.gov
Pabon-Ortiz, Carlos (GSC)	(301) 286-8560	pabon@dao.gsfc.nasa.gov
Park, Chung-Kyu (JCESS)	(301) 286-8695	park@dao.gsfc.nasa.gov
Pharo, Merritt (GSFC)	(301) 286-3468	pharo@dao.gsfc.nasa.gov
Philpot, Q. (GSC)	(301) 286-7562	philpot@dao.gsfc.nasa.gov
Rathod, Vipool (GSC)	(301) 286-1445	vip@dao.gsfc.nasa.gov
Redder, Chris (GSC)	(301) 805-8335	redder@dao.gsfc.nasa.gov
Riishojgaard, Lars Peter (USRA)	(301) 805-0258	riishojgaard@dao.gsfc.nasa.gov
Rood, Ricky, Head, (GSFC)	(301) 286-8203	rood@dao.gsfc.nasa.gov
Rosenberg, Jean (GSC)	(301) 286-3591	jeanr@dao.gsfc.nasa.gov
Rosenberg, Robert (GSC)	(301) 286-7126	bobr@pinhead.gsfc.nasa.gov
Rukhovets, Leonid (SUNY)	(301) 805-7961	leonidr@dao.gsfc.nasa.gov
Rumburg, Laura (GSC)	(301) 286-5691	rumburg@dao.gsfc.nasa.gov
Schubert, Siegfried (GSFC)	(301) 286-3441	schubert@dao.gsfc.nasa.gov
Sienkiewicz, Meta (GSC)	(301) 805-7956	meta@dao.gsfc.nasa.gov
da Silva, Arlindo (GSFC)	(301) 805-7959	dasilva@dao.gsfc.nasa.gov
Sivakumaran, N. (Siva) (GSC)	(301) 805-7957	siva@dao.gsfc.nasa.gov
Stajner, Ivanka (USRA)	(301) 805-6999	ivanka@dao.gsfc.nasa.gov
Stobie, Jim (GSC)	(301) 805-8441	stobie@dao.gsfc.nasa.gov
Strahan, Susan (GSC)	(301) 286-1448	strahan@dao.gsfc.nasa.gov
Takacs, Larry (GSC)	(301) 286-2510	w3llt@dao.gsfc.nasa.gov
Terry, Joe (GSC)	(301) 286-2509	terry@gmsb06.gsfc.nasa.gov
Thorpe, Felicia (IDEA, Inc.)	(301) 286-2466	thorpe@dao.gsfc.nasa.gov
Todling, Ricardo (USRA)	(301) 286-9117	todling@dao.gsfc.nasa.gov
Trenholme,Alice (GSC)	(301) 805-1079	trenholme@dao.gsfc.nasa.gov
Turkelson, Bob (GSFC)	(301) 286-7600	turkelson@dao.gsfc.nasa.gov
Vick, Tonya (GSFC)	(301) 286-5210	vick@carioca.gsfc.nasa.gov
Wu, Chung-Yu (John) (GSC)	(301) 286-1539	wu@dao.gsfc.nasa.gov
Wu, Man-Li (GSFC)	(301) 286-4087	frmlw@dao.gsfc.nasa.gov
Yang, Qiulian	(301) 286-0143	qyang@daac.gsfc.nasa.gov
Yang, Runhua (GSC)	(301) 805-8443	ryang@hera.gsfc.nasa.gov
Zero, Jose (GSC)	(301) 262-2034	zero@dao.gsfc.nasa.gov

Contents

List of Figures

List of Tables

Chapter 1

Scope of Algorithm Theoretical Basis Document

This Algorithm Theoretical Basis Document (ATBD) describes the basic algorithms of the Goddard Earth Observing System (GEOS) Data Assimilation System (DAS). The GEOS, DAS is being developed by the Data Assimilation Office (DAO) at NASA's Goddard Space Flight Center (GSFC). The GEOS DAS represents a series of incremental developments, with major releases identified by version numbers. GEOS-1 refers to the system described in Schubert *et al.* (1993) and was the first frozen version of GEOS.

This document focuses on GEOS-2, which is in the process of being validated at the time of writing. GEOS-2 is an engineering version, and fallback system, of GEOS-3 which is the version planned for the 1998 support of the Earth Observing System (EOS) AM-1 launch. The enhancements of GEOS-2 that will be included in GEOS-3 will be discussed.

The document describes the primary algorithms that form the data assimilation system; namely,

- statistical analysis algorithm
- predictive model
- quality control
- new data type infrastructure

The document does not provide the rigorous derivation of these algorithms. Those details are left to refereed journal articles, Technical Memoranda, and DAO Office Notes listed in Chapter 3. Only those details needed to express fundamental principles or special features will be described. The document is meant to be reviewable as a stand alone document. It is meant to show the theoretical basis of the GEOS system and to convey competence in the design and implementation of the data assimilation system.

The GEOS-2 and GEOS-3 systems will address problems of atmospheric, land surface, and ocean surface modeling and assimilation. The document does not describe all of the advanced methods that are being pursued for implementation beyond GEOS-3. While the

DAO will provide products from these advanced systems, they will not be routinely part of the GEOS system at the time of the AM-1 launch.

The document will not describe the file structure, data format, and operational scenario of the data assimilation system. The document will not describe in detail the data preprocessing algorithms for future systems. Likewise, the document will not detail the issues of computational implementation of the algorithm.

Reference

Schubert, S. D., R. B. Rood, J. W. Pfaendtner, 1993: An assimilated data set for earth science applications. *Bull. Amer. Meteor. Soc.*, **74**, 2331-2342.

Chapter 2

Background

Contents

2.1 Data Assimilation for Mission to Planet Earth

The capability of assimilating observations into comprehensive models of the atmosphere is increasingly recognized as an essential part of global and regional observational programs. As data assimilation methods mature, capabilities to assimilate data into land-surface, oceanic, and other component models are being developed. Ultimately, assimilation of data into coupled models will be an integral part of extracting the maximum information from Earth-system observations as well as driving quantitative model development.

Data assimilation for the atmosphere is described by Daley (1991), and has been developed primarily for numerical weather prediction (NWP) applications. Much of the improvement in weather forecasts over the past 15 years can be directly linked to improvements in data assimilation to provide better forecast initial conditions (NAS, 1991). In 1991 in the report, Four-Dimensional Model Assimilation of Data: A Strategy for the Earth System Sciences (NAS1991), a panel of the National Academy of Sciences recognized the need to develop more general data assimilation capabilities for observational programs in the coming decades. Within NASA, for the Upper Atmospheric Research Satellite (UARS), a proposal from the United Kingdom Meteorology Office (UKMO) was awarded to provide data assimilation support for the mission. Despite the fact that the standard UKMO product does not directly assimilate any UARS data, the UKMO product has been the fabric that integrates together the observations from the different instruments (see, Rood and Geller 1994). The UKMO analysis has been the most requested data set from the UARS data archive (personal communication, M. Schoeberl, UARS Project Scientist). The Data Assimilation Office was formed at NASA/GSFC in February 1992 in response to the National Research Council report and to support Mission to Planet Earth (MTPE) observational programs.

The decision by NASA to develop a comprehensive data assimilation capability for the Earth Observing System (EOS), and more generally MTPE, was visionary. However, the scope of such an effort was not well understood, the requirements were not well defined, and the expectations were very high. In reality, the construction of an assimilated data set for Earth science can take on unmanageable and unaffordable proportions. This is due to at least three reasons:

1. The inherent complexity of the science means that comprehensive modeling and analysis systems are just beginning to be constructed from simpler systems. Often, even the simple systems themselves are parameterizations of complex processes. Therefore, first principle development can quickly expand to consume all available resources.

2. The science of both modeling and analysis is computer constrained. Significant simplifications of the algorithms are required to achieve computational viability. Therefore, algorithm development is influenced by the decision of which parts of the algorithm get a premium of computer resources. Conversely, seemingly reasonable assimilation algorithms can be developed to consume any available computer resource.

3. Earth-science data assimilation has been developed primarily in the numerical weather prediction community, and this permeates the culture of the discipline. Therefore most of the thought has gone into predictive capabilities on the time scale of days using observations that are available in near real time. As more general applications are considered, it is possible to choose many development paths.

Therefore, the development of the Goddard Earth Observing System Data Assimilation System (GEOS DAS) is not straightforward. Requirements have had to be developed, refined, and mapped to a changing budget profile. Early products have been generated and used by many scientists to help characterize the performance of basic GEOS components. This experience has been used to help make priorities on which development paths to follow.

Broadly, the expectations of the data assimilation system are:

E1: To organize the observations from diverse sources with heterogeneous space and time distribution into a regularly gridded, time continuous product.

E2: To complement the observations by propagating information from observed to unobserved regions.

E3: To supplement observations by producing estimates of unobserved quantities, using the model parameterizations constrained directly and indirectly by the observations.

E4: To maximize the physical and, ultimately, chemical consistency between the observations through the comprehensive parameterizations of the model.

E5: To provide a variety of quality control functions for the observations.

E6: To provide, ultimately, an instrument calibration capability, especially with regard to the definition of biases and instrument drift.

These six general expectations are made possible by the melding of the model prediction and the observations through the statistical analysis scheme. At this point in development, Items 1 and 2 have become so ingrained, that they are taken for granted. Items number 3 and 4 are where the greatest expectations of most users exist. Item 5, and especially Item 6, are powerful future capabilities that will develop as the accuracy of the GEOS assimilation system is validated.

The model provides the data assimilation system with many of its special attributes. Conversely, because of the constant confrontation of the model with the observations, the model in the GEOS DAS should become one of the most extensively validated models in the world on time scales ranging from diurnal to decadal. Therefore, the data assimilation system should provide MTPE with:

> A systematic, quantitative method of climate model development which will contribute to the reduction of uncertainties in model predictions and assessments.

If successful, then the data assimilation system developed by the DAO becomes a resource for the MTPE and broader community. This extends far beyond the production of data sets. The GEOS DAS algorithms themselves should be a resource that is attractive to the broader community. The model should (and must) attract outside scientists to install and validate leading-edge parameterizations. The analysis system should be portable and applicable to other assimilation efforts within NASA. The GEOS system is being planned to provide such a resource.

2.2 Overview of GEOS Data Assimilation System (DAS)

Data assimilation is a process that is both explicitly and implicitly imbedded in scientific evolution. Fundamentally, data assimilation is the concurrent use of models and observations to both extract the maximum amount of information from the observations and improve quantitative abilities of the model. Real applications of modern data assimilation were pioneered at NASA during the 1960's during the Apollo missions (Battin and Levine 1970). More practically, Earth scientists usually think of data assimilation as the intermittent insertion of data into a model. From a theoretical point of view, data assimilation can be viewed as the quantitative analysis of information using the principles of estimation theory. In particular, the model provides a source of information in the form of an estimate of the expected state and the observations provide a measurement of the state. Given meaningful error characteristics of the model estimate and the observations, the two can be combined in an optimal way to produce the best estimate of the state given all of the available information

Earth-science data assimilation is characterized by immense complexity and large data sets. The type and scale of processes which must be modeled are large. The ability to prescribe error characteristics is limited. Techniques to measure many of the important parameters are nascent or unknown. The amount of data needed to represent global processes is large. The system is nonlinear with poorly understood feedback loops. The statistical methods to meld the information from the observations with the information from the model are just beginning to evolve from the highly approximated algorithms required to allow computational viability (Cohn 1996).

The GEOS DAS is represented in Figure 2.1. Currently the system cycles in six hour windows, with insertion of observations into the model every six hours. Focusing on the cycle at 6 UTC (Universal Coordinated Time) the atmospheric general circulation model (GCM) provides a three hour forecast from 3 UTC. Needed boundary conditions, for instance, sea surface temperature, are prescribed from various sources. The model predictions are then transformed from the vertical levels in the model (currently sigma) to the vertical levels used in the statistical objective analysis (currently pressure). The model prediction on pressure surfaces provides the first guess for the objective analysis algorithm.

Prior to and integrated with the analysis is quality control functionality. This includes pre-processing of the observations prior to use in the objective analysis and objective quality control through comparison of the first guess estimates with the observations. Somewhat parallel to the boundary conditions in the model, statistics which describe the model and observational error are needed for the analysis. Using these statistics the objective analysis combines the observations with the first guess to form the analysis. The analysis is then transformed back to the model vertical levels and used to calculate the increments that must be added to the model to represent the state of the atmosphere on the model grid. Then in the GEOS DAS, rather than adding the entire impact of the increment instantaneously, a second model forecast is initiated from 3 UTC, adding the impact of the increments over a six hour window. This data-constrained forecast at 9 UTC then becomes the initial condition for the three hour forecast used in the 12 UTC cycle. The process of gradually introducing the analysis increments over a six hour period is called the Incremental Analysis Update (IAU) and is a feature unique to the GEOS DAS. It will be discussed more fully in Chapter 5. Because of the IAU, there is currently not a formal initialization scheme in the

Figure 2.1: GEOS Data Assimilation System. See text for details.

GEOS DAS.

At the bottom of the figure are the currently archived products from the GEOS DAS: 1) the full three-dimensional state of the atmosphere on standard pressure surfaces at 6 UTC (what most researchers use), 2) the full three-dimensional state of the atmosphere on model vertical levels at 6 UTC (the most accurate data set, used, for instance, in off-line chemistry applications and budget studies), and 3) surface quantities at 3, 6, and 9 UTC. The analysis is also archived, as well as the observation data stream (ODS) file. The ODS file is used in quality assurance and monitoring candidate data sets to build error statistics prior to assimilation.

All aspects of the process represented in Figure 2.1 are subject to discussion and improvement. Attention is usually given to the fundamental components of the model and the objective analysis which are widely known to contain parameterizations and simplifications of complex processes. However, decisions in the quality control algorithms strongly impact the final assimilated data product. The process of transforming between model vertical levels and objective analysis vertical levels introduces errors. Sources of boundary conditions influence output quality. The issues for increased coupling to make parameters that are currently boundary conditions predictive quantities in the data assimilation system complicate an already complex problem. The development of error statistics is an enormous

fields are computationally demanding. In the algorithms discussed in this document there will be constant weighing and compromising of the development decisions as these different attributes are considered.

2.3 Scope of GEOS Data Assimilation System (DAS)

GEOS-1, GEOS-2, and GEOS-3 represent a series of developments of the GEOS DAS from 1992 to 1998, with GEOS-3 being the proposed initial system in support of the EOS AM-1 platform.

The scope of the GEOS-3 DAS is to assimilate operational and MTPE data of the:

- atmosphere
- land surface
- ocean surface

At the time of launch the input data stream will be primarily atmospheric, with the bulk of the observations coming from the operational weather satellites. The operational data provide the core of any Earth-science assimilation system, and optimal use of the operational data by the DAO is mandatory.

The Strategic Plan of the Mission to Planet Earth (1996), and the MTPE Science Initiatives (1996) help to define the choices of development paths. These have been distilled to two general areas which focus current algorithm decisions:

1. global hydrological and energy cycles, including interaction between the atmosphere ocean and land surfaces and storage in the soil
2. transport processes in the atmosphere in order to calculate quantitatively dynamic variability of tropospheric and stratospheric trace constituents

Improvement in both of these general Earth-science fields requires improvements to the objective analysis, the predictive model, and the use of currently available observations. In addition, improvement of the quality of the assimilated data product requires use of the new observation types that will become available through MTPE and other observing programs.

In order to address the science priorities of MTPE, it is necessary for the GEOS DAS to be accurate on time scales from hours to years. Figure 2.2 shows a wavelet analysis of moisture flux over the United States from the GEOS-1 product for the time period 1 May — 31 August 1993. As the season changes from spring to summer the moisture flux develops a regular diurnal component (period 1 day) which dominates the variability through July and August. In May, at the end of spring, variability in the synoptic times scales (period 4–8 days) is more important. What is pictured is the decline in late spring of the passage of weather fronts and storms, followed by the formation of the U.S. Great Plains Low Level Jet in the summertime convective regime. The figure shows that the fundamental components of seasonal variability are linked to dynamical regimes with much shorter time scales. Therefore, to study processes on seasonal and longer time scales it is necessary to have fidelity in the assimilated data set down to time scales of hours.

GEOS-1, which is discussed more fully in Chapter4, provided a scientifically useful data set early in the EOS program and a baseline to start incremental development of

the GEOS DAS. GEOS-2 will represent a major improvement to GEOS-1 and includes many features that serve as the infrastructure for improved representation of model and observational errors. GEOS-2 also provides the infrastructure for incorporation of new data types. GEOS-2 will be used to provide:

- data sets in support of the Advanced Earth Observing System (ADEOS) platform launched by Japan in August 1996 with particular emphasis on the NASA Scatterometer (NSCAT).
- data sets in support of the Tropical Rainfall Measuring Mission (TRMM) with expected launch by Japan in the later half of 1997 with particular emphasis on TMI, PR, and CERES.
- a 1979 re-analysis data set for intercomparison with ECMWF and NCEP, all using the same input data stream.

These applications prior to AM-1 launch will help define the enhanced scientific capabilities of GEOS-3. The applications prior to AM-1 and the expected capabilities provided by AM-1 have a major focus on near-surface processes, one of the most difficult and inadequately modeled parts of the Earth system. Successful implementation will significantly improve the two general areas of Earth science mentioned above and the ability of the GEOS DAS to address MTPE science priorities

Figure 2.2 shows a wavelet analysis of moisture flux over the United States from the GEOS-1 product for the time period 1 May — 31 August 1993.

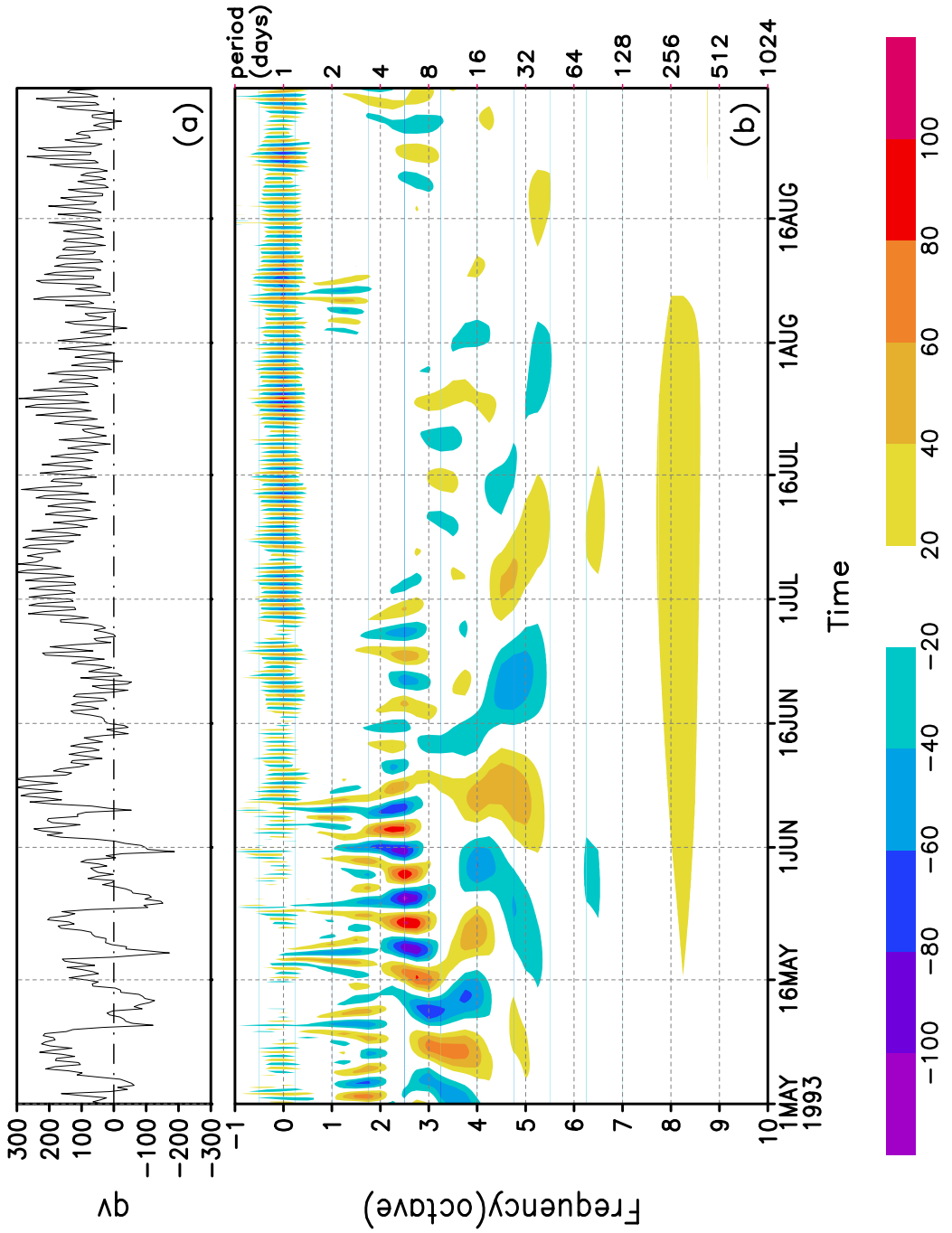

Figure 2.2: Wavelet analysis of moisture flux over the United States from GEOS-1.

2.4 Data Assimilation Office Advisory Panels

Since its inception the DAO has received critical guidance from its Science Advisory Panel. More recently a Computer Advisory Panel has been convened. These panels report to the Division Chief of the Laboratory for Atmospheres, the organization in which the DAO resides. Originally the Panels were chosen to assure minimal possible conflicts of interest with specific internal NASA programs. More recently, since EOS is the primary funding source of DAO activities, members from the EOS Interdisciplinary Studies have been included. The past and present members of the panels are given at the end of this chapter.

The Advisory Panels were formed in recognition of the immense challenge to produce a data assimilation capability for MTPE, and the potential open-ended development that was possible. The Advisory Panels consider both the scientific and operational aspects of the DAO. They assure that the DAO development does not take place in isolation. They challenge theoretical and computational decisions. They infuse both scientific and technological information into DAO development. The guidance from the Advisory Panels helps to prioritize DAO development paths. Therefore, the DAO development and the algorithms described in this document have received significant and continual scrutiny in an objective, critical process.

The Advisory Panels have already recognized many of the strengths and weaknesses of the DAO algorithms in five written reports. These will be summarized here in order to provide an over-arching framework for the Algorithm Theoretical Basis Document.

2.4.1 Summary of Scientific Advisory Panel's Comments on Objective Analysis Development

The Panel has recognized the DAO activities in development of objective analysis routines as unique, innovative, and first class. Original concerns about pragmatic considerations using the Kalman filter and estimation theory as a guiding paradigm have been reduced as the DAO has developed specific algorithms for GEOS-2 and GEOS-3. In particular they have recognized the advances manifested by the Physical-space Statistical Analysis System to be used in GEOS-2 and GEOS-3.

They have expressed concern that the specification of forecast and observational errors was primitive - primitive enough to both undermine the credibility of the GEOS system and to under-utilize the capabilities of the Physical-space Statistical Analysis System. Recent advances in representation of error statistics have reduced many of these concerns.

The Panel has praised the development of advanced capabilities such as the Kalman filter used in constituent assimilation and retrospective analysis that will allow the use of data after the analysis time.

The primary concern with respect to the objective analysis routine are the pragmatic ones of actual implementation of such a complex system in such a short time.

2.4.2 Summary of Scientific Advisory Panel's Model Development

The Panel has expressed concern over the leadership of the model development and how decisions are made in model development. In their most recent report (June 1996), however, they were laudatory about the current leadership, and the advances that had been made in GEOS-2.

Concerns remain because the model development is not an activity under control of the DAO. Rather, the DAO has a small internal model group and is dependent upon modeling activities within GSFC, within NASA, and even more broadly for model development. This process is not well defined, and many of these outside developments do not have a direct stake in DAO success. Improved process is needed here.

The Panel suggests DAO participation in community intercomparison experiments such as the Atmospheric Model Intercomparison Project (AMIP), which the DAO has done. Given the importance of numerical weather prediction to the data assimilation culture the Panel is concerned about how to establish model credibility without forecasting as the primary metric of model performance.

The Panel points out that the model in GEOS must be well documented and have an excellence comparable to the best models in the world. Concerns remain about how to achieve and maintain this objective in the current management and resource structure.

2.4.3 Summary of Scientific Advisory Panel's Comments on Quality Control

In the original concept of the DAO, input data quality control was to be achieved through collaboration with the National Centers for Environmental Prediction (NCEP). This was in recognition of the excellence of the NCEP quality control algorithms and the idea that much of the quality control functionality was portable.

Later the Panel recognized logistical problems in the actual technology transfer. Also, the desired functionality of the GEOS DAS and the range of new data that needed to be addressed required much more attention to quality control. The DAO hired a scientist for quality control functions in 1995, and the panel recognized her accomplishments in the most recent report. However, there is significant concern about the capabilities and the modernity of the quality control algorithms in the GEOS DAS. Appropriate NCEP algorithms remain part of the DAO strategy.

2.4.4 Summary of Scientific Advisory Panel's Comments on New Data Types

The Panel recognizes the use of new data types as core to the DAO mission, and something that separates the DAO activities from all others in the world. The Panel has expressed concern at the lack of resources to adequately address new data type initiatives. The Panel has also expressed concern about the ability or inability to directly use the expertise of the Instrument Teams in the development of the data assimilation system.

In early 1995 the DAO hired a leader for the new data types initiative and the Panel

has praised her excellent work of defining strategies, developing priorities, and accelerating the development of the new data types infrastructure. This includes developments of some important theoretical breakthroughs that enable assimilation of the massive future MTPE data sets. The Panel feels as if this is still the area of most critical scientific shortfalls and recommends immediate augmentation.

The Panel was supportive of DAO decisions to scale back originally unrealistic plans about assimilation of new data types and to focus on a handful of high priority data types. The Panel was also supportive of the strategy to monitor candidate data types for a year prior to assimilation to assess data quality and define error statistics. However, they noted that the DAO decision and the lack of resources in the new data types effort cut at the core of the DAO mission to support MTPE.

2.5 Relationship of the GEOS Data Assimilation System to Numerical Weather Prediction Data Assimilation Systems

Given the development of data assimilation techniques in the operational numerical weather prediction (NWP) centers, most notably the National Centers for Environmental Prediction (NCEP) and the European Center for Medium-range Weather Forecasts (ECMWF), it is natural to question why the DAO is developing assimilation capabilities largely independent of these organizations. At the very least it is natural to ask whether or not data assimilation capabilities for MTPE should be developed directly from the NWP systems.

At the time the DAO was formed it was decided that the scope of the data assimilation problem for MTPE required new approaches to assimilation. Furthermore, even in the broader vision of the NWP products as represented by recent re-analyses (Gibson et al., 1994; Kalnay et al. 1996) and new initiatives in seasonal prediction (Shukla 1996), the NWP centers are required by their operational mission to focus on prediction problems primarily on time scales of days. This focused mission limits both the assimilation methodologies that have been tried and interest in data sets that do not have potential operational impact.

Although weather prediction encompasses many problems of the Earth system, assimilation techniques for weather prediction are often explicitly tuned to improve forecasts, possibly at the expense of the most accurate representation of the atmosphere. A common example is that for NWP near-surface water vapor observations have often not been used because they trigger spurious precipitation. This does not arise because the data are incorrect, but because biases in the prognostic fields restrict the use of the observed information. In addition the focus of NWP data assimilation developments until recently have been on methods that rely on overly simplistic representations of forecast and observation errors. For instance, the old optimal interpolation methods relied on the assumption that forecast errors were isotropic. The major assumption behind the new variational approaches has been that model error is negligible over the assimilation interval. These assumptions are clearly not justified for most applications, and in fact, undermine the credibility of assimilation techniques with some instrument teams. The Third (February, 1995) and Fourth (June, 1996) Reports of the DAO Science Advisory Panel recognize that the DAO's mission differs substantially from the NWP efforts and that the DAO is addressing the important and unique attributes of that mission.

However, the DAO itself was formed out of an organization at GSFC that was focused on the evaluation of the impact of satellite data on numerical weather prediction. Therefore, the first implementation of GEOS, GEOS-1, not only has many characteristics of an NWP system, but the characteristics of an NWP system with few distinguishing attributes. At the time of formation of the DAO, direct adoption of NCEP systems for incremental development was considered in order to bridge the state-of-the-art between NWP and the DAO system. Aside from the scientific motivation implied above, the NCEP system was not adopted because of logistical considerations. Without tremendous up-front planning, sharing of common infrastructure, and the development of controlled software environments, the rapidly changing and improving NWP systems undermine any effort to develop MTPE capabilities as incremental improvements to operational NWP systems. Further, if the more general problem required changes in the basic NWP approach, the overhead of assur-

ing no degradation to operational forecasts greatly inhibits the progress of the generalized data assimilation system. Direct linkage of DAO algorithms to NCEP algorithms is not scientifically or logistically justified.

Nonetheless, there are many similarities between efforts at NWP centers and the DAO. Both NCEP and ECMWF (Gibson et al. 1994; Kalnay et al. 1996) have produced re- analyses which confuses the issue. A major issue that the re-analyses addressed is the problem that the spurious signal from changes in the assimilation system obscures geophysical variability (Trenberth and Olson 1988). However, these re-analyses are being produced from systems that were developed for NWP, and any benefit from a more general approach is not realized. It is also not clear how experience from more general applications of these re-analyses feed back into development of future data assimilation systems. Therefore, while GEOS-1 might have many similarities with an NWP system, future versions of the GEOS system will develop distinct characteristics that make a sharper contrast between NWP and DAO algorithms more clear. Already development activities in the DAO, many of which are described in this document, are making the distinction to those intimate with assimilation methodology.

A relevant example of the how the NWP application defines the culture of the data assimilation field can be found in the use of observations from the operational polar orbit meteorological satellites. It has taken many years to develop a forecast/analysis system which showed a positive forecast impact in the northern hemisphere from temperature information from the TIROS Operational Vertical Sounder (TOVS) (Derber and Wu, 1996). One key in achieving a positive impact was the direct use of radiance information rather than using retrieved temperature products. From a theoretical point of view the use of radiances is better posed than the use of retrieved temperatures because error characteristics can be more precisely defined and because radiance data are not contaminated by a first guess. The weather prediction experience led, amongst other things, to the recommendation in the Second DAO Advisory Panel Report (December, 1993) for the DAO to adapt a radiance-based approach to the new data type problem.

To solely have a radiance-based strategy for new data types is not viable for the DAO. Many of the MTPE instruments have a large number of spectral bands and very large data rates. The computational requirements to perform an analysis based on these radiance data bases are impossible even with the most optimistic projections of computing capabilities. The network requirements to move these radiance data bases from archive to the DAO system are prohibitive. To have only a radiance-based approach would preclude the DAO from a primary part of its mission - inclusion of new data types. Re-examination of the radiance problem from a theoretical point of view led to the development of the Consistent Assimilation of Retrieved Data (CARD) technology, which will be described in Chapter 7. This technology allows more effective use of instrument team capabilities and reduces the data volume of some of the MTPE instruments by 2-3 orders of magnitude. The computational advantages are obvious. In the short history of the DAO we have found numerous examples where re-examination of the common knowledge of the data assimilation culture has led to quick breakthroughs. The pursuit of CARD was endorsed in the Third DAO Advisory Panel Report (February, 1995), and manuscripts are now being submitted for peer review.

Finally, with regard to use of TOVS data, the inability to achieve a positive forecast impact from the TOVS data led to the data often being withheld from forecasting applications. There was a general emotion that the TOVS data were of little value. However,

withholding the TOVS data in an assimilation that includes the stratosphere quickly leads to an assimilation that is of no use for stratospheric meteorology or chemistry. Therefore if there is a requirement for an accurate stratosphere, then it was (at one time, anyway) in direct conflict with the requirement for an accurate forecast. This example is representative of the differences between assimilation for NWP and assimilation for more generalized applications. There is no reason to expect that the same sort of conflicts will disappear in the near future.

The development and implementation of theoretical notions to distinguish between assimilation for NWP and more general applications is both profound and subtle. There are also a set of tangible requirements for the DAO product that at least for the next few years separate NWP and DAO products. These are listed below, with the full recognition that each are arguable in the abstract.

Diagnostics. Traditionally, diagnostic information and information from model parameterizations have not been archived from NWP systems. This limits their application in, for instance, off-line tropospheric tracer transport studies. The DAO archives a customer-driven list of generalized diagnostics. This includes high time resolution products designed for MTPE instrument teams.

Domain: The DAO is required to produce products from the land and ocean surface, through the depth of the stratosphere, into the mesosphere.

Time scales: The focus of DAO products is the accurate representation of time scales from hourly to interannual. Therefore DAO models are validated as much by climate data sets as forecast skill.

Data Types: The DAO mission includes assimilation of data types either of indirect interest to NWP or data with no chance of becoming part of the operational data stream.

Final Product: The final product from the DAO system is the assimilation analysis, not the weather forecast. Scrutiny of the analysis, and how to validate the general quality of the analysis, will lead to more robust assimilation products for Earth-system science.

Data assimilation for NWP and for more general applications will never be completely divorced. In fact, as NWP models are pushed into more climate-oriented applications, the two will converge to some extent. Since forecasting is central to data assimilation, the DAO must use forecasting as part of its validation plan. However, taken as a whole, the field of data assimilation for Earth science is remarkably young. Therefore, the complexity of the Earth system, and the complexity of modeling and analysis, is so great that only a very limited range of the theoretical possibilities have been investigated.

2.6 Customers, Requirements, Product Suite

The requirements definition process for GEOS was not well defined at the start of the effort. In general requirements were acquired by expectations from program managers, ad hoc input from the EOS science team, and funding for special development or data sets from the GEOS analysis. Requirements obtained in this way, a normal way for most scientific enterprises, are not very robust, are often conflicting, are difficult to justify, and quickly lead to more requirements than can possible be met.

In March 1996 the DAO started the difficult task to trying to define the requirements for the GEOS-3 system more precisely. The goal is to ultimately trace the requirements both upwards to a justifiable source and downwards to available resources. This allows better prioritization; however, ultimately there needs to be a more robust process for requirements definition that incorporates input from the user community. Part of the current process will be highlighted here. A list of the requirements for GEOS-3 is given in Chapter9.

2.6.1 Customers

The DAO has identified seven customer categories.

C1: Campaign and Shuttle Support

C2: Instrument Teams: Product Generation

C3: Instrument Teams: Validation

C4: Assessment Community

C5: DAO Research and Development

C6: Earth Science: Programmatic

C7: Earth Science: Non-programmatic

2.6.2 Requirements Definition Process

While there is some overlap of the needs of the different customer groups, each group has some sort of requirement (desire) that distinguishes it. Examples of requirements from the different groups include

- near-real time production for C1 and C2
- desire for the "best" system for some Earth-science applications
- desire for a non-varying system for some Earth-science applications
- production of 15 year assimilated data set in the MTPE strategic plan
- re-analysis with GEOS-2 or GEOS-3 for surface applications in late 1997

- highest resolution possible
- lower resolution, but with more new data types incorporated

The following process has been used to start requirement prioritization. The MTPE Strategic Plan (1996) was used to identify specific activities in assimilation and modeling to which GEOS development was directly relevant. In some cases, GEOS products provide the only Agency resource to achieve these objectives. Then the five MTPE Science Initiatives (1996) were used to identify more carefully science problems to be addressed by the GEOS system. In two of the White Papers for the Science Initiatives, Seasonal to Interannual Climate Variability Research and Atmospheric Ozone Research, assimilation capabilities are specifically discussed. In a third, Long-term Climate Natural Variability and Change Research, the characterization of climate variability and climate processes has been one of the driving features of GEOS development from the beginning. In the final two initiatives, Land-Cover/Land-Use Research and Natural Hazards Research and Applications, GEOS data sets are of direct utility to practitioners in the field.

The information from the MTPE Science Initiatives was then used in concert with the Draft EOS Science Plan to develop two key areas where DAO capabilities and realistic resource expectations allow substantive development. These two key areas are:

1. global hydrological and energy cycles, including transfer between the atmosphere ocean and land surfaces and storage in the soil
2. transport processes in the atmosphere in order to calculate quantitatively dynamic variability of tropospheric and stratospheric trace constituents

Based on both internal-user and external-user experience the DAO developed six primary Earth-science fields in which user-defined metrics of GEOS system performance were being generated.

ES1: Hydrological Cycle

ES2: Land-surface/Atmosphere Interactions

ES3: Marine-surface/Atmosphere Interactions

ES4: Radiation (Clouds, Aerosols, Greenhouse Gases)

ES5: Atmospheric Circulation

ES6: Constituent Transport and Chemistry

Within these six primary fields users are collecting information on real, embraceable applications that allow quantitative decision making. For instance,

ES1: Hydrological Cycle

Precipitation, Total
Precipitation, Convective
Precipitation, Large-scale
Precipitation, Frequency
Precipitation, Extreme Events
Precipitation - Evaporation
Runoff
Total Precipitable Water
Upper Tropospheric Water
Middle Tropospheric Water
Planetary Boundary Layer Water
Seasonal Variability
Interannual Variability
Stratospheric Water

Users have provided relative, and some absolute, measures on GEOS capabilities in all of these fields. These tangible applications become the basis for DAO Science Product Requirements. The DAO is currently identifying which of these Science Product Requirements are most important and where GEOS development can have a significant impact. All DAO development paths ultimately map back to ES1-ES6 and a subset of DAO Science Product Requirements such as the ones listed in the example for ES2. In Chapter 8.0 the application of this process to validation will be presented. Obviously, the requirements definition process is a formidable, imprecise task. There are many instances when improvements in performance of one science product metric might degrade another, leading to conflicting implementation decisions. As the ability of the assimilation system improves, these conflicts should decrease, providing an integrated metric of improving capabilities of the GEOS system.

2.6.3 Product Suite

The customer requirements leads to the generation of a Product Suite of standard DAO products.

SP1: First-look Analysis: This provides operational support to MTPE missions, especially AM-1, including ground and airborne campaigns to address specific Earth-science processes. This analysis is required within 12-24 hours of real-time. The input data will be observations available in near-real time and will be primarily non-EOS. This run provides the data set for EOS instrument retrieval algorithms, and is also expected to be used in a broad range of scientific studies. For campaign and shuttle support (Customer C1) 5-10 day forecasts are required. There are conflicting requirements on whether the first-look analysis should be with a non-varying or "best" system.

SP2: Multi-year Assimilations ("Re-analyses"): For most customers this is the primary DAO product. These are long assimilations with a non-varying system, using historical data archives. The DAO plans to run re-analyses from 1979 onwards approximately every four years. The re-analyses will take advantage of advances in the

assimilation system as well as improvements in the ability to extract information from older data sets. There are major research questions about the impact of the changing observation system.

SP3: Final Platform Analysis: This is a science product which uses the same information as the first-look analysis plus additional data from MTPE and other non-operational data streams. This product is expected to change as the assimilation system and data availability from the platforms change.

In addition to these standard products the DAO will also generate research products that could fall as subsets of any of the above standard products.

RP1: Pocket analyses: These are analyses that include or exclude specific data sets from the input data stream. They are focused on data impact. Some customers have requested that parallel archives of pocket analyses be maintained with the re-analyses in order to evaluate the impact of the varying observing system.

RP2: Off-line analyses: These are sequential analyses for specific applications. Examples include the present constituent assimilations that use winds from GEOS as input. Future capabilities might include high-resolution land surface products. These provide versatility and simplicity while comprehensive capabilities are being developed.

RP3: Research and Development Products: These are analysis and model experiments needed for research and development. These will be of interest to specific groups outside of the DAO.

The DAO currently produces prototypes of all of these products and is collecting information on user needs and user experience with the products. The near-real time products that support stratospheric field missions are equivalent to a first- look analysis. The GEOS-1 project (see Chapter 4) is a multi-year re-analysis. Any of the various experiments where we have looked at the impact of a particular instrument (for example, Ledvina and Pfaendtner 1995) represent final platform analyses. DAO product information can be obtained at `http://dao.gsfc.nasa.gov/`.

2.7 Computational Issues

Computer resources are at the very core of a successful assimilation system for MTPE. The numerical algorithms are computationally demanding, require high floating point operations speeds (flop/s), large memories, large memory bandwidths, large mass storage facilities, and large input/output data streams. Traditionally numerical weather prediction (NWP) centers have had access to the fastest and largest computers in the world. Until recently, this was synonymous with Cray.

Almost three years ago, the DAO took the strategic position that Cray-like "boutique" computing was not viable. This decision was based on economics, independent advice, and studying of industry trends. Fundamentally, the market for high-end scientific computing is too small to maintain the boutique computers in the face of ever increasing capabilities from commercial-off-the-shelf hardware. The only way to maintain the boutique computing industry was through government subsidies, a policy that is short- sighted and not compatible with DAO budget profiles. Also, the only way to obtain traditional boutique computing capabilities is to use Japanese vendors, currently an impossibility.

While there is some satisfaction of being correct about the decline of traditional supercomputing (Cray purchased by Silicon Graphics, general confusion in the industry), exactly what strategy to follow is not clear. DAO experience with massively parallel processors through the High Performance Computing and Communications (HPCC) program are mixed. While high flop/s rates were achieved with large memory applications, the machines did not prove very reliable. In addition, machine configurations did not allow integration of end-to-end systems. The experience in HPCC also suggested that the massively parallel paradigms under consideration in 1992-1994 were no more economically viable than Cray-like vector computing.

Alternatively, workstation capabilities are far from satisfying DAO computing needs. At the urging of outside advisors, the DAO has tested primary algorithms in distributed environments that include networks of workstations. The large interprocessor communications requirements of the assimilation algorithms make such an approach impractical. Thus the DAO is left in a position of needing to develop algorithms with no definitive computer platform to target.

In March 1996 the DAO released Strategy Statement: Evolution Towards the 1998 Computing Environment for review by the DAO Computer Advisory Panel. The basic premise of the Strategy Statement was that the hardware and software environment was impossible to define beyond some basic characteristics.

- processors will be cache-based
- high speed (Cray-like) memory paradigms would not be available
- peak performance from processors will be more difficult to achieve (compared with Cray C-90 and T-90 technology)
- processor families are relatively robust, individual processors are not high-performance computing will require use of 32 - 256 processors instead of 8-16 used in Cray multitasking paradigms

- Cray multi-tasking paradigms would not scale to enough processors to be viable on the cache-based processor machines
- distributed memory computing would be necessary
- vendor provided performance software could not be relied on hardware with adequate potential capabilities would be available, but significant user adaptation would be required to achieve the potential

Taken in total, it was concluded that DAO software, with many years of implicit vector programming, would have to be re-programmed for a distributed memory environment using the Message Passing Interface (MPI, Gropp et al. 1994) protocol. This mitigates the risk of having only one possible platform on which to run the software. In order for the software to be viable, a much higher level of software engineering is required. In order to accommodate for decreasing capabilities of performance software, more of the performance programming falls on the scientific developer. All of these considerations are in direct conflict with resources available for scientific development of the GEOS algorithm. The DAO Computer Advisory Panel found these conclusions generally sound.

The DAO has been seeking partners for the solution of their computing problems. We have identified six key areas of needed expertise:

a. Networking.

b. Mass Storage.

c. Queuing for distributed processing.

d. Large computing platform design.

e. Procurement of computer hardware.

f. Software engineering for scientific problems

Currently the DAO is working with the Numerical Aerospace Simulation Systems Division at NASA's Ames Research Center to develop the computing capabilities.

In terms of direct impact on the GEOS algorithm, the single largest difference between GEOS-2 and GEOS-3 in terms of effort expended will be the conversion to message passing. Incremental scientific developments will be incorporated. Most of this conversion will have to be done by DAO scientific and programming staff.

2.8 The Weak Underbelly of Data Assimilation

There is no doubt that data assimilation is a powerful approach to the organization and extraction of information from observations. It is a powerful approach to model development. Assimilation and assimilated data sets integrate information and science across any observing program. The information from assimilated data sets is valuable enough that a data assimilation capability can be viewed as a virtual instrument that uses all observed information as its input. The output is a product enhanced by our collective knowledge of the field as represented by quantitative models.

But just like an instrument, there are limitations to products from data assimilation. Some major ones are listed here.

WU1: If there are fundamental changes in Earth processes that are outside the range that parameterizations represent, then the data will be rejected from the analysis. Monitoring of error statistics should help establish increased data rejection, but will not identify the cause. It will identify the place to go look. However, such changes in rejection statistics may be subtle and difficult to trace back to particular causes.

WU2: The estimated unobserved quantities generated by assimilation systems are only as good as the parameterizations in the model are capable of using information from the observations. They require extensive validation, with independent data sets which usually do not exist.

WU3: There is currently no robust, complete, physically-based procedure to discern model biases from observational biases. There is also no way to properly account for biases in the assimilation process. The former arise from inadequate modeling of physical processes, small-scale variability, and discretization errors. The latter arise from calibration errors, thermal sensitivity of instruments, and inadequate forward observation models. Until such procedures are discovered, there will be spurious signals in assimilated data products due to changes in the observational data base. Resolution of this problem is a long-term goal. Quantitative, ongoing estimates of model bias calculated during the data assimilation process, for instance, could be of enormous benefit in driving model development.

WU4: At the current state of the art, direct analysis of assimilated data sets should not be relied on for trend detection. The strength of assimilated data sets is in process studies and defining dynamical variability that must be removed from geophysical observations before trend calculation. However, variability in the observing system and the combination of data from many different sources limits the direct utility of assimilated data sets for trends. As error statistics are better defined and assimilation systems develop more sophisticated error handling capabilities, trend detection becomes more feasible.

2.9 References

Battin, R. H., and G. M. Levine, 1970: Application of Kalman filtering techniques to the Apollo program, Agard Theory and Appl. of Kalman Filtering, pp 335-361.

Cohn, S. E., 1996: An introduction to estimation theory. *J. Meteor. Soc. Japan.* In press.

Daley, R., 1991: Atmospheric Data Analysis, Cambridge U. Press, 457 pp.

Derber, J. C., and W. S. Wu, 1996: The use of cloud-cleared radiances in the NCEP's SSI analysis system, Eleventh Conference on Numerical Weather Prediction, American Meteorological Society, Norfolk, Virginia.

Gibson, J. K., P. Kallberg, A. Nomura and S. Uppala, 1994: The ECMWF re-analysis (ERA) project-Plans and current status, Tenth International Conference on Interactive Information and Processing Systems for Meteorology, Oceanography and Hydrology, American Meteorological Society, Nashville, Tennessee.

Gropp, W., E. Lusk, and A. Skelljum, 1994: Using MPI: portable parallel programming with the message-passing interface, The MIT Press, Cambridge, Massachusetts.

Kalnay, E., M. Kanamitsu, R. Kistler, W. Collins, D. Deaven, L. Gandin, M. Iredell, S. Saha, G. White, J. Woollen, Y. Zhu, M. Chelliah, W. Ebisuzaki, W. Higgins, J. Janowiak, K. C.. Mo, C. Ropelwski, J. Wang, A. Leetmaa, R. Reynolds, R. Jenne, and D. Joseph, 1996: The NCEP/NCAR 40-Year Reanalysis Project, *Bull. Amer. Meteor. Soc.*, **77**, 437- 471.

Ledvina, D. V., and J. Pfaendtner, 1995: Inclusion of Special Sensor Microwave/Imager (SSM/I) total precipitable water estimates into the GEOS-1 Data Assimilation System, *Mon. Weath. Rev.*, **123**, 3003-3015.

Mission to Planet Earth Science Research Plan, Volume 1, Office of Mission to Planet Earth, NASA, Washington, DC, September 1996. Available on-line from `http://www.hq.nasa.gov/office/mtpe`.

Mission to Planet Earth Strategic Enterprise Plan 1996-2002, NASA, Washington, DC, March 1996. Available on-line from `http://www.hq.nasa.gov/office/mtpe`.

National Academy of Sciences (NAS), 1991: Four-Dimensional Model Assimilation of Data: A Strategy for the Earth System Sciences. Report of the Panel on Model- Assimilated Data Sets for Atmospheric and Oceanic Research, National Academy Press, 78 pp.

Rood, R. B., and M. A. Geller (Sp. Editors), 1994: The upper atmosphere research satellite: early scientific results, *J. Atmos. Sci.*, **51**, 2781-3108.

Trenberth, K. E., and J. G. Olson, 1988: ECMWF global analyses 1979-1986: Circulation statistics and data evaluation, NCAR Technical Note, NCAR/TN-300+STR, Boulder, CO.

Shukla, J., 1996: Dynamical Seasonal Prediction, Draft, October 1996.

2.10 Acronyms

2.10.1 General acronyms

DAO	Data Assimilation Office
GEOS	Goddard Earth Observing System (The name of the DAO data assimilation system)
GCM	General Circulation Model
DAS	Data Assimilation System
QC	Quality Control
NWP	Numerical Weather Prediction
CARD	Consistent Assimilation of Retrieved Data
PSAS	Physical-space Statistical Analysis System
NASA	National Aeronautics and Space Administration
GSFC	Goddard Space Flight Center
MTPE	Mission to Planet Earth
EOS	Earth Observing System
EOSDIS	Earth Observing System Data and Information System
NOAA	National Oceanic and Atmospheric Administration
NCEP	National Centers for Environmental Prediction (formerly, NMC)
NMC	National Meteorological Center
NESDIS	National Environmental Satellite Data and Information Service
ECMWF	European Center for Medium-range Weather Forecasts
UKMO	United Kingdom Meteorological Office

2.10.2 Instruments

ADEOS	Advanced Earth Observting Satellite (Mid-late 1996)
AIRS	Atmospheric Infrared Sounder (EOS PM)
AMSU A-B	Advanced Microwave Sounding Unit (POES, EOS PM)
AVHRR	Advanced Very High-Resolution Radiometer
ASTER	Advanced Spaceborne Thermal Emission and Reflection Radiometer (EOS AM)
ATOVS	Advanced TOVS; HIRS3/AMSU (POES)
CERES	Clouds and Earth's Radiation Energy System (TRMM, EOS AM)
CLAES	Cryogenic Limb Array Etalon Spectrometer (UARS)
DMSP	Defense Meteorological Satellite Program (currently operational)
EOS AM1	Earth Observting Satellite AM (June 98 launch)
EPS	EUMETSAT (European Meteorology Satellite) Polar System
ERBE	Earth Radiation Budget Experiment (ERBS)
ERBS	Earth Radiation Budget Satellite
ERS-1,2	European Remote Sensing Satellite (Scatterometer, 6 channel, IR-Visible radiometer)

GOES	Geostationary Observational Environmental Satellite (Imager and 18 channel visible and infrared sounder, currently operational)
GOME	Global Ozone Monitoring Experiment (ERS-2)
GPS	Global Positioning System
HALOE	Halogen Occultation Experiment (UARS)
HIRS2/3	High-Resolution InfraRed Sounder (POES)
HRDI	High Resolution Doppler Imager
IASI	Infrared Atmospheric Sounding Interferometer (EPS)
ILAS	Improved Limb Atmospheric Spectrometer (ADEOS)
IMG	Interferometric Monitor for Greenhouse Gases (ADEOS)
ISCCP	International Satellite Cloud Climatology Project (several IR and visible instruments aboard different satellite)
LIMS	Limb Infrared Monitor of the Stratosphere (Nimbus 7)
MAPS	Measurement of Atmospheric Pollution from Satellites
MHS	Microwave Humidity Sounder (EOS-PM)
MLS	Microwave Limb Sounder (UARS)
MODIS	Moderate-Resolution Imaging Spectrometer (EOS AM)
MSU	Microwave Sounding Unit
MOPITT	Measurement of Pollution in the Troposphere (EOS AM)
NSCAT	NASA Scatterometer (ADEOS)
POES	Polar Orbiting Environmental Satellite (Currently Operational)
PR	Precipitation Radar (TRMM)
SBUV	Satellite Backscatter Ultraviolet radiometer (Nimbus 7, POES)
SAGE	Stratospheric Aerosol and Gas Experiment (ERBS)
SMMR	Scanning Multispectral Microwave Radiometer (?)
SSM/I	Special Sensor Microwave/Imager (DMSP)
SSM/T	Special Sensor Microwave (Temperature sounder, DMSP)
SSM/T2	Special Sensor Microwave (Water vapor sounder) (DMSP)
SSU	Stratospheric Sounding Unit (POES)
TMI	TRMM Microwave Imager (TRMM)
TOMS	Total Ozone Mapping Spectrometer (ADEOS, Meteor, Earth Probe, Nimbus 7)
TOVS	TIROS Operational Vertical Sounder; HIRS2/MSU/SSU (POES)
TRMM	Tropical Rainfall Measuring Mission (summer '97 launch)
UARS	Upper Atmospheric Research Satellite (some instruments in operation)
WINDII	Wind Imaging Interferometer (UARS)

2.11 Advisory Panel Members

2.11.1 Science Advisory Panel

Roger Daley, Chairman
Naval Research Laboratory

Jeffrey Anderson
GFDL/NOAA
Department of Commerce
Princeton University

Andrew F. Bennett
College of Oceanography
Oregon State University

Philippe Courtier
European Centre for Medium-Range Weather Forecasts

Robert E. Dickinson
Department of Atmospheric Science
University of Arizona

Daniel J. Jacob
Harvard University

Donald R. Johnson
Space Science and Engineering Center
University of Wisconsin-Madison

James J. O'Brien
Professor of Meteorology and Oceanography

Alan O'Neill
The Center for Global Atmospheric Modelling
Department of Meteorology
University of Reading

Guy Brasseur
National Center for Atmospheric Research
(Past Member)

Anthony Hollingsworth
European Centre for Medium-Range Weather Forecasts
(Past member)

Kikuro Miyakoda
GFDL/NOAA
Department of Commerce
Princeton University
(Past Member)

2.11.2 Computer Advisory Panel

William E. Farrell (chairman)
SAIC, San Diego

Tony Busalacchi
NASA, Goddard Space Flight Center
Laboratory for Hydrospheric Processes, Code 970

Bill Dannevik
Lawrence Livermore National Laboratory
L262, Environmental Programs

Alan Davis
The Florida State University
Center for Ocean-Atmosphere Prediction Studies

Geerd-R. Hoffmann
European Centre for Medium-Range Weather Forecasts
Computer Division

Menas Kafatos
University Professor of Interdisciplinary Science, Director
George Mason University
Institute for Computational Sciences and Informatics

Reagan W. Moore
San Diego Supercomputer Center

John Sloan
NCAR/SCD

Thomas Sterling
NASA, Goddard Space Flight Center
Space Data and Computing Division, Code 930

Chapter 3

Supporting Documentation

Contents

The chapter contains primarily manuscripts generated by the DAO that are directly relevant to the algorithm description or product quality. They are divided by type of document. As much as possible we seek peer review on all algorithms and data sets.

3.1 DAO Refereed Manuscripts

3.1.1 Published

Atlas, R., R. N. Hoffman, S. C. Bloom, J. C. Jusem, and J. Ardizzone, 1996: A multiyear global surface wind velocity dataset using SSM/I wind observations, Bull. Amer. Meteor. Soc., 77, 869-882.

Bloom, S. C., L. L. Takacs, A. M. da Silva, and D. Ledvina, 1996: Data assimilation using incremental analysis updates, Mon. Wea. Rev., 124, 1256-1271.

Cohn, S. E., 1993: Dynamics of short-term univariate forecast error covariances, Mon. Wea. Rev., 121,3123-3149.

Cohn, S. E., 1996: An introduction to estimation theory, to appear J. Meteor. Soc. Japan.

Cohn, S. E., and R. Todling, 1996: Approximate data assimilation schemes for stable and unstable dynamics, J. Met. Soc. Japan, 74, 63-75.

Coy, L., R. Rood, and P. Newman, 1994: A comparison of winds from the STRATAN data assimilation system to balanced wind estimates, J. Atmos. Sci., 51, 2309-2315.

Dee, D. P., 1995: On-line estimation of error covariance parameters for atmospheric data assimilation, Mon. Wea. Rev., 123, 1128-1145.

Helfand, H. M., and S. D. Schubert, 1995: Climatology of the simulated Great Plains low-level jet and its contribution to the continental moisture budget of the United States, J. Climate, 784-806.

Ledvina, D. V., and J. Pfaendtner, 1995: Inclusion of Special Sensor Microwave/Imager (SSM/I) total precipitable water estimates into the GEOS-1 Data Assimilation System, Mon. Weath. Rev., 123, 3003-3015.

Molod, A., H. M. Helfand, L. L. Takacs, 1996: The climatology of parameterized physical processes in the GEOS-1 GCM and their impact on the GEOS-1 Data Assimilation System, J. Climate, 9, 764-785.

Riishojgaard, L. P., 1996: On four-dimensional variational assimilation of ozone data in weather prediction models, to appear Q. J. Roy. Meteor. Soc.

Schubert, S. D., R. B. Rood, J. W. Pfaendtner, 1993: An assimilated data set for earth science applications, Bull. Amer. Meteor. Soc., 74, 2331-2342.

Schubert, S. D. and Y. Chang, 1996: An objective method for inferring sources of model error, Mon. Wea. Rev., 124, 325-340.

Park, C.-K, and S. D. Schubert, 1996: On the nature of the 1994 East Asian summer drought, to appear J. Climate.

Sienkiewicz, M. E., and J. W. Pfaendtner, 1996: Assimilation variability in the GEOS-1 Data Assimilation System, to appear Mon. Wea. Rev.

3.1.2 Submitted

Chen M., R.B. Rood, and L. L. Takacs, 1996: Impact of a semi-lagrangian and an Eulerian dynamical core on climate simulations, submitted to J. Climate.

Gaspari, G. and S. E. Cohn, 1996: The construction of correlation functions in two and three dimensions, submitted to Math. Geol.

Joiner, J., and A. M. da Silva, 1996: Efficient methods to assimilate satellite retrievals based on information content, submitted Q. J. Roy. Meteor. Soc.

Min, W., and S. D. Schubert, 1996: The climate signal in regional moisture fluxes: a comparison of three global data assimilation products, submitted J. Climate.

3.1.3 Collaborations

Allen, D. J., P. Kasibhatla, A. M. Thompson, R. B. Rood, B. G. Doddridge, K. E. Pickering, R. D. Hudson, and S.-J. Lin, 1996: Transport-induced interannual variability of carbon monoxide determined using a chemistry and transport model, to appear in J. Geophys. Res.

Douglass, A. R., C. J. Weaver, R. B. Rood, and L. Coy, 1996: A three-dimensional simulation of the ozone annual cycle using winds from a data assimilation system, J. Geophys. Res., 101, 1463-1474.

Higgins, R. W., K. C. Mo and S. D. Schubert, 1996: The moisture budget of the central United States in spring as evaluated in the NMC/NCAR and the NASA/DAO reanalyses, Mon. Wea. Rev.,124, 939-963.

Rienecker, M. M., R. Atlas, S. D. Schubert, and C. A. Scholz, 1995: A comparison of surface wind products over the North Pacific Ocean, J. Geophys. Res.-Oceans, 101, 1011- 1023.

3.2 DAO Office Notes

DAO Office Notes are internal documents that describe requirements, strategies, and technical information about DAO system components, science activities, and data sets. Some have received formal technical review. Some are the basis for refereed papers and Technical Memoranda. DAO Office Notes have not been subjected to formal anonymous peer review.

Office Notes may be viewed at
http://dao.gsfc.nasa.gov/subpages/office-notes.html

ON 95-01: Documentation of the GEOS/DAS Observation Data Stream (ODS), Version 1.01: Arlindo da Silva and Christopher Redder, 12/95.

ON 96-02: Documentation of the Physical-space Statistical Analysis System (PSAS) Part I: The Conjugate Gradient Solver Version, PSAS-1.00: Arlindo da Silva and Jing Guo, 2/96.

ON 96-03: Construction of Correlation Functions in Two and Three Dimensions: Gregory Gaspari and Stephen E. Cohn, 4/96.

ON 96-04: Notes on the Icosahedral Domain Decomposition in PSAS: James W. Pfaendtner, 9/94.

ON 96-05: Documentation of the Multi-year GEOS-1 Assimilation Data Subset for Northern Africa, the Mediterranean, and the Middle East: Arlindo da Silva, 2/96.

ON 96-06: Efficient Methods to Assimilate Satellite Retrievals Based on Information Content: Joanna Joiner and Arlindo M. da Silva.

ON 96-07: A Study on Assimilating Potential Vorticity Data: Yong Li, Richard Menard, Stephen E. Cohn, Richard B. Rood.

ON 96-08: The GLA TOVS Rapid Algorithm Forward Radiance Modules and Jacobian Version 1.0: Meta Sienkiewicz, 9/96.

ON 96-11: On-line Estimation and Correction of Forecast Error Bias for Data Assimilation: Arlindo da Silva, Dick Dee and Lawrence Takacs.

ON 96-12: A Climatological Atlas of the Bermuda High from the GEOS-1 Multi-year Assimilation (Summers of 1985-93): Arlindo da Silva and Richard Rood, 5/96.

ON 96-13: New Data Types Working Document: Joanna Joiner, Robert Atlas, Steve Bloom, Genia Brin, Stephen Cohn, Arthur Hou, Dave Lamich, Dave Ledvina, Richard Menard, Lars-Peter Riishojgarrd, Richard Rood, Arlindo da Silva, Meta Sienkiewicz, Jim Stobie, and Runhua Yang, 6/96.

ON 96-14: Requirements for DAO's On-Line Monitoring System (DOLMS), Version 1.00: Arlindo da Silva, Ken Ekers and Austin Conaty, 6/96.

ON 96-15: GEOS/DAS Quality Control Strategy Document: Dick P. Dee and Alice R. Trenholme, 8/96.

ON 96-16: Data Assimilation Computing and Mass Storage Requirements for 1998: James G. Stobie, 1/96.

ON 96-17: A summary of precipitation statistics over the United States: W. Min and S. Schubert.

ON 96-18: Data assimilation in the presence of forecast bias, D. P. Dee and A. M. da Silva.

ON 96-19: GEOS-3/DAS Quality Control Requirements, Document Version 1: Alice Trenholme.

ON 96-20: Evaluation of RTTOV and GLA TOVS forward model and Jacobian: M. Sienkiewicz.

ON 96-21: Primary Requirements for the GEOS-3 Data Assimilation System: J. Stobie.

ON 96-22: Visualization and user interface: requirements documentation: P. Beaudoin and S. Schubert.

ON 96-23: Validation Plan for Version 2.0 of the Goddard Earth Observing System (GEOS) Data Assimilation System: S. D. Schubert, S. C. Bloom and K. Ekers.

ON 96-24: Monsoon Rainfall in the GEOS-1 Assimilation: Sensitivity to Input Data: Chung-Kyu Park, Siegfried D. Schubert, David J. Lamich, and Yelena Kondratyeva.

3.3 Technical Memoranda

The Technical Report Series on Global Modeling and Data Assimilation (Max J. Suarez, Editor. NASA Technical Memorandum 104606) provides details of model and assimilation algorithms, as well as results from workshops. This series is written by both DAO and non-DAO authors and describes algorithms that are at the basis of both GEOS and other efforts at GSFC.

In some instances the documents provide technical details or expanded graphics of refereed manuscripts. The Technical Memoranda have been edited and subjected to internal review. The Technical Memoranda have not been subjected to formal anonymous peer review.

The documents may be obtained from the DAO or from the NASA Center for AeroSpace Information, 800 Elkridge Landing Road, Linthicum Heights, MD 21090-2934 (phone 301-621-0390).

They can be viewed at

http://dao.gsfc.nasa.gov/subpages/tech-reports.html

TM Volume 1: Documentation of the Goddard Earth Observing System (GEOS) General Circulation Model-Version 1: Lawrence L. Takacs, Andrea Molod, and Tina Wang, 9/94.

TM Volume 2: Direct Solution of the Implicit Formulation of Fourth Order Horizontal Diffusion for Gridpoint Models on the Sphere: Yong Li, S. Moorthi, and J. Ray Bates, 10/94.

TM Volume 3: An Efficient Thermal Infrared Radiation Parameterization for Use in General Circulation Models: Ming-Dah Chou and Max J. Suarez, 12/94.

TM Volume 4: Documentation of the Goddard Earth Observing System (GEOS) Data Assimilation System-Version 1: J. Pfaendtner, S. Bloom, D. Lamich, M. Seablom, M. Sienkiewicz, J. Stobie, and A. da Silva, 1/95.

TM Volume 5: Documentation of the ARIES/GEOS Dynamical Core: Version 2: Max J. Suarez and Lawrence L. Takacs, 4/95.

TM Volume 6: A Multi-Year Assimilation with the GEOS-1 System: Overview and Results: S. Schubert, C.K. Park, C. Wu, W. Higgins, Y. Kondratyeva, A. Molod, L. Takacs, M. Seablom, and R. Rood, 4/95.

TM Volume 7: Proceedings of the Workshop on the GEOS-1 Five-Year Assimilation: Siegfried D. Schubert and Richard B. Rood, 9/95.

TM Volume 8: Documentation of the Tangent Linear Model and Its Adjoint of the Adiabatic Version of the NASA GEOS-1 C-Grid GCM (Version 5.2): Weiyu Yang and I. Michael Navon, 3/96.

TM Volume 9: Energy and Water Balance Calculations in the Mosaic LSM: Randal D. Koster and Max J. Suarez, 3/96.

TM Volume 10: Dynamical Aspects of Climate Simulations Using the GEOS General Circulation Model: Lawrence L. Takacs and Max J. Suarez, 4/96.

TM Volume xx: An intercomparison of assimilated and simulated atmospheric variance/covariance statistics, W. Min, S. Schubert and C.-K. Park. *In preparation.*

Other Technical Memoranda:

Schemm, J.-K., S. Schubert, J. Terry, and S. Bloom, 1992: Estimates of monthly mean soil moisture for 1979-89, NASA Tech. Memo. 104571, 252 pp.

3.4 Other DAO Documents

3.4.1 Planning, MOU and Requirements Documents

Data Assimilation Office Plan (1994-2000)

Data Assimilation Office (DAO) Strategy Statement: Evolution Towards the 1998 Computing Environment (March 1996)

NOAA-NASA Technical Implementation Agreement between the NASA/GSFC Earth Sciences Directorate and the NOAA/NWS National Meteorological Center for transferring NMC Operational Products to the Earth Sciences Directorate, 9 February 1993.

DAO/ESDISP Memorandum of Understanding, 21 January 1996.

Model Requirements for Data Assimilation at Launch, 4 May 1994.

Framework for Collaboration between The Data Assimilation Office (DAO) and The Numerical Aerospace Simulation Systems Division (NAS), December 1996.

3.4.2 Advisory Panel Reports

First Report of the Data Assimilation Office Advisory Panel (December, 1992)

Second Report of the Data Assimilation Office Advisory Panel (December, 1993)

Third Report of the Data Assimilation Office Advisory Panel (February, 1995)

Fourth Report of the Data Assimilation Office Advisory Panel (June, 1996)

Report of the Data Assimilation Office Computer Advisory Panel (May, 1996)

3.4.3 Conference Abstracts

Dee, D. P., and G. Gaspari, 1996: Development of anisotropic correlation models for atmospheric data assimilation, Preprint volume, 11th Conf. on Numerical Weather Prediction, August 19-23, 1996, Norfolk, VA, pp 249-251

Ding, H. D. and R. D. Ferraro, 1996: An 18GFLOPS Parallel Data Assimilation PSAS Package, Proceedings of Intel Supercomputer Users Group Conference 1996, June 1996, to be published in Journal of Computers and Mathematics.

Guo, J. and A. M. da Silva, 1995: Computational Aspects of Goddard's Physical-space Statistical Analysis System (PSAS), Preprints, Second UNAM-CRAYSupercomputing Conf. on Numerical Simulations in the Environmental and Earth Sciences, Mexico City, Mexico, 6 pp.

von Laszewski, G., M. Seablom, M. Makivic, P. M. Lyster, and S. Ranka, 1995: Design issues for the parallelization of an optimal interpolation algorithm, Coming of Age, Proceedings of the Sixth ECMWF Workshop on the Use of Parallel Processors in Meteorology, 290-302.

Ledvina, D. V. and A. Hou, 1996: Data impact studies using the GEOS-1 DAS during TOGA COARE: Inclusion of SSM/I total precipitable water and surface wind estimates, WMO TOGA 95, in press.

Lou, G.-P., A. da Silva, D. Dee, and C. Redder, 1996: Modeling fully anisotropic wind-mass error covariances in physical space, preprint volume, 11th Conf. on Numerical Weather Prediction, August 19-23, 1996, Norfolk, VA, p 253.

Menard, R., 1995: Middle atmosphere assimilation of UARS constituent data using Kalman filtering: Preliminary results, International symposium on assimilation of observations in meteorology and oceanography, Tokyo, Japan, 273-278.

da Silva, A. M., Pfaendtner, J., Guo, J., Sienkiewicz, M., and S. E. Cohn, 1995: Assessing the effects of data selection with DAO's Physical-space Statistical Analysis System, International symposium on assimilation of observations in meteorology and oceanography, Tokyo, Japan, 273-278.

da Silva, A. M., C. Redder, and D. P. Dee, 1996: Modeling retrieval error covariances for atmospheric data assimilation. *Eighth Conference on Satellite Meteorology,* Atlanta, GA, 28 January–2 February, 1996.

da Silva, A. M., Redder, C., and D. P. Dee, 1996a: Modeling retrieval error covariances for global data assimilation, Proc. 8th Conf. Satell. Meteor., Atlanta, GA., in press.

Chapter 4

GEOS-1 Data Assimilation System

Contents

4.1 GEOS-1 Multi-year Re-analysis Project

GEOS-1 is version number 1 of the GEOS data assimilation system. The model and objective analysis algorithms (see Figure 2.1) were frozen in 1993 and the basic algorithms are described in the Takacs et al. (1994, TM Volume1) and Pfaendtner et al. (1995, TM Volume 4). A multi-year re-analysis was performed with GEOS-1, and the GEOS-1 re-analysis has been distributed to hundreds of users. The GEOS-1 re-analysis provides a data set with a non-varying assimilation system from 1980-1993. Plans are to continue the re-analysis to the beginning of 1979 through the end of 1994. Schubert et al. (1995, TM Volume 6) is an atlas of results from the 1985-1989 portion of the re-analysis. Schubert and Rood (1995, TM Volume 7) is a record from a user workshop held in 1995. Schubert and Rood also list the strengths and weaknesses of the GEOS-1 product which provides the baseline for evaluating improvements in future versions of the GEOS system.

Since the completion of the first five-year segment of GEOS-1 both NCEP and ECMWF have completed multi-year re-analyses. These products have been subjected to numerous intercomparisons and will be the subject of an international workshop in Fall 1997.

The GEOS-1 re-analysis project is described in Schubert et al. (1993). The goals of the GEOS-1 project included building a data set of scientific value prior to the launch of the EOS platforms. Objectives included evaluation of the interseasonal and multi-year information in applications of an atmospheric assimilated data set to climate dynamics, global hydrology, and stratospheric and tropospheric chemistry.

There are numerous configurations of early GEOS systems. The GEOS-1 system covers the global atmosphere from the ground to the pressure altitude of 10 hPa (approx. 30 km). A stratospheric configuration (not used in the GEOS-1 re-analysis project) covers the altitude range from the ground to 0.4 hPa (approx. 55 km). GEOS-1 was run at a horizontal resolution of 2 degrees latitude and 2.5 degrees longitude. The stratospheric configuration was originally run at 4 degrees latitude and 5 degrees longitude for computational viability. Since 1994 the stratospheric experiments are run at 2 degrees latitude and 2.5 degrees longitude. In some publications the early stratospheric system was named STRATAN (STRATospheric ANalysis; Coy et al.(1994) and references therein). This distinction is not made in later versions. All products are now linked by name to the GEOS system. The current stratospheric configuration used for production is known as GEOS-STRAT.

As a system development exercise there were numerous goals of the GEOS-1 project:

- Characterize performance of initial algorithm capabilities.
- Provide baseline performance criteria to help guide development path.
- Develop validation strategies for generalized data assimilation.
- Prototype data flows, develop a production capability, identify production bottlenecks.
- Collect and pre-process the historical input data stream for future re-analyses.
- Determine diagnostics needed by extended Earth-science community.
- Determine user needs in data set structure.

From the point of view of all original goals the GEOS-1 project has been successful. The information has been critical to GEOS-2 development. The rest of this chapter will highlight some of the results of the GEOS-1 re-analysis as well as results from the stratospheric configurations of the system. Attention will be focused on issues relevant to algorithm definition and improvement.

4.2 GEOS-1 DAS Algorithms

The basic algorithms of GEOS-1 are described in Takacs et al. (1994, TM Volume1) and Pfaendtner et al. (1995, TM Volume 4). A general schematic of the system is given in Figure 2.1. Since the objective analysis routine is a conventional optimal interpolation (OI) that is completely replaced in GEOS-2, the analysis will only be very briefly described. The same is true for the error statistics used in GEOS-1; therefore, they will only be discussed in passing. The optimal interpolation and statistics are a direct descendent of the scheme described in Baker et al. (1987). The model in GEOS-2 is an incremental development from GEOS-1; therefore, the GEOS-1 model will be described in some detail. The model and analysis are integrated together through the incremental analysis update (IAU) routine. The primary discussion of the IAU implementation is in Chapter 5.

The GEOS-1 DAS analyzes global sea level pressure and near surface winds over the oceans, as well as geopotential height, vector wind, and water vapor mixing ratio on constant pressure surfaces. The upper air height/wind analyses and the sea level pressure/surface wind analyses are done using multivariate statistical interpolation algorithms in which mass (height/pressure) and wind data affect both the mass and wind analyses. The moisture analysis is done with a univariate statistical algorithm, and only at levels from 1000 hPa to 300 hPa. The input data are from rawinsondes, dropwindsondes, rocketsondes, aircraft winds, cloud tracked winds, and thicknesses from the historical TOVS soundings produced by NOAA NESDIS.

The basic GEOS-1 DAS configuration consists of a 2° latitude by 2.5° longitude, 14-level analysis (20, 30, 50, 70, 100, 150, 200, 250, 300, 400, 500, 700, 850, 1000 hPa) coupled to a 20-level, 2° by 2.5° model for the troposphere and lower stratosphere. The system used in the current stratospheric applications, GEOS-STRAT, consists of a 2o by 2.5o, 18- level (surface to 0.4 hPa) analysis coupled to a 46-level, 2o by 2.5o model.

4.2.1 The GEOS-1 Objective Analysis Scheme (Optimal Interpolation)

The GEOS-DAS optimal interpolation (OI) analysis scheme uses up to 75 observations to analyze all grid-points within a small three-dimensional cluster. The data selection algorithm, which chooses the observations to be used from those that have passed the quality control procedures, is an empirically tuned decision tree which uses a priori observation error estimates in making its choices. All observations used in the analysis have passed a two stage quality check (Seablom et al. 1991). The first stage, the gross check, makes use of the assimilation's forecast error variance fields to estimate expected innovation (observation increments) vector variances. In a second stage a buddy check compares suspect observations with neighboring data by means of a successive correction analysis to the location of the suspect datum. Forecast error correlations are modeled with the damped cosine function as in Baker et al. (1987), but the fit parameters have been recalculated using GEOS-1 DAS.

A feature of the GEOS-1 DAS which has been eliminated in GEOS-2 is the localization of the analysis. The GEOS-1 DAS global analyses are performed as a series of localized analyses on smaller regions referred to as mini-volumes. This was done to make the algorithm computationally viable on the computers available when GEOS-1 was developed. However, the localization process leaves significant algorithmic artifacts in the final prod-

uct. A mathematical description of the localization and data selection processes, as well as assessments of their consequences is given in Chapter 5

The GEOS-1 mini-volumes are a set of non-overlapping groups of analysis grid-points. Associated with each mini-volume is an approximately cylindrical search region, having 3200 km diameter, from which the data are selected for the generation of the analysis in the mini-volume. There are three distinct types of mini-volumes, each containing a different number of horizontal grid-points. In the tropics and low latitudes, each mini-volume contains six horizontal grid-points, rectangularly arranged. The mid-latitude region, between 30 degrees and 82 degrees latitude, contains mini-volumes with eight horizontal grid-points, while the polar regions place an entire latitude band of grid-points into each mini-volume. Additionally, each mini-volume contains two vertical layers of grid-points. The total analysis contains nearly 12,000 mini-volumes.

A data search within each search region selects the 75 observations closest to the volume midpoint, with 60% of these from rawinsondes if available. The covariance matrix is then formed and a linear system of equations is solved for the weights of the observations. With the GEOS-1 configuration of mini-volumes, neighboring search regions have an approximate 85% overlap. Because only 75 observations are selected, however, the actual overlap could be substantially less.

The mini-volume approach to performing the analysis is preferable to a single grid-point approach for two computational reasons. First, solving a local problem centered on a region rather than on a particular grid-point significantly reduces the number of covariance matrices that need be set up and solved. The data search, also computationally expensive, is minimized by avoiding redundant calculations. Second, the independent nature of the mini-volumes allows the GEOS-1 DAS to operate well in a parallel computing environment. The major drawback is that the limitation of 75 observations per mini-volume reduces the search region overlap, particularly in areas of high data density, leading to the adverse effect of boxiness in the analysis increments.

Mini-volumes, large volume, and single grid point approaches of OI schemes are all local approximations for solving the analysis problem, which is, in fact, a global problem. One of the primary improvements in GEOS-2 is the development of a global solver. One of the scientific goals of GEOS-2 is to investigate the real advantages of a global solve that does not require the data selection of the mini-volume approach of GEOS-1.

4.2.2 GEOS-1 General Circulation Model (GCM)

This section presents a summary of the main features of the GEOS-1 GCM. This model is fully documented in Takacs et al. (1994, TM Volume1). The GEOS GCM is designed to be completely time continuous with tendencies from the physics parameterizations and filters being incrementally added at every dynamics time step. Earlier versions had intermittent applications of these processes.

The GEOS-1 GCM uses the second-order potential enstrophy and energy conserving horizontal differencing scheme on a C-grid developed by Sadourney (1975), and further described by Burridge and Haseler (1977). An eighth-order Shapiro filter with a reduced coefficient is applied to the wind, potential temperature and specific humidity to avoid non-

linear computational instability. The reduced-coefficient filter is applied at every step in such a way that the amplitude of the two-grid interval wave is essentially removed in six hours. Applying the filter weakly at each step eliminates the shock that occurred in earlier assimilations using an intermittent application of the filter. The model also uses a polar Fourier filter to avoid linear instability due to violation of the linear stability condition for the Lamb wave and interval gravity waves. This polar filter is applied only to the tendencies of the winds, potential temperature, specific humidity and surface pressure. The model's vertical finite differencing scheme is that of Arakawa and Suarez (1983). The dynamics routines are organized into a plug-compatible module called the ARIES/GEOS dynamical core which is described in Suarez and Takacs (1995, TM Volume 5).

The infrared and solar radiation parameterizations follow closely those described by Harshvardhan et al. (1987). In the longwave, water vapor absorption is parameterized as in Chou (1984), the 15 micron band of carbon dioxide as in Chou and Peng (1983), and ozone absorption as in Rodgers (1968) with modifications suggested by Rosenfield et al. (1987). The shortwave follows Davies (1982), as described in Harshvardhan et al. (1987). Shortwave absorption by water vapor uses a k-distribution approach as in Lacis and Hansen (1974). Cloud albedo and transmissivity for the model layers are obtained from specified single-scattering albedo and cloud optical thickness using the delta- Eddington approximation (Joseph et al. 1976; King and Harshvardhan 1986). The penetrative convection originating in the boundary layer is parameterized using the Relaxed Arakawa-Schubert scheme (Moorthi and Suarez 1992) which is a simplified Arakawa-Schubert (1974) type scheme. As an approximation to the full interaction between the different allowable cloud types in the original Arakawa-Schubert scheme, many clouds are simulated frequently with each modifying the large scale environment some fraction of the total adjustment. The parameterization thereby relaxes the large scale environment towards neutrality. In addition to the Relaxed Arakawa-Schubert cumulus convection scheme, the GEOS-1 GCM employs a Kessler-type scheme for the re-evaporation of falling rain (Sud and Molod 1988). The scheme accounts for the rainfall intensity, the drop size distribution, and the temperature, pressure and relative humidity of the surrounding air.

Super-saturation or large-scale convection is defined in the GEOS-1 GCM whenever the specific humidity in any grid-box exceeds its super-saturation value. The large-scale precipitation scheme rains at super-saturation, and re-evaporates during descent to partially saturate lower layers in a process that accounts for some simple micro-physics.

The GEOS-1 GCM turbulence parameterization consists of elements which handle vertical diffusion (Helfand and Labraga 1988) and surface fluxes of heat, moisture and momentum (Helfand et al 1991; Helfand and Schubert 1995). The vertical regime is divided into a free atmosphere, a surface layer, and a viscous sub-layer above the surface roughness elements. The turbulent eddy fluxes are calculated using a variety of methods depending on the vertical location in the atmosphere.

Turbulent eddy fluxes of momentum, heat and moisture in the surface layer are calculated using stability-dependent bulk formulae based on Monin-Obukhov similarity functions. For an unstable surface layer, the chosen stability functions are the KEYPS function (Panofsky, 1973) for momentum, and its generalization for heat and moisture. The function for heat and moisture assures non-vanishing heat and moisture fluxes as the wind speed approaches zero. For a stable surface layer, the stability functions are those of Clarke (1970), slightly modified for the momentum flux. The moisture flux also depends on a specified

evapo- transpiration coefficient.

Above the surface layer, turbulent fluxes of momentum, heat and moisture are calculated by the Level 2.5 Mellor-Yamada type closure scheme of Helfand and Labraga (1988), which predicts turbulent kinetic energy and determines the eddy transfer coefficients used for vertical diffusion.

4.2.3 The Incremental Analysis Update

The Incremental Analysis Update (IAU) (Bloom et al. 1996) is the interface between the objective analysis routine and the assimilating model. The IAU reduces initial imbalances and spin-up. The IAU is effective enough that the GEOS-1 DAS does not contain a formal initialization routine. The IAU procedure is a unique feature of the GEOS-1 DAS, and the IAU will be implemented in GEOS-2. IAU theory and filtering qualities are described more fully in Chapter 5.

For an assimilation system to be used for climate and chemistry applications the IAU also offers a set of particular advantages. In traditional numerical weather prediction schemes the precipitation products were usually derived from a multi-hour forecast. This allows for the hydrological cycle spin up. In the IAU the precipitation products are from the analysis; therefore, closer to the actual data insertion time. In addition, because the assimilated product is given by a continuous integration, there can be frequent output of products. This has proven useful for archiving surface products every hour (on request) and is the reason the GEOS DAS can produce the special sub-orbital data sets requested by AM-1 instruments. Finally, with the analysis increments archived, it is possible to re- generate the assimilation products, with additional diagnostics or increased time frequency, for only the computational cost of the model simulation.

4.3 Performance/Validation of GEOS-1 Algorithms

This section will highlight some of the performance characteristics of the GEOS-1 system. Both some successes and failures will be presented, revealing some of the issues that must be addressed in improvement of the GEOS system. Since it is crucial that model performance be verified and credible, model performance will be discussed separately.

4.3.1 GEOS-1 General Circulation Model

The primary development and validation strategy for the GEOS-1 GCM was focused on interseasonal and multi-year simulations. This is in contrast with models used in numerical weather prediction (NWP) which are evaluated primarily on multi-day forecast capabilities. For NWP models there is a clear driving metric - the better the forecast, the better the analysis. There is not such a clear metric for assimilated data products for more general applications. This strategy of using longer model integrations for development and validation was chosen for GEOS-1 GCM because of the desire to investigate the impact of model physics parameterizations on the multi-year assimilated data product. The strategy has proven to have both advantages and disadvantages as will be summarized in Section 4.4.

4.3.1.1 Atmospheric Model Intercomparison Project (AMIP)

On the DAO's initiative, as well as requested by the DAO Scientific Advisory Panel and members of the EOS community, the GEOS-1 GCM was used to generate a simulation for the Atmospheric Model Intercomparison Project (AMIP, Gates 1992). The AMIP simulations are of ten year duration with a specified set of boundary conditions and model parameters. The strengths of AMIP include a relatively controlled research experiment with teams focused on particular projects. Disadvantages include both the fact that the models are so complex and varied that a rigorously controlled experiment is not accomplished and the process is such a large undertaking that models have evolved substantially by the time results are obtained and published. AMIP and similar projects, however, do provide valuable steps in identifying model uncertainties and initiating systematic improvement.

In general the GEOS-1 GCM has performed credibly in the AMIP studies, and in some cases the relative performance has been outstanding. This is a mixed statement, because by some perspectives the performance of all the models is significantly flawed. Furthermore, as discussed below, the assumptions drawn from the AMIP studies have not provided definitive information about particular model weaknesses.

Some of the best characteristics of the GEOS-1 GCM include the sensitivity to sea surface temperature changes and the representation of low level, boundary layer, jets. The response to sea surface temperature changes is demonstrated in Figure 4.1 which shows the outgoing longwave radiation at the equator as a function of latitude and time from the GEOS-1 GCM, the GEOS-1 DAS, and National Oceanic and Atmospheric Administration (NOAA) satellite measurements. The general shape of the variability as simulated by the model is good, and the migration into the eastern Pacific in 1987 during the El Niño is well simulated. The characteristics of the low level jet over the United States is documented in Helfand and Schubert (1995). This jet is responsible for the flux of moisture into the central

United States, and is closely related to drought and flood conditions. The GEOS-1 model has proven capable of simulating many important processes that maintain the climate.

Many of the teams in AMIP have focused attention on atmospheric hydrology, including the representation of precipitation, clouds, tropospheric water, global and regional moisture budgets, and interseasonal and interannual variability. Aside from being important climate parameters, moist processes are difficult to model and highly parameterized. Therefore, they are one of the most uncertain and difficult to validate processes in the model.

Weare et al. (1995) investigate total cloudiness and its variability. The summary of relative performance of all the models in representing seasonal differences in cloudiness is given in Figure 4.2. The GEOS-1 model is labeled GSFC. The verification data set is the International Satellite Cloud Climatology Project (ISCCP) C2 data set (Rossow and Schiffer 1991). In this ranking the higher the numbers the better, and GEOS-1 performs near the top. The first shading in the bar represents the ability to model the summer minus winter differences in zonal mean cloudiness, the second shading the correlations between ISCCP C2 and modeled seasonal variability, and the unshaded part the correlations during an El Niño cycle. While GEOS-1 performance is relatively high, the absolute performance of the models is only ephemerally satisfying. Weare at al. point out that often the correlation between different observation data sets is much higher than the correlation of observations with any model. Further, some models obtain relatively accurate representations of averaged diagnostics such as the ones presented here, but have very poor representation of the spatial distribution of the cloudiness. In general there remain significant problems with model simulations of cloudiness. Furthermore, this AMIP study was not able to identify any strong relationship between model parameterizations and performance.

Gaffen et al. (1996) study the ability of the AMIP models to represent total precipitable water as verified with both radiosonde and satellite microwave data. With regard to model algorithms, they reach the same conclusion as Weare et al. (1995); namely, there is no distinct relationship of model performance to formulation. With respect to GEOS-1 GCM performance, the simulation of seasonal values and variability of precipitable water over North America is very good. Decadal mean values over North America in the GEOS-1 GCM are slightly wetter than observed, but relative to other model simulations better than most. In the global decadal mean the GEOS-1 GCM is dry, and in the middle of the pack relative to other models.

Lau et al. (1996) look at the integrated hydrologic cycles in the AMIP model. In this evaluation the overall performance of GEOS-1 GCM was in the third quartile. The strongest aspect of the GEOS-1 GCM is in the global rainfall distribution. The weakest aspect is the precipitation and evaporation balance over land.

The summary of the AMIP exercise, to date, shows that the GEOS-1 GCM is a credible basis on which to build future systems. The model has its set of strengths and weaknesses. One disturbing message from the AMIP simulations for all of the models is the inconsistency between different parts of the hydrological cycle. Individual models will get one part of the cycle accurately, but another part poorly. Since the different parts of the hydrological cycle are physically related, the AMIP results suggest we are often investigating, as a discipline, model tuning rather than the representation of physical processes. This is a situation that must be changed to reduce the uncertainties of climate models. Further, as we use assimilation techniques to investigate model response to input data sets, we can develop new

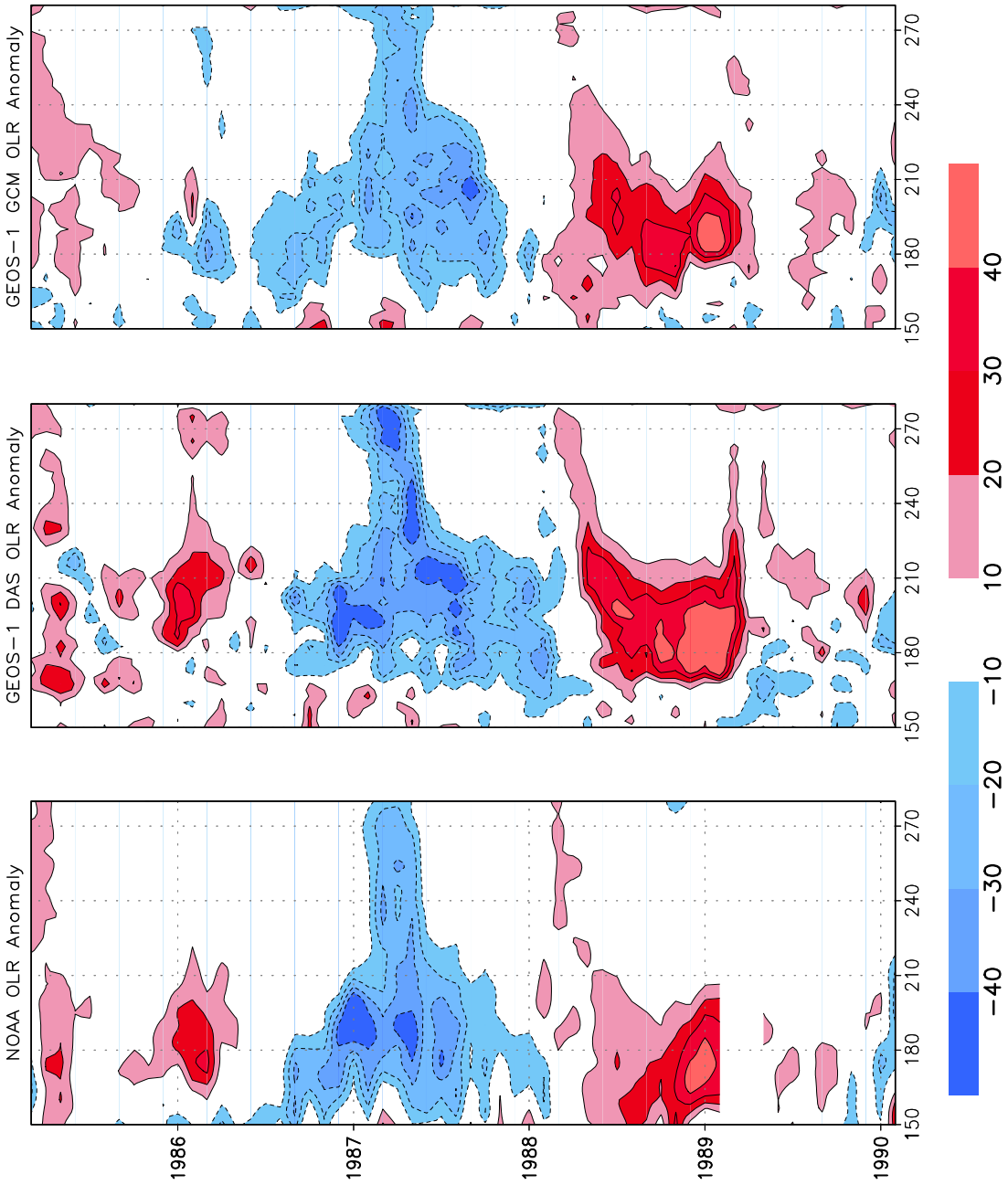

Figure 4.1: Time series between 150 and 270 degrees longitude of the anomaly (time mean removed) of outgoing longwave radiation (OLR) centered over the equator. The GEOS-1 GCM OLR simulation is on the right, and the NOAA satellite derived OLR on the left. The results from the GEOS-1 data assimilation are in the center. Note that the simulation captures the major features of the OLR variation, and in particular the migration of the anomaly to the eastern Pacific during the 1987 El Niño. The ability to capture interannual variability is one of the strengths of the GEOS-1 GCM (See also Chapter 8).

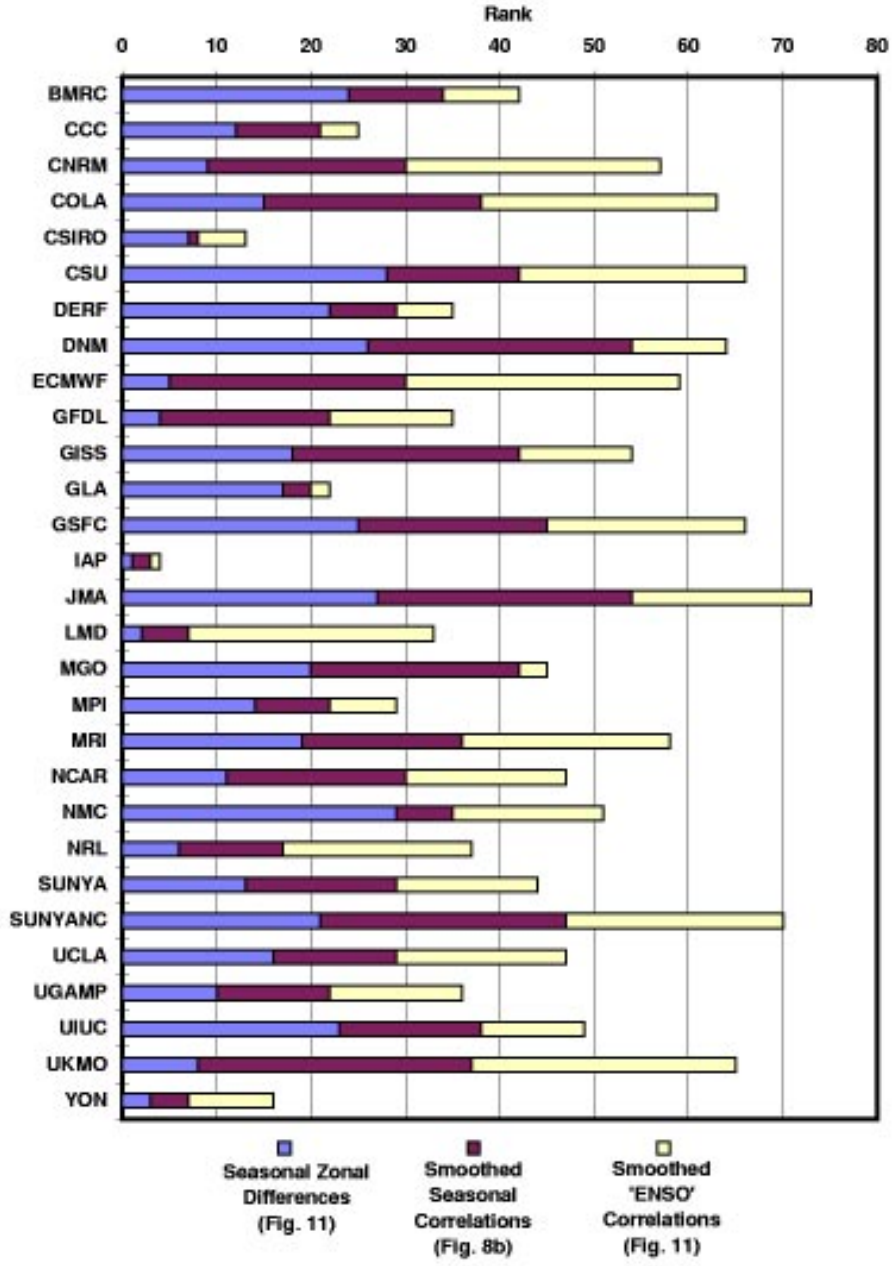

Figure 4.2: Relative ranks of AMIP GCMs from Weare et al. (1995). The GEOS-1 model is labeled GSFC. The verification data set is the International Satellite Cloud Climatology Project (ISCCP) C2 data set (Rossow and Schiffer 1991). In this ranking the higher the numbers the better, and GEOS-1 performs near the top. The first shading in the bar represents the ability to model the summer minus winter differences in zonal mean cloudiness, the second shading the correlations between ISCCP C2 and modeled seasonal variability, and the unshaded part the correlations during an El Niño cycle.

ways of model development that more closely link parameterizations to observed processes.

4.3.1.2 Model Impact on Assimilated Data Products

In a unique study, the DAO generated a five year simulation that parallels the 1985-1989 portion of the GEOS-1 re-analysis. This is the only multi-year simulation that parallels a multi-year assimilation using the same model that was used in the assimilation. The purpose of the experiment was to validate model performance and to understand the impact of model parameterizations on the assimilated product. The results are reported in Molod et al. (1996).

Using independent data sets as validation, Molod et al. showed that the assimilated data product often provided a very accurate representation of observed Earth-system parameters. Therefore, the GEOS-1 GCM is capable of using information from the observations to generate data sets that are more complete in both coverage and number of geophysical parameters than the observations alone. However, there are some significant zeroth-order shortcomings that require attention for future developments. Many of these are related to clouds and precipitation. Some of the same disturbing inconsistencies, as discussed in the previous subsection on the AMIP results, are seen in the assimilated data set.

As discussed in Molod et al., there are four general ways which the model responds to the assimilation of observations:

Re1: GCM inadequacies are corrected by the data, even in cases when the biased quantity is not directly observed. Example, surface fluxes of latent heat, sensible heat, and momentum.

Re2: GCM inadequacies are partially corrected by the input observations. Example, the model dry bias in the moisture field is only partially corrected.

Re3: GCM inadequacies are not corrected by the input observations. Example, extratropical cloud forcing.

Re4: GCM representation is made worse by the input observations, suggesting a spurious feedback loop. Example, tropical cloud forcing and surface energy balance.

By and large, Re1 and Re2 are the most common responses to the insertion of currently available data. The responses Re3 and, especially, Re4 demand special scrutiny. An example of the Re4 situation is given in Figure 4.3. The figure shows the longwave cloud forcing from the Earth Radiation Budget Experiment (ERBE, Harrison et al. 1990), the validation data set, as the dashed line. The GEOS-1 GCM simulation is the solid line, and the GEOS-1 assimilation is dashed line. In the tropics the assimilation is further from the ERBE data than the simulation. The reason is that the model was designed to the represent the current climate in simulation mode. The model has a dry bias. When the data are inserted during the assimilation process, the atmosphere is moistened and the cloud forcing is increased. Interestingly, the total precipitation is improved in the assimilation as verified with the Legates-Wilmont (1990) data (there is significant controversy about verification data sets for precipitation). This inconsistency between the clouds and precipitation fields exemplifies the difficulties of data assimilation for climate applications. In order to address these problems,

the physics of the hydrological cycle must be more robustly modeled. Statistical models of isolated processes are inadequate. The use of new data types with new assimilation techniques will allow us to constrain the uncertainties in the hydrological cycle and will let us improve not only the quality and completeness of the assimilated data sets, but the integrity of the model.

4.3.2 GEOS-1 Data Assimilation System

The production of the data multi-year data set with the GEOS-1 DAS has established a credible baseline for GEOS system development. Aside from obtaining important logistical information as enumerated in Section4.1, the data sets have proven scientifically valuable. In fact, there have been some unique discovery results obtained from applications of the GEOS-1 data set. Furthermore, GEOS-1 has proven competitive with the re-analysis from NCEP, and intercomparisons of the two products have done much to help the efforts of both organizations. This section will briefly highlight some results from the GEOS-1 DAS. The examples will show the breadth of applications, the ability of the assimilated data to provide unique science capabilities, and the manner in which Earth-science applications contribute to validation and system design.

4.3.2.1 Regional Moisture Budgets

One of the important components of the moisture budget over continental regions is moisture transport associated with low level, planetary boundary layer, jets. These jets are located in the lowest part of the atmosphere and are often linked to topographical features. They have a strong diurnal component. In Figure 2.2 the low level jet over the United States is responsible for the strong summertime diurnal variation.

One of the strengths of the GEOS-1 GCM was the representation of the Great Plains Low Level Jet (GPLLJ). The model performance was discussed in Helfand and Schubert (1995). From an assimilation point of view, the observing network is not frequent enough to resolve the diurnal jet. Even when there is wind information in the boundary level observations, it is not enough to constrain the GPLLJ wind profile. Therefore, if the analysis is to provide information about the GPLLJ, then it has to be through the model's capabilities.

Figure 4.4 shows time series of moisture flux over the south-central United States for 1988 and 1993. These two years were record drought and flood years, respectively. The difference in the moisture flux is obvious, with the flood year having larger values. Thus the wind and moisture from the assimilation is capable, at least, of providing qualitative information on the regional moisture budget in these two extreme years.

Min and Schubert (1996) have completed a study of low level jets in three different regions: the Great Plains of the United States, Argentina east of the Andes, and the Indian monsoon. These regions are distinguished by having different dynamical regimes as well as different levels of data coverage by the observations. Min and Schubert also intercompare the GEOS-1 DAS with the NCEP re-analysis and operational analyses from ECMWF. One goal is to try to understand the quantitative attributes of the assimilated data products.

Min and Schubert conclude that the qualitative ability of the assimilated data sets in

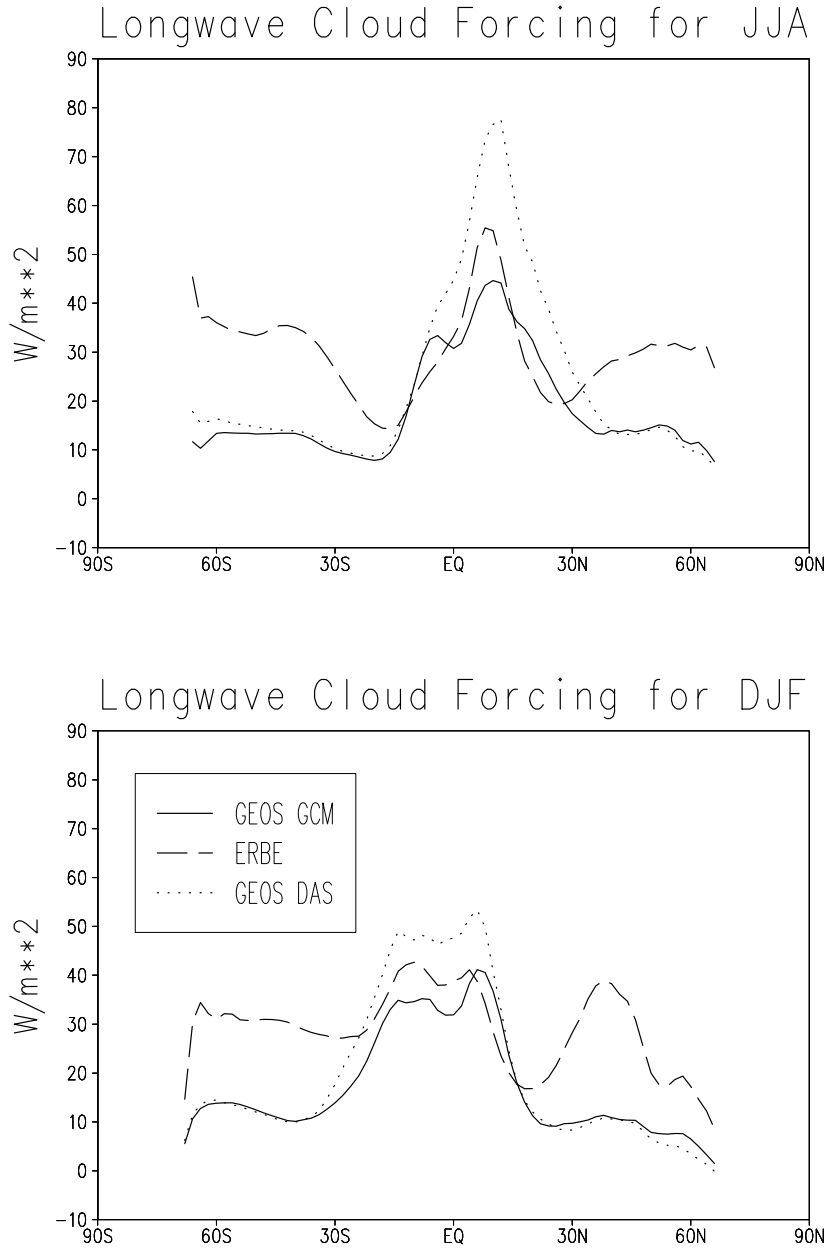

Figure 4.3: Longwave cloud forcing for northern hemisphere summer (JJA) and winter (DJF). The dashed line is the ERBE (Harrison et al. 1990) data which is used for verification. The solid line is the GEOS-1 GCM model simulation, and the dotted line is from the GEOS-1 data assimilation. This is an example of the assimilation of data degrading the performance of the model simulation. The insertion of water and temperature observations moistens the model dry bias in the tropics and increases the cloud forcing too much. In middle latitudes the inability of either the model or assimilation to represent middle latitude stratus is revealed by the weak cloud forcing.

capturing interannual anomalies is robust. However, there is significant uncertainty in the quantitative information. The uncertainties are traced back to the incompleteness of the observations, as well as model representations of topography and near-surface physics. In addition, they are able to identify an impact of quality control decisions on the input data stream to the end product. Finally, post-processing of the assimilated data sets also plays an important role in quantitative applications. This includes interpolation to pressure levels and grids different from the assimilating model.

4.3.2.2 East Asian Monsoon

The Asian monsoon and the interactions of the monsoon with the large-scale El Niño-Southern Oscillation circulation is an important feature of global climate dynamics. Direct observations of tropical dynamics and precipitation are inadequate for defining a complete specification of climate processes. One of the important challenges of assimilation is to provide information about tropical processes and their role in regional and global climate anomalies. Park and Schubert (1996) study the East Asian summer drought of 1994 with the GEOS-1 assimilated data set.

Park and Schubert show the onset of the drought is closely linked to an acceleration of the seasonal transition, where a normal August-like flow pattern occurs in July. This is related to large-scale dynamics, and the early formation of the Tibetan anticyclone. After recognizing this process in the 1994 case, Park and Schubert are able to define an index based on zonal wind over the Tibetan Plateau which correlates strongly with Korean precipitation. They are also able to clarify the relationships between western Pacific sea surface temperature and East Asian drought. The sea surface temperature is driven by the atmospheric circulation, and it is not the local sea surface temperature changes that are initiating the drought.

The high values of mosture flux are in red. The plot shows the significant difference between the US drought year, 1988, and the US flood year, 1993.

4.3.2.3 Atmospheric Chemistry and Transport

Some of the most successful applications of GEOS data sets have been to atmospheric chemistry and transport problems. Original efforts were focused on the stratosphere, and in particular ozone transport and chemistry. With the assimilation algorithms that immediately preceded GEOS-1 at GSFC, Rood et al. (1991) were able to use assimilated winds to calculate ozone transport accurately for time-scales of approximately two months. After this amount of time, errors in the background mean-meridional circulation altered the mean ozone gradients enough that ozone transport was no longer well represented. Using winds from a stratospheric configuration of GEOS-1, that uses the Incremental Analysis Update (see Chapter 5.0), Douglass et al. (1996) have been able to calculate ozone transports accurately for more than one year. The use of assimilated winds from stratospheric analyses either in off-line chemistry and transport models or in trajectory models, has tremendously increased the quantitative use of satellite constituent observations. Fundamentally, the winds from the assimilation are often good enough that dynamical variability can be extracted from the constituent observations and the chemical source and sink terms can be

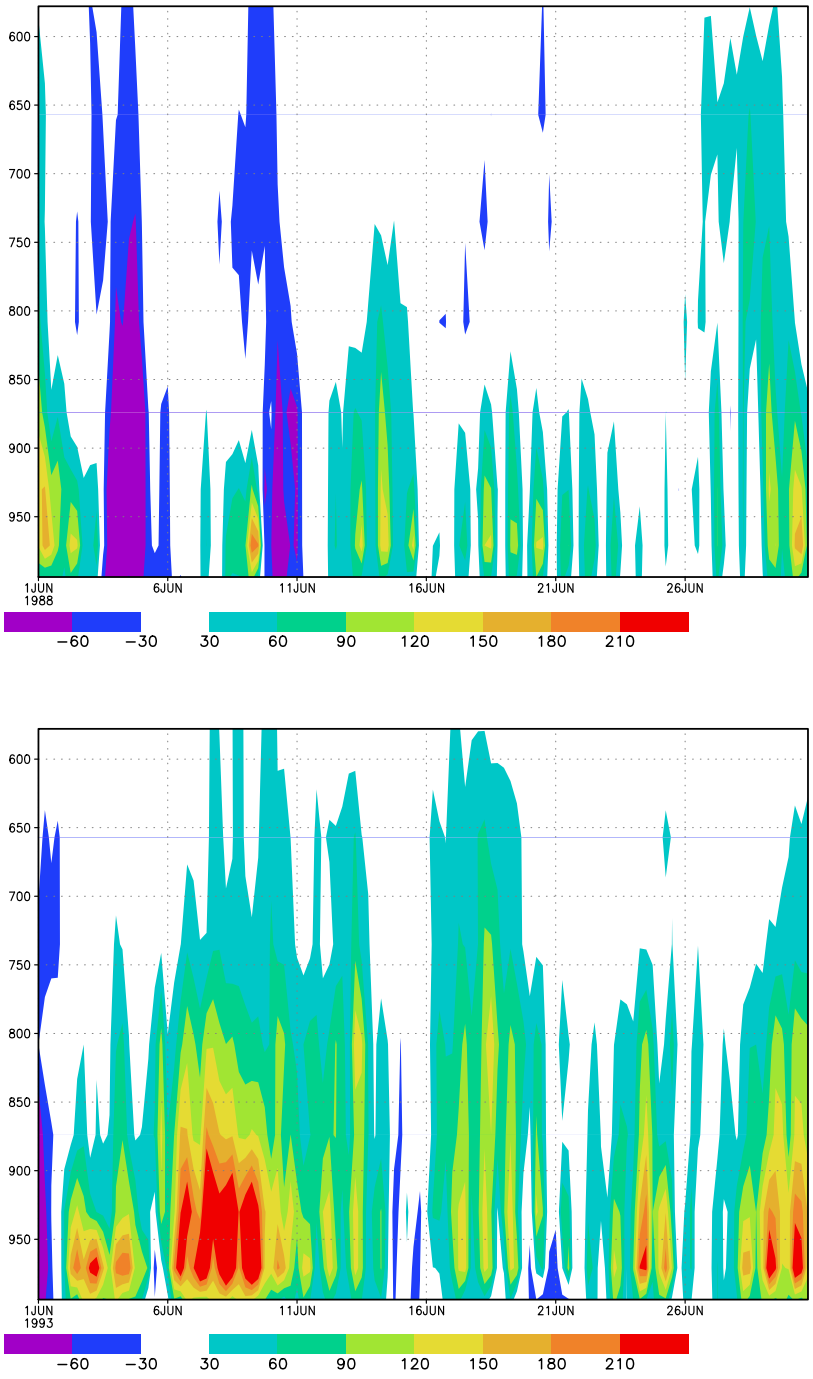

Figure 4.4: Height time series of moisture flux ppm m/sec in the lower troposphere at 32 N and 97.5 W (southern United States), pressure in hPa is plotted on the vertical axis: a) summer of 1988, and b) summer of 1993.

directly investigated.

More recently, Allen et al. (1996) have started to investigate tropospheric applications. A major problem in tropospheric chemistry is transport by cloud systems. Allen et al. have used the cloud mass flux and planetary boundary layer heights archived with GEOS-1 to study carbon monoxide transport. Figure 4.5 shows the surface carbon monoxide measurements and carbon monoxide calculated from an off-line chemistry and transport model driven by GEOS-1 winds and cloud mass fluxes. They show the ability to represent both the seasonal and daily variability with significant accuracy. Allen et al. were able to isolate, for the first time, interannual variability due to meteorological changes at North Atlantic carbon monoxide observing stations.

4.4 Lessons Learned from the GEOS-1 Re-analysis Project

In terms of its primary objectives the GEOS-1 re-analysis project has been a success. The data sets have proven scientifically useful, and they have attracted a variety of applications that have tested both particular aspects and the general fidelity of GEOS-1 product.

In terms of the requirements and expectations discussed in Section 2.6.2, GEOS-1 establishes that assimilated data sets can and will contribute directly to the scientific initiatives of MTPE and the mercurial MTPE strategic plan. GEOS-1 establishes that the base data assimilation system for the 1998 MTPE support can use observational information, and that in many cases it can complement and supplement that information. Useful estimates of unobserved quantities have been produced and used.

The broad primary goals of the GEOS-1 re-analysis project, to provide a comprehensive data set with meaningful interseasonal and interannual variability, has been verified in several applications. In some cases, such as those associated with clouds, the interannual signal is represented, despite biased representations of mean quantities. In other cases, such as in the study of tropospheric carbon monoxide, new capabilities to study interannual variability have been achieved. In some instances the science remains discovering and process oriented, and in other instances, increased quantitative capabilities are achieved.

In terms of developing generalized validation strategies, at the very least representative problems are being addressed which provide baseline performance criteria. Also, in many cases the different problems provide varying perspectives on shortcomings in the system. These perspectives provide insight into physically-based improvements of the model and estimation-theory based improvements of the analysis. In some instances, such as the case of the constituent transport studies, news ways to evaluate both meteorological parameters and the general circulation are being revealed.

The workshop in 1995 on the GEOS-1 re-analysis provided many reports on GEOS-1 performance (Schubert and Rood 1995, TM Volume 7). These reports identified strengths and weaknesses which are being prioritized and integrated in the GEOS-2 validation plan (see Chapter 8.0). If we look, in total, at the performance of the GEOS-1 system, the theoretical constructs of the GEOS-1, the reports of the DAO Science Advisory Panel, and the internal development decisions made since GEOS-1 was frozen, the following conclusions can be made.

1. The GEOS-1 data assimilation system can enhance the information content of the observations for certain problems. Instances where the model simulation of Earth-system parameters are degraded by the data insertion reveal instances where the system is far from optimal. There are unwanted and spurious artifacts in the assimilated data set which must be removed, or reduced, in future versions.

2. In some cases the design of the model to simulate climate parameters, such as outgoing longwave radiation, has not proven to benefit the assimilated data product. The data insertion process changes the background moisture and temperature fields, which propagates through the hydrological and cloud parameterizations. This reveals the fragility of tuned climate models, which are collections of explicit parameterizations and implicit assumptions designed to operate within a pre-derived range of parameter space. The GEOS-1 experience underscores the requirement to build physically-based

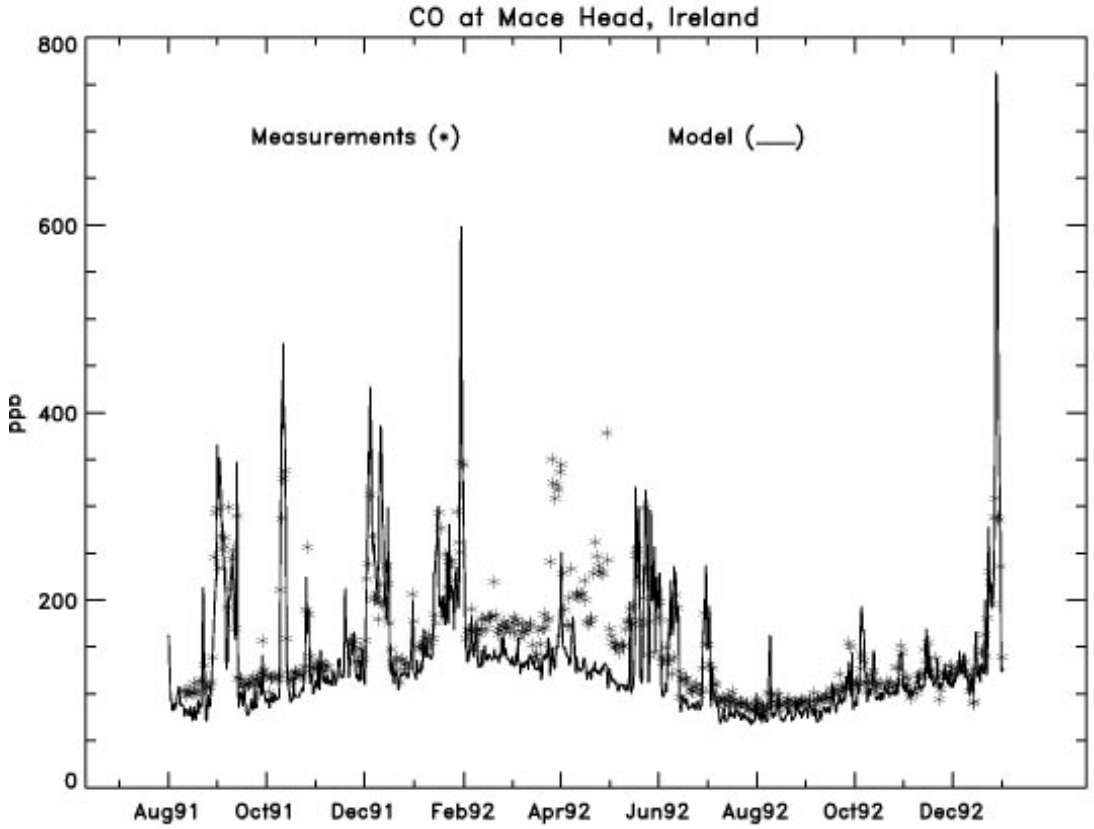

Figure 4.5: Carbon monoxide (CO) surface measurements compared with model calculations from an off-line chemistry transport model. Winds and cloud mass fluxes from GEOS-1 to transport CO given source distributions and chemical destruction. This time series for 1991-1992 shows that the winds and cloud mass fluxes capture synoptic variability and seasonal variability. The winds have been able to explain interannual variability in the northern hemisphere middle latitudes, (from Allen et al. 1996).

parameterizations with correctly defined feedback loops. It also emphasizes the need to define model parameters in the assimilation cycle, something the GEOS system is uniquely suited for because of the Incremental Analysis Update algorithm.

3. The objective analysis scheme in GEOS-1, especially with the partitioning into mini-volumes, is not very sensitive to statistical representations of model and observational errors. This is believed to be largely due to the mini-volume and data selection required for computational viability. For this reason, GEOS-1 performed reasonably well with crude statistics. However, to reduce the analysis artifacts in future systems, the objective analysis system needs to be exquisitely sensitive to statistics in order to use the information that describes model and observational error. This is especially true when considering the use of new data types from MTPE that do not have a heritage of assimilation applications.

4. The quality control decisions have a strong impact on final analysis quality, and impact different applications in different ways. Because future GEOS systems will diverge

from numerical weather prediction assimilation systems, reliance on NCEP quality control is short-sighted. This is especially true when new data types are considered.

5. Evaluation of long-term assimilated data sets with parallel model integrations is a powerful way to understand system performance. Preconceived ideas that the model and assimilation would be so closely intertwined as to defy definitive identification of problems are found to be untrue. In fact, Chen et al. (1996) find that a parallel integration with a different model often compares better with the GEOS-1 assimilation than does the GEOS-1 GCM. As a model validation technique, the comparison of parallel simulations and assimilations, help to bridge the gap between integrated and process oriented model diagnostics.

6. Model forecasts have been underutilized in the GEOS development strategy. Despite relatively low resolution, the current GEOS GCM can provide numerical weather forecasts that only trail the operational forecast skill scores for the northern hemisphere winter by approximately half a day at seven days. However, the GEOS model falls behind in the first 48 hours of the forecast. The lack of predictability on the shortest time scales implies that information propagation is not as good as it should be (Fourth Report of the DAO Science Advisory Panel).

7. The ability of the assimilated data to advance quantitative science might be more dependent on post-processing algorithms than previously thought. Interpolation routines and output strategies strongly impact the ability to calculate closed budgets of tracers, heat, momentum or energy from archived data sets. The impact of third party post-processing and subsetting tools must be evaluated.

8. There are many potential bottlenecks in the production stream. Some of the most difficult have been related to finding historical data and performing basic quality control on these data sets. In addition, the interaction of computers in a distributed production environment requires the development of new types of backup capabilities to assure operational production.

4.5 References

Allen, D. J., P. Kasibhatla, A. M. Thompson, R. B. Rood, B. G. Doddridge, K. E. Pickering, R. D. Hudson, and S.-J. Lin, 1996: Transport-induced interannual variability of carbon monoxide determined using a chemistry and transport model, to appear in J. Geophys. Res.

Arakawa, A. and S. D. Schubert, 1974: Interaction of a cumulus ensemble with the large-scale environment, Part I., J. Atmos. Sci., 31, 674-701.

Arakawa, A. and M. J. Suarez, 1983: Vertical differencing of the primitive equations in the sigma coordinates, Mon. Wea. Rev., 111, 34-45.

Baker, W. E., S. C. Bloom, J. S. Woollen, M. S. Nestler, E. Brin, T. W. Schlatter, and G. W. Branstator, 1987: Experiments with a three-dimensional statistical objective analysis scheme using FGGE data, Mon. Wea. Rev., 115, 273-296.

Bloom, S. C., L. L. Takacs, A. M. da Silva, and D. Ledvina, 1996: Data assimilation using incremental analysis updates, Mon. Wea. Rev., 124, 1256-1271.

Burridge, D. M., and J. Haseler, 1977: A model for medium range weather forecasting, Tech. Rep. No. 4, European Centre for Medium Range Weather Forecasts, Bracknell, Berks., U. K., 46 pp.

Chen M., R.B. Rood, and L. L. Takacs, 1996: Impact of a semi-lagrangian and an Eulerian dynamical core on climate simulations, submitted to J. Climate.

Chou, M. D., 1984: Broadband water vapor transmission functions for atmospheric IR flux computations, J. Atmos. Sci., 41, 1775-1778.

Chou, M. D., and L. Peng, 1983: A parameterization of the absorption in the spectral region with application to climate sensitivity studies, J. Atmos. Sci., 40, 2183-2192.

Clarke, R. H., 1970: Observational studies in the atmospheric boundary layer, Q. J. Roy. Meteor. Soc., 96, 91-114.

Coy, L., R. Rood, and P. Newman, 1994: A comparison of winds from the STRATAN data assimilation system to balanced wind estimates, J. Atmos. Sci., 51, 2309-2315.

Davies, R., 1982: Documentation of the solar radiation parameterization in the GLAS climate model, NASA Tech. Memo 83961, 57 pp.

Douglass, A. R., C. J. Weaver, R. B. Rood, and L. Coy, 1996: A three-dimensional simulation of the ozone annual cycle using winds from a data assimilation system, J. Geophys. Res., 101, 1463-1474.

Gaffen, D. J., R. D. Rosen, D. A. Salstein, and J. S. Boyle, 1996: Evaluation of tropospheric water vapor simulations from the Atmospheric Model Intercomparison Project, submitted J. Climate.

Gates, W. L., 1992: AMIP: The atmospheric model intercomparison project, Bull. Amer. Meteor. Soc., 73, 1962-1970.

Harrison, E. F., P. Minnis, B. R. Barkstrom, V. Ramanathan, R. D. Cess, and G. G. Gibson, 1990: Seasonal variation of cloud radiative forcing derived from the Earth Radiation Budget Experiment, J. Geophys. Res., 95, 18687-18703.

Harshvardhan, R. Davies, D. A. Randall, and T. G. Coresetti, 1987: A fast radiation parameterization for atmospheric general circulation models, J. Geophys. Res., 92, 1009- 1016.

Helfand, H. M., and J. C. Labraga, 1988: Design of a non-singular level 2.5 second-order closure model for the prediction of atmospheric turbulence, J. Atmos. Sci., 45, 113-132.

Helfand, H. M., M. Fox-Rabinovitz, L. Takacs, and A, Molod, 1991: Simulation of the planetary boundary layer and turbulence in the GLA GCM, Proc. AMS Ninth Conf. on Numerical Weather Prediction, Denver, CO.

Helfand, H. M., and S. D. Schubert, 1995: Climatology of the simulated Great Plains low-level jet and its contribution to the continental moisture budget of the United States, J. Climate, 784-806.

Joseph, J. H., W. J. Wiscombe, and J. E. Weinman, 1976: The delta-Eddington approximation for radiative flux transfer, J. Atmos. Sci., 33, 2452-2459.

King, M. D., and Harshvardhan, 1986: Comparative accuracy of selected multiple scattering approximations, J. Atmos. Sci., 43, 784-801.

Lacis, A. A., and J. E. Hansen, 1974: A parameterization for the absorption of solar radiation in the Earth's atmosphere, J. Atmos. Sci., 31, 118-133.

Lau, K.-M., J. H. Kim, and Y. Sud, 1996: Intercomparison of hydrologic processes in AMIP GCMs, Bull. Amer. Meteor. Soc., 77, 2209-2227.

Legates, D. R., and C. J. Wilmott, 1990: Mean seasonal and spatial variability in gage-corrected global precipitation, Int. J. Climate, 10, 111-127.

Min, W., and S. D. Schubert, 1996: The climate signal in regional moisture fluxes: a comparison of three global data assimilation products, submitted J. Climate.

Molod, A., H. M. Helfand, L. L. Takacs, 1996: The climatology of parameterized physical processes in the GEOS-1 GCM and their impact on the GEOS-1 Data Assimilation System, J. Climate, 9, 764-785.

Panofsky, H. A., 1973: Tower micrometeorology. In Workshop on Micrometeorology, D. A. Haugen (ed.), American Meteorological Society, Boston, 392 pp.

Park, C.-K, and S. D. Schubert, 1996: On the nature of the 1994 East Asian summer drought, to appear J. Climate.

Pfaendtner, J., S. Bloom, D. Lamich, M. Seablom, M. Sienkiewicz, J. Stobie, A. da Silva, 1995: Documentation of the Goddard Earth Observing System (GEOS) Data Assimilation System-Version 1, NASA Tech. Memo. No. 104606, Vol. 4, Goddard Space Flight Center, Greenbelt, MD 20771.

Rodgers, C. D., 1968: Some extensions and applications of the new random model for molecular band transmission, Q. J. Roy. Meteor. Soc., 94, 99-102.

Rood, R. B., A. R. Douglass, J. A. Kaye, M. A. Geller, Y. Chi, D. J. Allen, E. M. Larson, E. R. Nash, and J. E. Nielsen, 1991: Three-dimensional simulations of wintertime ozone variability in the lower stratosphere, J. Geophys. Res., 96, 5055-5071.

Rosenfield, J. E., M. R. Schoeberl, and M. A. Geller, 1987: A computation of the stratospheric diabatic circulation using an accurate radiative transfer model, J. Atmos. Sci., 44, 859-876.

Rossow, W. L, and R. A. Schiffer, 1991: ISCCP cloud data products, Bull. Amer. Meteor. Soc., 72, 2-21.

Sadourney, R., 1975: The dynamics of finite difference models of the shallow water equations, J. Atmos. Sci., 32, 680-689.

Schubert, S., C.-K. Park, Chung-Yu Wu, W. Higgins, Y. Kondratyeva, A. Molod, L. Takacs, M. Seablom, and R. Rood, 1995: A Multiyear Assimilation with the GEOS-1 System: Overview and Results, NASA Tech. Memo. 104606, Vol. 6, Goddard Space Flight Center, Greenbelt, MD 20771.

Schubert, S. D. and R. Rood, 1995: Proceedings of the Workshop on the GEOS-1 Five-Year Assimilation, NASA Tech. Memo. 104606, Vol. 7, Goddard Space Flight Center, Greenbelt, MD 20771.

Seablom, M. S., J. W. Pfaendtner, and P. E. Piraino, 1991: Quality control techniques for the interactive GLA retrieval/assimilation system, preprint volume, Ninth Conf. on Numerical Weather Prediction, Amer. Meteor. Soc., 28-29.

Sud, Y., and A. Molod, 1988: The roles of dry convection, cloud-radiation feedback processes and the influences of recent improvements in the parameterization of convection in the GLA AGCM, Mon. Wea. Rev., 116, 2366-2387.

Takacs, L., A. Molod and T. Wang, 1994: Documentation of the Goddard Earth Observing System (GEOS) General Circulation Model -Version 1, NASA Tech. Memo. 104606, Vol. 1.

Weare, B. C., I. I. Mokhov, and Project Members, 1995: Evaluation of total cloudiness and its variability in the Atmospheric Model Intercomparison Project, J. Climate, 8, 2224- 2238.

4.6 Acronyms

4.6.1 General acronyms

DAO	Data Assimilation Office
GEOS	Goddard Earth Observing System (The name of the DAO data assimilation system)
GCM	General Circulation Model
DAS	Data Assimilation System
QC	Quality Control
NWP	Numerical Weather Prediction
CARD	Consistent Assimilation of Retrieved Data
PSAS	Physical-space Statistical Analysis System
NASA	National Aeronautics and Space Administration
GSFC	Goddard Space Flight Center
MTPE	Mission to Planet Earth
EOS	Earth Observing System
EOSDIS	Earth Observing System Data and Information System
NOAA	National Oceanic and Atmospheric Administration
NCEP	National Centers for Environmental Prediction (formerly, NMC)
NMC	National Meteorological Center
NESDIS	National Environmental Satellite Data and Information Service
ECMWF	European Center for Medium-range Weather Forecasts
UKMO	United Kingdom Meteorological Office

4.6.2 Instruments

ADEOS	Advanced Earth Observting Satellite (Mid-late 1996)
AIRS	Atmospheric Infrared Sounder (EOS PM)
AMSU A-B	Advanced Microwave Sounding Unit (POES, EOS PM)
AVHRR	Advanced Very High-Resolution Radiometer
ASTER	Advanced Spaceborne Thermal Emission and Reflection Radiometer (EOS AM)
ATOVS	Advanced TOVS; HIRS3/AMSU (POES)
CERES	Clouds and Earth's Radiation Energy System (TRMM, EOS AM)
CLAES	Cryogenic Limb Array Etalon Spectrometer (UARS)
DMSP	Defense Meteorological Satellite Program (currently operational)
EOS AM1	Earth Observting Satellite AM (June 98 launch)
EPS	EUMETSAT (European Meteorology Satellite) Polar System
ERBE	Earth Radiation Budget Experiment (ERBS)
ERBS	Earth Radiation Budget Satellite
ERS-1,2	European Remote Sensing Satellite (Scatterometer, 6 channel, IR-Visible radiometer)

GOES	Geostationary Observational Environmental Satellite (Imager and 18 channel visible and infrared sounder, currently operational)
GOME	Global Ozone Monitoring Experiment (ERS-2)
GPS	Global Positioning System
HALOE	Halogen Occultation Experiment (UARS)
HIRS2/3	High-Resolution InfraRed Sounder (POES)
HRDI	High Resolution Doppler Imager
IASI	Infrared Atmospheric Sounding Interferometer (EPS)
ILAS	Improved Limb Atmospheric Spectrometer (ADEOS)
IMG	Interferometric Monitor for Greenhouse Gases (ADEOS)
ISCCP	International Satellite Cloud Climatology Project (several IR and visible instruments aboard different satellite)
LIMS	Limb Infrared Monitor of the Stratosphere (Nimbus 7)
MAPS	Measurement of Atmospheric Pollution from Satellites
MHS	Microwave Humidity Sounder (EOS-PM)
MLS	Microwave Limb Sounder (UARS)
MODIS	Moderate-Resolution Imaging Spectrometer (EOS AM)
MSU	Microwave Sounding Unit
MOPITT	Measurement of Pollution in the Troposphere (EOS AM)
NSCAT	NASA Scatterometer (ADEOS)
POES	Polar Orbiting Environmental Satellite (Currently Operational)
PR	Precipitation Radar (TRMM)
SBUV	Satellite Backscatter Ultraviolet radiometer (Nimbus 7, POES)
SAGE	Stratospheric Aerosol and Gas Experiment (ERBS)
SMMR	Scanning Multispectral Microwave Radiometer (?)
SSM/I	Special Sensor Microwave/Imager (DMSP)
SSM/T	Special Sensor Microwave (Temperature sounder, DMSP)
SSM/T2	Special Sensor Microwave (Water vapor sounder) (DMSP)
SSU	Stratospheric Sounding Unit (POES)
TMI	TRMM Microwave Imager (TRMM)
TOMS	Total Ozone Mapping Spectrometer (ADEOS, Meteor, Earth Probe, Nimbus 7)
TOVS	TIROS Operational Vertical Sounder; HIRS2/MSU/SSU (POES)
TRMM	Tropical Rainfall Measuring Mission (summer '97 launch)
UARS	Upper Atmospheric Research Satellite (some instruments in operation)
WINDII	Wind Imaging Interferometer (UARS)

Chapter 5

The Goddard Earth Observing System – Version 2 Data Assimilation System (GEOS-2 DAS)

Contents

5.1 Overview of the Data Assimilation Algorithm

This Chapter and the following two chapters on Quality Control and New Data Types describe the core capabilities of the GEOS-2 Data Assimilation System (DAS). The basic components of the GEOS DAS were described in section 2.2 and a schematic of the system was given in Figure 2.1. The major components of the system were identified as the statistical objective analysis, the model, and the quality control algorithm. In addition it was noted that there are major tasks to develop forecast and observational error statistics for the objective analysis and to develop boundary conditions for the model. In this chapter the objective analysis and the model are discussed, along with the efforts to develop improved statistics and boundary conditions.

The GEOS-2 Physical-space Statistical Analysis System (PSAS) is an entirely new algorithm. It is a state-of-the-art system, with the versatility and capability to accommodate future developments in data assimilation methodology in a manner consistent with estimation theory. The DAO Advisory Panel identified the successful development and implementation of PSAS as crucial to the success of the GEOS system. The DAO Plan (1994-2000) identified the ambitious development of PSAS as one of four high-risk activities. This chapter will show that many major hurdles in developing PSAS have been overcome. The current GEOS-2 validation exercises are demonstrating the successful implementation of PSAS.

The GEOS-2 General Circulation Model (GCM) is an incremental development over GEOS-1. The model description includes several developments that are aimed at addressing specific problems discovered in GEOS-1. In addition, the model has been prepared for broader future capabilities to meet the science requirements and scope outlined in Chapter 2.

Both the analysis and the model have been designed to accommodate new data types. This includes the ability to implement arbitrary observation operators in the analysis and to generalize the specification of error statistics. The model design incorporates more physically-based parameterizations, including the introduction of new variables that improve the link to the expanded observation suite. A major model development to follow GEOS-2 is the inclusion of an interactive land-surface model. Many aspects of GEOS-2 provide the foundation for the integration of the land-surface model. The incorporation of new data types is discussed extensively in Chapter 7. Development beyond GEOS-2 is discussed in Chapter 9.

The development detailed here follows from the GEOS-1 project in many ways. The lessons learned from GEOS-1 (see Chapter 4) are either explicitly or implicitly addressed in the GEOS-2 development. In some ways the development is aimed at meeting a baseline credibility requirement for the GEOS DAS. More broadly, the development builds the infrastructure to anticipate future requirements as Earth science and the data assimilation mission evolve. Developments that are directed at solving explicit shortcomings identified in the GEOS-1 data sets and their applications are aimed as much as possible at improving the underlying physics of the model or the statistical basis of the analysis system. Fixes targeting specific problems are avoided as much as possible.

5.2 The Physical-space Statistical Analysis System (PSAS)

5.2.1 Design objectives

At the time the DAO was formed, in February 1992, plans were initiated to develop a new statistical analysis system called the Physical-space Statistical Analysis System (PSAS). PSAS was designed to meet the following five requirements.

1. To establish and remove the effects of data selection in the GEOS-1 optimal interpolation (OI) system. This objective requires PSAS to be capable of using forecast and observation error covariance models identical to those specified in the OI system, but to solve the analysis equations globally rather than locally.

2. To obtain proper sensitivity to all data and to all error covariance specifications. In Baker *et al.* (1987), for instance, it was shown that introducing geographically-dependent forecast error covariances had little impact on OI analyses. It is likely that global solution of the analysis equations demanded by objective (1) would reveal much more robust responsiveness, forcing one to pay careful attention to error covariance formulations. Recent experiments with the PSAS system (not described here) have in fact demonstrated strong sensitivity to these formulations and will be described in future publications.

3. To permit assimilation of new data types that are not state variables. A great wealth of data, mostly from space-borne remote-sensing devices, will become available in coming years. Data selection would become an increasingly onerous and *ad hoc* procedure for these data. More importantly, many of these data, especially if assimilated in raw form (e.g., radiances or backscatter) rather than as retrieved products, are neither state variables nor linearly related to state variables. While some types of data that are not state variables, such as total precipitable water, have been successfully assimilated with the OI methodology (Ledvina and Pfaendtner 1995), global formulation of the analysis problem, in which observation operators are defined explicitly, provides a natural framework for assimilating these data types (e.g., Eyre *et al.* 1993, Derber and Wu 1996, Joiner and da Silva 1996). The version of PSAS described in this Chapter incorporates linear (*i.e.*, state-independent) observation operators only. A version of the PSAS algorithm for nonlinear observation operators is described in Chapter 9 (see also Cohn 1996, section 5).

4. To allow maximum flexibility in forecast and observation error covariance modeling. While much effort has been directed toward covariance modeling in recent years, it is likely that additional efforts will result in improved analyses. For instance, while global spectral analysis systems rely explicitly on an assumption that forecast errors are horizontally isotropic, it is well-known (*e.g.*, Courtier *et al.* 1994, Thépaut *et al.* 1996, Cohn and Todling 1996 and references therein) that these errors are in fact highly anisotropic. Although the first implementation of GEOS-2 does not take advantage of this capability, much of the GEOS-3 development is focused on improved error statistics. The development of anisotropic correlation modeling in PSAS is discussed in Chapter 9.

5. To enable flexibility for future developments in data assimilation methodology. The PSAS system was envisioned from the outset to provide a computational framework for the development of techniques for fixed-lag Kalman smoothing (Todling *et al.* 1996, Cohn *et al.* 1994), approximate Kalman filtering (*e.g.*, Cohn and Todling 1996), forecast bias estimation (Dee and da Silva 1996), and other topics known from the estimation theory literature but not yet implemented in operational data assimilation systems (see Chapter 9). Solution of the innovation covariance equation, a key component of the PSAS system described below, is a need common to all of these techniques.

Because of these design features PSAS has the following attributes:

a. PSAS solves the analysis equations globally rather than locally. The local approximation and data selection of OI schemes is eliminated. In this respect, PSAS is similar to the global *variational* spectral analysis systems that have recently replaced OI schemes at NCEP (Parrish and Derber 1992) and at ECMWF (Heckley *et al.* 1993, Courtier *et al.* 1993).

b. PSAS works directly in physical space, like OI schemes but unlike spectral analysis schemes.

c. PSAS performs a large part of its calculations in observation space, also unlike operational spectral analysis schemes, which operate in state space. This results in computational savings, since the dimension of the observation space is currently an order of magnitude smaller than that of the forecast model state. The computational efficiency of spectral analysis schemes arises from an assumption that horizontal forecast error covariances or correlations are isotropic, *i.e.*, diagonal in spectral space, an assumption which is not made in the PSAS algorithm.

d. PSAS is fundamentally independent of the model formulation, and hence, is a portable algorithm suitable for many applications. While compatible with the grid-point system of the GEOS GCM, nothing in the design restricts PSAS applications to this grid. In particular PSAS is suitable for regional assimilation and problems on irregular grids.

5.2.2 Background: the statistical analysis equations

A statistical analysis scheme attempts to obtain an *optimal* estimate, or analysis, of the state of the system by combining observations with a forecast model first guess. Let $w^f \in I\!R^n$ denote the vector representing the forecast first guess, defined on a grid in our case, and let $w^t \in I\!R^n$ denote the true state approximated by w^f,

$$w^f = w^t + \epsilon^f, \tag{5.1}$$

where $\epsilon^f \in I\!R^n$ denotes the forecast error. Let $w^o \in I\!R^p$ denote the vector of p observations available at the analysis time, assumed to be related linearly to the state variables,

$$w^o = H\, w^t + \epsilon^o. \tag{5.2}$$

Here $H \in I\!R^p \times I\!R^n$ is the observation operator, or generalized interpolation operator; $\epsilon^o \in I\!R^p$ denotes the observation error, which is the sum of the measurement error and the error of representativeness (*e.g.*, Cohn 1996). Currently the number of model degrees of freedom is $n \sim 10^6$ and the current observing system has $p \sim 10^5$.

The probabilistic assumptions common to most operational analysis systems are that ϵ^f and ϵ^o are Gaussian-distributed with zero mean, and are not correlated with either the state or with each other. While these assumptions can be relaxed in a variety of ways (*cf.* Cohn 1996 and references therein), the current implementation of PSAS invokes all of them. Efforts directed toward relaxing the assumption that ϵ^f has zero mean $\left(\left\langle \epsilon^f \right\rangle = 0\right)$, that is, that the forecast is unbiased, are described in section 5.2.6 and in Chapter 9.

The two most common optimality criteria, arising from minimum variance estimation and maximum likelihood estimation, lead to identical analysis equations under these assumptions (*e.g.*, Lorenc 1986, Cohn 1996). These equations also yield the *best linear unbiased estimate* (BLUE), or analysis, without an assumption that the errors ϵ^f and ϵ^o are Gaussian-distributed.

The *minimum variance* analysis $w^a \in I\!R^n$ is obtained by requiring $\left\langle \left(w^a - w^t\right)^T S \left(w^a - w^t\right) \right\rangle$ to be minimum for all positive definite matrices $S \in I\!R^n \times I\!R^n$, and under the stated assumptions is given by the *analysis equations*

$$w^a = w^f + K\left(w^o - H w^f\right) \tag{5.3}$$

$$K = P^f H^T \left(H P^f H^T + R\right)^{-1}. \tag{5.4}$$

Here the matrix K is the *gain matrix*, which ascribes appropriate weights to the observations. The gain matrix depends on the *forecast error covariance matrix*

$$P^f \equiv \left\langle \left(\epsilon^f - \left\langle \epsilon^f \right\rangle\right) \left(\epsilon^f - \left\langle \epsilon^f \right\rangle\right)^T \right\rangle \in I\!R^n \times I\!R^n \tag{5.5}$$

and on the *observation error covariance matrix*

$$R \equiv \left\langle \left(\epsilon^o - \left\langle \epsilon^o \right\rangle\right) \left(\epsilon^o - \left\langle \epsilon^o \right\rangle\right)^T \right\rangle \in I\!R^p \times I\!R^p. \tag{5.6}$$

Both are symmetric and positive semi-definite by definition; R is in fact positive definite under an assumption that no linear combination of the observations is perfect. While these matrices are *defined* as above, in practice they must be *modeled*. The modeling strategy of PSAS for GEOS-2 is detailed in section 5.2.7.

5.2.3 The global PSAS solver

The PSAS algorithm solves the analysis equations in a straightforward manner. First, one $p \times p$ linear system is solved for the quantity y,

$$\left(H P^f H^T + R\right) y = w^o - H w^f, \tag{5.7}$$

and then the analyzed state w^a is obtained from the equation

$$w^a = w^f + P^f H^T y. \tag{5.8}$$

Equations (5.7) and (5.8) will be referred to as the *PSAS equations*. The *innovation covariance matrix*

$$M \equiv H P^f H^T + R \tag{5.9}$$

is symmetric positive definite, making a standard pre-conditioned conjugate gradient (CG) algorithm (Golub and van Loan 1989) the method of choice for solving the large linear system (5.7). For the current observing system, setting up and solving the linear system (5.7) costs about half the computational effort of PSAS, and involves computation in observation space: $M \in I\!R^p \times I\!R^p$ and $y \in I\!R^p$. The other half of the computational expense is taken by step (5.8) which transfers the solution y to the state space: $P^f H^T y \in I\!R^n$.

The GEOS-2 version of PSAS analyzes global sea level pressure and near surface winds over the oceans, as well as geopotential height, vector wind, and water vapor mixing ratio on constant pressure surfaces. The upper air height/wind analyses and the sea level pressure/surface wind analyses are multivariate using the wind-mass error covariance models described in subsection 5.2.7. The moisture analysis is done with a univariate statistical algorithm, and only at levels from 1000 hPa to 300 hPa. The basic GEOS-2 DAS configuration consists of a 2° latitude by 2.5° longitude, and 18 vertical levels (0.4, 1, 5, 7, 10, 30, 50, 70, 100, 150, 200, 250, 300, 400, 500, 700, 850, 1000 hPa). Details of the model/analysis interface are given in subsection 5.4.3.

For typical models of P^f and R the innovation covariance matrix M is not sparse, although entries associated with remote pairs of observation locations are negligibly small. To introduce some sparseness in M and thereby to save computational effort, the sphere is divided into N regions, and matrix blocks associated with regions separated by more than 6,000 km are assumed to be zero; these blocks never enter the CG computations. The same procedure is applied to the matrix P^f itself in (5.8). While this procedure could in principle destroy the positive-definiteness of M, causing lack of convergence of the CG solver, this has not been observed in the experiments reported in section 5.2.5 using the covariance models P^f and R of the GEOS-1 OI system. A rigorous approach based on space-limited covariance models (Gaspari and Cohn 1996), which are exactly zero beyond a specified distance, is used in GEOS-2, as described in section 5.2.7.

A good pre-conditioner for the CG algorithm must have two important characteristics: 1) it must be inexpensive to compute, and 2) it must retain the essentials of the original problem if it is to effectively improve the convergence rate of the algorithm. For the statistical interpolation problem that PSAS implements, a natural candidate for pre-conditioner is an OI-like approximation, in which the problem is solved separately for each of the N regions used to partition the data. For the Cray C-90 implementation the globe is divided into 80 equal-area regions using an *icosahedral* grid (Pfaendtner 1996) [1]. With $p \sim 100{,}000$ observations and $N \sim 80$ regions, each of these regional problems have on average more

[1] In the massively parallel implementation of PSAS being developed at JPL the globe is divided in 256 or 512 geographically irregular regions, each having approximately the same number of observations. This strategy is necessary to achieve load balance (Ding and Ferraro 1996).

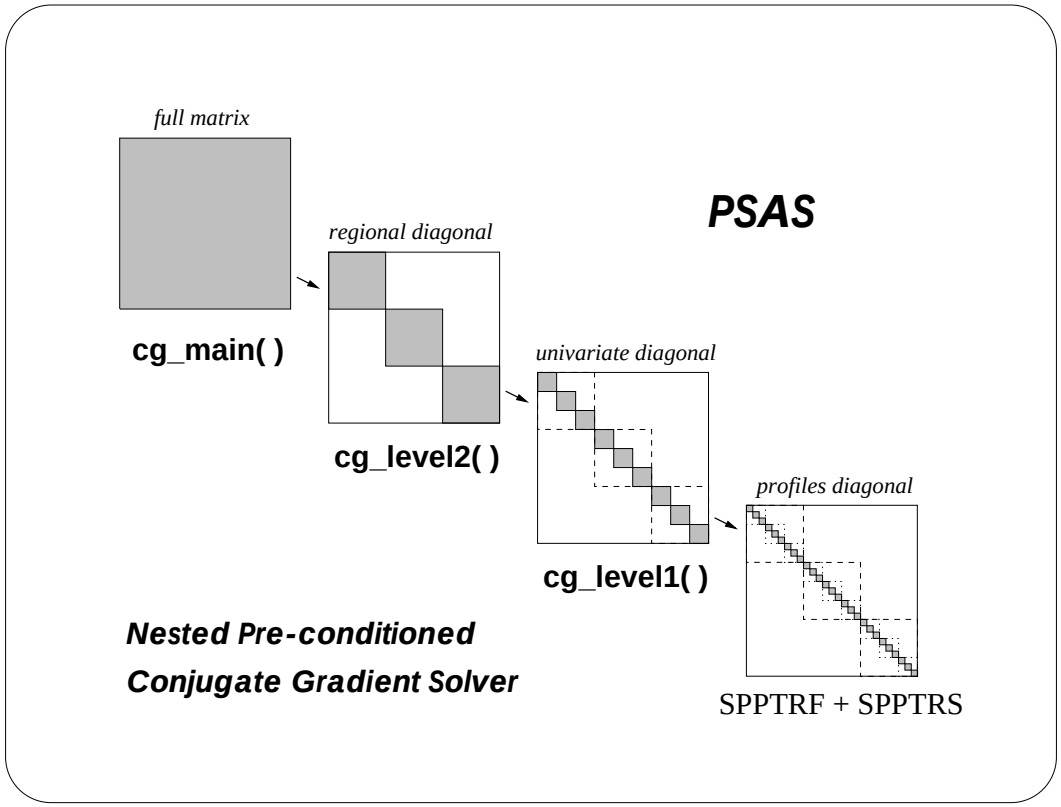

Figure 5.1: PSAS nested pre-conditioned conjugate gradient solver. Routine `cg_main()` contains the main conjugate gradient driver. This routine is pre-conditioned by `cg_level2()`, which solves a similar problem for each region. This routine is in turn pre-conditioned by `cg_level1()` which solves the linear system univariately. See text for details.

than 1,000 observations, too many for an efficient pre-conditioner. These regional problems are therefore solved by another pre-conditioned conjugate gradient algorithm; we refer to this solver as the *CG level 2*. As a pre-conditioner for *CG level 2* the same problem is solved univariately for each data type, *i.e.*, observations of u-wind, v-wind, geopotential height, etc., are treated in isolation. However, these univariate problems are still too large to be efficiently solved by direct methods and yet another iterative solver is used; this is the *CG level 1* algorithm. As a pre-conditioner for CG level 1 we make use of LAPACK (Anderson *et al.* 1992) to perform a direct Cholesky factorization of diagonal blocks of the *level 1* correlation sub-matrix. These diagonal blocks are typically of size 32, and are carefully chosen to include full vertical profiles, a desirable feature for the implementation of new data types. These nested pre-conditioned conjugate gradient solvers are illustrated in Figure 5.1. Additional details about the pre-conditioner can be found in da Silva and Guo (1996).

In the current serial implementation of PSAS, the matrix M is first normalized by its main diagonal, the normalized matrix is provided to the global CG solver as an operator, and the matrix elements are recomputed each CG iteration. In the parallel implementation of PSAS being developed at the Jet Propulsion Laboratory (Ding and Ferraro 1996), blocks of the matrix M are pre-computed and stored in memory. As a convergence criterion for the CG solver we specify that the residual must be reduced by 1 or 2 orders of magni-

tude. Experiments with reduction of the residual beyond 2 orders of magnitude produced differences much smaller than expected analysis errors. This is mainly due to the filtering properties of the operator $P^f H^T$ in (5.8), which attenuates the small-scale details in the linear system variable y.

5.2.4 Differences between PSAS, OI and spectral variational schemes

In this subsection we discuss the main distinctions between the PSAS approach to solving the analysis equations (5.3), (5.4), the approach of OI schemes, and the approach of spectral variational schemes.

Optimal interpolation schemes solve equations (5.3)–(5.4) approximately, as follows. Denote by k_j the j^{th} column of the transposed gain matrix K^T defined by (5.4), so that $k_j \in I\!R^p$. Then (5.4) can be written as

$$\left(H P^f H^T + R\right) k_j = (H P^f)_j \tag{5.10}$$

for $j = 1, \ldots, n$, where $(H P^f)_j \in I\!R^p$ denotes the j^{th} column of the matrix $H P^f$. This equation represents n linear systems, each of the same form as the PSAS equation (5.7). Similarly, equation (5.3) can be written as n scalar equations,

$$w^a_j = w^f_j + (k_j)^T \left(w^o - H w^f\right) \tag{5.11}$$

for $j = 1, \ldots, n$, where w^a_j and w^f_j denote the j^{th} elements of w^a and w^f, respectively. This equation makes it clear that the weight vector k_j solved for in (5.10) determines the correction, or analysis increment, at the j^{th} grid point.

Equations (5.10) and (5.11) would yield the same analysis w^a as the PSAS equations (5.7) and (5.8), but at far greater computational expense since there are n linear systems to be solved in (5.10) but only one in (5.7). Optimal interpolation schemes do in fact solve (5.10) and (5.11), but with a *local approximation* and hence the need for *data selection*. These schemes differ widely in the details of the local approximation and the data selection algorithm (*cf.* McPherson *et al.* 1979; Lorenc 1981; Baker *et al.* 1987; Pfaendtner *et al.* 1995), but all can be described in a generic way as follows.

Instead of involving all p observations in the solution of each of the j equations (5.10) and (5.11), some much smaller number q of observations nearby the j^{th} grid location is selected for the analysis at that location, and a different subset of observations, $q = q(j)$, is selected for different locations j. [In the GEOS-1 OI system, $q = 75$ and a fixed subset of observations is selected for a given mini-volume.] Thus w^o, H, and R become lower-dimensional and are made to depend on the grid-point index j: $w^o = w^o_j \in I\!R^q$, $H = H_j \in I\!R^q \times I\!R^n$, and $R = R_j \in I\!R^q \times I\!R^q$. [This is a slight abuse of notation; for these quantities the subscript j simply denotes dependence on the grid-point index, while otherwise it denotes a column of a matrix or an element of a vector.] Thus in OI schemes the analysis equations (5.10) and (5.11) can be written as

$$\left(H_j P^f H_j^T + R_j\right) k_j = \left(H_j P^f\right)_j \tag{5.12}$$

and

$$w_j^a = w_j^f + (k_j)^T \left(w_j^o - H_j w^f \right) \tag{5.13}$$

for $j = 1, \ldots, n$, where now $k_j \in I\!R^q$. While there are still n systems to solve in (5.12), each is now only $q \times q$ (this is the local approximation), and q is small enough that a direct method such as the standard Cholesky algorithm can be used to solve them. In addition, the matrix $M_j = H_j P^f H_j^T + R_j$ in (5.12) itself is fixed for a given volume, so that the Cholesky decomposition can be re-used for each grid point j in a given volume, reducing computational effort.

An important distinction between OI schemes and the PSAS scheme is that the weights k_j themselves are solved for in (5.12), albeit approximately, rather than the vector y in (5.7). This gives OI schemes the ability to calculate approximately the *analysis error variances* in the following simple fashion. Under the same probabilistic assumptions noted above equation (5.3), the *analysis error covariance matrix*

$$P^a \equiv \left\langle \left(\epsilon^a - \langle \epsilon^a \rangle\right) \left(\epsilon^a - \langle \epsilon^a \rangle\right)^T \right\rangle \in I\!R^n \times I\!R^n, \tag{5.14}$$

where

$$\epsilon^a = w^a - w^t \tag{5.15}$$

is the analysis error, is given by

$$P^a = P^f - KHP^f, \tag{5.16}$$

whose $(i,j)^{th}$ element is

$$P_{ij}^a = P_{ij}^f - (k_i)^T \left(HP^f \right)_j . \tag{5.17}$$

The diagonal elements P_{jj}^a, or analysis error variances, are then

$$P_{jj}^a = P_{jj}^f - (k_j)^T \left(HP^f \right)_j , \tag{5.18}$$

which under the local approximation becomes

$$P_{jj}^a = P_{jj}^f - (k_j)^T \left(H_j P^f \right)_j . \tag{5.19}$$

The ingredients for this simple computation are available from equation (5.12). A similar computation could be carried out at small additional cost in the PSAS algorithm at CG level 2, but has not been implemented at present. This would have the desirable effect of *overestimating* the analysis error variances, since not all of the data would enter the computation (*cf.* Jazwinski 1970, Sec. 7.8). The GEOS-1 OI system uses equation (5.19) to calculate approximate analysis error variances, after which a simple empirical error growth

model is applied to obtain forecast error variances for the subsequent analysis time, as described in Pfaendtner *et al.* (1995).

Variational spectral analysis schemes are based on the *maximum likelihood* optimality criterion which, under the probabilistic assumptions noted above equation (5.3), is identical to the minimum variance criterion, and hence leads to a formulation of the analysis problem which is algebraically equivalent to that of PSAS. The actual equations solved by these schemes, however, are different from those of PSAS, as described here.

The maximum likelihood criterion seeks to maximize the *a posteriori* (conditional) probability density $p\left(w^t|w^f, w^o\right)$, which under the stated assumptions is the Gaussian density

$$p\left(w^t \mid w^f, w^o\right) = c \exp\left[-\tilde{J}\left(w^t\right)\right], \tag{5.20}$$

where

$$c = (2\pi)^{-n/2}|R|^{-1/2}|P^f|^{-1/2}|HP^fH^T + R|^{1/2}, \tag{5.21}$$

the symbol $|\cdot|$ denoting the matrix determinant, and where

$$\begin{aligned}\tilde{J}\left(w^t\right) &= \frac{1}{2}\left(w^t - w^f\right)^T \left(P^f\right)^{-1}\left(w^t - w^f\right) + \frac{1}{2}\left(Hw^t - w^o\right)^T R^{-1}\left(Hw^t - w^o\right) \\ &\quad -\frac{1}{2}\left(w^o - Hw^f\right)^T \left(HP^fH^T + R\right)^{-1}\left(w^o - Hw^f\right);\end{aligned} \tag{5.22}$$

cf. Jazwinski 1970, Sec. 7.2; Cohn 1996, Sec. 4. Since the constant c is independent of w^t, as is the final term in (5.22), and since $\exp\left(-\tilde{J}\right)$ is a monotonically decreasing function of $\tilde{J}$, maximizing the density (5.20) with respect to w^t is equivalent to minimizing with respect to w the functional

$$J(w) = \frac{1}{2}\left(w - w^f\right)^T \left(P^f\right)^{-1}\left(w - w^f\right) + \frac{1}{2}\left(Hw - w^o\right)^T R^{-1}\left(Hw - w^o\right). \tag{5.23}$$

Since this functional is a positive definite quadratic form in w, it has a unique minimum. This minimum is denoted by w^a, the analysis vector. Variational analysis schemes are called such because they take minimization of (5.23), or of a similar functional, as the starting point.

Details of the minimization procedure differ between the two operational implementations, namely the 3DVAR (three-dimensional variational) system of ECMWF (Heckley *et al.* 1993, Courtier *et al.* 1993), which became operational in early 1996, and the SSI (spectral statistical interpolation) system of NCEP (Parrish and Derber 1992; hereafter referred to as PD92), which became operational in early 1992. Here we follow PD92. Setting

$$\left.\frac{\partial J(w)}{\partial w}\right|_{w=w^a} = 0 \tag{5.24}$$

gives the equation

$$\left[\left(P^f\right)^{-1} + H^TR^{-1}H\right]\left(w^a - w^f\right) = H^TR^{-1}\left(w^o - Hw^f\right). \tag{5.25}$$

Now let B be any matrix such that

$$BB^T = P^f \tag{5.26}$$

(this decomposition, carried out spectrally, is discussed later), and define the vector $z \in \mathbb{R}^n$ such that

$$z = B^{-1}\left(w^a - w^f\right). \tag{5.27}$$

Algebraic manipulation of (5.25) leads to the equation

$$\left(I + B^T H^T R^{-1} H B\right) z = B^T H^T R^{-1}\left(w^o - H w^f\right), \tag{5.28}$$

which along with (5.27) written in the form

$$w^a = w^f + Bz, \tag{5.29}$$

comprise the analysis equations of PD92. These can be compared directly with the PSAS analysis equations (5.7) and (5.8). Observe that (5.28) is an equation solved in state space, that is, $z \in \mathbb{R}^n$, whereas the matrix problem (5.7) of PSAS is solved in the lower-dimensional observation space $\mathbb{R}^p$. Solving (5.28) involves additionally the solution of observation-space systems of the form $Ru = v$.

To establish the equivalence of the analysis equations of PD92 with those of PSAS when presented with the same data w^o, w^f, and the same matrices P^f, R, and H, note from the Sherman-Morrison-Woodbury formula (*e.g.* Golub and van Loan 1989) that

$$\left(I + B^T H^T R^{-1} H B\right)^{-1} = I - B^T H^T \left(H P^f H^T + R\right)^{-1} H B, \tag{5.30}$$

so that (5.28) can be written as

$$\begin{aligned} Bz &= B\left[I - B^T H^T \left(H P^f H^T + R\right)^{-1} H B\right] B^T H^T R^{-1}\left(w^o - H w^f\right) \\ &= P^f H^T \left[I - \left(H P^f H^T + R\right)^{-1} H P^f H^T\right] R^{-1}\left(w^o - H w^f\right) \\ &= P^f H^T \left(H P^f H^T + R\right)^{-1}\left(w^o - H w^f\right) \\ &= P^f H^T y, \end{aligned} \tag{5.31}$$

where y was defined by the PSAS equation (5.7). This result, along with (5.8) and (5.29), establishes the formal algebraic equivalence between the SSI scheme of PD92 and the PSAS scheme. The differences, therefore, are in the solution algorithm and, perhaps more importantly, in the covariance modeling. The matrix P^f is modeled directly in physical space in PSAS, whereas in variational schemes such as SSI it is modeled spectrally.

In the SSI scheme, as well as in the 3DVAR scheme of ECMWF, the forecast w^f, and hence the true state w^t and the analysis w^a, consists of spectral coefficients rather than

grid-point values as in the GEOS system. Thus the observation operator in (5.28) consists of a transformation to physical space followed by interpolation to observation locations [see equation (5.2)] which, as reported in PD92, comprises most of the computational effort in solving (5.28). The spectral forecast error covariance matrix P^f, still defined by (5.5), is assumed to be diagonal. This renders the decomposition (5.26) trivial, but is an explicit assumption of horizontal isotropy. In particular, the forecast wind error variances of PD92 are independent of geographical location.

The linear system (5.28) of PD92 is solved by a standard CG algorithm without pre-conditioning; this is equivalent computationally to solving (5.25) by a preconditioned CG algorithm with the (diagonal) matrix P^f as the pre-conditioner. The eigenvalues μ of the matrix of the linear system (5.28) have the form

$$\mu = 1 + \lambda\left(\tilde{M}\right), \tag{5.32}$$

where

$$\tilde{M} \equiv B^T H^T R^{-1} H B, \tag{5.33}$$

and $\lambda\left(\tilde{M}\right)$ denotes an eigenvalue of the matrix $\tilde{M}$. The matrix $\tilde{M}$ is symmetric positive semi-definite, and has at least $n - p$ zero eigenvalues, assuming $p < n$. Thus the condition number σ of the matrix of (5.28), which controls the convergence rate of the CG algorithm (*cf.* Golub and van Loan 1989), is

$$\sigma = 1 + \lambda_{max}\left(\tilde{M}\right). \tag{5.34}$$

Accurate observational data (reflected by small diagonal entries of R) increase the largest eigenvalue of $\tilde{M}$ according to (5.33), and therefore increase the condition number σ and reduce the convergence rate of the CG iterations. It can be shown that, were the PSAS equation (5.7) to be preconditioned by the matrix R rather than by the strategy described in section 5.2.3, its condition number would be identical to that of (5.34).

5.2.5 Comparison of the global PSAS solver with the localized OI solver

The *Optimal Interpolation* (OI) algorithm implemented in GEOS-1 DAS is a statistical interpolation scheme which includes the following assumptions: a) isotropic horizontal correlation functions, b) separable vertical and horizontal correlation structures, c) multivariate wind and height analysis with a "geostrophic" constraint built into the covariance model, d) *local approximation:* each mini-volume analysis incorporates data only in the neighborhood of that mini-volume, e) *data selection:* only a relatively small portion of the observations in the neighborhood of the grid point is actually included in the analysis (Pfaendtner *et al.* 1995).

In order to investigate incremental improvements over the OI analysis scheme of GEOS-1 DAS, observation and forecast error covariance statistics were specified the same way as in the GEOS-1 OI scheme (Pfaendtner *et al.* 1995). In this configuration, PSAS only differs

from OI in the numerical method used to solve for the analysis increments: a global conjugate gradient solver includes all available observations to produce the analyzed field. Before improved error covariance statistics are introduced in section 5.2.7, we assess the impact of global analysis, with no local approximation and no data selection, on the assimilation system.

For this comparison we rely on the data base prepared through the GEOS-1 project described in Chapter 4. This data bank provides not only the analysis increments produced by the OI-based system, but also the innovation vectors used by the OI (before data selection) which will be used for the right-hand-side of (5.7) in the present study. A number of synoptically relevant events have been identified by R. Atlas (*personal communication*) for the purpose of data assimilation experiments. The five cases selected for this study are summarized in Table 5.1. The experiments reported here all have 12Z as the synoptic time. Unless otherwise noted, the PSAS analyses described in this section are carried out in static mode: both innovation vectors and forecast error statistics are specified exactly as in the OI system.

Table 5.1: Five synoptically relevant cases used in this study. For all cases the synoptic time is 12Z.

Case	*Date*	*Description*
1	08/28/85	Tropical easterly waves
2	10/15/87	Explosive cyclogenesis (Europe)
3	12/01/87	Cyclogenesis (South Australia)
4	12/15/87	Explosive cyclogenesis (US)
5	01/30/89	Cold surge (US)

Although PSAS has the capability of including data on all mandatory levels, for this comparison we chose to include only data on the same vertical levels as in the OI system, this way focusing on the horizontal aspects of data selection. For the 500 hPa analysis, only data from 850 to 400 hPa are included. For brevity, we present only results concerning the spectral characteristics of 500 hPa analysis increments $w_a - w_f$ obtained with the OI and PSAS systems. Analysis increments are expanded in terms of spherical harmonics and the 5-case mean power spectra are displayed as functions of total wavenumber in Figs. 5.2–5.4.

Fig. 5.2 depicts the power spectra of 500 hPa geopotential height analysis increments obtained with PSAS (solid) and OI (points) systems. Overall, there is very little difference between the spectra for wavenumbers in the range 3-15. For wavenumbers lower than 3 the OI analysis increments have less power than the corresponding PSAS increments. However, for higher wavenumbers the OI analysis increments have considerably more power than the PSAS increments. This is due to the relatively flat spectral slope of the OI increments, a shortcoming related to the local approximation and data selection. Notice that the PSAS increments also show signs of saturation at around wavenumber 70. However, there is a negligible amount of power at these wavenumbers.

The impact of the local approximation and data selection of OI on the wind field are presented in Figs. 5.3–5.4 in terms of the power spectra of divergence and vorticity. There is a good agreement between the OI and PSAS analysis increments of relative vorticity (Fig. 5.3) up to about wavenumber 40. At higher wavenumbers the OI increments again

show much more power than the PSAS increments. For the divergence field (Fig. 5.4), both OI and PSAS increments show a rather flat spectrum for wavenumbers greater than about 20. For wavenumbers beyond 20 the OI increments have 1 to 2 orders of magnitude more power than the PSAS increments. The upshot is that the ratio of divergence to vorticity in the OI increments is much larger than in PSAS. This large amount of divergence in the OI increments is likely to contribute to an unbalanced analyzed state contaminated by gravity waves. Therefore, the imbalances often found in OI analyses are not entirely due to the crude geostrophic balance used to relate wind forecast error statistics to height error statistics. A great deal of spurious divergence is due to the local approximation and data selection.

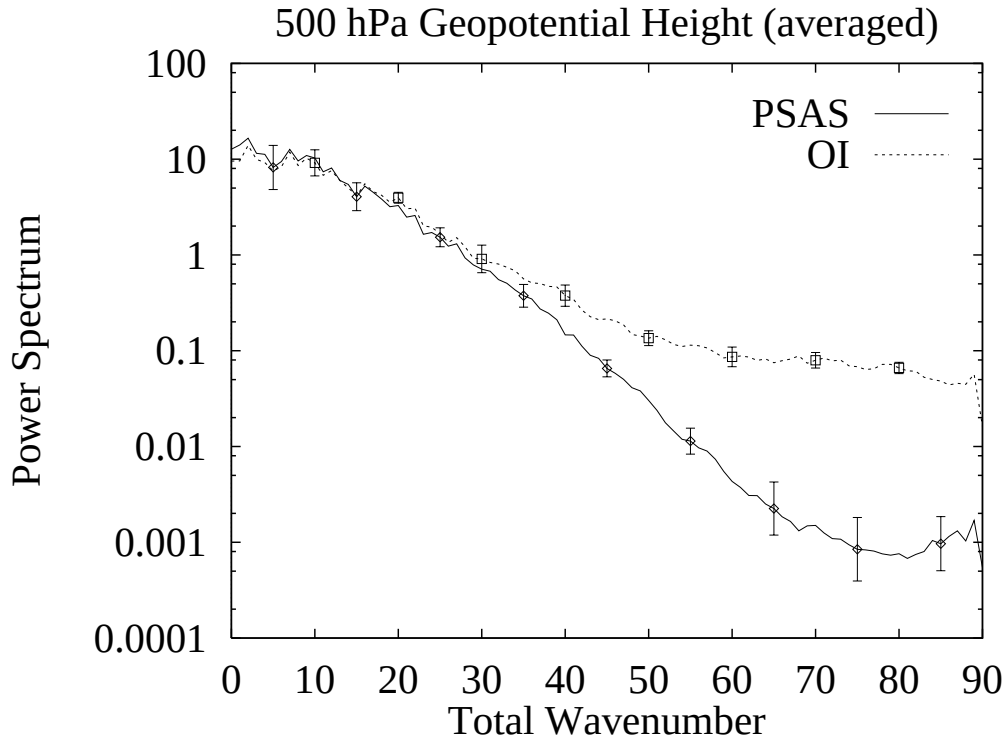

Figure 5.2: Power spectra as a function of spherical harmonic total wavenumber for PSAS (solid) and OI (points) analysis increments of geopotential height at 500 hPa (5 case average, see table 5.1). Units: m^2.

The power spectra of water vapor mixing ratio analysis increments (not shown) indicate that the OI increments show a greater amount of noise reflected by excessive power in higher wavenumbers. Although similar to the increments of geopotential heights, the discrepancies between OI and PSAS are not as accentuated in this case. This fact is consistent with the smaller correlation lengths assigned to the water vapor forecast error covariance. The tighter correlation function for the water vapor is more amenable to the local approximation of the OI system. However, at large scales the OI increments have considerably less power than the PSAS increments.

A version of GEOS DAS has been configured using a 46-level version of the GEOS-1 GCM (Takacs *et al.* 1994), and PSAS with the error statistics of the GEOS-1 OI system (Pfaendtner *et al.* 1995). Figure 5.5 depicts the time-mean (bias) and standard deviation

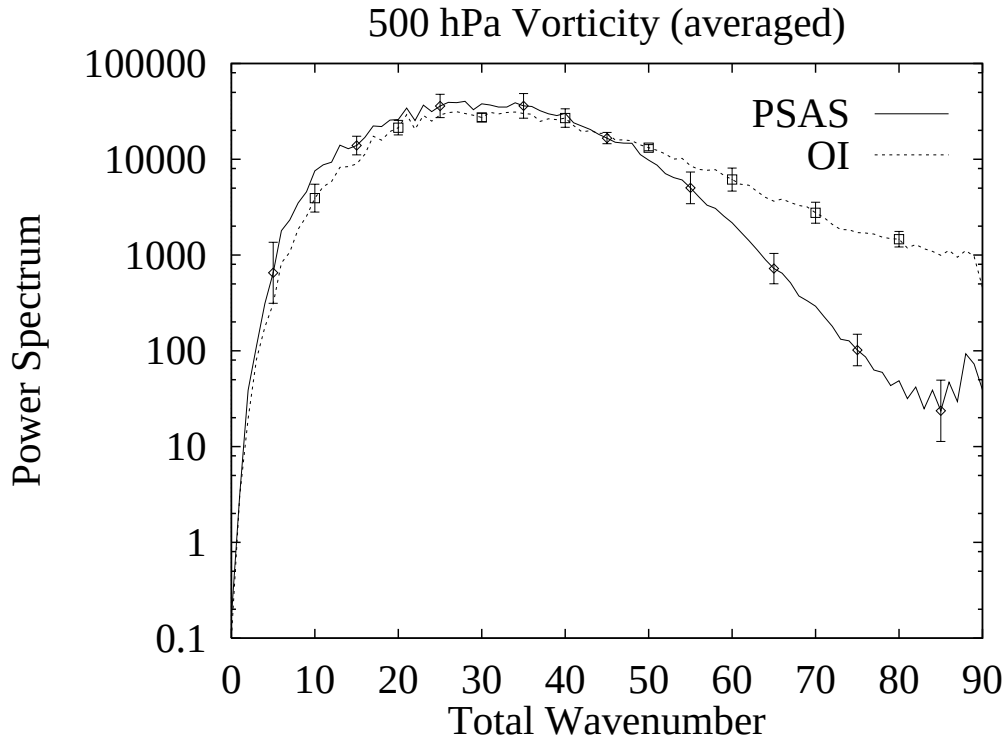

Figure 5.3: As in fig. 1, but for 500 hPa relative vorticity. Units: $10^{-15}s^{-2}$.

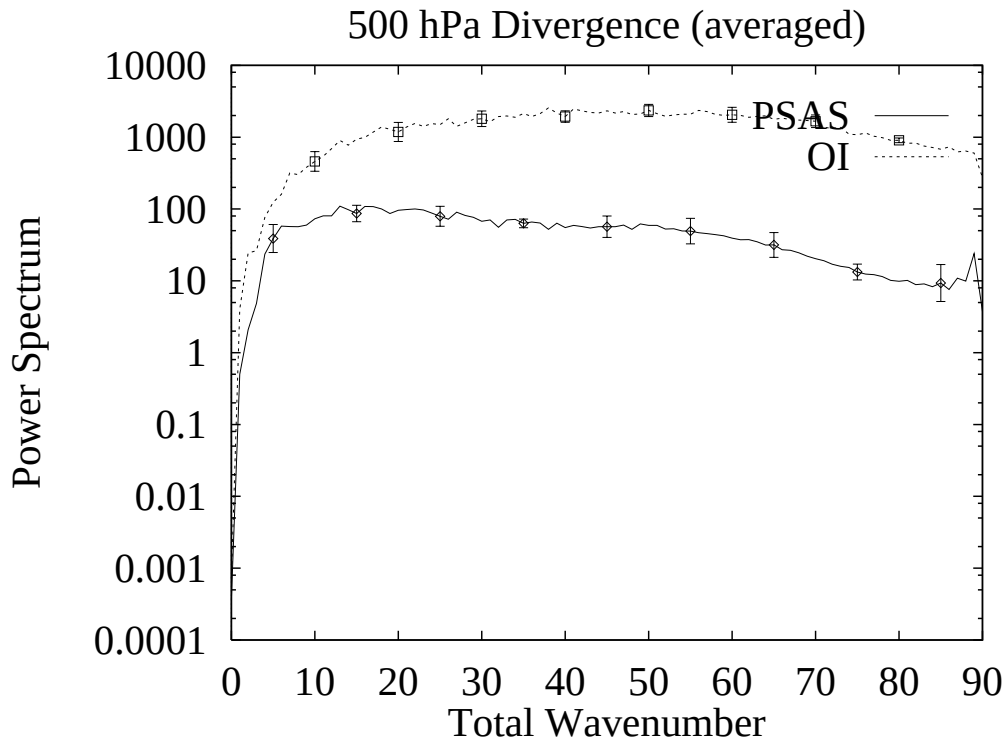

Figure 5.4: As in fig. 1, but for 500 hPa divergence. Units: $10^{-15}s^{-2}$.

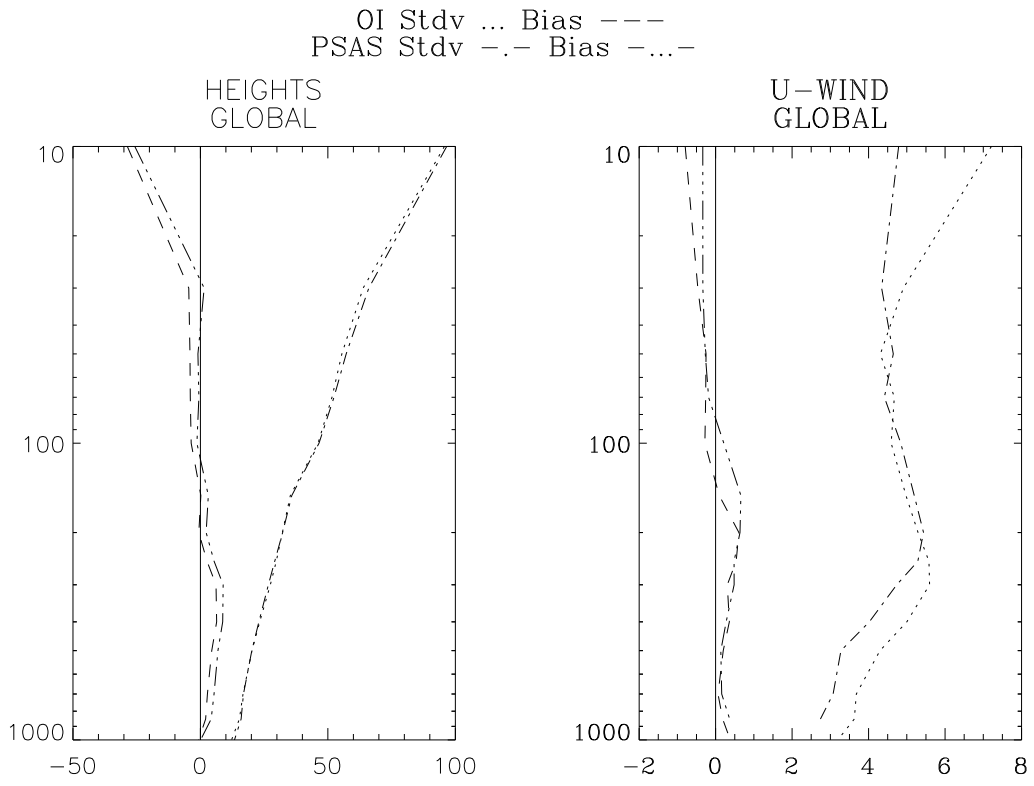

Figure 5.5: Bias (time-mean) and standard deviation of radiosonde observation minus 6-hour forecast residuals (O-F) for the last 10 days of a one-month assimilation experiment (February 1992). See text for details.

(stdv) of observation minus forecast (O-F) residuals for the last 10 days of a one-month assimilation (February 1992). For geopotential height, PSAS shows a slight increase in the O-F time-mean in the troposphere, but a decrease above 100 hPa; geopotential height O-F standard deviations are practically the same for both systems. For winds (only statistics for the zonal component of the wind are shown in Fig. 5.5), the PSAS run shows a slight improvement in time-mean O-F, but a more significant improvement in the wind standard deviations. The O-F statistics for mixing ratio (not shown) are practically identical for both systems. These results are consistent with the analysis increment characteristics depicted in Figs. 5.2–5.4. The noise in the height and mixing ratio analysis increments introduced by the local approximation in OI is filtered by the IAU procedure (section 5.4). However, the dynamical imbalances associated with the spurious OI analysis increments of wind divergence have a deleterious impact on the 6-hour wind forecast.

In summary, 500 hPa OI analysis increments have a large amount of noise in geopotential heights and mixing ratio, and an unrealistically large ratio of divergence to vorticity compared to PSAS. These problems with the OI system impact negatively the dynamical balance of the OI analyzed state as demonstrated by the one-month assimilation experiment.

5.2.6 The analysis equations in the presence of forecast bias

In this section we show that a biased forecast invariably leads to a biased analysis, independently of the weights used in the analysis update. Bias can be reduced by drawing more to the observations, but the side effect will be an increasingly noisy analysis.

If the forecast bias $b^f = \left\langle \epsilon^f \right\rangle$ were known, one could compute an unbiased forecast

$$\widetilde{w}^f = w^f - b^f. \tag{5.35}$$

Similarly, if $b^o = \langle \epsilon^o \rangle$ is the observation bias, then

$$\widetilde{w}^o = w^o - b^o \tag{5.36}$$

would be a set of unbiased observations.

The statistical analysis equation which properly accounts for bias is

$$\widetilde{w}^a = \widetilde{w}^f + K[\widetilde{w}^o - H\widetilde{w}^f], \tag{5.37}$$

where $\widetilde{w}^a$ is the analysis and K is a *gain matrix* which takes into account the relative accuracies of forecast and observations. Independently of the specification of this gain, the analysis here is an unbiased estimate of the true state:

$$b^a \equiv \langle \epsilon^a \rangle = 0, \qquad \epsilon^a \equiv \widetilde{w}^a - w^t. \tag{5.38}$$

If, in particular,

$$K = P^f H^T [H P^f H^T + R]^{-1}, \tag{5.39}$$

where P^f and R were defined in (5.5) and (5.6), respectively, then (5.37) provides the *linear minimum variance estimate* of the true state given the observations w^o and forecast w^f (Anderson and Moore, 1979, section 5.2).

In operational data assimilation systems the bias terms b^o, b^f are usually unknown and hence neglected. Using w^o, w^f in place of $\widetilde{w}^o, \widetilde{w}^f$ the analysis equation is

$$w^a = w^f + K[w^o - Hw^f]. \tag{5.40}$$

Independently of the gain K this analysis is biased:

$$b^a = b^f + K[b^o - Hb^f], \tag{5.41}$$

unless the observations as well as the forecast happen to be unbiased.

Given an analysis equation of the form (5.40) in which bias is not explicitly accounted for, it is nevertheless interesting to consider the gain K which leads to the smallest analysis error variance. This is important from a practical point of view since (5.40) is precisely the

equation being solved in operational sequential data assimilation systems. It is not difficult to show that the analysis error variance due to (5.40) is minimal when

$$K \equiv \bar{K} = \bar{P}^f H^T [H \bar{P}^f H^T + \bar{R}]^{-1}, \tag{5.42}$$

with

$$\bar{P}^f \equiv \left\langle \epsilon^f (\epsilon^f)^T \right\rangle = P^f + b^f (b^f)^T, \tag{5.43}$$

$$\bar{R} \equiv \left\langle \epsilon^o (\epsilon^o)^T \right\rangle = R + b^o (b^o)^T. \tag{5.44}$$

The analysis resulting from (5.40) with $K = \bar{K}$ is still biased, as is true for *any* gain K. The estimate of analysis error "variances" described in subsection 5.2.7.2 takes into account a crude estimate of the forecast error bias according to (5.43). A truly unbiased analysis can be produced only if explicit estimates of forecast bias and observation bias are available. A practical algorithm for properly accounting for forecast bias in the analysis equation is described in Chapter 9.

A scalar example.

Suppose that w^f and w^o are both scalars, with

$$b^f = \langle \epsilon^f \rangle = b, \qquad P^f = \langle (\epsilon^f - b)^2 \rangle = \sigma^2, \tag{5.45}$$

$$b^o = \langle \epsilon^o \rangle = 0, \qquad R = \langle (\epsilon^o)^2 \rangle = \sigma^2. \tag{5.46}$$

Using (5.37), the optimal analysis is given by

$$\widetilde{w}^a = \frac{1}{2}(\widetilde{w}^f + w^o) = \frac{1}{2}(w^f - b + w^o), \tag{5.47}$$

for which

$$b^a = 0, \qquad \langle (\epsilon^a)^2 \rangle = \frac{1}{2}\sigma^2. \tag{5.48}$$

Ignoring forecast bias as in (5.40) would give instead

$$w^a = \frac{1}{2}(w^f + w^o), \tag{5.49}$$

which is biased:

$$b^a = \frac{1}{2}b, \qquad \langle (\epsilon^a)^2 \rangle = \frac{1}{4}b^2 + \frac{1}{2}\sigma^2. \tag{5.50}$$

Note that the analysis reduces the bias (by a factor of two) but does not remove it. Suppose now that $b = \sigma$, *i.e.* the typical magnitude of the random component of forecast error is

equal to that of the systematic component. Increasing the weight of the observation as in (5.42) then gives

$$w^a = \frac{1}{3}(w^f + 2w^o), \tag{5.51}$$

which is still biased, although less so, and has somewhat less total variance:

$$b^a = \frac{1}{3}b, \qquad \langle(\epsilon^a)^2\rangle = \frac{1}{9}b^2 + \frac{5}{9}\sigma^2. \tag{5.52}$$

Drawing the analysis even closer to the observation would further reduce the bias but increase the total analysis error variance, due to the random error component. Figure 1 summarizes this example; it shows the dependence on the weight K of the analysis bias, the standard deviation of the random component of analysis error, and the total expected analysis error if (5.41) is used. This example shows clearly that, unless bias is explicitly accounted for, it can be reduced only at the expense of increasing the noisiness of the analysis.

5.2.7 Specification of error statistics

As pointed out in the Third Report of the DAO Science Advisory Panel (February, 1995) the specification of error statistics inherited from previous data assimilation efforts at GSFC was primitive. These statistics had been used in GEOS-1, but the GEOS-1 OI scheme was not very sensitive to the specification of the statistics. As discussed in the previous sections, this is likely related to the data selection used in GEOS-1 to allow computational viability. With the development of PSAS, much more accurate modeling of error statistics is demanded.

This section documents the specification of error statistics for GEOS-2. We first introduce the general formulation of a three-dimensional, non-separable, horizontally isotropic, univariate covariance model, largely based on Gaspari and Cohn (1996). Next, the method for estimating covariance parameters from time-series of observed-minus forecast residuals is described; this is an off-line version of the maximum-likelihood scheme developed in Dee (1995). We then discuss the specific implementations of the multivariate forecast error covariance model and of the observation error covariance models implemented in PSAS.

It is to be expected that, as validation of GEOS-2 progresses, several aspects of the covariance models as described in this section will be modified and adjusted. The general formulation of the models, described in the next sections, as well as their implementation in PSAS, have been designed to allow considerable flexibility in this regard. These designs have been based on the premise that adjustments to the covariance modeling formulations and re-tuning of the statistics will take place continuously.

5.2.7.1 Statistical modeling methodology

5.2.7.1.1 General covariance model formulation. Several important aspects of the formulation described here rely on the theory developed in Gaspari and Cohn (1996). First,

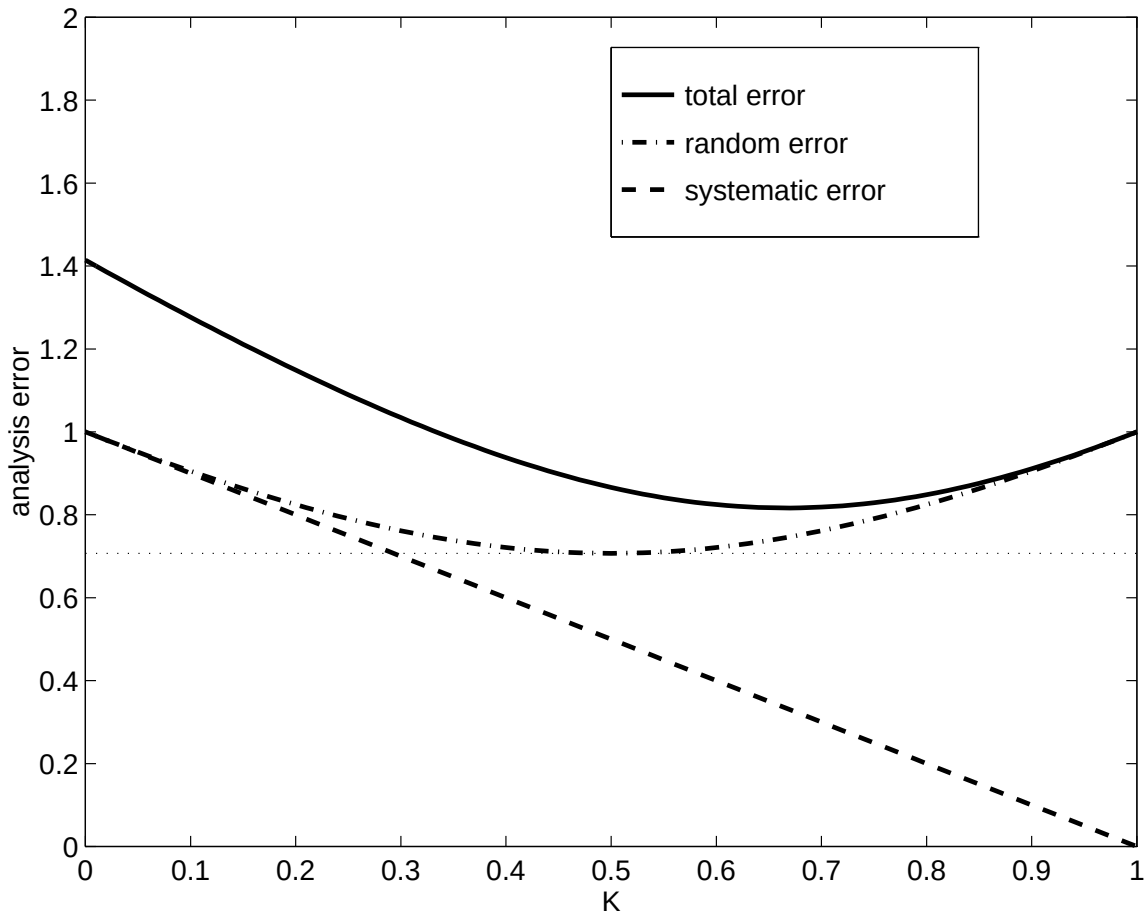

Figure 5.6: Analysis error as a function of the scalar gain coefficient K, when bias is not explicitly accounted for in the analysis, for the scalar example presented in section 5.2.6. The dotted horizontal line indicates the optimal analysis error level, obtained when bias is explicitly accounted for in the analysis equation.

PSAS employs compactly supported spline functions for modeling all single-level univariate correlations. This means that the modeled horizontal correlations are exactly zero beyond a certain finite distance; the PSAS global solver takes advantage of this fact. Second, the non-separable three-dimensional covariance formulation, based on multi-level cross-correlation functions, is positive-semidefinite by construction. This is, of course, an essential requirement for the convergence of the global solver.

Three-dimensional covariances are constructed in terms of single-level isotropic covariances, which we will describe first, together with some important special cases. In the following, superscripts denote vertical pressure levels and subscripts correspond to pairs of horizontal longitude-latitude coordinates. The quantity r_{ij} denotes the horizontal distance between two three-dimensional locations, which is defined as the chordal distance between the vertical projection of the two locations onto the earth's surface. Thus, the horizontal distance between a pair of three-dimensional locations $P_i^{(m)} = (p_m, \lambda_i, \varphi_i)$ and

$P_j^{(n)} = (p_n, \lambda_j, \varphi_j)$ is given by

$$r_{ij} = [(\mathbf{p}_i - \mathbf{p}_j) \cdot (\mathbf{p}_i - \mathbf{p}_j)]^{\frac{1}{2}} = a\,[2(1 - \mathbf{q}_i \cdot \mathbf{q}_j)]^{\frac{1}{2}}\,, \tag{5.53}$$

where a is the earth's radius and

$$\mathbf{p}_j = a\mathbf{q}_j = a\,[\cos\varphi_j \cos\lambda_j, \cos\varphi_j \sin\lambda_j, \sin\varphi_j]\,. \tag{5.54}$$

5.2.7.1.1.1 Single-level univariate isotropic covariances

The general single-level univariate isotropic covariance model is of the form

$$[\mathrm{Cov}]_{ij}^{(m)} = \sigma_i^{(m)} \sigma_j^{(m)} \rho^{(m)}(r_{ij}), \tag{5.55}$$

where $\rho^{(m)}(r)$ is a correlation function and $\sigma^{(m)} > 0$.

Although PSAS does not contain any restrictions on the type of correlation models it can handle, only a few families of single-level correlation models are actually employed. For errors which are assumed horizontally uncorrelated,

$$\rho^{(m)}(r) = \delta(r) \tag{5.56}$$

where

$$\delta(r) = \begin{cases} 1 & \text{if } r = 0 \\ 0 & \text{otherwise} \end{cases} \tag{5.57}$$

Horizontally correlated errors may be modeled using the powerlaw function, given by

$$\rho^{(m)}(r) = \rho_p(r; L^{(m)}) = \left[1 + \frac{1}{2}\left(\frac{r}{L^{(m)}}\right)^2\right]^{-1}. \tag{5.58}$$

Alternatively, the compactly supported spline function (Gaspari and Cohn, section 4.3) can be used:

$$\rho^{(m)}(r) = \rho_c(r; L^{(m)}) \tag{5.59}$$

where

$$\rho_c(r; L^{(m)}) = \begin{cases} -\frac{1}{4}\left(\frac{r}{c}\right)^5 + \frac{1}{2}\left(\frac{r}{c}\right)^4 + \frac{5}{8}\left(\frac{r}{c}\right)^3 - \frac{5}{3}\left(\frac{r}{c}\right)^2 + 1, & \text{if } 0 \le r \le c, \\ \frac{1}{12}\left(\frac{r}{c}\right)^5 - \frac{1}{2}\left(\frac{r}{c}\right)^4 + \frac{5}{8}\left(\frac{r}{c}\right)^3 + \frac{5}{3}\left(\frac{r}{c}\right)^2 - 5\left(\frac{r}{c}\right) + 4 - \frac{2}{3}\left(\frac{r}{c}\right)^{-1}, & \text{if } c \le r \le 2c, \\ 0 & \text{otherwise} \end{cases} \tag{5.60}$$

with

$$c = L^{(m)}\sqrt{\frac{10}{3}}. \tag{5.61}$$

The parameter $L^{(m)}$ is the de-correlation length scale for the correlation function $\rho^{(m)}(r)$, defined by

$$L^{(m)} = \sqrt{\frac{-1}{\rho_c''(0)}}. \tag{5.62}$$

Note that $\rho_c(r; L^{(m)}) = 0$ for $r > 2L^{(m)}\sqrt{\frac{10}{3}} \approx 3.65L^{(m)}$.

The compactly supported spline function is twice continuously differentiable. Figure 5.7 shows the function for two different values of the length scale parameter $L^{(m)}$, as well as the discrete Legendre spectra for these two examples.

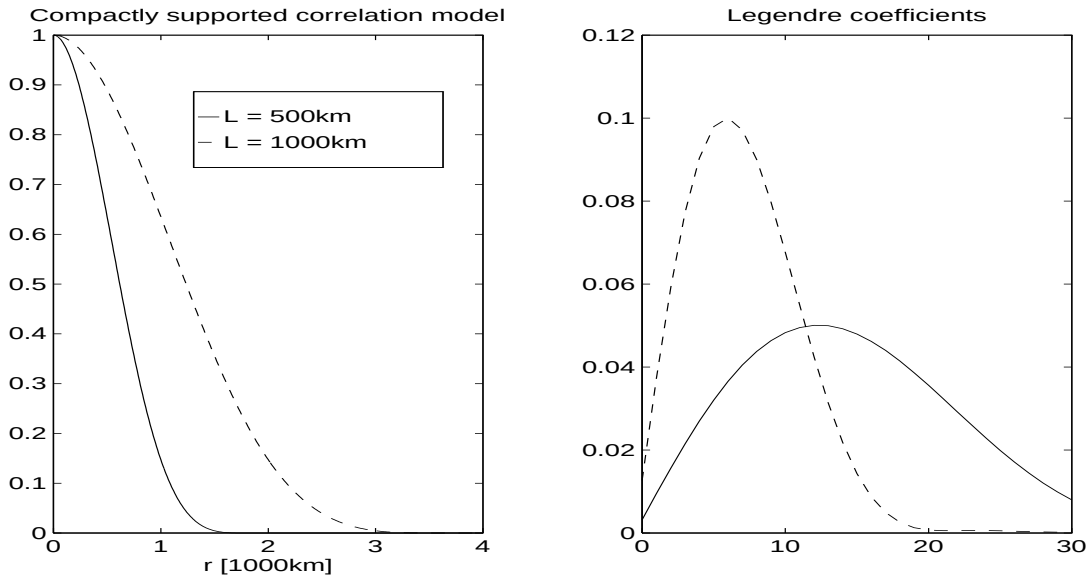

Figure 5.7: Compactly supported single-level correlation model and Legendre coefficients.

5.2.7.1.1.2 Multi-level univariate covariances

The general multi-level univariate covariance model is of the form

$$[\mathrm{Cov}]_{ij}^{(mn)} = \sigma_i^{(m)} \sigma_j^{(n)} \nu^{(mn)} \rho^{(mn)}(r_{ij}), \tag{5.63}$$

where the $\rho^{(mn)}(r)$ are cross-correlation functions, $\nu^{(mn)}$ are vertical correlation coefficients, and $\sigma^{(m)}$ are positive functions. Note that r_{ij} is horizontal distance, as defined by (5.53).

Gaspari and Cohn (1996) (Theorem 3.1) show how to construct a covariance model of the form (5.63) with $\rho^{(mm)}(r) = \rho^{(m)}(r)$; i.e., a three-dimensional covariance model which reduces to the single-level model (5.55) at each pressure level. Since these single-level models may be different at different pressure levels, the three-dimensional model is non-separable. For the special case when horizontal correlations are modeled by the compactly supported spline function, i.e. when $\rho^{(m)}(r) = \rho_c(r; L^{(m)})$, the cross-correlations are defined by

$$\rho^{(mn)}(r) = \rho_{c \times c}(r; L^{(m)}, L^{(n)}); \tag{5.64}$$

the formula for this family of functions is rather cumbersome and will not be included here. Figure 5.8 shows an example of a compactly supported spline cross-correlation function.

The covariance model 5.63 is positive-semidefinite by construction, provided the vertical correlation matrix $[\nu]^{(mn)}$ is positive-semidefinite.

When all single-level correlation functions are identical, i.e., $\rho^{(m)}(r) = \rho(r)$ for all m, (5.63) reduces to the separable model

$$[\mathrm{Cov}]_{ij}^{(mn)} = \sigma_i^{(m)} \sigma_j^{(n)} \nu^{(mn)} \rho(r_{ij}). \tag{5.65}$$

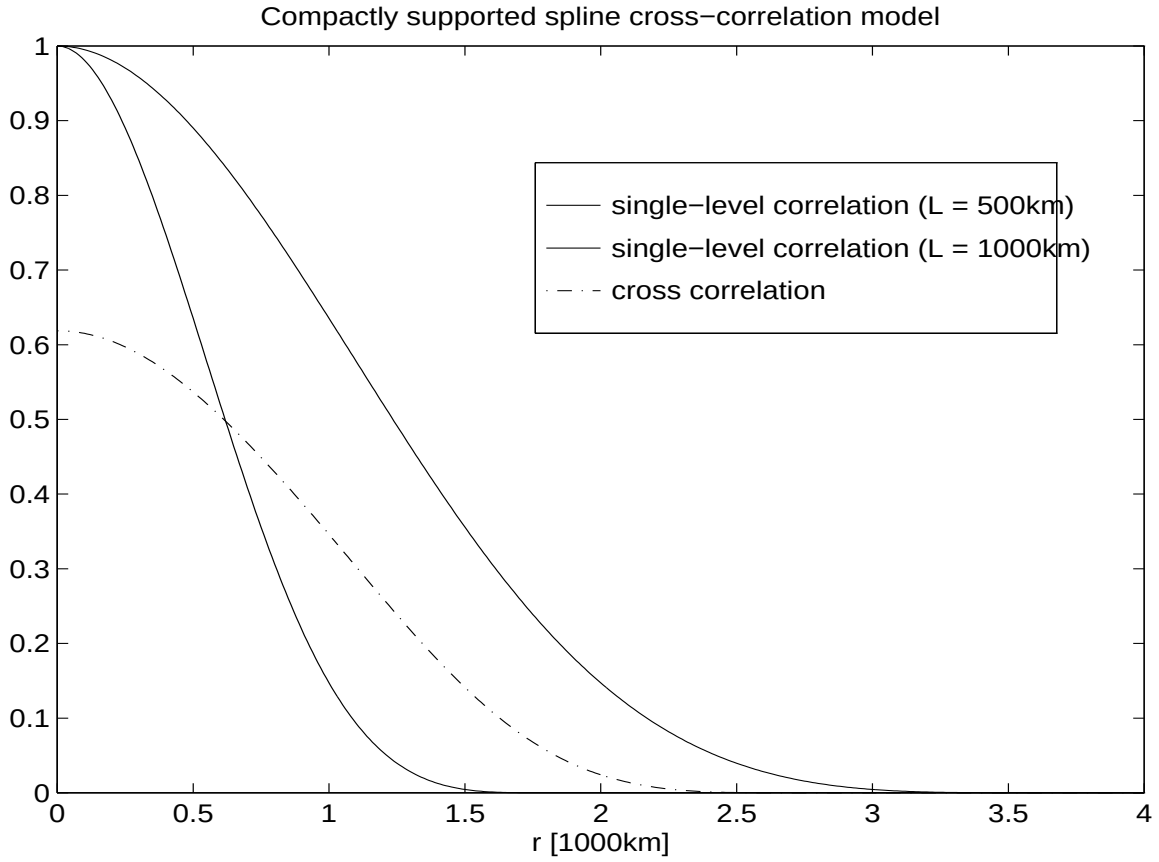

Figure 5.8: Compactly supported spline cross-correlation function.

5.2.7.1.2 Tuning methodology. The actual multivariate error covariance formulations employed by PSAS can all be expressed in terms of the general univariate model presented in the previous section. In general, assumptions about forecast and observation errors (which will be described below, in sections 5.2.7.2 and 5.2.7.3) lead to parameterized covariance models of the form

$$P_k^f \approx P_k^f(\alpha^f), \qquad R_k \approx R_k(\alpha^o), \tag{5.66}$$

where P_k^f, R_k are the forecast and observation error covariances at time t_k, respectively. The α^f, α^o are covariance parameters which must be estimated from data; these may include observation error standard deviations, horizontal de-correlation length scales, vertical correlation coefficients, etc.

Observational information about the covariance parameters α^f, α^o is contained in the observed-minus-forecast residuals (O-F's)

$$v_k \equiv w_k^o - h_k(w_k^f). \tag{5.67}$$

Here w_k^o is any vector of observations and w_k^f is the forecast valid at time t_k. The observation operator h_k maps model state variables to the observables; if the state variables are observed directly then h_k is just an interpolation operator, but in case of radiance data, for example, the observation operator involves a radiative transfer model. In general one can define the linearized observation operator H_k:

$$H_k \equiv \left.\frac{\partial h_k}{\partial w}\right|_{w=w_k^f}. \tag{5.68}$$

The forecast as well as the observations themselves contain errors, and therefore the residual (5.67) depends on both forecast errors and observation errors. In fact, it is easy to show that the covariance of the O-F's equals the sum of the forecast and observation error covariances:

$$S_k \equiv \left\langle (v_k - \langle v_k \rangle)(v_k - \langle v_k \rangle)^T \right\rangle \tag{5.69}$$

$$\approx R_k + H_k P_k^f H_k^T, \tag{5.70}$$

under the assumption that forecast and observation errors are statistically independent. In case of direct observations of state variables, the matrix $H_k P_k^f H_k^T$ is just the evaluation of the forecast error covariance model at the observation locations.

The residual covariance equation (5.69) provides the basis for tuning forecast and observation error statistics for given covariance formulations. Substitution of the covariance models (5.66) yields

$$S_k \approx S_k(\alpha) = S_k(\alpha^f, \alpha^o). \tag{5.71}$$

Estimates of α can be obtained by finding the best fit of the covariance model $\S_k(\alpha)$ to a sequence of residuals

$$\{v_k\} \equiv \{v_k, k = 1, \ldots, K\}. \tag{5.72}$$

In doing so we assume that the mean $\langle v_k \rangle$ is zero; in practice the (time) mean of $\{v_k\}$ is removed prior to covariance tuning.

The criterion of fit is based on the maximum-likelihood principle, in which the likelihood function of the data is maximized as a function of the unknown parameters α. We assume

that the time-series of O-F's is white and Gaussian, with mean zero and covariance at time t_k given by $S_k(\alpha)$ for some α. Then

$$p(\{v_k\};\alpha) = \prod_{k=1}^{K} p(v_k;\alpha) \propto \prod_{k=1}^{K} (\det S_k(\alpha))^{-\frac{1}{2}} \exp\left[-\frac{1}{2} v_k^T S_k^{-1}(\alpha) v_k\right]. \tag{5.73}$$

The maximum-likelihood estimate $\hat{\alpha}$ is obtained by maximizing (5.73), or, equivalently, by minimizing the *log-likelihood function*

$$f(\alpha) = \sum_{k=1}^{K} \left[\log\det S_k(\alpha) + v_k^T S_k^{-1}(\alpha) v_k\right]. \tag{5.74}$$

In case the covariance model (5.71) is stationary, i.e.

$$S_k(\alpha) = S(\alpha), \tag{5.75}$$

the log-likelihood function simplifies to

$$f(\alpha) = K \times \left[\log\det S(\alpha) + \mathrm{tr}(S^{-1}(\alpha)\widehat{S})\right]. \tag{5.76}$$

Here $\widehat{S}$ is the sample covariance of the data defined by

$$\widehat{S} = \frac{1}{K}\sum_{k=1}^{K} v_k v_k^T, \tag{5.77}$$

where, if necessary, the mean of the time series $\{v_k\}$ has been removed. For a stationary observing system, such as a rawinsonde observing network, (5.76) is easier to evaluate than (5.74).

The tuning method just described is quite general, and can be used to tune all kinds of covariance parameters. To illustrate the method we describe its application to the tuning of the forecast height error horizontal correlation length scales based on single-level rawinsonde height observed-minus-forecast residuals. At a fixed pressure level, the covariance of these residuals is given by

$$S_{ij} = \sigma^o \delta(r_{ij}) + \sigma^f \rho_c(r_{ij};L), \tag{5.78}$$

where σ^o is the rawinsonde height observation error standard deviation, σ^f is the forecast height error standard deviation, and L is the length scale parameter for the forecast height error horizontal correlations. These parameters can be estimated from, say, a month of data, by computing the sample covariance $\widehat{S}$ of the data defined at the station locations, and then minimizing (5.76) as a function of the three parameters $\alpha = (\sigma^o, \sigma^f, L)$.

As an example we take 500hPa data from 80 North-American rawinsonde stations for the month of February, 1995. For this case one obtains the estimates $\sigma^o = 9.2m, \sigma^f = 12.4m$, and $L = 617 \times 10^3 m$. Individual elements of $\widehat{S}$ are plotted in figure 5.9 together with the

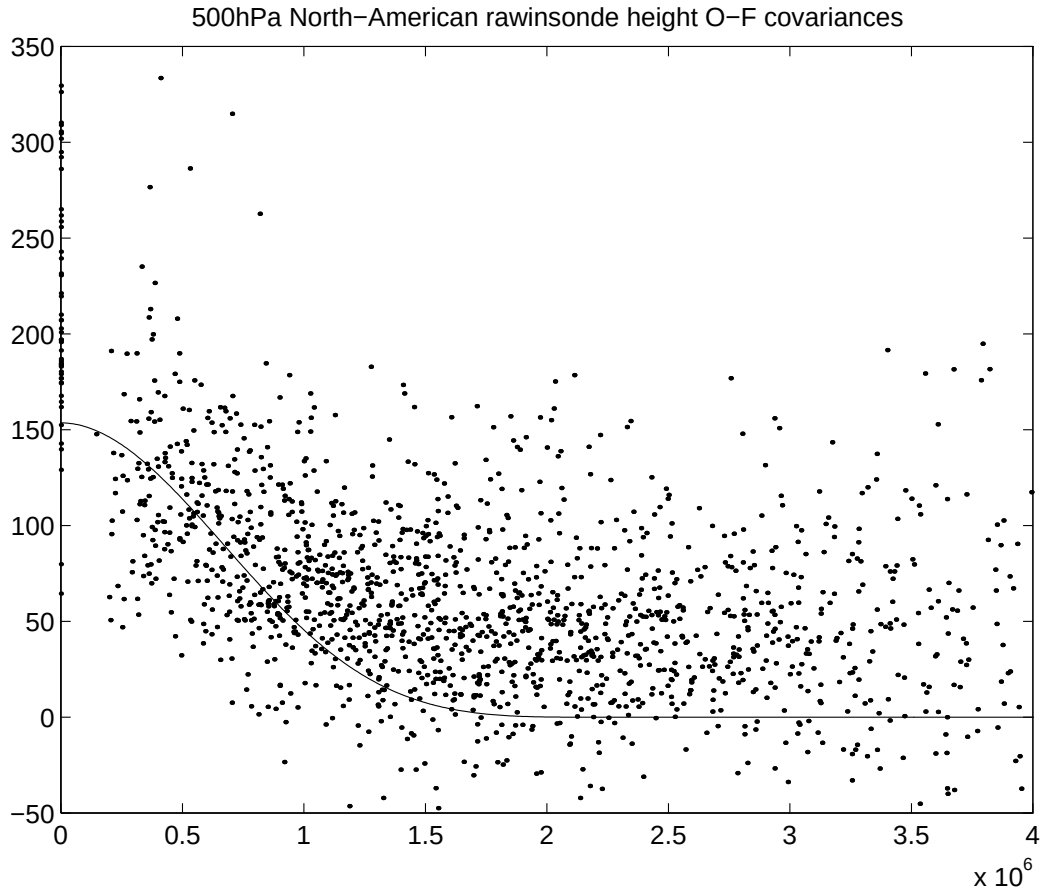

Figure 5.9: Sample and tuned model covariances for 500hPa North-American rawinsonde height observed-minus-forecast residuals.

model fit. The scatter in the sample covariances is due to sampling error as well as to the fact that actual errors are neither isotropic nor stationary. The model fit is plotted as well. At first glance it may seem that the model underestimates the covariances, however upon closer inspection this is primarily due to the large scatter of the sample covariances beyond $10^3 m$. The maximum-likelihood criterion apparently rejects this scatter as being statistically insignificant.

5.2.7.2 Specification of forecast error statistics

This section describes the multivariate, three-dimensional formulation of the forecast error covariance model.

5.2.7.2.1 Forecast height errors. The forecast height error covariance model is of the form

$$[\mathrm{Cov}]_{ij}^{(mn)} = \sigma_i^{(m)} \sigma_j^{(n)} \nu^{(mn)} \rho_{c\times c}(r_{ij}; L^{(m)}, L^{(n)}). \tag{5.79}$$

The main features of this model are:

1. the height error variances are three-dimensional, spatially variable fields which are updated on-line;
2. the correlation model has compact support;
3. correlations are horizontally isotropic (correlations at fixed pressure levels depend on distance only);
4. the model is non-separable (horizontal de-correlation length scales may vary with pressure).

The length scale parameters $L^{(m)}$ in the model (5.79) are estimated from single-level rawinsonde height O-F's. The vertical correlation coefficients $\nu^{(mn)}$ are estimated from multi-level rawinsonde height O-F's. The forecast height error standard deviations σ are estimated from global time series of TOVS height retrievals, as follows.

5.2.7.2.1.1 Specification of height error variances

The height forecast error variances are again estimated from observed-minus-forecast residuals (O-F's). The maximum-likelihood methodology described earlier provides spatially averaged estimates of the forecast variances valid at the tuning region, usually North America. In order to account for the regional variability of the forecast error variances, we use global residual time series instead.

We start by binning the residuals on a 4° by 5° latitude-longitude grid, computing mean and standard deviations for each grid-box. This calculation is performed separately for radiosonde height observations (RAOB) and NESDIS TOVS A/B retrievals (TOVS). For those grid-boxes with more than 10 radiosonde observations in a given month, we assume

$$\left(\sigma_j^{f|h}\right)^2 \approx \left(s_j^{RAOB}\right)^2 - \left(\sigma^{RAOB}\right)^2 \tag{5.80}$$

where s_j^{RAOB} is the radiosonde O-F standard deviation for grid-box j at a given level (we have omitted the vertical level index (m) for notational convenience), and σ^{RAOB} is the radiosonde observation error standard deviation, tuned over North America and assumed constant over the globe. We have also assumed statistical independence of forecast and observation errors. Because radiosonde coverage is mostly restricted to the northern hemisphere land areas, the only hope for obtaining a global estimate of forecast error variances is to use satellite observations. The TOVS O-F variance can be written

$$\left(s_j^{TOVS}\right)^2 = \left(\sigma_j^{f|h}\right)^2 + \left(\sigma_u^{TOVS}\right)^2 + \left(\sigma_c^{TOVS}\right)^2 - 2x_j \tag{5.81}$$

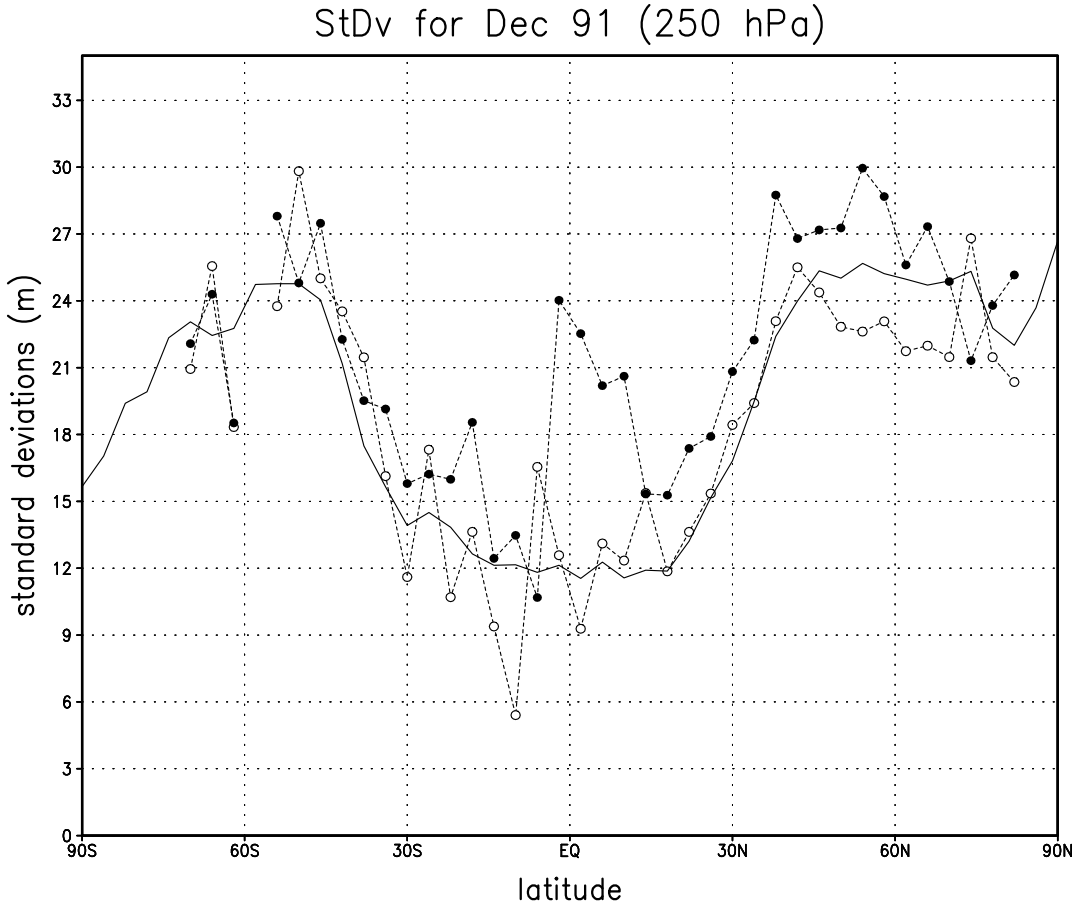

Figure 5.10: Square-root of zonal average of forecast height error variances estimated from radiosondes (eq. 5.80, open circles), modified TOVS height innovation variances ($\left(s_j^{TOVS}\right)^2 - \left(\sigma_u^{TOVS}\right)^2$, closed circles), and forecast height error variances estimated from TOVS (eq. 5.82, solid line). Monthly means for December 1991, at 250 hPa. Units: meters

where $\sigma_u^{TOVS}, \sigma_c^{TOVS}$ are the standard deviations of the spatially uncorrelated and correlated components of the retrieval error, respectively (see section 5.2.7.3.2 below), and x_j is the cross-covariance between the retrieval and forecast errors at locations i and j. Da Silva *et al.* (1996) present a method for estimating each term on the RHS of (5.81); however these estimates are only valid regionally. Terms such as σ_c^{TOVS} and x_j are likely to vary spatially as much as the forecast error standard deviation itself; the uncorrelated portion of the retrieval error, σ_u^{TOVS}, has been verified to have a modest variation over the globe. In view of this, we adopt the following parameterization for $\sigma_j^{f|h}$ in terms of TOVS O-F's:

$$\left(\sigma_j^{f|h}\right)^2 \approx \kappa^2(\varphi_j)\left[\left(s_j^{TOVS}\right)^2 - \left(\sigma_u^{TOVS}\right)^2\right] + d \tag{5.82}$$

where κ is an empirical function of latitude defined by

$$\kappa^2(\varphi_j; a, b, c) = a \exp\left[-(\varphi_j/b)^2\right] + c, \tag{5.83}$$

and a, b, c, d are constants. These four parameters are determined separately for each vertical level by means of a non-linear least-square fit of the model (5.80) to co-located radiosonde estimates of $\left(\sigma_j^{f|h}\right)^2$, obtained from (5.80). Once model parameters (a, b, c, d) are determined for each level (levels above 20 hPa use the same value of the parameters at 20 hPa), forecast error variances determined from radiosondes and TOVS retrievals are merged together and smoothed with a simple successive correction method. An example of zonally averaged forecast error standard deviations obtained by this procedure is shown in Fig. 5.10.

As discussed in subsection (5.2.6), unless forecast bias is explicitly accounted for, the forecast error variances must be inflated based on an estimate of this bias. A zonally symmetric estimate of the time-averaged forecast error can be obtained by fitting the model

$$b^f(\varphi_j; a, b, c, d) = a \exp\left[-\left(\frac{\varphi_j - d}{b}\right)^2\right] + c \tag{5.84}$$

to gridded, zonal-time mean radiosonde O-F's, for each level. An example of such a fitted forecast bias model is shown in Fig. 5.11. The final three-dimensional gridded field of forecast error variances used by PSAS is:

$$\left(\overline{\sigma}_j^{f|h}\right)^2 = \left(\sigma_j^{f|h}\right)^2 + \left(b^f(\varphi_j)\right)^2 \tag{5.85}$$

Running monthly means of O-F standard deviations are re-computed on a daily basis, model parameters re-tuned, and $\overline{\sigma}_j^{f|h}$ updated. Although model parameters are robust and do not change much on a daily basis, this adaptive system is capable of capturing the seasonal cycle in the forecast error variances and to automatically keep up with modifications made in the data assimilation system.

5.2.7.2.2 Forecast wind errors. The multivariate height-wind covariance formulation is based on the following model for wind errors. Denoting the wind error field by u, v, it is assumed that

$$\begin{bmatrix} u \\ v \end{bmatrix} = \begin{bmatrix} u_h \\ v_h \end{bmatrix} + \begin{bmatrix} u_d \\ v_d \end{bmatrix} \tag{5.86}$$

where u_h, v_h is the height-coupled wind error component (correlated with height errors) and u_d, v_d is the height-decoupled wind error component (statistically independent from height errors). The two wind error components are assumed mutually independent, and a separate model exists for each.

5.2.7.2.2.1 Height-coupled wind error component

The height-coupled wind error component is modeled by assuming a linear relationship of the form

$$\begin{bmatrix} u_h \\ v_h \end{bmatrix} = \frac{g}{2\Omega} \begin{bmatrix} a_{11}(\varphi, p) & a_{12}(\varphi, p) \\ a_{21}(\varphi, p) & a_{22}(\varphi, p) \end{bmatrix} \begin{bmatrix} \frac{\partial h}{\partial x} \\ \frac{\partial h}{\partial y} \end{bmatrix} \tag{5.87}$$

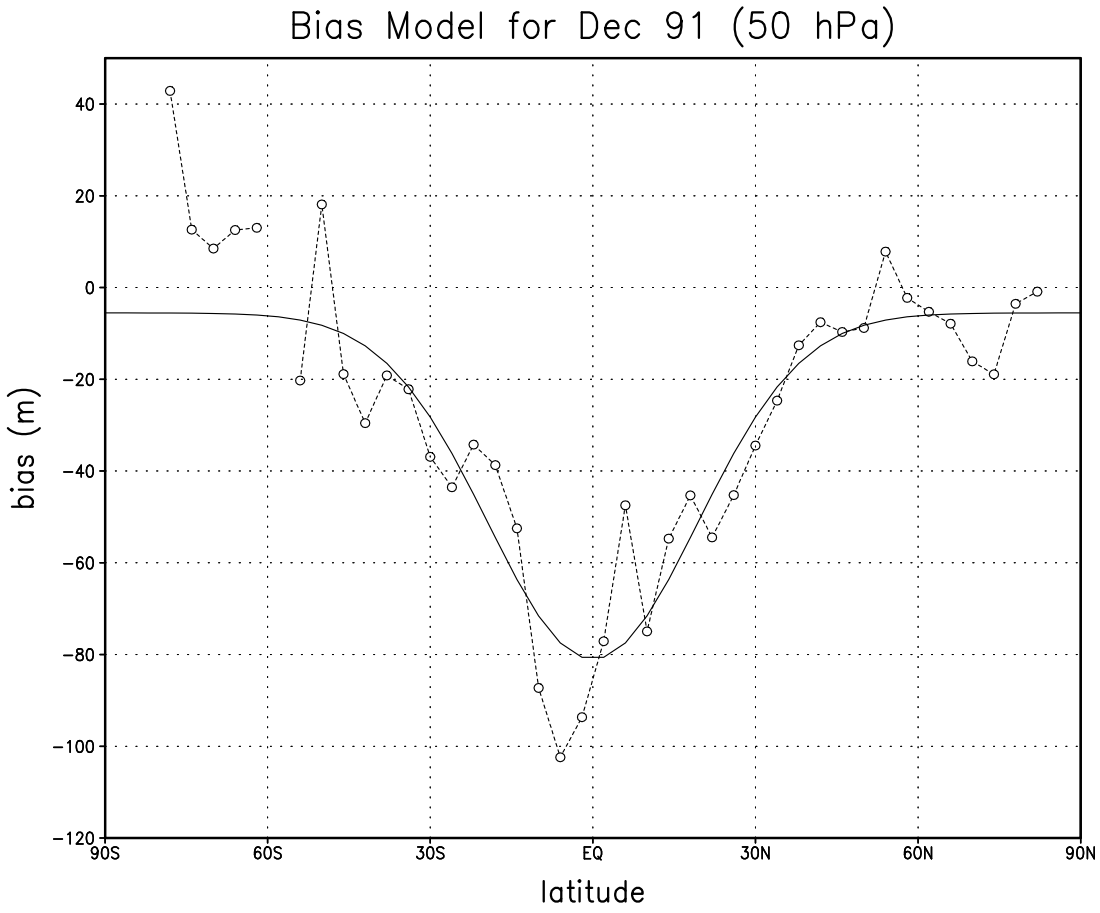

Figure 5.11: Monthly means for December 1991 of radiosonde height innovations at 50 hPa (open circles), and zonally symmetric fit (solid line). Units: meters

The coefficients a_{ij} are parameterized by

$$a_{11} = a_{22} = \frac{-c_0^{(m)}\epsilon(\varphi,p)}{\epsilon^2(\varphi,p)+\sin^2(\varphi)} \tag{5.88}$$

$$-a_{12} = a_{21} = \frac{sin(\varphi)}{\epsilon^2(\varphi,p)+\sin^2(\varphi)} \tag{5.89}$$

where

$$\epsilon^2(\varphi,p) = c_1^{(m)} \exp\left[-\left(\frac{\varphi}{c_2^{(m)}}\right)^2\right]. \tag{5.90}$$

Note that $\epsilon(\varphi,p)$ for $p = p_m$ fixed attains a maximum value of $c_1^{(m)}$ at the equator, and decays exponentially away from the equator. When $\epsilon \to 0$, the model (5.87) reduces to the geostrophic balance relation. The values of the model parameters $c_0^{(m)}, c_1^{(m)}, c_2^{(m)}$ are obtained by regression to a time-series of 48h-24h forecast residuals.

Given the height error covariance (5.79), the model (5.87) completely determines the multivariate height-coupled wind error covariance.

5.2.7.2.2.2 Height-decoupled wind error component

The height-decoupled wind error component is modeled in terms of a stream function ψ and a velocity potential χ by

$$\begin{bmatrix} u_d \\ v_d \end{bmatrix} = \begin{bmatrix} -\frac{\partial \psi}{\partial y} + \frac{\partial \chi}{\partial x} \\ \frac{\partial \psi}{\partial x} + \frac{\partial \chi}{\partial y} \end{bmatrix} \tag{5.91}$$

The stream function and velocity potential are assumed mutually independent, and the covariance model for each is of the form

$$[\mathrm{Cov}]_{ij}^{(mn)} = \sigma^{(m)}\sigma^{(n)}\nu^{(mn)}\rho_{c\times c}(r_{ij}; L^{(m)}, L^{(n)}). \tag{5.92}$$

The model parameters $\sigma^{(m)}, L^{(m)}$ for both stream function and velocity potential are estimated from single-level rawinsonde height and wind O-F's. The vertical correlation coefficients $(\nu)^{(mn)}$ for both stream function and velocity potential are estimated from multi-level rawinsonde height and wind O-F's.

5.2.7.2.3 Forecast moisture errors. The forecast moisture error covariance model is of the form

$$[\mathrm{Cov}]_{ij}^{(mn)} = (\sigma^{(m)})^2\delta(m-n)\rho_c(r_{ij}; L^{(m)}). \tag{5.93}$$

The main features of this model are:

1. the variances are constant at each pressure level;
2. correlations have compact support;
3. correlations are horizontally isotropic, i.e. at fixed pressure levels;
4. horizontal de-correlation length scales vary in the vertical direction.

The model parameters $\sigma^{(m)}, L^{(m)}$ are estimated from rawinsonde mixing ratio observations.

5.2.7.3 Specification of observation error statistics

5.2.7.3.1 Rawinsonde errors. Rawinsonde errors are assumed to be vertically correlated but uncorrelated in the horizontal direction. Height, wind, and moisture observation errors are assumed independent of each other. Each of the univariate rawinsonde observation error covariance models are of the form

$$[\mathrm{Cov}]_{ij}^{(mn)} = \sigma^{(m)}\sigma^{(n)}\nu^{(mn)}\delta(r_{ij}). \tag{5.94}$$

Height error observation error standard deviations are estimated from single-level rawinsonde height O-F's; the vertical correlation coefficients are estimated from multi-level rawinsonde height O-F's. Similarly, the error statistics for mixing ratio observations are estimated from rawinsonde mixing ratio O-F's. Wind observation error statistics are estimated from multivariate (height and wind) O-F's.

5.2.7.3.2 TOVS height retrieval errors. TOVS height retrieval errors are assumed to consist of two components, one of which is horizontally uncorrelated. The covariance model is of the form

$$[\mathrm{Cov}]_{ij}^{(mn)} = \sigma_u^{(m)}\sigma_u^{(n)}\nu_u^{(mn)}\delta(r_{ij}) + \sigma_c^{(m)}\sigma_c^{(n)}\nu_c^{(mn)}\rho_c(r_{ij}; L^{(m)}). \tag{5.95}$$

The main features of this model are:

1. height retrieval errors contain a component which is horizontally uncorrelated;
2. the retrieval error standard deviations are constant at each pressure level;
3. the correlation model has compact support;
4. correlations are horizontally isotropic: correlations at fixed pressure levels depend on distance only;
5. horizontal de-correlation length scales vary in the vertical direction.

The parameters $\sigma_u^{(m)}$ are estimated from single-level retrieval O-F's. The vertical correlation coefficients $\nu_u^{(mn)}$ are estimated from multi-level retrieval O-F's. The parameters $\sigma_c^{(m)}, L^{(m)}$ are estimated from single-level co-located retrieval-minus-rawinsonde observations (O-O's). The vertical correlation coefficients $\nu_c^{(mn)}$ are estimated from multi-level co-located retrieval-minus-rawinsonde O-O's.

Details of this procedure are described in da Silva *et al.* (1996), where it is also shown how the tuning methodology can be applied to the estimation of the cross-covariance between forecast and observation errors.

5.3 The GEOS-2 General Circulation Model

5.3.1 Introduction and Model Lineage

The Goddard Earth Observing System-2 (GEOS-2) General Circulation Model (GCM) is an incremental development of the GEOS-1 GCM. The develop paths have been chosen based on the major Earth-science priorities discussed in Chapter 2.0 as well as the experience gained in both model and data assimilation applications. Many of the changes made in GEOS-2 are in preparation for extended capabilities in GEOS-3. Major GEOS-3 developments will focus on the implementation of an interactive land-surface model and prognostic cloud water parameterization. These improvements are driven not only by the need to improve cloud and hydrological processes, but the need to monitor and assimilate new data types.

Unlike the development of PSAS and the associated error statistics, much of the GCM development is linked with other modeling efforts within Goddard. While this potentially saves resources by leveraging off of existing expertise, it is not without cost. Often seemingly appropriate algorithms are not easily integrated into the GEOS GCM. This can occur because the native model in which the algorithm was developed has its own set of compensating errors, for which the algorithm has been explicitly or implicitly tuned. Sometimes the software engineering of candidate algorithms is so poor that it is easier to start an independent development rather than implement foreign code. In addition, the management structure of GSFC is not conducive for entraining non-DAO scientists into a product- and time- driven development. It is one of the management goals of the DAO to develop a model infrastructure that facilitates inside and outside collaboration. The GEOS model and analysis system must become a resource that attracts visiting scientists and outside experts, if the GEOS DAS is to achieve its full potential.

The GEOS-2 GCM was developed by the Data Assimilation Office (DAO) at the Goddard Laboratory for Atmospheres (GLA), in collaboration with the Climate and Radiation Branch, for use in the system being developed to analyze EOS data. Based on extensive analysis and evaluation of the GEOS-1 system (see Takacs and Suarez (1996), Molod et al. (1996), Schubert et al. (1995), Schubert and Rood (1995)), the GEOS-2 GCM addresses some of the fundamental limitations of GEOS-1. The GEOS-2 GCM also provides the next benchmark and infrastructure base in the DAO's effort to develop the GEOS-3 system for the EOS observing period. Development advances of the GEOS-2 GCM relative to the GEOS-1 GCM will be specifically highlighted at the beginning of the appropriate sections.

As noted, the immediate predecessor of the GEOS-2 GCM was the GEOS-1 GCM which was used to produce a multi-year global atmospheric data set for climate research (Schubert et al., 1993). The GEOS-1 GCM was also used to produce multiple 10-year climate simulations as part of the DAO's participation in the Atmospheric Model Intercomparison Project (AMIP) sponsored by the Program for Climate Model Diagnostics and Intercomparison (PCMDI) (see Gates, 1992). A stratospheric version of the GEOS DAS (Version 1.2) has been used operationally to provide scientific flight guidance during NASA's participation in the Measurements for Assessing the Effects of Stratospheric Aircraft (MAESA) and other field experiments.

The earliest predecessor of the GEOS-1 GCM was developed in 1989 based on the

"plug- compatible" concepts outlined in Kalnay et al. (1989), and subsequently improved in 1991 (Fox- Rabinovitz, et al., 1991, Helfand et al., 1991). The plug-compatibility of the physical parameterizations together with the plug-compatible "Dynamical Core" introduced by Suarez and Takacs (1995) facilitate the development and testing of new algorithms. Together the DAO and the Climate and Radiation Branch at GLA have produced a library of physical parameterizations and dynamical algorithms which can be utilized for various GCM applications.

Relevant Model Documentation

Descriptions of aspects of the the GEOS Data Assimilation System (DAS) may be found in Schubert et al. (1993), Pfaendtner et al. (1995) and Bloom et al. (1996). The GEOS-1 GCM is documented in Takacs et al. (1994), and for completeness much of the GEOS-1 documentation is included here to provide a self-contained report of the GEOS-2 GCM. A comprehensive documentation of the Aries/GEOS Dynamical Core incorporating the horizontal and vertical discretization and finite-difference schemes used is given in Suarez and Takacs (1995). The Relaxed Arakawa-Schubert cumulus convective parameterization and the re-evaporation of falling rain are based upon the works of Moorthi and Suarez (1992) and Sud and Molod (1988). The longwave radiative processes are described by Chou and Suarez (1994) and the shortwave by Chou (1990) and Chou (1992). The turbulence parameterization is based on the Level 2.5 second order closure scheme of Helfand and Labraga (1988), and the surface layer parameterization in described in Helfand and Schubert (1995). The gravity wave drag parameterization is based on Zhou et al. (1996).

5.3.2 Atmospheric Dynamics

The momentum equations used in the GEOS-2 GCM are written in the "vector invariant" form, as in Sadourney (1975) and Arakawa and Lamb (1981), to facilitate the derivation of the energy and potential enstrophy conserving differencing scheme. The thermodynamic (potential temperature) and moisture (specific humidity) equations are written in flux form to facilitate potential temperature and moisture conservation. A complete description of the finite-difference scheme used can be found in Suarez and Takacs (1995).

The GEOS GCM uses a σ coordinate defined by

$$\sigma = \frac{p - p_T}{\pi}, \tag{5.96}$$

where p is the pressure, $\pi \equiv p_s - p_T$, p_s is the surface pressure, and p_T is a constant prescribed pressure at the top of the model atmosphere. With $p_T = 0$ this coordinate reduces to the conventional σ coordinate proposed by Phillips (1957).

With this vertical coordinate, the continuity equation becomes

$$\frac{\partial \pi}{\partial t} = -\nabla_\sigma \cdot (\pi \mathbf{v}) - \frac{\partial (\pi \dot{\sigma})}{\partial \sigma}, \tag{5.97}$$

where $\mathbf{v}$ is the horizontal velocity vector. Integrating (5.97) and assuming $\dot{\sigma} = 0$ at $p = p_s$

and $p = p_T$, we obtain the forms used in the model:

$$\frac{\partial \pi}{\partial t} = -\int_0^1 \nabla_\sigma \cdot (\pi \mathbf{v})\, d\sigma \tag{5.98}$$

and

$$(\pi \dot{\sigma}) = -\sigma \frac{\partial \pi}{\partial t} - \int_0^\sigma \nabla_\sigma \cdot (\pi \mathbf{v})\, d\sigma. \tag{5.99}$$

The equation of state for an ideal gas is $\alpha = RT/p$, where α is the specific density, T is the temperature, and R is the gas constant. The following alternative forms will be used below

$$\alpha = R\theta \frac{P}{p} = c_p \theta \frac{\partial P}{\partial p} = \frac{c_p \theta}{\pi} \left(\frac{\partial P}{\partial \sigma} \right)_\pi = \frac{c_p \theta}{\sigma} \left(\frac{\partial P}{\partial \pi} \right)_\sigma , \tag{5.100}$$

where $\theta \equiv T/P$ is the potential temperature, $P \equiv (p/p_0)^\kappa$, $\kappa = R/c_p$, c_p is the specific heat at constant pressure, and p_0 is a reference pressure. In obtaining the forms in (5.100) we have used $\frac{\partial P}{\partial p} = \kappa \frac{P}{p}$ and the relation

$$\left(\frac{dP}{d\sigma} \right)_\pi = \frac{\pi}{\sigma} \left(\frac{dP}{d\pi} \right)_\sigma . \tag{5.101}$$

For the time being virtual effects are neglected.

The hydrostatic equation is

$$\frac{\partial \Phi}{\partial p} = -\alpha,$$

where Φ is the geopotential. Using (5.100) and (5.101), this can be written:

$$\frac{\partial \Phi}{\partial \sigma} = -\pi\alpha = -c_p \theta \frac{\pi}{\sigma} \left(\frac{dP}{d\pi} \right)_\sigma = -c_p \theta \left(\frac{dP}{d\sigma} \right)_\pi . \tag{5.102}$$

From (5.102) we obtain

$$\frac{\partial \Phi}{\partial P} = -c_p \theta, \tag{5.103}$$

which, following Arakawa and Suarez (1983), is the form used in the model.

The momentum equation is written in "vector-invariant" form, as in Sadourney (1975) and Arakawa and Lamb (1981), to facilitate the derivation of an energy- and enstrophy-conserving differencing scheme:

$$\frac{\partial \mathbf{v}}{\partial t} = -(f + \zeta)\, \mathbf{k} \times \mathbf{v} - \dot{\sigma} \frac{\partial \mathbf{v}}{\partial \sigma} - \nabla_\sigma (\Phi + K) - c_p \theta\, \nabla_\sigma P - \frac{g}{\pi} \frac{\partial \mathcal{T}}{\partial \sigma}, \tag{5.104}$$

$$= -\eta\, \mathbf{k} \times (\pi \mathbf{v}) - \dot{\sigma} \frac{\partial \mathbf{v}}{\partial \sigma} - \nabla_\sigma (\Phi + K) - c_p \theta \left(\frac{dP}{d\pi} \right)_\sigma \nabla \pi - \frac{g}{\pi} \frac{\partial \mathcal{T}}{\partial \sigma}, \tag{5.105}$$

where

$$\eta = \frac{(f+\zeta)}{\pi}$$

is an "external" potential vorticity, f is the Coriolis parameter, $\mathbf{k}$ is the unit vector in the vertical,

$$\zeta \equiv \nabla_\sigma \times \mathbf{v}$$

is the vertical component of the vorticity along σ surfaces,

$$K \equiv \frac{1}{2}(\mathbf{v} \cdot \mathbf{v})$$

is the kinetic energy per unit mass, g is the acceleration of gravity, and $\mathcal{T}$ is the horizontal frictional stress.

The thermodynamic equation is written in flux form to facilitate the derivation of a θ-conserving differencing scheme:

$$\frac{\partial(\pi\theta)}{\partial t} = -\nabla_\sigma \cdot (\pi \mathbf{v}\theta) - \frac{\partial(\pi\dot{\sigma}\theta)}{\partial\sigma} + \frac{\pi\mathcal{Q}}{c_p P}, \tag{5.106}$$

where $\mathcal{Q}$ is the diabatic heating per unit mass.

In addition to the equations of motion, the Aries/GEOS Dynamical Core computes tendencies for an arbitrary number of atmospheric contituents, such as water vapor and ozone. These are also written in flux form:

$$\frac{\partial(\pi q^{(k)})}{\partial t} = -\nabla_\sigma \cdot (\pi \mathbf{v} q^{(k)}) - \frac{\partial(\pi\dot{\sigma}q^{(k)})}{\partial\sigma} + \pi\mathcal{S}^{(k)}, \tag{5.107}$$

where $q^{(k)}$ is the specific mass of the kth constituent, and $\mathcal{S}^{(k)}$ is its source per unit mass of air.

5.3.2.1 Horizontal and Vertical Discretization

The GEOS-2 GCM is constructed in the horizontal using the staggered Arakawa C-grid (see Figure 5.12) and employs Version 2 of the Aries/GEOS Dynamical Core for the finite-differencing algorithm. Important differences relative to GEOS-1 include

- fourth order horizontal differences instead of second order
- raising the model top to 0.01 hPa
- increasing the vertical resolution to 70 levels

The use of fourth order differencing substantially improves the phase propagation of synoptic scale waves. The raising of the model lid is directed at improving stratospheric descent over the winter pole and addressing the stratospheric cold pole problem. Increasing the number of level is directed at improving the representation of the planetary boundary layer, the troposphere at the altitude of the sub-tropical jet stream, and the stratosphere.

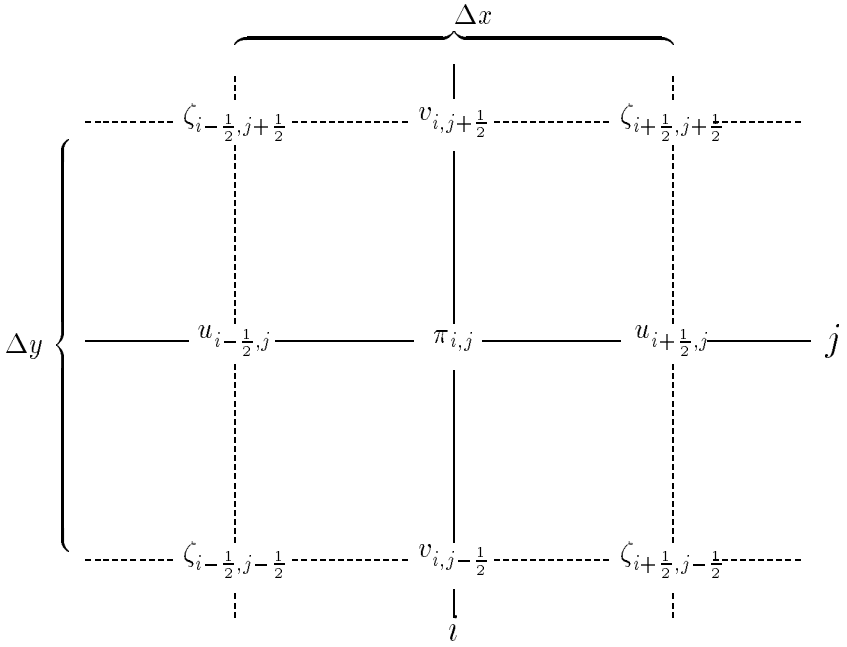

Figure 5.12: Stencil showing the position and indexing of the prognostic fields u, v, π, and ζ.

The Aries/GEOS Dynamical Core is a plug-compatible dynamics module which is used at both the DAO in the GEOS GCM as well as at the Climate and Radiation Branch in the Aries GCM. The Aries GCM has been extensively used in many climate and coupled ocean/atmosphere simulations (eg. Schubert et al. 1993, Higgins and Schubert, 1993). Version 2 of the Aries/GEOS Dynamical Core is a fourth-order version of the Sadourny energy and potential enstrophy conserving scheme described by Burridge and Haseler (1977), and is fully derived in Suarez and Takacs (1995). This scheme conserves total energy and potential enstrophy for the non-divergent component of the flow in the shallow water equations. It is fourth-order in the sense that it reduces to the fourth-order Arakawa (1966) Jacobian for non-divergent flow. It thus provides fourth-order accuracy for the advection of a second-order vorticity by the non-divergent part of the flow. Horizontal advection of potential temperature and moisture is performed using the fourth-order scheme in use in the UCLA GCM (Arakawa, personal communication). It also is fourth-order only in the advection by the non-divergent part of the flow.

The Aries/GEOS Dynamical Core uses a Lorenz or unstaggered vertical grid in generalized sigma coordinates (see Figure 5.13). The vertical differencing scheme is that of Arakawa and Suarez (1983) which ensures that:

- The pressure gradient force generates no circulation of vertically integrated momentum along a contour of surface topography
- The finite-difference analogues of the energy-conversion term have the same form in the kinetic energy and thermodynamic equations
- The global mass integral of the potential temperature is conserved under adiabatic processes

- The hydrostatic equation for the lowest thickness has a local form
- The hydrostatic equation is exact for vertically isentropic atmospheres
- The pressure-gradient force is exact for three-dimensionally isentropic atmospheres

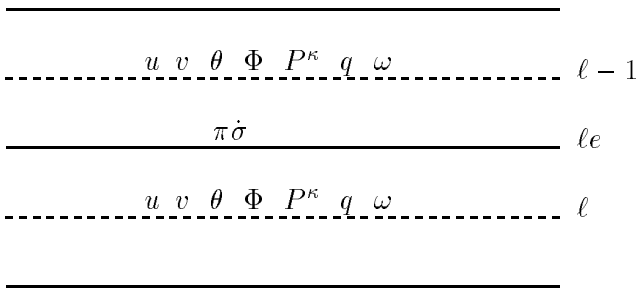

Figure 5.13: Vertical placement and index notation for sigma levels in the GEOS-2 GCM

The standard, or "production", resolution of the GEOS-2 GCM is a global 2° x 2.5° latitude-longitude grid in the horizontal, together with 70 sigma levels in the vertical. The vertical distribution of the sigma levels (shown in Table 5.2) is chosen to provide enhanced resolution in the planetary boundary layer and at the tropospheric jet level, as well as providing a well resolved stratosphere. The model top pressure used in this configuration is set at 0.01 hPa. Figure 5.14 shows the distribution of levels based on 1000 hPa surface pressure. The logarithm of pressure and Δpressure are used to show detail in the upper levels. There are 8 levels within the lowest 100 hPa, and approximately 40 levels below 10 hPa (note, GEOS-1 had 2 and 20 levels, respectively). Figure 5.15 shows the distribution of the lowest 10 levels in detail.

5.3.2.2 Time Integration Scheme

The GEOS GCM has the ability to use the Matsuno time integration scheme or the Leapfrog time integration scheme together with an Asselin (1972) time filter. The GEOS-1 GCM multi-year simulations cited in Takacs and Suarez (1996) and Molod et al. (1996) used the Leapfrog time scheme together with the Asselin averaging parameter equal to 0.05. The GEOS-1 DAS multi-year Re-analysis used the Matsuno time scheme. The GEOS GCM employs a unique method for incorporating adjustments due to diabatic processes (ie, moist convection, radiation and turbulence) and the analysis increments during an assimilation. At every model time step, all prognostic fields are updated due to both dynamical and

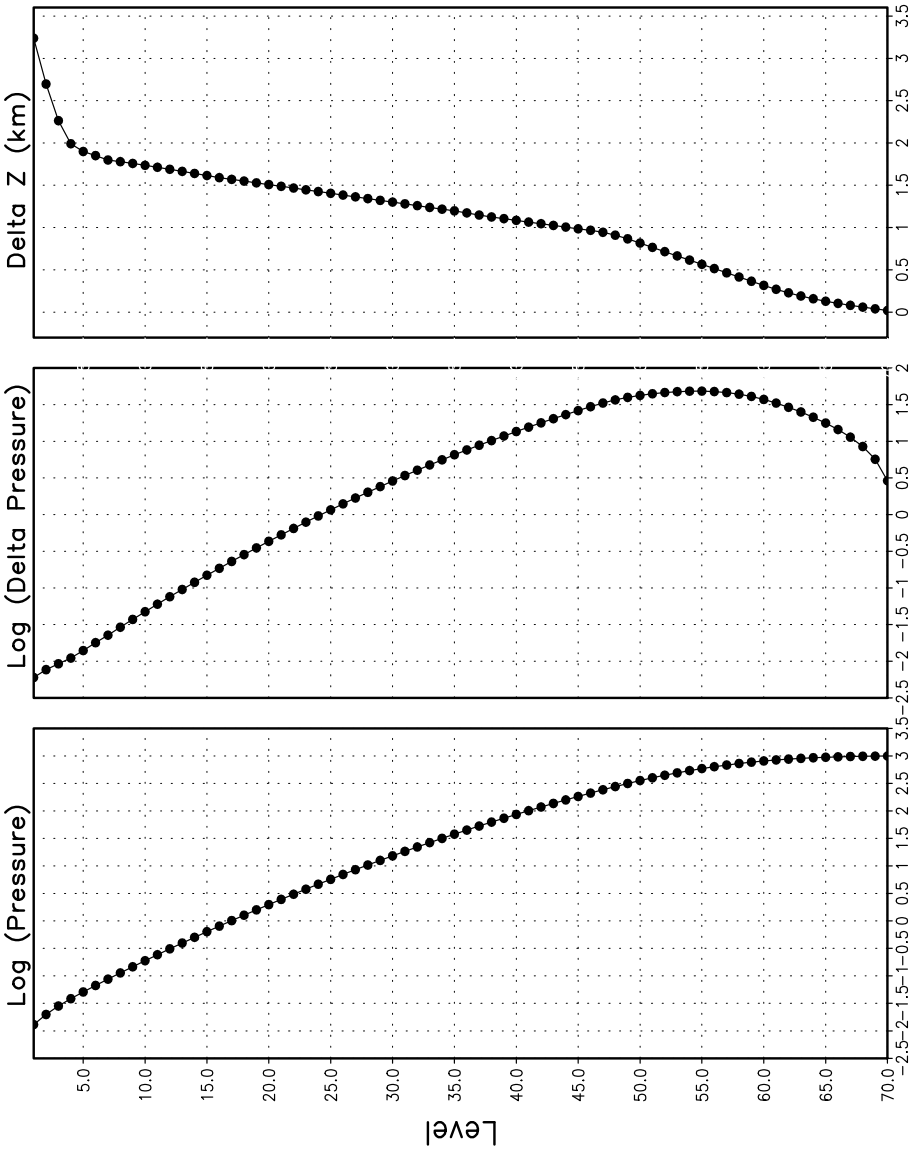

Figure 5.14: Vertical distribution used in the 70-level GEOS-2 GCM.

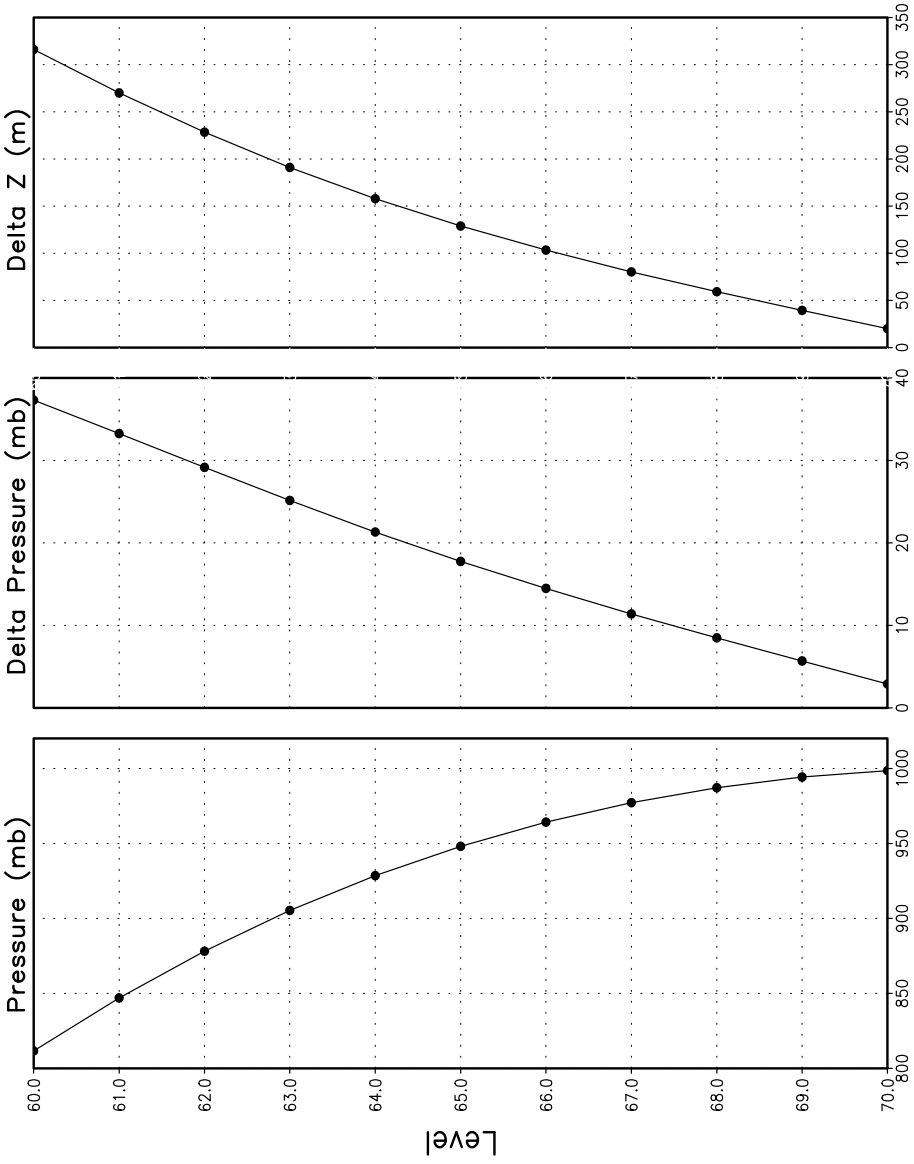

Figure 5.15: Vertical distribution used in the lowest 10 levels of the GEOS-2 GCM.

Table 5.2: GEOS-2 Sigma Level Distribution

Level	Sigma	Δ Sigma	Level	Sigma	Δ Sigma	Level	Sigma	Δ Sigma
1	.000003	.000006	25	.005699	.001162	49	.316175	.039790
2	.000010	.000008	26	.006982	.001402	50	.357260	.042380
3	.000018	.000009	27	.008526	.001687	51	.400740	.044580
4	.000028	.000011	28	.010381	.002022	52	.446215	.046370
5	.000041	.000014	29	.012600	.002416	53	.493218	.047635
6	.000057	.000018	30	.015247	.002878	54	.541227	.048384
7	.000077	.000023	31	.018394	.003416	55	.589634	.048431
8	.000103	.000029	32	.022123	.004042	56	.637724	.047750
9	.000136	.000037	33	.026527	.004767	57	.684748	.046297
10	.000179	.000047	34	.031710	.005600	58	.729920	.044048
11	.000232	.000060	35	.037793	.006566	59	.772457	.041026
12	.000300	.000076	36	.044898	.007644	60	.811635	.037330
13	.000386	.000095	37	.053147	.008854	61	.846935	.033270
14	.000494	.000120	38	.062692	.010237	62	.878157	.029174
15	.000628	.000149	39	.073724	.011825	63	.905322	.025156
16	.000795	.000185	40	.086444	.013616	64	.928565	.021330
17	.001003	.000230	41	.101065	.015626	65	.948115	.017770
18	.001261	.000285	42	.117817	.017877	66	.964250	.014500
19	.001579	.000352	43	.136943	.020375	67	.977200	.011400
20	.001971	.000433	44	.158715	.023170	68	.987150	.008500
21	.002453	.000531	45	.183425	.026250	69	.994248	.005695
22	.003043	.000649	46	.211400	.029700	70	.998548	.002905
23	.003763	.000791	47	.242900	.033300			
24	.004638	.000960	48	.277915	.036730			

sub-grid scale diabatic processes, shown schematically using the Leapfrog time scheme for an arbitrary prognostic field q as:

$$q^{n+1} = q^{n-1} + 2\Delta t \left(\frac{\partial q}{\partial t}^{n}\right)_{total} \tag{5.108}$$

where

$$\begin{aligned}\left(\frac{\partial q}{\partial t}^{n}\right)_{total} &= \left(\frac{\partial q}{\partial t}^{n}\right)_{Dynamics} + \left(\frac{\partial q}{\partial t}^{n-1}\right)_{Shapiro\ Filter} \\ &+ \left(\frac{\partial q}{\partial t}\right)_{Moist\ Processes} + \left(\frac{\partial q}{\partial t}\right)_{Turbulence} + \left(\frac{\partial q}{\partial t}\right)_{GravityWaveDrag}\end{aligned}$$

$$+ \left(\frac{\partial q}{\partial t}\right)_{Longwave\ Radiation} + \frac{S_0}{R_a^2} \cdot cos\phi_z \left(\frac{\partial q}{\partial t}\right)_{Shortwave\ Radiation}$$
$$+ \left(\frac{\partial q}{\partial t}\right)_{Analysis\ Increment} \tag{5.109}$$

with S_0 defined as the solar contant, R_a as the earth-sun distance in Astronomical Units, and $cos\phi_z$ as the cosine of the zenith angle. The Dynamics and Shapiro Filter time tendencies are updated every model time step using the time index indicated in (5.109). The diabatic time tendencies are updated at a time step appropriate to the physical parameterizations using the current time index, and are held constant between Physics calls. The time tendency for Moist Convection is updated every 10 minutes, and for Turbulence every 30 minutes. The time tendency for Longwave Radiation is updated every 3 hours. Shortwave Radiation is updated once every three hours assuming a normalized incident solar radiation, and adjusted at every model time step by the true incident radiation. During GEOS-2 DAS assimilations, the Analysis Increment is updated every synoptic time period, or 6 hours. By gradually incorporating the diabatic adjustments during the model integration, shocks and dynamical imbalances are greatly reduced (cf. Bloom, et al. 1996).

5.3.2.3 Coordinate Rotation

In GEOS-2 the capability to perform a coordinate rotation of the finite difference grid has added. This was implemented to address polar noise problems, especially in the stratosphere. In addition, the coordinate rotation is at the basis for adaptive resolution capabilities to provide the infrastructure for possible regional applications.

As previously mentioned, the Eulerian grid-point dynamics module used in the GEOS GCM is the Aries/GEOS Dynamical Core (Suarez and Takacs, 1995). This module allows the spherical coordinate system used for the computations to be displaced relative to the geographical latitude-longitude coordinates. The relation between the two coordinate systems is fully determined by specifying the coordinates of the geographical north pole in the computational system, which are denoted by $(\lambda_{NP}, \phi_{NP})$, and by a third parameter, λ_0, which represents a rotation about the geographical pole. These parameters are determined by the user, and are stored on the model restart as part of the model state description. The relation between the geographical and computational axes is shown schematically in Figure 5.16.

The only effect on the dynamical core of displacing the geographical pole away from the computational pole is on the form of the Coriolis parameter:

$$f = 2\Omega \sin\tilde{\phi} = 2\Omega \left[\cos\phi_{NP}\cos(\lambda - \lambda_{NP}) + \sin\phi_{NP}\sin\phi\right], \tag{5.110}$$

where $\tilde{\phi}$ is the geographical latitude and (λ, ϕ) are the computational longitude/latitude coordinates. Although there are no other references to quantities in geographical coordinates within the dynamical core, it is generally necessary to transform between the two grids when other specific processes are computed within a geographical framework (eg., physics, analysis, output). In the GEOS-2 GCM, bi-cubic interpolation is used for this transformation.

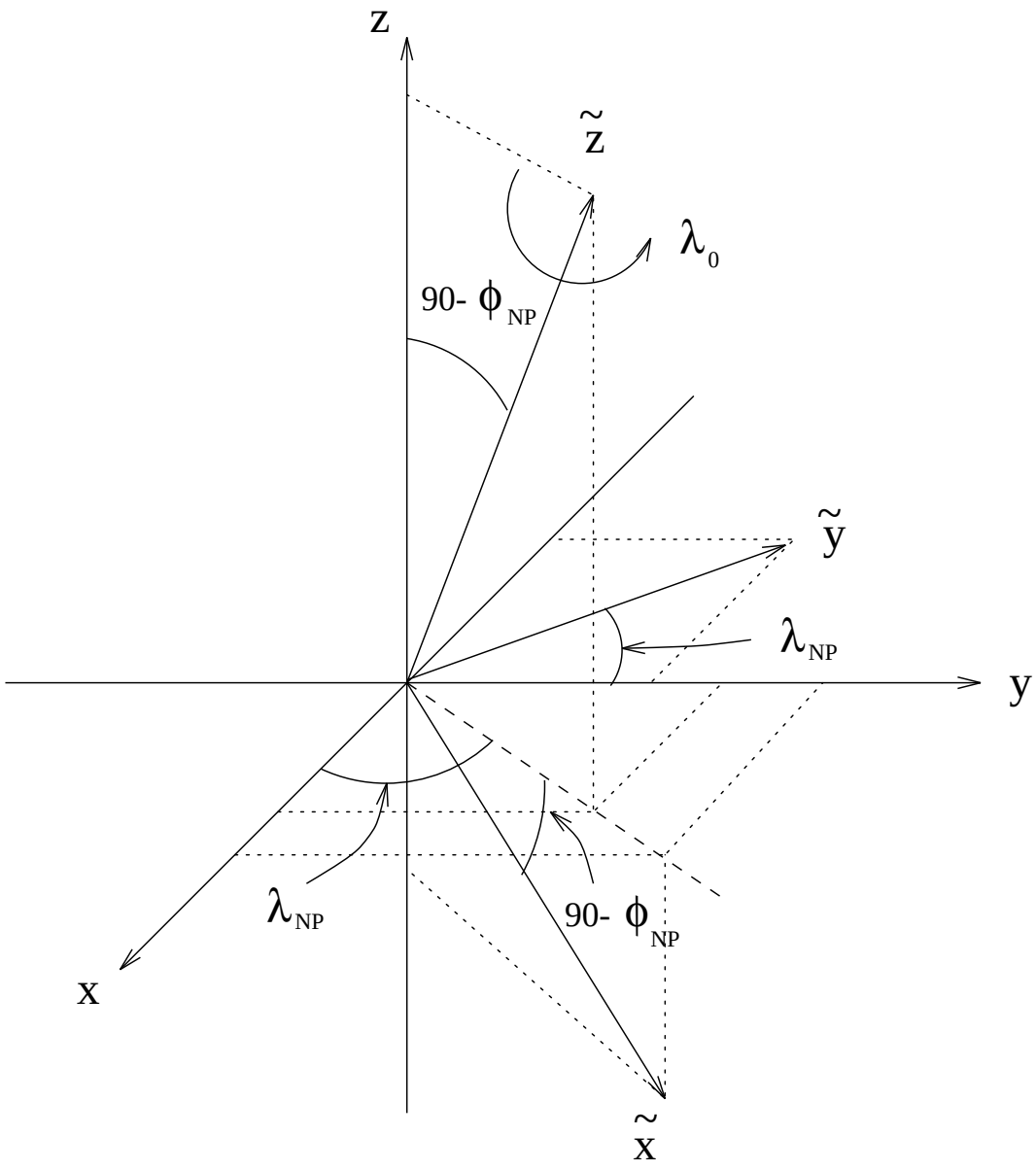

Figure 5.16: Rotation parameters used in the GEOS-2 GCM.

The use of coordinate rotation has had a profound affect on the quality of the GEOS stratospheric system. The momentum equations in the Aries/GEOS dynamical core are written in vector-invariant form. Inherent in many schemes of this type is the computational instability discussed by Hollingsworth et al. (1983). This instability arises from the non-cancellation in finite-difference form of the underlined terms illustrated in the following shallow water example:

$$\frac{\partial v}{\partial t} + \left(fu + u\frac{\partial v}{\partial x} - \underline{u\frac{\partial u}{\partial y}} \right) = -\underline{\frac{\partial}{\partial y}\left(\frac{1}{2}u^2\right)} - \frac{\partial}{\partial y}\left(\frac{1}{2}v^2 + gh\right) \tag{5.111}$$

An analysis of the linearized system shows that the instability is proportional to the mean zonal wind speed, U, and the coriolis parameter f. While this instability is easily controlled away from the poles by using a slightly modified kinetic energy formulation (see Suarez and Takacs, 1995, for details), variations of the scheme near the poles required from conservation constraints still result in polar noise when confronted with strong cross-polar flow. By rotating the computational grid to the geographic equator, however, the instability near the computational pole is removed due to the vanishing coriolis term. In addition, the geographic pole now using the transformed grid is also free of noise.

Figure 5.17 shows instantanious results at 1 hPa of wind speed, vorticity, and divergence from a 2° x 2.5° 70-level GEOS-DAS assimilation, using both the rotated (with the computational pole placed on the geophysical equator) and non-rotated systems. The plots are of the northern hemisphere from 50° N to 90° N.

It should be noted that placing the computational pole on the geophysical equator does cause a reduction in the accuracy at mid-latitudes. The physical area represented by the computational latitude/longitude grid is larger in mid- and high-latitudes than that of the non-rotated grid. Thus, in the region of maximum mid-latitude transports of heat and momentum by transient waves, the physical resolution is somewhat degraded. At 4° x 5° resolution, this degradation can be seen in the statistics related to the dynamical circulation and reveals itself as a "2nd-order" climate (ie., the climate simulated using the 2nd-order Aries/GEOS Dynamical Core). At higher resolutions (eg. 2° x 2.5°) and within data assimilation, no significant differences in the quality of the integrations have been revealed. Examination of propagation of tropical disturbances in model simulations show no apparent ill effect of the coordinate rotation. However, in the model simulation tropical variability is weak. Further evaluation in data assimilation applications is needed.

5.3.2.4 Smoothing / Filling

A Shapiro (1970) filter adjustment is computed for the winds, potential temperature, and specific humidity in order to globally damp small-scale dispersive waves. In order to reduce the dynamical imbalances generated by intermittent use of the full filter, a Shapiro filter tendency for any quantity q is defined as:

$$\left(\frac{\partial q}{\partial t}\right)_{Shapiro\ Filter} = \frac{q^F - q}{\tau} \tag{5.112}$$

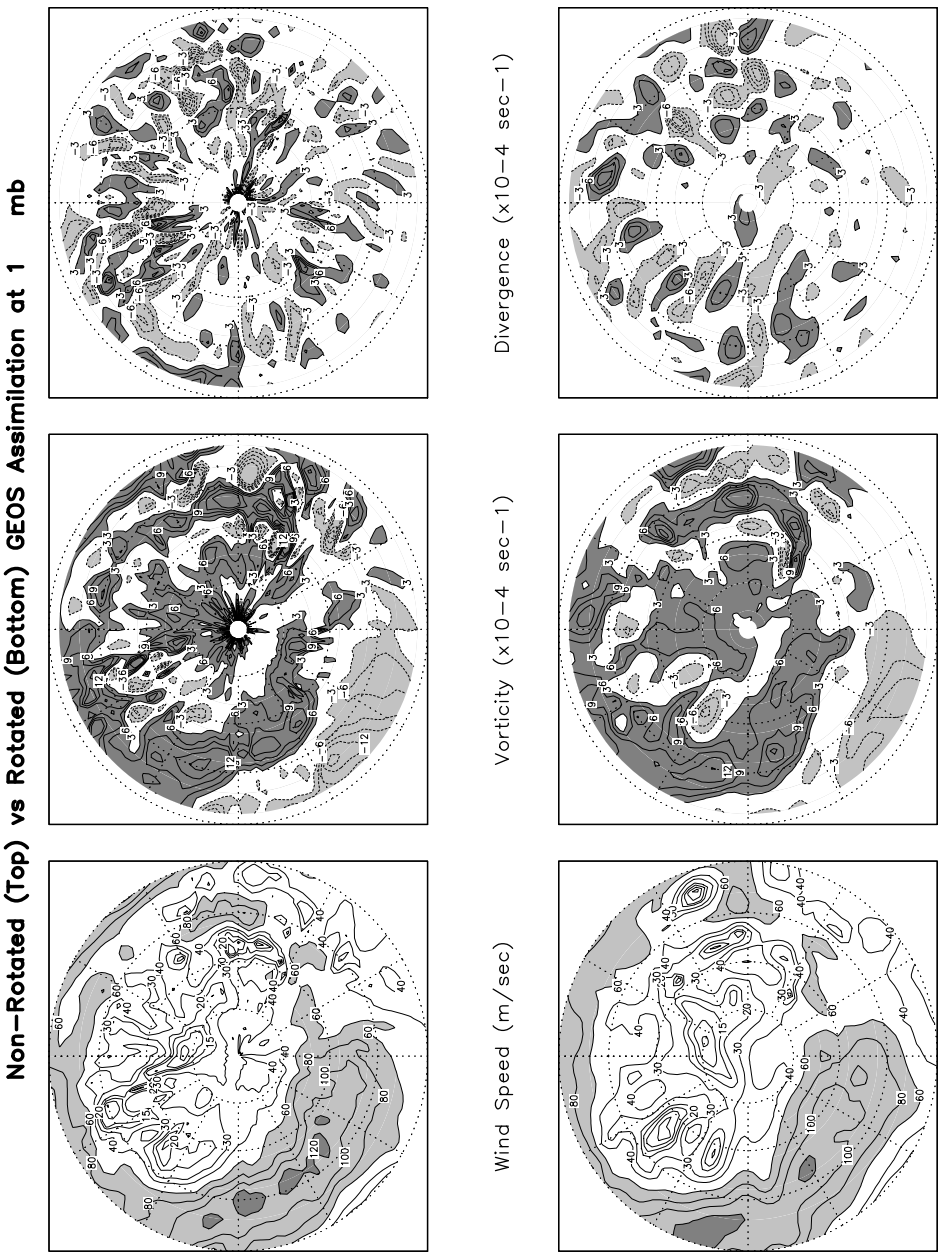

Figure 5.17: Wind Speed, Vorticity, and Divergence at 1 hPa using the rotated and non-rotated 2° x 2.5° 70-level GEOS DAS.

where q^F is the quantity after application of the full Shapiro filter, q is the unfiltered quantity, and τ is an adjustable time scale. Thus, a fraction $\frac{\Delta t}{\tau}$ of the full Shapiro filter is incorporated at each model timestep. In the GEOS-2 GCM, the time scale τ is equal to 1.5 hours, and has been chosen so as to remove the two-grid interval wave in about six hours. For the 2° x 2.5° x 70 level GEOS-2 GCM, an 8th-order Shapiro filter is used below 10 hPa and a 4th-order filter above. The response function of the 8th-order filter is shown in Figure 5.18. The GEOS-2 GCM also uses a high-latitude Fourier filter to avoid linear instability due to violation of the CFL condition for the Lamb wave and internal gravity waves near the poles. This polar filter is only applied to the time-tendencies of the prognostic fields, ie. winds, potential temperature, specific humidity, and surface pressure.

For the moisture equation, negative values computationally generated through advection are filled by "borrowing" from below while conserving the vertically integrated moisture, ie.,

$$\left(\int_{le+1}^{le-1} \rho q dz\right)_{final} = \left(\int_{le+1}^{le-1} \rho q dz\right)_{initial} . \tag{5.113}$$

Using the hydrostatic relation $\rho \delta z = -\frac{\delta p}{g} = -\frac{\pi}{g}\delta\sigma$, we may write

$$\left(\int_{le+1}^{le-1} \pi q d\sigma\right)_{final} = \left(\int_{le+1}^{le-1} \pi q d\sigma\right)_{initial} . \tag{5.114}$$

Approximating equaton (5.114) by

$$(\pi q_l \Delta\sigma_l + \pi q_{l-1}\Delta\sigma_{l-1})_{final} = (\pi q_l \Delta\sigma_l + \pi q_{l-1}\Delta\sigma_{l-1})_{initial} , \tag{5.115}$$

an expression for the updated moisture at level l is given by

$$\pi q_{l_{final}} = \left(\pi q_l + \pi q_{l-1}\frac{\Delta\sigma_{l-1}}{\Delta\sigma_l}\right)_{initial} - \left(\pi q_{l-1}\frac{\Delta\sigma_{l-1}}{\Delta\sigma_l}\right)_{final} . \tag{5.116}$$

Assuming that πq_{l-1} is initially negative, we require that its final value is set to zero. Thus

$$\begin{aligned} \pi q_{l-1_{final}} &= 0, \\ \pi q_{l_{final}} &= \left(\pi q_l + \pi q_{l-1}\frac{\Delta\sigma_{l-1}}{\Delta\sigma_l}\right)_{initial} . \end{aligned} \tag{5.117}$$

This process is repeated until the lowest level is reached. If the resulting πq_{nlay} is negative, the mass-weighted specific humidity in the lowest model level is simply set to zero.

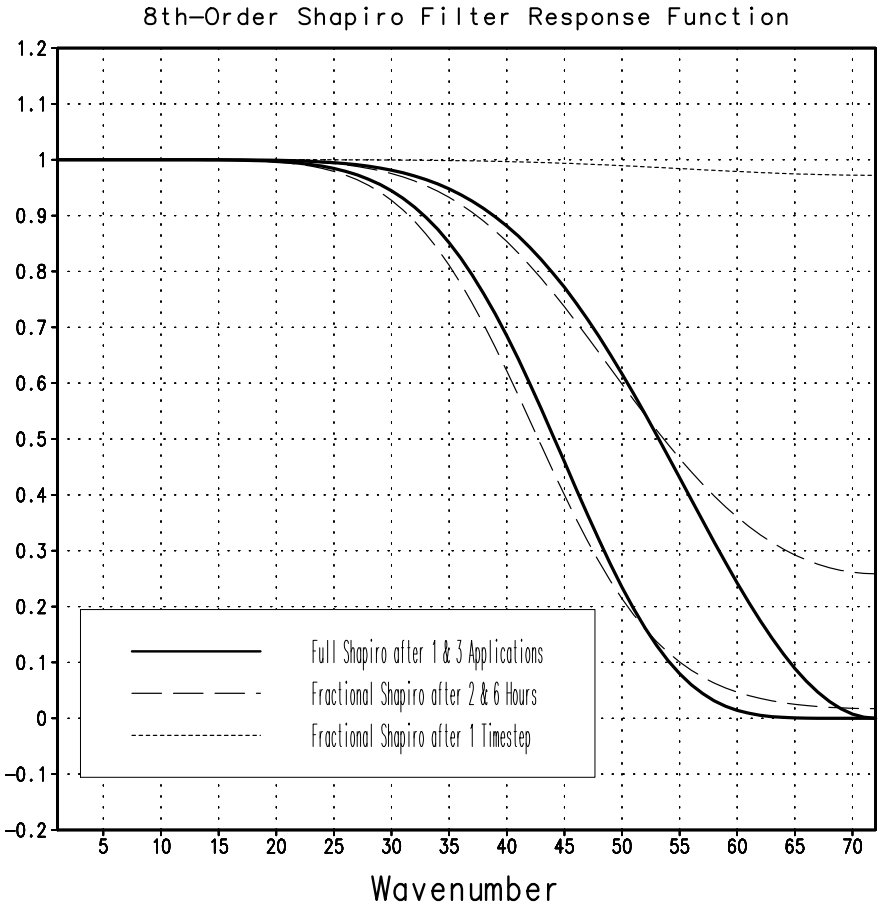

Figure 5.18: Shapiro filter response function used in the 2° x 2.5° GEOS-2 GCM.

5.3.3 Atmospheric Physics

5.3.3.1 Moist Convective Processes

5.3.3.1.1 Sub-grid and Large-scale Convection Sub-grid scale cumulus convection is parameterized using the Relaxed Arakawa Schubert (RAS) scheme of Moorthi and Suarez (1992), which is a linearized Arakawa Schubert type scheme. RAS predicts the mass flux from an ensemble of clouds. Each subensemble is identified by its entrainment rate and level of neutral bouyancy which are determined by the grid-scale properties.

The thermodynamic variables that are used in RAS to describe the grid scale vertical profile are the dry static energy, $s = c_pT + gz$, and the moist static energy, $h = c_pT + gz + Lq$. The conceptual model behind RAS depicts each subensemble as a rising plume cloud, entraining mass from the environment during ascent, and detraining all cloud air at the level of neutral buoyancy. RAS assumes that the normalized cloud mass flux, η, normalized by the cloud base mass flux, is a linear function of height, expressed as:

$$\frac{\partial \eta(z)}{\partial z} = \lambda \quad or \quad \frac{\partial \eta(P^\kappa)}{\partial P^\kappa} = -\frac{c_p}{g}\theta\lambda$$

where we have used the hydrostatic equation written in the form:

$$\frac{\partial z}{\partial P^\kappa} = -\frac{c_p}{g}\theta$$

The entrainment parameter, λ, characterizes a particular subensemble based on its detrainment level, and is obtained by assuming that the level of detrainment is the level of neutral buoyancy, ie., the level at which the moist static energy of the cloud, h_c, is equal to the saturation moist static energy of the environment, h^*. Following Moorthi and Suarez (1992), λ may be written as

$$\lambda = \frac{h_B - h^*_D}{\frac{c_p}{g}\int_{P_D}^{P_B} \theta(h^*_D - h)dP^\kappa},$$

where the subscript B refers to cloud base, and the subscript D refers to the detrainment level.

The convective instability is measured in terms of the cloud work function A, defined as the rate of change of cumulus kinetic energy. The cloud work function is related to the buoyancy, or the difference between the moist static energy in the cloud and in the environment:

$$A = \int_{P_D}^{P_B} \frac{\eta}{1+\gamma}\left[\frac{h_c - h^*}{P^\kappa}\right] dP^\kappa$$

where γ is $\frac{L}{c_p}\frac{\partial q^*}{\partial T}$ obtained from the Claussius Clapeyron equation, and the subscript c refers to the value inside the cloud.

To determine the cloud base mass flux, the rate of change of A in time *due to dissipation by the clouds* is assumed to approximately balance the rate of change of A *due to the*

generation by the large scale. This is the quasi-equilibrium assumption, and results in an expression for m_B:

$$m_B = \frac{-\left.\frac{dA}{dt}\right|_{ls}}{K}$$

where K is the cloud kernel, defined as the rate of change of the cloud work function per unit cloud base mass flux, and is currently obtained by analytically differentiating the expression for A in time. The rate of change of A due to the generation by the large scale can be written as the difference between the current $A(t + \Delta t)$ and its equillibrated value after the previous convective time step $A(t)$, divided by the time step. $A(t)$ is approximated as some critical A_{crit}, computed by Lord (1982) from *insitu* observations.

The predicted convective mass fluxes are used to solve grid-scale temperature and moisture budget equations to determine the impact of convection on the large scale fields of temperature (through latent heating and compensating subsidence) and moisture (through precipitation and detrainment):

$$\left.\frac{\partial \theta}{\partial t}\right|_c = \alpha \frac{m_B}{c_p P^\kappa} \eta \frac{\partial s}{\partial p}$$

and

$$\left.\frac{\partial q}{\partial t}\right|_c = \alpha \frac{m_B}{L} \eta \left(\frac{\partial h}{\partial p} - \frac{\partial s}{\partial p}\right)$$

where $\theta = \frac{T}{P^\kappa}$, $P = (p/p_0)$, and α is the relaxation parameter.

As an approximation to a full interaction between the different allowable subensembles, many clouds are simulated frequently, each modifying the large scale environment some fraction α of the total adjustment. The parameterization thereby "relaxes" the large scale environment towards equillibrium.

In addition to the RAS cumulus convection scheme, the GEOS-2 GCM employs a Kessler-type scheme for the re-evaporation of falling rain (Sud and Molod, 1988), which correspondingly adjusts the temperature assuming h is conserved. RAS in its current formulation assumes that all cloud water is deposited into the detrainment level as rain. All of the rain is available for re-evaporation, which begins in the level below detrainment. The scheme accounts for some microphysics such as the rainfall intensity, the drop size distribution, as well as the temperature, pressure and relative humidity of the surrounding air. The fraction of the moisture deficit in any model layer into which the rain may re-evaporate is controlled by a free parameter, which allows for a relatively efficient re-evaporation of liquid precipitate and larger rainout for frozen precipitation.

Due to the increased vertical resolution near the surface, the lowest model layers are averaged to provide a 50 hPa thick sub-cloud layer for RAS. Each time RAS is invoked (every ten simulated minutes), a number of randomly chosen subensembles are checked for the possibility of convection, from just above cloud base to 10 hPa.

Supersaturation or large-scale precipitation is initiated in the GEOS GCM whenever the relative humidity in any grid-box exceeds a critical value, currently 100 %. The large-scale precipitation re-evaporates during descent to partially saturate lower layers in a process identical to the re-evaporation of convective rain.

5.3.3.1.2 Cloud Formation Convective and large-scale cloud fractons which are used for cloud-radiative interactions are determined diagnostically as part of the cumulus and large-scale parameterizations. Convective cloud fractions produced by RAS are proportional to the detrained liquid water amount given by

$$F_{RAS} = \min\left[\frac{l_{RAS}}{l_c}, 1.0\right]$$

where l_c is an assigned critical value equal to 1.25 g/kg. A memory is associated with convective clouds defined by:

$$F^n_{RAS} = \min\left[F_{RAS} + (1 - \frac{\Delta t_{RAS}}{\tau})F^{n-1}_{RAS}, 1.0\right]$$

where F_{RAS} is the instantanious cloud fraction and F^{n-1}_{RAS} is the cloud fraction from the previous RAS timestep. The memory coefficient is computed using a RAS cloud timescale, τ, equal to 1 hour. RAS cloud fractions are cleared when they fall below 5 %.

Large-scale cloudiness is defined, following Slingo and Ritter (1985), as a function of relative humidity:

$$F_{LS} = \min\left[\left(\frac{RH - RH_c}{1 - RH_c}\right)^2, 1.0\right]$$

where

$$\begin{aligned}
RH_c &= 1 - s(1-s)(2 - \sqrt{3} + 2\sqrt{3}\,s)r \\
s &= p/p_{surf} \\
r &= \left(\frac{1.0 - RH_{min}}{\alpha}\right) \\
RH_{min} &= 0.75 \\
\alpha &= 0.573285.
\end{aligned}$$

These cloud fractions are suppressed, however, in regions where the convective sub-cloud layer is conditionally unstable. The functional form of RH_c is shown in Figure (5.19).

The total cloud fraction in a grid box is determined by the larger of the two cloud fractions:

$$F_{CLD} = \max[F_{RAS}, F_{LS}].$$

Finally, cloud fractions are time-averaged between calls to the radiation packages.

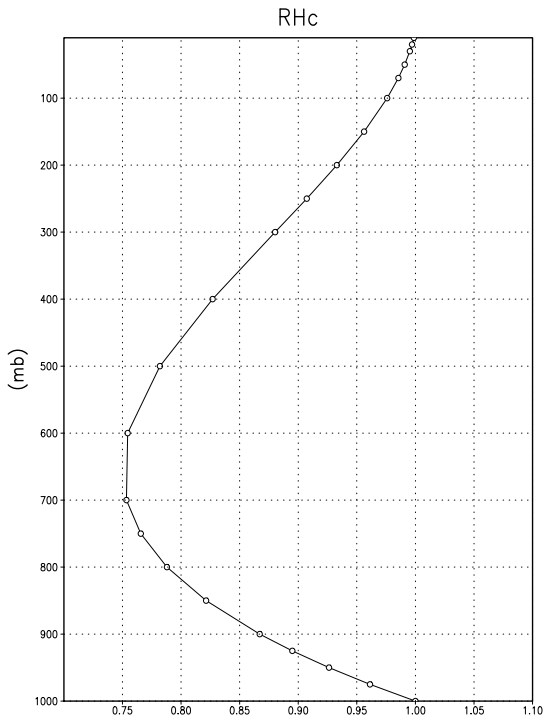

Figure 5.19: GEOS-2 GCM Critical Relative Humidity for Clouds.

5.3.3.2 Radiation

The parameterization of radiative heating in the GEOS-2 GCM includes effects from both shortwave and longwave processes. The radiation parameterization in GEOS-2 has been completely update from GEOS-1. The motivation for this was to improve the radiative transfer in the stratosphere and to model photosynthetically active radiation for the land-surface model. In addition the new radiative routine allows more accurate cloud radiative computations. Finally, the new radiation package is suitable for both aerosols and minor trace gases.

Radiative fluxes are calculated at each model edge-level in both up and down directions. The heating rates/cooling rates are then obtained from the vertical divergence of the net radiative fluxes.

The net flux is

$$F = F^{\uparrow} - F^{\downarrow}$$

where F is the net flux, $F^{\uparrow}$ is the upward flux and $F^{\downarrow}$ is the downward flux.

The heating rate due to the divergence of the radiative flux is given by

$$\frac{\partial \rho c_p T}{\partial t} = -\frac{\partial F}{\partial z}$$

or

$$\frac{\partial T}{\partial t} = \frac{g}{c_p \pi} \frac{\partial F}{\partial \sigma}$$

where g is the acceleration due to gravity and c_p is the heat capacity of air at constant pressure.

The time tendency for Longwave Radiation is updated every 3 hours. The time tendency for Shortwave Radiation is updated once every three hours assuming a normalized incident solar radiation, and subsequently modified at every model time step by the true incident radiation. The solar constant value used in the GEOS-2 GCM is equal to 1365 W/m^2 and a CO_2 mixing ratio of 330 ppm. For the ozone mixing ratio, monthly mean zonally averaged climatological values specified as a function of latitude and height (Rosenfield, et al., 1987) are linearly interpolated to the current time. The GEOS-2 GCM also uses climatological water vapor data above 100 hPa from the Stratospheric Aerosol and Gas

5.3.3.2.1 Shortwave Radiation The shortwave radiation package used in the GEOS-2 GCM computes solar radiative heating due to the absoption by water vapor, ozone, carbon dioxide, oxygen, clouds, and aerosols and due to the scattering by clouds, aerosols, and gases. The shortwave radiative processes are described by Chou (1990,1992). This shortwave package uses the Delta-Eddington approximation to compute the bulk scattering properties of a single layer following King and Harshvardhan (1986). The transmittance and reflectance of diffuse radiation follow the procedures of Sagan and Pollock (1967) and Lacis and Hansen (1974).

Highly accurate heating rate calculations are obtained through the use of an optimal grouping strategy of spectral bands. By grouping the UV and visible regions as indicated in Table 5.3, the Rayleigh scattering and the ozone absorption of solar radiation can be accurately computed in the ultraviolet region and the photosynthetically active radiation (PAR) region. The computation of solar flux in the infrared region is performed with a broadband parameterization using the spectrum regions shown in Table 5.4. The solar radiation algorithm used in the GEOS-2 GCM can be applied not only for climate studies but also for studies on the photolysis in the upper atmosphere and the photosynthesis in the biosphere.

Within the shortwave radiation package, both ice and liquid cloud particles are allowed to co-exist in any of the model layers. Two sets of cloud parameters are used, one for ice paticles and the other for liquid particles. Cloud parameters are defined as the cloud optical thickness and the effective cloud particle size. In the GEOS-2 GCM, the effective radius for water droplets is given as 10 microns, while 65 microns is used for ice particles. The absorption due to aerosols is currently set to zero.

To simplify calculations in a cloudy atmosphere, clouds are grouped into low ($p > 700$ hPa), middle (700 hPa $\geq p >$ 400 hPa), and high ($p <$ 400 hPa) cloud regions. Within each of the three regions, clouds are assumed maximally overlapped, and the cloud cover of the group is the maximum cloud cover of all the layers in the group. The optical thickness

UV and Visible Spectral Regions

Region	Band	Wavelength (micron)
UV-C	1.	.175 - .225
	2.	.225 - .245
		.260 - .280
	3.	.245 - .260
UV-B	4.	.280 - .295
	5.	.295 - .310
	6.	.310 - .320
UV-A	7.	.320 - .400
PAR	8.	.400 - .700

Table 5.3: UV and Visible Spectral Regions used in shortwave radiation package.

Infrared Spectral Regions

Band	Wavenumber(cm^{-1})	Wavelength (micron)
1	1000-4400	2.27-10.0
2	4400-8200	1.22-2.27
3	8200-14300	0.70-1.22

Table 5.4: Infrared Spectral Regions used in shortwave radiation package.

of a given layer is then scaled for both the direct (as a function of the solar zenith angle) and diffuse beam radiation so that the grouped layer reflectance is the same as the original reflectance. The solar flux is computed for each of the eight cloud realizations possible within this low/middle/high classification, and appropriately averaged to produce the net solar flux.

5.3.3.2.2 Longwave Radiation The longwave radiation package used in the GEOS-2 GCM is thoroughly described by Chou and Suarez (1994). As described in that document, IR fluxes are computed due to absorption by water vapor, carbon dioxide, and ozone. The spectral bands together with their absorbers and parameterization methods, configured for the GEOS-2 GCM, are shown in Table 5.5.

The longwave radiation package accurately computes cooling rates for the middle and lower atmosphere from 0.01 hPa to the surface. Errors are < 0.4 C day^{-1} in cooling rates and $< 1\%$ in fluxes. From Chou and Suarez, it is estimated that the total effect of neglecting all minor absorption bands and the effects of minor infrared absorbers such as nitrous oxide (N_2O), methane (CH_4), and the chlorofluorocarbons (CFCs), is an underestimate of ≈ 5 W/m^2 in the downward flux at the surface and an overestimate of ≈ 3 W/m^2 in the upward flux at the top of the atmosphere.

Similar to the procedure used in the shortwave radiation package, clouds are grouped into three regions catagorized as low/middle/high. The net clear line-of-site probability (P) between any two levels, p_1 and p_2 $\quad (p_2 > p_1)$, assuming randomly overlapped cloud groups, is simply the product of the probabilities within each group:

IR Spectral Bands

Band	Spectral Range (cm^{-1})	Absorber	Method
1	0-340	H_2O line	T
2	340-540	H_2O line	T
3a	540-620	H_2O line	K
3b	620-720	H_2O continuum	S
3b	720-800	CO_2	T
4	800-980	H_2O line	K
		H_2O continuum	S
5	980-1100	H_2O line	K
		H_2O continuum	S
		O_3	T
6	1100-1380	H_2O line	K
		H_2O continuum	S
7	1380-1900	H_2O line	T
8	1900-3000	H_2O line	K

K: k-distribution method with linear pressure scaling
T: Table look-up with temperature and pressure scaling
S: One-parameter temperature scaling

Table 5.5: IR Spectral Bands, Absorbers, and Parameterization Method (from Chou and Suarez, 1994)

$$P_{net} = P_{low} \times P_{mid} \times P_{hi}.$$

Since all clouds within a group are assumed maximally overlapped, the clear line-of-site probability within a group is given by:

$$P_{group} = 1 - F_{max},$$

where F_{max} is the maximum cloud fraction encountered between p_1 and p_2 within that group. For groups and/or levels outside the range of p_1 and p_2, a clear line-of-site probability equal to 1 is assigned.

5.3.3.2.3 Cloud-Radiation Interaction The cloud fractions and diagnosed cloud liquid water produced by moist processes within the GEOS-2 GCM are used in the radiation packages to produce cloud-radiative forcing. The cloud optical thickness associated with large-scale cloudiness is made proportional to the diagnosed large-scale liquid water, ℓ, detrained due to super-saturation. Two values are used corresponding to cloud ice particles and water droplets. The range of optical thickness for these clouds is given as

$$0.0002 \leq \tau_{ice}(hPa^{-1}) \leq 0.002 \quad \text{for} \quad 0 \leq \ell \leq 2 \quad \text{mg/kg},$$
$$0.02 \leq \tau_{h_2o}(hPa^{-1}) \leq 0.2 \quad \text{for} \quad 0 \leq \ell \leq 10 \quad \text{mg/kg}.$$

The partitioning, α, between ice particles and water droplets is achieved through a linear scaling in temperature:

$$0 \leq \alpha \leq 1 \quad \text{for} \quad 233.15 \leq T \leq 253.15.$$

The resulting optical depth associated with large-scale cloudiness is given as

$$\tau_{LS} = \alpha \tau_{h_2o} + (1 - \alpha)\tau_{ice}.$$

The optical thickness associated with sub-grid scale convective clouds produced by RAS is given as

$$\tau_{RAS} = 0.16 \quad hPa^{-1}.$$

The total optical depth in a given model layer is computed as a weighted average between the large-scale and sub-grid scale optical depths, normalized by the total cloud fraction in the layer:

$$\tau = \left(\frac{F_{RAS} \ \tau_{RAS} + F_{LS} \ \tau_{LS}}{F_{RAS} + F_{LS}} \right) \Delta p,$$

where F_{RAS} and F_{LS} are the time-averaged cloud fractions associated with RAS and large-scale processes described in Section 5.3.3.1.2. The optical thickness for the longwave radiative feedback is assumed to be 75 % of these values.

The entire Moist Convective Processes Module is called with a frequency of 10 minutes. The cloud fraction values are time-averaged over the period between Radiation calls (every 3 hours). Therefore, in a time-averaged sense, both convective and large-scale cloudiness can exist in a given grid-box.

5.3.3.3 Turbulence

Turbulence is parameterized in the GEOS-2 GCM to account for its contribution to the vertical exchange of heat, moisture, and momentum. The turbulence scheme is invoked every 30 minutes, and employs a backward-implicit iterative time scheme with an internal time step of 5 minutes. The tendencies of atmospheric state variables due to turbulent diffusion are calculated using the diffusion equations:

$$\begin{aligned}
\frac{\partial u}{\partial t}_{turb} &= \frac{\partial}{\partial z}(-\overline{u'w'}) = \frac{\partial}{\partial z}(K_m \frac{\partial u}{\partial z}) \\
\frac{\partial v}{\partial t}_{turb} &= \frac{\partial}{\partial z}(-\overline{v'w'}) = \frac{\partial}{\partial z}(K_m \frac{\partial v}{\partial z}) \\
\frac{\partial T}{\partial t} = P^\kappa \frac{\partial \theta}{\partial t}_{turb} &= P^\kappa \frac{\partial}{\partial z}(-\overline{w'\theta'}) = P^\kappa \frac{\partial}{\partial z}(K_h \frac{\partial \theta_v}{\partial z}) \\
\frac{\partial q}{\partial t}_{turb} &= \frac{\partial}{\partial z}(-\overline{w'q'}) = \frac{\partial}{\partial z}(K_h \frac{\partial q}{\partial z})
\end{aligned}$$

Within the atmosphere, the time evolution of second turbulent moments is explicitly modeled by representing the third moments in terms of the first and second moments. This approach is known as a second-order closure modeling. To simplify and streamline the computation of the second moments, the level 2.5 assumption of Mellor and Yamada (1974) and Yamada (1977) is employed, in which only the turbulent kinetic energy (TKE),

$$\frac{1}{2}q^2 = \frac{1}{2}\left[\overline{u'^2} + \overline{v'^2} + \overline{w'^2}\right],$$

is solved prognostically and the other second moments are solved diagnostically. The prognostic equation for TKE allows the scheme to simulate some of the transient and diffusive effects in the turbulence. The TKE budget equation is solved numerically using an implicit backward computation of the terms linear in q^2 and is written:

$$\frac{d}{dt}(\frac{1}{2}q^2) - \frac{\partial}{\partial z}(\frac{5}{3}\lambda_1 q \frac{\partial}{\partial z}(\frac{1}{2}q^2)) = -\overline{u'w'}\frac{\partial U}{\partial z} - \overline{v'w'}\frac{\partial V}{\partial z} + \frac{g}{\Theta_0}\overline{w'\theta_v{}'} - \frac{q^3}{\Lambda_1}$$

where q is the turbulent velocity, u', v', w' and θ' are the fluctuating parts of the velocity components and potential temperature, U and V are the mean velocity components, ${\Theta_0}^{-1}$ is the coefficient of thermal expansion, and λ_1 and Λ_1 are constant multiples of the master length scale, ℓ, which is designed to be a characteristic measure of the vertical structure of the turbulent layers.

The first term on the left-hand side represents the time rate of change of TKE, and the second term is a representation of the triple correlation, or turbulent transport term. The first three terms on the right-hand side represent the sources of TKE due to shear and bouyancy, and the last term on the right hand side is the dissipation of TKE.

In the level 2.5 approach, the vertical fluxes of the scalars θ_v and q and the wind components u and v are expressed in terms of the diffusion coefficients K_h and K_m, respectively. In the statisically realizable level 2.5 turbulence scheme of Helfand and Labraga (1988), these diffusion coefficients are expressed as

$$K_h = \begin{cases} q\,\ell\,S_H(G_M, G_H) & \text{for decaying turbulence} \\ \frac{q^2}{q_e}\,\ell\,S_H(G_{M_e}, G_{H_e}) & \text{for growing turbulence} \end{cases}$$

and

$$K_m = \begin{cases} q\,\ell\,S_M(G_M, G_H) & \text{for decaying turbulence} \\ \frac{q^2}{q_e}\,\ell\,S_M(G_{M_e}, G_{H_e}) & \text{for growing turbulence} \end{cases}$$

where the subscript e refers to the value under conditions of local equillibrium (obtained from the Level 2.0 Model), ℓ is the master length scale related to the vertical structure of the atmosphere, and S_M and S_H are functions of G_H and G_M, the dimensionless buoyancy and wind shear parameters, respectively. Both G_H and G_M, and their equilibrium values G_{H_e} and G_{M_e}, are functions of the Richardson number:

$$\mathbf{RI} = \frac{\frac{g}{\theta_v}\frac{\partial \theta_v}{\partial z}}{(\frac{\partial u}{\partial z})^2 + (\frac{\partial v}{\partial z})^2} = \frac{c_p \frac{\partial \theta_v}{\partial z}\frac{\partial P^\kappa}{\partial z}}{(\frac{\partial u}{\partial z})^2 + (\frac{\partial v}{\partial z})^2}.$$

Negative values indicate unstable buoyancy and shear, small positive values (< 0.2) indicate dominantly unstable shear, and large positive values indicate dominantly stable stratification.

Turbulent eddy diffusion coefficients of momentum, heat and moisture in the surface layer, which corresponds to the lowest GCM level (see 5.2), are calculated using stability-dependant functions based on Monin-Obukhov theory:

$$K_m(surface) = C_u \times u_* = C_D W_s$$

and

$$K_h(surface) = C_t \times u_* = C_H W_s$$

where $u_* = C_u W_s$ is the surface friction velocity, C_D is termed the surface drag coefficient, C_H the heat transfer coefficient, and W_s is the magnitude of the surface layer wind.

C_u is the dimensionless exchange coefficient for momentum from the surface layer similarity functions:

$$C_u = \frac{u_*}{W_s} = \frac{k}{\psi_m}$$

where k is the von Karman constant and ψ_m is the surface layer non-dimensional wind shear given by

$$\psi_m = \int_{\zeta_0}^{\zeta} \frac{\phi_m}{\zeta} d\zeta.$$

Here ζ is the non-dimensional stability parameter, and ϕ_m is the similarity function of ζ which expresses the stability dependance of the momentum gradient. The functional form of ϕ_m is specified differently for stable and unstable layers.

C_t is the dimensionless exchange coefficient for heat and moisture from the surface layer similarity functions:

$$C_t = -\frac{(\overline{w'\theta'})}{u_* \Delta\theta} = -\frac{(\overline{w'q'})}{u_* \Delta q} = \frac{k}{(\psi_h + \psi_g)}$$

where ψ_h is the surface layer non-dimensional temperature gradient given by

$$\psi_h = \int_{\zeta_0}^{\zeta} \frac{\phi_h}{\zeta} d\zeta.$$

Here ϕ_h is the similarity function of ζ, which expresses the stability dependance of the temperature and moisture gradients, and is specified differently for stable and unstable layers according to Helfand and Schubert, 1995.

ψ_g is the non-dimensional temperature or moisture gradient in the viscous sublayer, which is the mosstly laminar region between the surface and the tops of the roughness elements, in which temperature and moisture gradients can be quite large. Based on Yaglom and Kader (1974):

$$\psi_g = \frac{0.55(Pr^{2/3} - 0.2)}{\nu^{1/2}}(h_0 u_* - h_{0_{ref}} u_{*_{ref}})^{1/2}$$

where Pr is the Prandtl number for air, ν is the molecular viscosity, z_0 is the surface roughness length, and the subscript *ref* refers to a reference value. $h_0 = 30 z_0$ with a maximum value over land of 0.01

The surface roughness length over oceans is is a function of the surface-stress velocity,

$$z_0 = c_1 u_*^3 + c_2 u_*^2 + c_3 u_* + c_4 + \frac{c_5}{u_*}$$

where the constants are chosen to interpolate between the reciprocal relation of Kondo(1975) for weak winds, and the piecewise linear relation of Large and Pond(1981) for moderate to large winds. Roughness lengths over land are specified from the climatology of Dorman and Sellers (1989).

For an unstable surface layer, the stability functions, chosen to interpolate between the condition of small values of β and the convective limit, are the KEYPS function (Panofsky, 1973) for momentum, and its generalization for heat and moisture:

$$\phi_m{}^4 - 18\zeta\phi_m{}^3 = 1 \qquad ; \qquad \phi_h{}^2 - 18\zeta\phi_h{}^3 = 1 \qquad .$$

The function for heat and moisture assures non-vanishing heat and moisture fluxes as the wind speed approaches zero.

For a stable surface layer, the stability functions are the observationally based functions of Clarke (1970), slightly modified for the momemtum flux:

$$\phi_m = \frac{1 + 5\zeta_1}{1 + 0.00794\zeta_1(1 + 5\zeta_1)} \qquad ; \qquad \phi_h = \frac{1 + 5\zeta_1}{1 + 0.00794\zeta(1 + 5\zeta_1)}.$$

The moisture flux also depends on a specified evapotranspiration coefficient, set to unity over oceans and dependant on the climatological ground wetness over land.

Once all the diffusion coefficients are calculated, the diffusion equations are solved numerically using an implicit backward operator.

5.3.3.3.1 Atmospheric Boundary Layer The depth of the atmospheric boundary layer (ABL) is diagnosed by the parameterization as the level at which the turbulent kinetic energy is reduced to a tenth of its maximum near surface value. The vertical structure of the ABL is explicitly resolved by the lowest few (3-8) model layers.

5.3.3.3.2 Surface Energy Budget The ground temperature equation is solved as part of the turbulence package using a backward implicit time differencing scheme:

$$C_g \frac{\partial T_g}{\partial t} = R_{sw} - R_{lw} + Q_{ice} - H - LE$$

where R_{sw} is the net surface downward shortwave radiative flux and R_{lw} is the net surface upward longwave radiative flux.

H is the upward sensible heat flux, given by:

$$H = P^\kappa \rho c_p C_H W_s (\theta_{surface} - \theta_{NLAY}) \qquad where: \;\; C_H = C_u C_t$$

where $\rho =$ the atmospheric density at the surface, c_p is the specific heat of air at constant pressure, and θ represents the potential temperature of the surface and of the lowest σ-level, respectively.

The upward latent heat flux, LE, is given by

$$LE = \rho\beta L C_H W_s (q_{surface} - q_{NLAY}) \qquad where: \; C_H = C_u C_t$$

where β is the fraction of the potential evapotranspiration actually evaporated, L is the latent heat of evaporation, and $q_{surface}$ and q_{NLAY} are the specific humidity of the surface and of the lowest σ-level, respectively.

The heat conduction through sea ice, Q_{ice}, is given by

$$Q_{ice} = \frac{C_{ti}}{H_i}(T_i - T_g)$$

where C_{ti} is the thermal conductivity of ice, H_i is the ice thickness, assumed to be $3\,m$ where sea ice is present, T_i is 273 degrees Kelvin, and T_g is the surface temperature of the ice.

C_g is the total heat capacity of the ground, obtained by solving a heat diffusion equation for the penetration of the diurnal cycle into the ground (Blackadar, 1977), and is given by:

$$C_g = \sqrt{\frac{\lambda C_s}{2\omega}} = \sqrt{(0.386 + 0.536W + 0.15W^2)2 \times 10^{-3} \frac{86400}{2\pi}} \; .$$

Here, the thermal conductivity, λ, is equal to $2 \times 10^{-3} \; \frac{ly}{sec} \frac{cm}{^oK}$, the angular velocity of the earth, ω, is written as 86400 sec/day divided by 2π $radians/day$, and the expression for C_s, the heat capacity per unit volume at the surface, is a function of the ground wetness, W.

5.3.3.4 Gravity Wave Drag

A gravity wave drag scheme has been added to the GEOS-2 GCM. This provides a physically-based momentum dissipation in the model. The gravity wave drag was added primarily to address excessive zonality of tropospheric winds. The scheme has a dramatic positive impact on sea level pressure and tropospheric momentum and heat fluxes. Gravity wave processes in the stratosphere and mesosphere require further development of the scheme.

The GEOS-2 GCM employs the gravity wave drag scheme of Zhou et al. (1996). This scheme is a modified version of Vernekar et al. (1992), which was based on Alpert et al. (1988) and Helfand et al. (1987). In this version, the gravity wave stress at the surface is based on that derived by Pierrehumbert (1986) and is given by:

$$|\vec{\tau}_{sfc}| = \frac{\rho U^3}{N\ell^*} \left(\frac{F_r^2}{1 + F_r^2} \right) \; , \tag{5.118}$$

where $F_r = Nh/U$ is the Froude number, N is the *Brunt - Väisälä* frequency, U is the surface wind speed, h is the standard deviation of the sub-grid scale orography, and ℓ^* is

the wavelength of the monochromatic gravity wave in the direction of the low-level wind. A modification introduced by Zhou et al. allows for the momentum flux to escape through the top of the model, although this effect is small for the current 70-level model. The subgrid scale standard deviation is defined by h, and is not allowed to exceed 400 m.

The effects of using this scheme within the GEOS GCM are shown in Takacs and Suarez (1996). Experiments using the gravity wave drag parameterization yielded significant and beneficial impacts on both the time-mean flow and the transient statistics of the GEOS GCM climatology, and have eliminated most of the worst dynamically driven biases in the GEOS-1 GCM simulation. An examination of the angular momentum budget during climate runs indicates that the resulting gravity wave torque is similar to the data-driven torque introduced by the GEOS-1 DAS analysis which was performed without gravity wave drag. It was shown that the inclusion of gravity wave drag results in large changes in both the mean flow and in eddy fluxes. The result is a more accurate simulation of surface stress (through a reduction in the surface wind strength), of mountain torque (through a redistribution of mean sea-level pressure), and of momentum convergence (through a reduction in the flux of westerly momentum by transient flow eddies).

5.3.4 Boundary Conditions and other Input Data

Development and maintenance of boundary condition data sets is a major task. Improvement of some boundary condition data sets is required to accommodate the land-surface model. Increased flexibility to use different boundary data sets, perhaps prescribed directly from MTPE observations is also required. Finally, much of the work of future development is to make some of the current boundary condition data sets interactive. This allows even more model degrees of freedom which must be properly defined.

Required fields which are not explicitly predicted or diagnosed during model execution must either be prescribed internally or obtained from external data sets. In the GEOS-2 GCM these fields include the boundary conditions: surface geopotential, surface geopotential variance, vegetation index, sea surface temperature, ground wetness, sea ice, snow, surface roughness and surface albedo, and the radiation-related background levels of: ozone, carbon dioxide, and stratospheric moisture.

Boundary condition data sets are available at the model's 4° x 5° and 2° x 2.5° resolutions for either climatological or yearly varying conditions. Any frequency of boundary condition data can be used in the GEOS-2 GCM; however, the current selection of data is summarized in Table 5.6. The time mean values are interpolated during each model timestep to the current time. Future model versions will incorporate boundary conditions at higher spatial (1° x 1°) resolutions.

5.3.4.1 Topography and Topography Variance

Surface geopotential heights are provided from an averaging of the Navy 10 minute by 10 minute dataset supplied by the National Center for Atmospheric Research (NCAR) to the model's grid resolution. The original topography is first rotated to the proper grid-orientation which is being run, and then averages the data to the model resolution. The averaged topography is then passed through a Lanczos (1966) filter in both dimensions

GEOS-2 GCM Input Datasets

Variable	Frequency	Years
Ground Wetness	monthly	1979-1992, climatology
Sea Ice Extent	monthly	1979-1992, climatology
Sea Ice Extent	weekly	1982-1992, climatology
Sea Surface Temperature	monthly	1979-1992, climatology
Sea Surface Temperature	weekly	1982-1995, climatology
Snow Extent	monthly	climatology
Snow Extent	weekly	1982-1992, climatology
Zonally Averaged Upper-Level Moisture	monthly	climatology
Zonally Averaged Ozone Concentration	monthly	climatology

Table 5.6: Boundary conditions and other input data used in the GEOS-2 GCM. Also noted are the current years and frequencies available.

which removes the smallest scales while inhibiting Gibbs phenomena.

In one dimension, we may define a cyclic function in x as:

$$f(x) = \frac{a_0}{2} + \sum_{k=1}^{N} \left(a_k \cos(kx) + b_k \sin(kx) \right) \tag{5.119}$$

where $N = \frac{\mathrm{IM}}{2}$ and IM is the total number of points in the x direction. Defining $\Delta x = \frac{2\pi}{\mathrm{IM}}$, we may define the average of $f(x)$ over a $2\Delta x$ region as:

$$\overline{f(x)} = \frac{1}{2\Delta x} \int_{x-\Delta x}^{x+\Delta x} f(x')dx' \tag{5.120}$$

Using equation (5.119) in equation (5.120) and integrating, we may write:

$$\overline{f(x)} = \frac{a_0}{2} + \frac{1}{2\Delta x} \sum_{k=1}^{N} \left[a_k \frac{\sin(kx')}{k} \Big/_{x-\Delta x}^{x+\Delta x} - b_k \frac{\cos(kx')}{k} \Big/_{x-\Delta x}^{x+\Delta x} \right] \tag{5.121}$$

or

$$\overline{f(x)} = \frac{a_0}{2} + \sum_{k=1}^{N} \frac{\sin(k\Delta x)}{k\Delta x} \left(a_k \cos(kx) + b_k \sin(kx) \right) \tag{5.122}$$

Thus, the Fourier wave amplitudes are simply modified by the Lanczos filter response function $\frac{\sin(k\Delta x)}{k\Delta x}$. This may be compared with an *mth*-order Shapiro (1970) filter response function, defined as $1 - \sin^m(\frac{k\Delta x}{2})$, shown in Figure 5.20. It should be noted that negative values in the topography resulting from the filtering procedure are *not* filled.

The standard deviation of the subgrid-scale topography is computed from a modified version of the the Navy 10 minute by 10 minute dataset. The 10 minute by 10 minute

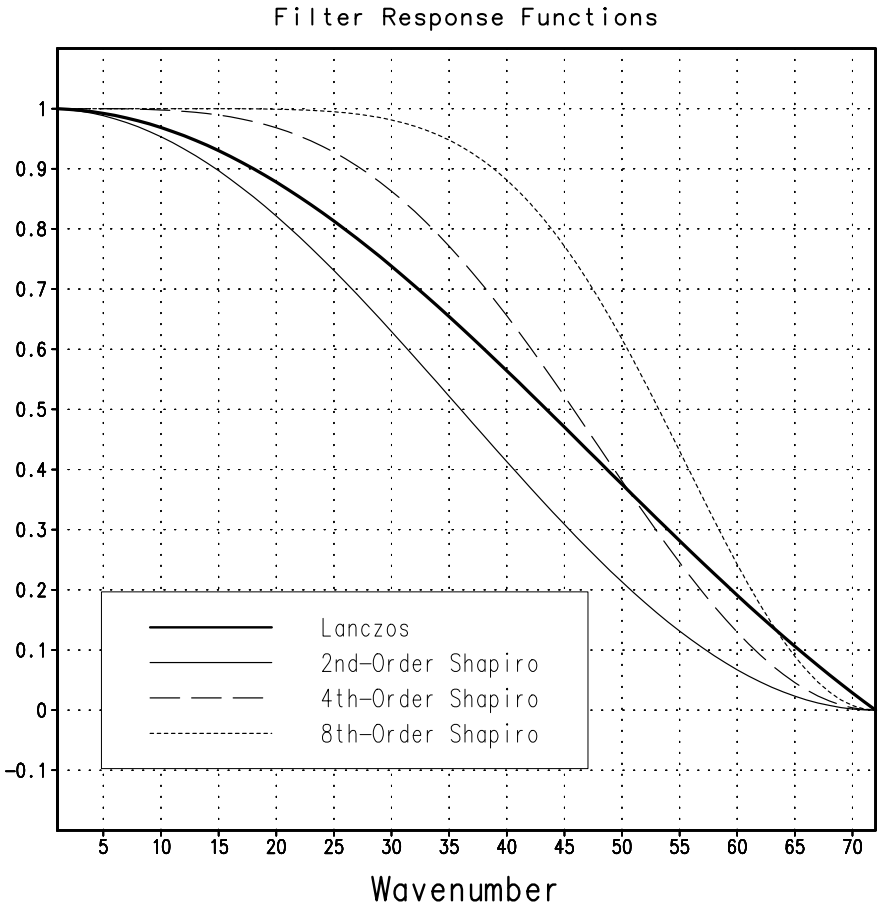

Figure 5.20: Comparison between the Lanczos and *mth*-order Shapiro filter response functions for $m = 2$, 4, and 8.

GEOS-2 GCM Surface Type Designation

Type	Vegetation Designation
1	Broadleaf Evergreen Trees
2	Broadleaf Deciduous Trees
3	Needleleaf Trees
4	Ground Cover
5	Broadleaf Shrubs
6	Dwarf Trees (Tundra)
7	Bare Soil
8	Desert (Bright)
9	Glacier
10	Desert (Dark)
100	Ocean

Table 5.7: GEOS-2 GCM surface type designations used to compute surface roughness (over land) and surface albedo.

topography is passed through a wavelet filter in both dimensions which removes the scale smaller than 20 minutes. The topography is then averaged to 1°x1° grid resolution, and then re-interpolated back to the 10 minute by 10 minute resolution. The sub-grid scale variance is constructed based on this smoothed dataset.

5.3.4.2 Surface Type

GEOS-2 GCM Surface Types are designated using the Koster-Suarez (1992) mosaic philosophy which allows multiple "tiles", or multiple surface types, in any one grid cell. The Koster-Suarez Land Surface Model (LSM) surface type classifications are shown in Table 5.7. The surface types and the percent of the grid cell occupied by any surface type were derived from the surface classification of Defries and Townshend (1994), and information about the location of permanent ice was obtained from the classifications of Dorman and Sellers (1989). The surface designation at 1°x1° resolution is shown in Figure 5.21. The determination of the land or sea category of surface type was made from NCAR's 10 minute by 10 minute Navy topography dataset, which includes information about the percentage of water-cover at any point. The data were averaged to the model's 4° x 5° and 2° x 2.5° grid resolutions, and any grid-box whose averaged water percentage was $\geq 60\%$ was defined as a water point. The 4° x 5° grid Land-Water designation was further modified subjectively to ensure sufficient representation from small but isolated land and water regions.

5.3.4.3 Sea Surface Temperature

Yearly varying monthly mean sea surface temperatures for the 4° x 5° grid resolution are from AMIP specified monthly mean fields (Gates, 1992). All other monthly varying data sets were interpolated from data of Reynolds (1988). The weekly varying data was provided by the National Centers for Environmental Prediction (NCEP) using an optimum interpolation sea surface temperature analysis (Reynolds and Smith, 1994) with bias correction (Reynolds,

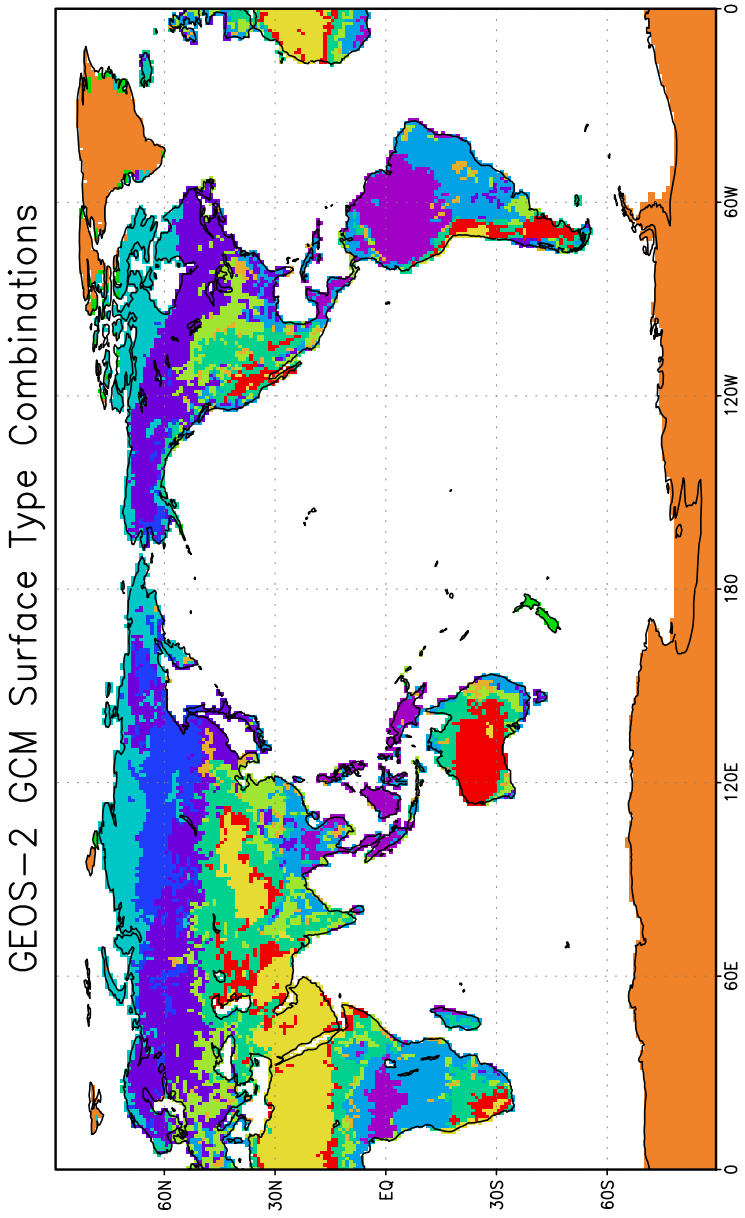

Figure 5.21: GEOS-2 GCM Surface Type Compinations at 2° x 2.5° resolution.

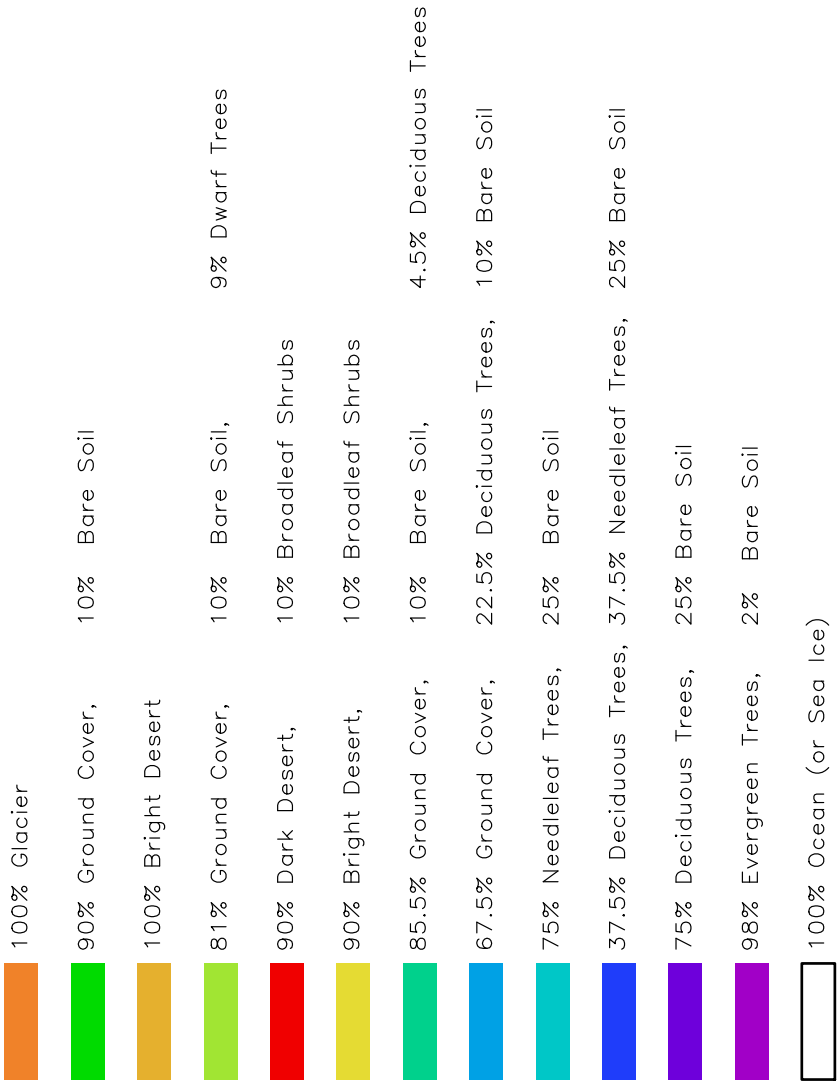

Figure 5.22: GEOS-2 GCM Surface Type Descriptions.

1988; Reynolds and Marsico, 1993). The satellite data were provided by the National Environmental Satellite, Data and Information Service (NESDIS). During 1981-1989, the in situ data was obtained from the Comprehensive Ocean Atmosphere Data Set (COADS) (Slutz, et al., 1985; Woodruff, et al., 1993). For 1990-1995, the in situ data was obtained from radio messages carried on the Global Telecommunication System. A binomial time filter of $(\frac{1}{4}, \frac{1}{2}, \frac{1}{4})$ was applied to the weekly data as well as a minimum temperature limit of 271.36K.

5.3.4.4 Surface Roughness

The surface roughness length over oceans is computed iteratively with the wind stress by the surface layer parameterization (Helfand and Schubert, 1995). It employs an interpolation between the functions of Large and Pond (1981) for high winds and of Kondo (1975) for weak winds.

5.3.4.5 Albedo

The surface albedo computation, described in Koster and Suarez (1991), employs the "two stream" approximation used in Sellers' (1987) Simple Biosphere (SiB) Model which distinguishes between the direct and diffuse albedos in the visible and in the near infra-red spectral ranges. The albedos are functions of the observed leaf area index (a description of the relative orientation of the leaves to the sun), the greenness fraction, the vegetation type, and the solar zenith angle. Modifications are made to account for the presence of snow, and its depth relative to the height of the vegetation elements.

5.3.4.6 Sea Ice

Monthly mean sea ice extents were interpolated to the model's 4° x 5° and 2° x 2.5° grid resolutions from the AMIP monthly mean fields (Gates, 1992). The weekly sea ice extent data, originally from the Navy/NOAA Joint Ice Center (Reynolds and Smith, 1994), were provided by NCEP at a 2° x 2° resolution. The data were then interpolated to the 4° x 5° and 2° x 2.5° grid resolutions consistent with the GEOS-2 GCM land/water mask. Sea ice thickness is assumed to be three meters and is used in the calculation of conduction through sea ice accounted for in the surface energy budget. Note that unlike the GEOS-1 GCM, the permanent Ross and Ronne ice shelves of Antartica were not included in the vegetation data set which defines glacier extent; therefore, the marine ice shelves have been classified as sea ice.

5.3.4.7 Snow Cover

The monthly mean snow extent is based on climatological albedo values which are greater than 0.4 (Posey and Clapp, 1964; Kitzmiller, personal communication). The climatological monthly mean data set was created to reproduce the snow extent used in GEOS-1. The weekly snow extent data were provided by NCEP at a 2° x 2° grid resolution (Dewey and Heim, 1981) and were interpolated to the 4° x 5° and 2° x 2.5° grid resolutions consistent

with the GEOS-2 GCM land/water mask. A binomial $(\frac{1}{4}, \frac{1}{2}, \frac{1}{4})$ time filter was applied to the weekly snow extent data. Also, a persistant block of snow from 46N-56N and 70E-92E which resembled a misplaced plateau of Tibet was removed when neighboring grid-boxes were free of snow. Snow depth is assumed to be a constant and set equal to a water equivalent of 50 mm. Snow amounts are used in the GEOS-2 GCM in the calculation of albedo and surface conductive characteristics.

5.3.4.8 Upper Level Moisture

The GEOS-2 GCM uses climatological water vapor data above 100 hPa from the Stratospheric Aerosol and Gas Experiment (SAGE) as input into the model's radiation packages. The SAGE data is archived as monthly zonal means at 5° latitudinal resolution. The data is interpolated to the model's grid location and current time, and blended with the GCM's moisture data. Below 300 hPa, the model's moisture data is used. Above 100 hPa, the SAGE data is used. Between 100 and 300 hPa, a linear interpolation (in pressure) is performed using the data from SAGE and the GCM.

5.3.4.9 Ground Temperature and Moisture

Ground temperature over land is predicted from a surface energy balance equation. The ground wetness used in the GEOS-2 GCM is obtained from the monthly estimates of Schemm, et al. (1992) based on the procedure developed by Mintz and Serafini (1984) using an inverted single layer "bucket" model together with observed fields of surface air temperature and precipitation.

5.4 Combining model and analysis: the IAU process

The IAU procedure was introduced in Chapter 4. It is an integral part of the GEOS-DAS, smoothly integrating the information from the model and the analysis. Its use has been controversial. The IAU process has also been confused with linear nudging techniques. This section establishes the theoretical basis of the IAU, clarifies the relation with linear nudging, and gives an example of performance enhancements achieved by the IAU.

The intermittent insertion of analyses has been the most commonly used strategy for operational data assimilation. This approach typically begins with a statistical interpolation scheme (such as OI or PSAS) that combines observations in a 6-hour time window with a 6 hour model forecast to produce an *analysis*. This analysis is then used as an initial condition for the next 6 hour forecast, and so on. Two related problems arise with the intermittent approach: shocks to the model and data rejection. Sudden localized changes to GCM fields can spur large non-physical adjustment processes, the result of which can be the unnecessary diminution of the effect of valid observations. For example, a large, localized change to a model's mass field will likely produce (in mid-latitudes) a geostrophic adjustment in which the change to the mass field would then largely disappear in the form of gravity waves radiating away from the analysis location.

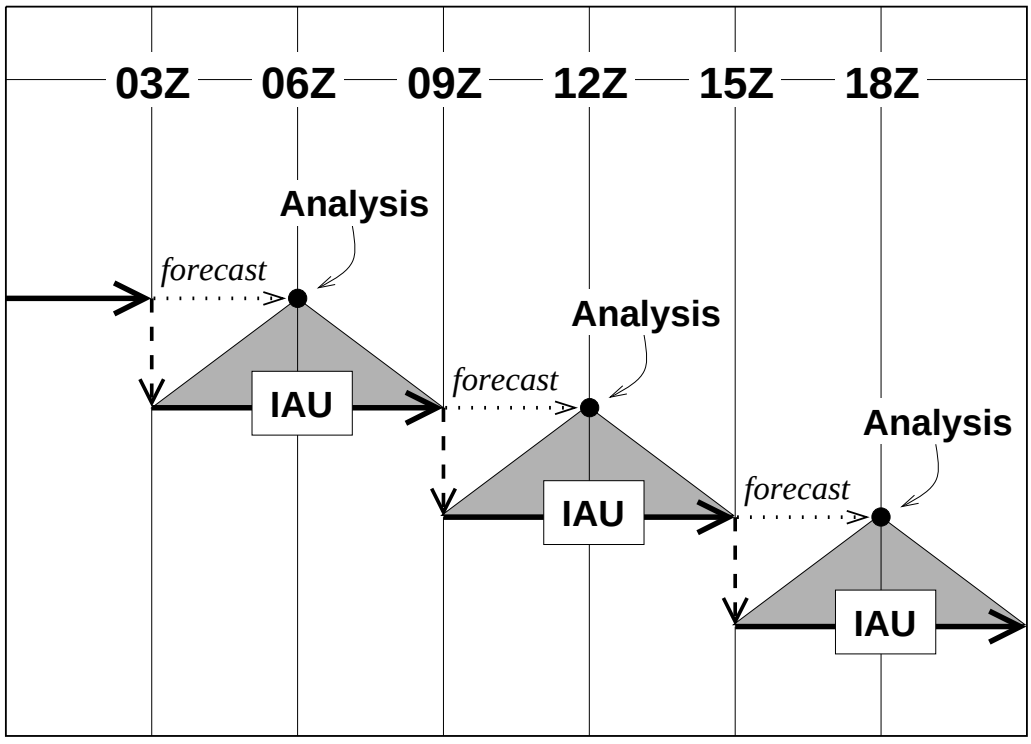

Figure 5.23: Schematic of the incremental analysis update (IAU) scheme employed in the GEOS DAS. Statistical analyses (OI or PSAS) are performed at synoptic times (0000, 0600, 1200 and 1800 UTC). The assimilation is restarted three hours prior to the analysis time (heavy dashed lines), and the model is integrated forward for 6 hours using the analysis increments as *constant* forcing (data influence shown by shaded regions). At the end of the IAU interval, an *un-forced* forecast is made (dotted line) to provide the first guess for the next analysis.

There have been a number of strategies for coping with the problems inherent in intermittent assimilation: damped time-differencing schemes in the forecast model, initialization methods, and balance constraints. A former version of the Goddard Laboratory for Atmospheres (GLA) data assimilation system used a Matsuno time-differencing scheme (cf. Baker *et al.*, 1987), which damps high frequency oscillations. Even with this high-frequency damping the previous GLA system still suffered from shocks and unrealistic precipitation (examples of which will be shown in below). Further elaborations of this approach, using dynamical initialization techniques, have been explored in Fox-Rabinovitz and Gross (1993) and Fox-Rabinovitz (1995). Operational centers have made frequent use of normal mode initialization methods. While quite effective at eliminating imbalances, these initialization methods (even diabatic methods) tend to have unwanted side-effects on physical processes, such as the loss of divergent wind structures in the tropics (Puri, 1985). In addition, such methods make non-local changes to the analyses, most notably in areas where there were no data. The NCEP SSI system (Parrish and Derber 1992) uses a linear balance constraint as well as a non-linear pressure tendency constraint as integral parts of variational analysis system.

The *Incremental Analysis Updating* (IAU) approach combines aspects of the intermittent and continuous data assimilation approaches. A statistical analysis is performed intermittently every 6 hours but used as a continuous forcing for the model prognostic variables as illustrated in Fig. 5.23. Analysis increments are computed in a conventional way at the analysis times (00, 06, 12, 18 UTC) by an analysis scheme such as PSAS or OI. These increments are then inserted gradually into the model by restarting the short-term forecast that provided the analysis background and adding a fraction of the analysis increment at each model time-step. Over the six hour period centered on the analysis time, the full effect of the analysis increment is realized. The final assimilation product thus effectively consists of a model forecast produced using additional heat, momentum, moisture and mass tendency terms which are updated every six hours from observations. This update scheme for the assimilation is similar to the way the forcing tendencies from the model's physical parameterizations and filters are recomputed intermittently (usually every 30 minutes) and gradually introduced into the ongoing integration at every time-step (section 5.3).

For an assimilation system to be used for climate and chemistry applications the IAU also offers a set of particular advantages. In traditional numerical weather prediction schemes precipitation and other diagnostic products are usually derived from multi-hour forecast. These diagnostics are accumulated after discarding the first few hours of the forecast when more severe spin-up processes take place. In the IAU, precipitation and other diagnostic products are computed from a continuous model integration; therefore, closer to the actual data time. In addition, because of its continuous nature, there can be frequent output of diagnostics. This has proven useful for archiving surface products every hour (on request) and is the reason the GEOS DAS can produce the special sub-orbital data sets requested by AM-1 instrument teams. Finally, with the analysis increments archived, it is possible to regenerate the assimilation products with additional diagnostics or increased time frequency, for only the computational cost of the model simulation.

Although similar in nature, IAU differs from the UKMO *Analysis Correction* scheme (Lorenc *et al.* 1991) in one important respect: IAU uses *one* analysis as assimilation forcing while the UKMO system *reanalyzes* the data continuously through a 6 hour period. There is also an important difference between IAU and the usual Newtonian nudging procedure

(Anthes 1974; Stauffer and Seaman 1990): IAU forcing terms are held *constant* over the insertion period, while in Newtonian nudging the forcing terms are proportional to the changing difference between a target analysis and the instantaneous current model state; this difference in forcing terms result in much different filtering properties (Bloom *et a.* 1996; see also next subsection).

Significant improvements in terms of assimilation accuracy, noise control, and the hydrological cycle spin-up are obtained using the IAU technique (Bloom *et al.* 1996). These results are summarized in subsections 5.4.1—5.4.2. Details of the model/analysis interface are given in subsection 5.4.3.

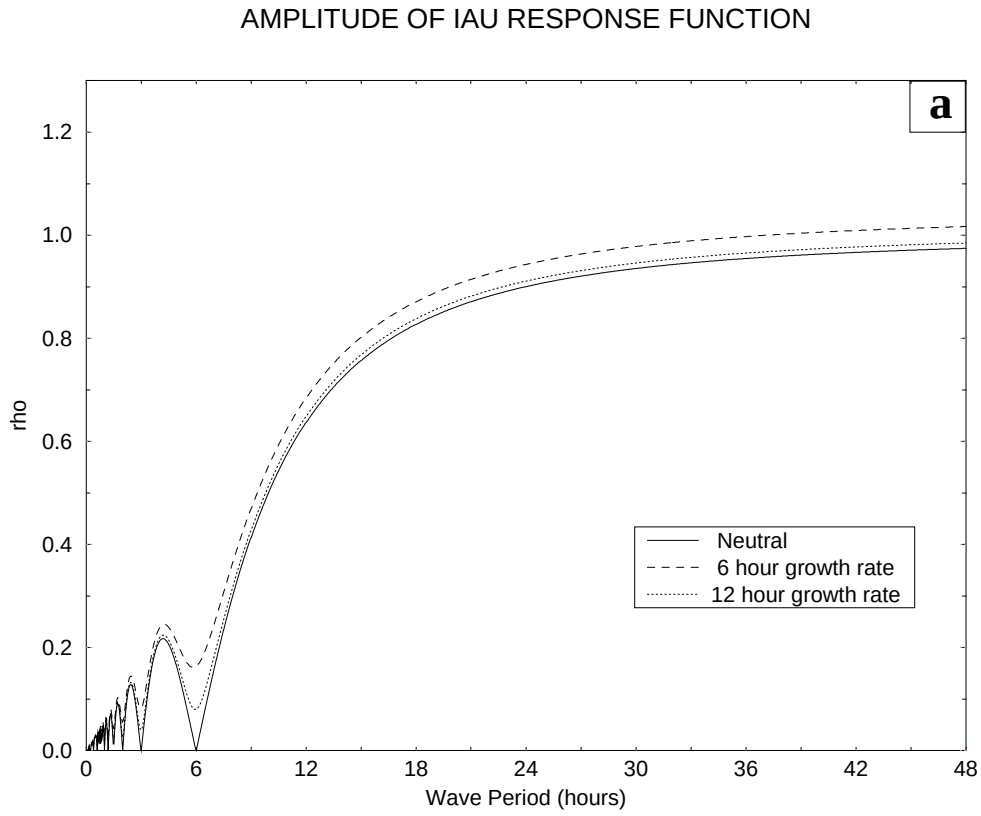

Figure 5.24: Amplitude of the IAU response function as a function of the disturbance period in hours. Results are shown for 3 values of the growth/decay rate, $\sigma = 0$ (neutral case, *solid*), $1/\sigma = 12$ hours (*dashed*) and $1/\sigma = 6$ hours (*dotted*). See Bloom *et al.* 1996 for details.

5.4.1 Filtering properties of IAU

Bloom *et al.* (1996) derive the linear response functions associated with the assimilation of analysis increments into a generic linear model. Such an analysis of various assimilation approaches (intermittent, IAU, and dynamical relaxation or "nudging") within the context of a linear system does give an indication of the behavior of these methods in a full assimilation system. A number of important conclusions can be drawn from this linear analysis:

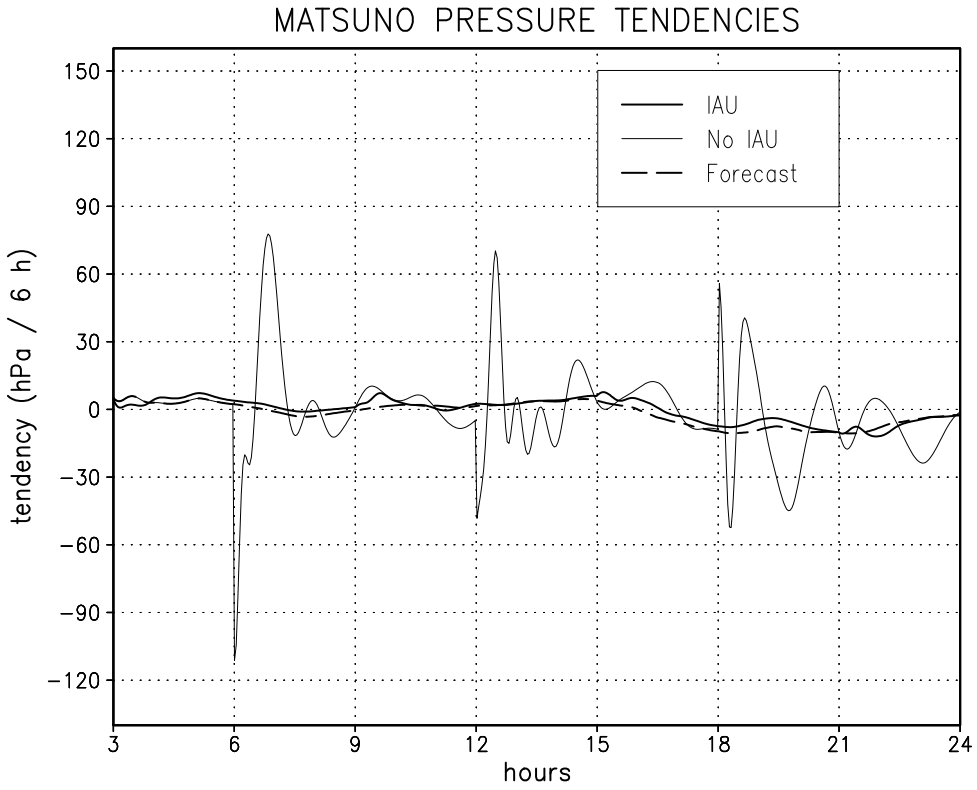

Figure 5.25: Surface Pressure Tendency traces at a gridpoint over North America, results displayed from every time-step over the course of a 1-day assimilation: IAU (*heavy solid*); no IAU (*light solid*); model forecast, no data assimilation *heavy dashed*).

- In the linear system, IAU acts only on the contribution to the assimilation state by the analysis increments. This is a confirmation of one of the design goals of IAU; that the process should not make any changes to the background state where there were no data.

- The response function amplitude (IAU response compared to intermittent assimilation response), Figure 5.24, indicates that the 6 h IAU update cycle acts as a low-pass filter. Disturbances forced by analysis increments and that have periods longer than one day retain over 90% of their initial amplitude. The response decreases to zero for disturbances having a period of 6 h, the IAU process update interval. These results are true for a wide range of disturbances having growth or decay rates slower than 12 h.

- Dynamical Relaxation (nudging) is a much more intrusive process, affecting both high frequency phenomena introduced by imbalances in the analysis, as well as high frequency phenomena generated by physical processes in the model. While the IAU forcing is significant only in regions where observations induce an analysis increment, the DR forcing is operative at every grid point of the model, independent of the presence of observations. Compared to the simple implementation of DR used for this linear analysis, IAU has a much sharper response function with much less phase

distortion.

5.4.2 Impact of IAU on GEOS-1 DAS

Bloom *et al.* (1996) documents the impact of IAU on the GEOS-1 DAS. Figure 5.25 shows the impact of IAU on the behavior of the surface pressure tendencies for the three runs for a gridpoint over North America. The variations in the surface pressure tendency in the IAU assimilation have similar amplitudes and time scales to those obtained from the forecast with no IAU forcing starting from the same initial condition. This indicates that the contribution from the IAU terms is on a par with the forcings from the other Physics-related terms in the model's tendency equations. The sudden, sharp adjustments evident in the non-IAU run occur after each analysis, and their influence clearly extends from one analysis time to the next.

The manner in which data are assimilated can have a profound effect on moist processes in the assimilation system. This point is illustrated in Figure 5.26, where we compare globally averaged precipitation rates from assimilation runs with and without IAU. Figure 5.26 shows a trace of total global precipitation for the IAU/non-IAU runs. A series of regular spikes is apparent in the non-IAU time-series with similar counterpart in the IAU time-series. These precipitation spikes align well with the synoptic analysis times indicating that the non-IAU adjustment processes trigger sharp, intense responses from the GCM's parameterization of moist processes.

One measure of an improvement to a data assimilation system lies in how well forecasts from the modified assimilation states predict future data. Observation-minus-forecast (O-F) statistics are readily available as a by-product of the analysis step in an assimilation system. Figure 5.27 depicts O-F standard deviations computed from radiosonde observations over North America and NESDIS TOVS-A retrievals over the oceans. The O-F standard deviations from the IAU cases are consistently smaller than their non-IAU counterparts.

5.4.3 Model/analysis interface

The actual implementation of IAU in GEOS-2 DAS involves the following steps:

1. The analysis fields must be interpolated from mandatory levels to the sigma-levels required by the GEOS GCM. To minimize the adverse effects of the vertical interpolation, only the analysis increments are vertically interpolated, and then added to the original model first guess in sigma-coordinates. For details of the interpolation algorithm refer to Takacs *et al.* (1994).

2. The analysis variables must be converted to the GCM prognostic variables. For example, the potential temperature field is first computed from analyzed heights and mixing ratio. Because the model thermodynamic equation is formulated in flux form (Takacs *et al.* 1994, eq. 9), the *after analysis* potential temperature must be mass-weighted, *i.e.*, the potential temperature field must be multiplied by the factor $\Pi = p_s - p_T$, where p_s is the surface pressure and p_T hPa is the pressure at the top of the model.

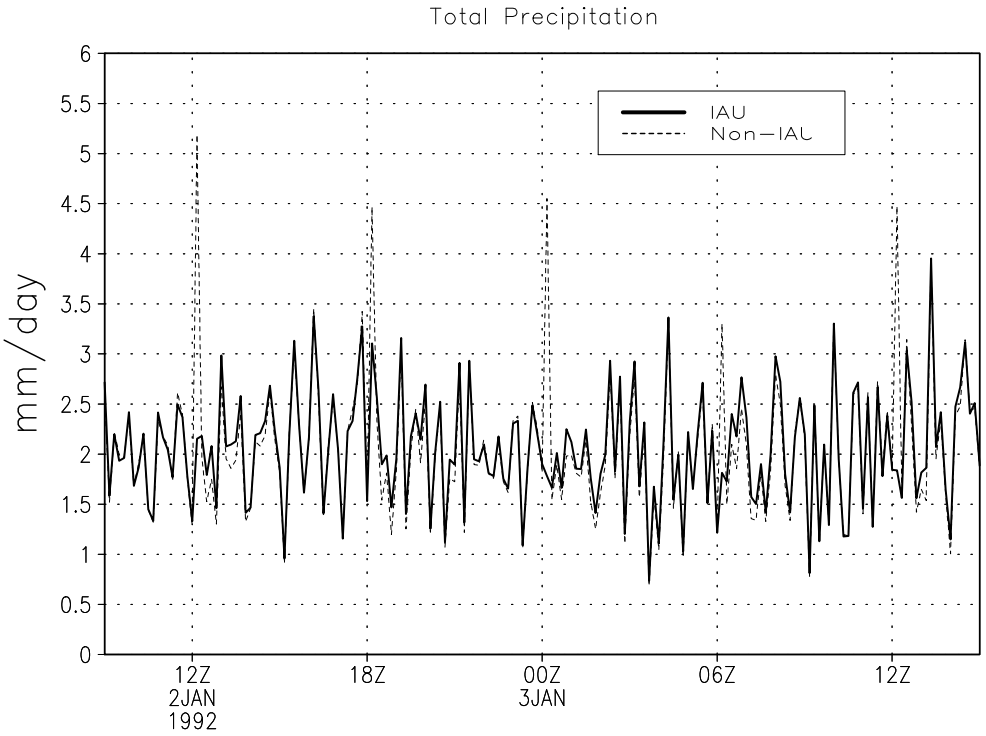

Figure 5.26: Globally averaged precipitation, plotted in 10 minute intervals, for a 24 hour period. IAU (solid) and non-IAU (dashed) results.

3. The IAU forcing terms are formed by subtracting the after analysis prognostic fields from the corresponding first guess fields, and then dividing this difference by the number of seconds in 6 hours. IAU forcing fields are produced for surface pressure, wind components, mass-weighted temperature and mass-weighted moisture.

4. The model integration is restarted 3 hours before the synoptic time and continues for 6 hours with the IAU forcing held constant in time. After these 6 hours, the forcing terms are set to zero and the model integration continues for another 3 hours up to next synoptic time when the model state is used as first guess for the next analysis.

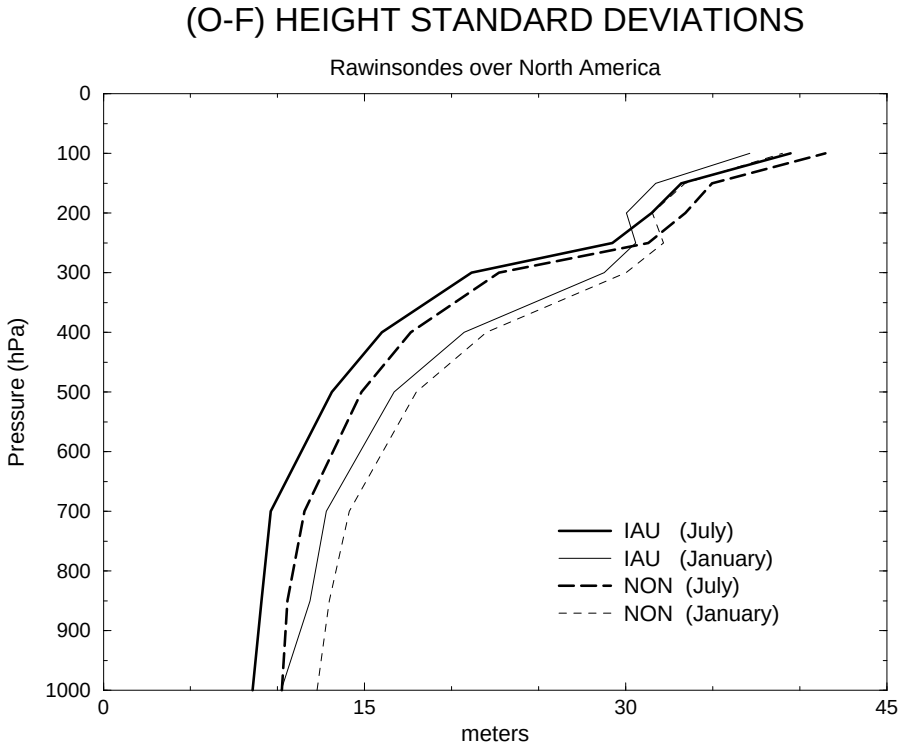

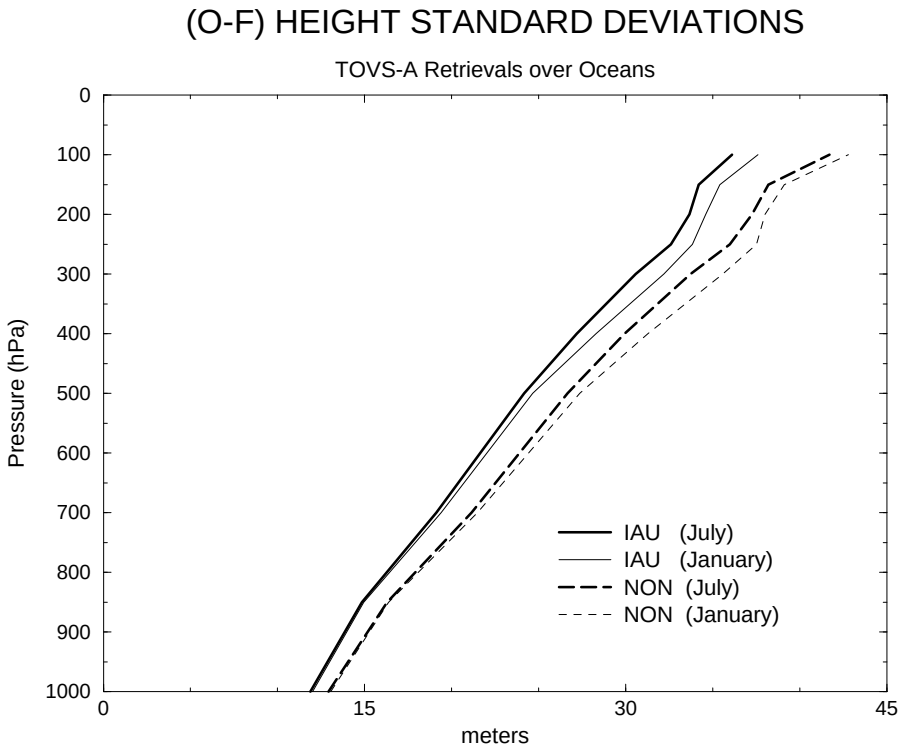

Figure 5.27: O-F standard deviations for geopotential heights. Four cases include: IAU, July 1978 (*heavy solid*); no IAU, July 1978 (*heavy dashed*); IAU, January 1978 (*light solid*); no IAU, January 1978 (*light dashed*). a) Rawinsondes over North America, b) TOVS-A retrievals over oceans.

5.5 References

Anderson, B. D. O., and J. B. Moore, 1979: *Optimal Filtering.* Prentice-Hall, 357pp.

Anderson, E., Z. Bai, C. Bischof, J. Demmel, J. Dongarra, J. du Croz, A. Greenbaum, S. Hammarling, A. McKenney, S. Ostrouchov, D. Sorensen, 1992: LAPACK User's Guide. *Society for Industrial and Applied Mathematics*, Philadelphia, PA, 235pp.

Arakawa, A. and V.R. Lamb, 1981: A potential enstrophy and energy conserving scheme for the shallow water equations. *Mon. Wea. Rev.*, **109**, 18-36.

Arakawa, A. and M.J. Suarez, 1983: Vertical differencing of the primitive equations in sigma coordinates. *Mon. Wea. Rev.*, **111**, 34-45.

Asselin, R., 1972: Frequency filter for time integrations. *Mon. Wea. Rev.*, **100**, 487-490.

Baker, N. L., 1991: An adaptive correction procedure for radiosonde geopotential height biases. *Preprints, Ninth Conference on Numerical Weather Prediction,* Denver CO, 192–194.

Baker, W.E., S.C. Bloom, J.S. Woollen, M.S. Nestler, E.Brin, T.W. Schlatter, and G.W. Branstator, 1987: Experiments with a three-dimensional statistical objective analysis scheme using FGGE data. *Mon. Wea. Rev.*, **115**, 273–296.

Blackadar, A.K.,1977: High Resolution Models of the Planetary Boundary Layer. *Advances in Environmental Science and Engineering, Vol 1* Editors Pfafflin and Zeigler, Gordon and Breach, Scientific Publishers.

Bloom, S.C., L.L. Takacs, A.M. da Silva, and D. Ledvina, 1996: Data Assimilation Using Incremental Analysis Updates. *Mon. Wea. Rev.*, **124**, 1256-1271.

Burridge, D.M. and J. Haseler, 1977: A model for medium range weather forecasting—adiabatic formulation, *Tech. Report. No. 4, European Center for Medium Range Weather Forecasts*, Brachnell, Berkshire, UK.

Cohn, S.E., 1996: An introduction to estimation theory. *J. Met. Soc. Japan*, submitted.

Cohn, S.E., and R. Todling, 1996: Approximate data assimilation schemes for stable and unstable dynamics. *J. Met. Soc. Japan*, **74**, 63–75.

Cohn, S.E., N.S. Sivakumaran, and R. Todling, 1994: A fixed-lag Kalman smoother for retrospective data assimilation. *Mon. Wea. Rev.*, **122**, 2838–2867.

Chou, M.-D., 1992: A solar radiation model for use in climate studies. *J. Atmos. Sci.*, **49**, 762-772.

Chou, M.-D., 1990: Parameterizations for the absorption of solar radiation by O_2 and CO_2 with applications to climate studies. *J. Climate*, **3**, 209-217.

Chou, M. -D., and M.J.Suarez, 1994: An efficient thermal infrared radiation parameterization for use in general circulation models. *NASA Tech. Memorandum 104606*, Vol **3**. NASA Goddard Space Flight Center, Greenbelt, MD 20771. Available on-line from `http://dao.gsfc.nasa.gov/subpages/tech-reports.html`.

Clarke, R. H., 1970: Observational studies in the atmospheric boundary layer. *Quart. J. Roy. Meteor. Soc.*, **96**, 91-114.

Courtier, P., E. Andersson, W. Heckley, G. Kelly, J. Pailleux, F. Rabier, J.-N. Thepaut, P. Unden, D. Vasiljevic, C. Cardinali, J. Eyre, M. Hamrud, J. Haseler, A. Hollingsworth, A. Mc Nally, and A. Stoffelen, 1993: Variational Assimilation at ECMWF. *ECMWF Technical Memorandum*, No. 194. Reading, England, 84pp.

Courtier, P., J.-N. Thépaut and A. Hollingsworth, 1994: A strategy for operational implementation of 4D-Var, using an incremental approach. *Q. J. R. Meteorol. Soc.*, **120**, 1367-1388.

Daley, R., 1991: *Atmospheric Data Analysis.* Cambridge University Press. New York, 457pp. ISBN 0-521-38215-7.

Dee, D. P., 1995: On-line estimation of error covariance parameters for atmospheric data assimilation. *Mon. Wea. Rev.*, **123**, 1128–1145.

Dee, D. P., and A. M. da Silva, 1996: Data assimilation in the presence of forecast bias. DAO Office Note 96-18. Data Assimilation Office, Goddard Space Flight Center, Greenbelt, MD 20771. Available on-line from
`http://dao.gsfc.nasa.gov/subpages/office-notes.html`.

Defries, R. S., and J. R. G. Townshend, 1994: NDVI-derived Land Cover Classification at Global Scales. *Int'l J. Rem. Sens.* **15**, 3567-3586. Special Issue on Global Data Sets.

Derber, J.C., and W.S. Wu, 1996: The use of cloud-cleared radiances in the NCEP's SSI analysis system. *Preprint volume, 11th Conf. on Numerical Weather Prediction*, August 19-23, 1996, Norfolk, VA.

Dewey, K. F. and R. Heim Jr., 1981: Satellite Observations of Variations in Northern Hemisphere Seasonal Snow Cover. NOAA Tech. Report NESS 87, National Technical Information Service (NTIS), Springfield, VA.

Ding, H. D. and R. D. Ferraro, 1996: An 18GFLOPS Parallel Data Assimilation PSAS Package, *Proceedings of Intel Supercomputer Users Group Conference 1996*, June 1996. To be published in Journal of Computers and Mathematics.

Dorman, J. L., and P. J. Sellers, 1989: A global climatology of albedo, roughness length and stomatal resistance for atmospheric general circulation models as represented by the Simple Biosphere model (SiB). *J. Appl. Meteor.*, **28**, 833-855.

Eyre, J. R., 1992: A bias correction scheme for simulated TOVS brightness temperatures. ECMWF Tech. Memo 176.

Eyre, J. R., Kelly, A. P., McNally, A. P., Andersson, E., and A. Persson, 1993: Assimilation of TOVS radiance information through one-dimensional variational analysis. *Q. J. R. Meteorol. Soc.*, **119**, 1427-1463.

Fox-Rabinovitz, M., H. M. Helfand, A. Hou, L. L. Takacs, and A. Molod, 1991: Numerical experiments on forecasting, climate simulation and data assimilation with the new 17 layer GLA GCM. Ninth Conference on Numerical Weather Prediction. 21-25 October 1991, Denver, CO, 506-509.

Gates, W. Lawrence, 1992: AMIP: The Atmospheric Model Intercomparison Project. *Bull. Am Met. Soc.*, **73**, 1962-1970

Gaspari, G., and S. E. Cohn, 1996: Construction of correlation functions in two and three dimensions. Submitted to *Mathematical Geology.* Also available as *DAO Office Note 96-03.* Data Assimilation Office, Goddard Space Flight Center, Greenbelt, MD 20771. Available on-line from
`http://dao.gsfc.nasa.gov/subpages/office-notes.html`.

Ghil, M., S. Cohn, J. Tavantzis, K. Bube, and E. Isaacson, 1981: Applications of estimation theory to numerical weather prediction. Pp. 139–225 in: Bengtsson, L., M. Ghil, and E. Källén, *Dynamic Meteorology: Data Assimilation Methods*, Springer-Verlag, New York, 330pp.

Golub, G. H. and C. F. van Loan, 1989: *Matrix Computations*, 2nd Edition, The John Hopkins University Press, 642pp.

Heckley, W. A., P. Courtier, J. Pailleux, and E. Anderson, 1993: The ECMWF Variational Analysis: general formulation and use of background information. *Proc. ECMWF Workshop on Variational Assimilation*, Reading, U.K., 49-94.

Helfand, H. M., and J. C. Labraga, 1988: Design of a non-singular level 2.5 second-order closure model for the prediction of atmospheric turbulence. *J. Atmos. Sci.*, **45**, 113-132.

Helfand, H. M., M. Fox-Rabinovitz, L. Takacs, and A. Molod, 1991: Simulation of the planetary boundary layer and turbulence in the GLA GCM. Proceedings of the AMS Ninth Conference on Numerical Weather Predicition, 21-25 October 1991, Denver, CO, 514-517.

Helfand, H. M., M. and S. D. Schubert, 1995: Climatology of the Simulated Great Plains Low-Level Jet and Its contribution to the Continental Moisture Budget of the United States. *J. Climate*, **8**, 784-806.

Higgins, R. W., and S. D. Schubert, 1993: Low-frequency synoptic-eddy activity in the Pacific storm track. *J. Atmos. Sci.*, **50**, 1672-1690.

Hollingsworth, A., P. Kållberg, V. Renner, and D.M. Burridge, 1983: An internal symmetric computational instability, *Quart. J. R. Met Soc.* , **109**, 417-428.

Jazwinski, A. H., 1970: *Stochastic Processes and Filtering Theory*, Academic Press, New York, 376pp.

Joiner, J. and A. M. da Silva, 1996: Efficient methods to Assimilate Satellite Retrievals Based on Information Content. *DAO Office Note 96-06.*. Data Assimilation Office, Goddard Space Flight Center, Greenbelt, MD 20771. Available on-line from `http://dao.gsfc.nasa.gov/subpages/office-notes.html`.

Julian, P. R., 1991: RADCOR91 - The new radiosonde radiation error correction procedure. NMC Office Note 374.

Kalnay, E., M. Kanamitsu, J. Pfaendtner, J. Sela, M. Suarez, J. Stackpole, J. Tuccillo, L. Umscheid, and D. Williamson, 1989: Rules for the interchange of physical parameterizations, *Bull. Am Met. Soc.*, **70**, 620-622.

King, M.D. and Harshvardhan, 1986: Comparative Accuracy of Selected Multi ple Scattering Approximations. *J. Atmos. Sci.*, **43**, 784-801.

Kondo, J., 1975: Air-sea bulk transfer coefficients in diabatic conditions. *Boundary Layer Meteor.*, **9**, 91-112.

Koster, Randal D. and Max J. Suarez, 1991: A Simplified Treatment of SiB's Land Surface Albedo Parameterization. *NASA Technical Memorandum 104538.* Goddard Space Flight Center, Greenbelt, MD 20771. Available on-line from `http://dao.gsfc.nasa.gov/subpages/tech-reports.html`, 11pp.

Koster, Randal D. and Max J. Suarez, 1992: Modeling the Land Surface Boundary in Climate Models as a Composite of Independent Vegetation Stands. *J. Geophys. Res.* **97** No. D3, 2697-2715.

Lacis, A. A., and J. E. Hansen, 1974: A parameterization for the absorption of solar radiation in the Earth's atmosphere. *J. Atmos. Sci.*, **31**, 118-133.

Lanczos, C., 1966: *Discourse on Fourier Series.* Hafner Publishing, 255 pp.

Large, W. G., and S. Pond, 1981: Open ocean momentum flux measurements in moderate to strong winds. *J. Phys. Oceanogr.*, **11**, 324-336.

Ledvina, D. V., and J. Pfaendtner, 1995: Inclusion of Special Sensor Microwave/Imager (SSM/I) total precipitable water estimates into the GEOS-1 Data Assimilation System, *Mon. Weath. Rev.,* **123**, 3003-3015.

Lorenc, A.C., 1981: A global three-dimensional multivariate statistical interpolation scheme. *Mon. Wea. Rev.*, **109**, 701–721.

Lorenc, A.C., 1986: Analysis methods for numerical weather prediction. *Quart. J. Roy. Meteor. Soc.*, **112**, 1177–1194.

Lou, G.-P., A. da Silva, D. Dee, and C. Redder, 1996: Modeling fully anisotropic wind-mass error covariances in physical space. *Preprint volume, 11th Conf. on Numerical Weather Prediction,* August 19–23, 1996, Norfolk, VA, p 253.

McPherson, R.D., K.H. Bergman, R.E. Kistler, G.E. Rasch, and D.S. Gordon, 1979: The NMC operational global data assimilation system. *Mon. Wea. Rev.*, **107**, 1445–1461.

Mintz, Y. and Y. Serafini, 1984: Global fields of monthly normal soil moisture as derived from observed precipitation and an estimated potential evapotranspiration. Final scientific report under NASA grant NAS 5-26, Part V, Dept. of Meteorology, University of Maryland, College Park, MD

Miyakoda, K., and J. Sirutis, 1990: Subgrid scale physics in 1-month forecasts. Part II: Systematic error and blocking forecasts. *Mon. Wea. Rev.*, **118**, 1065–1081.

Molod, Andrea, H.M. Helfand, and L.L. Takacs, 1996: The Climatology of Parameterized Physical Processes in the GEOS-1 GCM and their Impact on the GEOS-1 Data Assimilation System. *J. Climate*, **9**, 764-785.

Moorthi, S., and M. J. Suarez, 1992: Relaxed Arakawa Schubert: A parameterization of moist convection for general circulation models. *Mon. Wea. Rev.*, **120**, 978-1002.

Panofsky, H. A., 1973: Tower Micrometeorology. In Workshop on Micrometeorology, D. A. Haugen (ed.), American Meteorological Society, Boston, 392 pp.

Parrish, D.F. and J.C. Derber, 1992: The National Meteorlogical Center's statistical spectral interpolation analysis system. *Mon. Wea. Rev.*, **109**, 1747-1763.

Pfaendtner, J., S. Bloom, D. Lamich, M. Seablom, M. Sienkiewicz, J. Stobie, A. da Silva, 1995: Documentation of the Goddard Earth Observing System (GEOS) Data Assimilation System–Version 1. *NASA Tech. Memo. No. 104606*, Vol. **4**, NASA Goddard Space Flight Center, Greenbelt, MD 20771. Available on-line from `http://dao.gsfc.nasa.gov/subpages/tech-reports.html`.

Pfaendtner, J., 1996: Notes on the Icosahedral Domain Decomposition in PSAS. *DAO Office Note 96-04*. Data Assimilation Office, Goddard Space Flight Center, Greenbelt, MD 20771. Available on-line from `http://dao.gsfc.nasa.gov/subpages/office-notes.html`.

Phillips, N. A., 1957: A coordintate system having some special advantages for numerical forecasting. *J. Meteor.*, **14**, 184-185.

Posey, J. W., and P. F. Clapp, 1964: Global distribution of normal surface albedo. *Geofis. Int.*, **4**, 33-48.

Reynolds, R. W., 1988: A real time global sea surface temperature analysis. *J. Climate*, **1**, 75-86.

Reynolds, R. W. and D. C. Marsico, 1993: An improved real-time global sea surface temperature analysis. *J. Climate*, **6**, 114-119.

Reynolds, R. W. and T. M. Smith, 1994: Improved global sea surface temperature analyses using optimum interpolation. *J. Climate*, **7**, 929-948.

Reynolds, C., R. Gelaro, and T. Murphree, 1996: Observed and simulated Northern Hemisphere intraseasonal circulation anomalies and the influence of model bias. *Mon. Wea. Rev.*, **124**, 1100–1118.

Rosenfield, J. E., M. R. Schoeberl, and M. A. Geller, 1987: A computation of the stratospheric diabatic circulation using an accurate radiative transfer model. *J. Atmos. Sci.*, **44**, 859-876.

Sadourney, R., 1975: The dynamics of finite difference models of the shallow water equations, *J. Atmos. Sci.*, **32**, 680-689.

Sagan, C. and J.B. Pollack, 1967: Anisotropic Nonconservative Scattering and the Clouds of Venus. *J. Geophys. Res.*, **72**, 469-477.

Schemm, J., S. Schubert, J. Terry, and S. Bloom, 1992: Estimates of monthly mean soil moisture for 1979-1989. *NASA Tech. Memo. No. 104571.* Goddard Space Flight Center, Greenbelt, MD 20771.

Schubert, S. D., J. Pfaendtner and R. Rood, 1993: An assimilated data set for Earth Science applications, *Bull. Am Met. Soc.*, **74**, 2331-2342

Schubert, S., M. Suarez, C. K. Park, and S. Moorthi, 1993: GCM Simulations of intraseasonal variability in the Pacific/North American region. *J. Atmos. Sci.*, **50**, 1991-2007.

da Silva, A., and J. Guo, 1996: Documentation of the Physical-Space Statistical Analysis System (PSAS) Part I: The Conjugate Gradiant Solver version PSAS-1.00 *DAO Office Note 96-02.* Data Assimilation Office, Goddard Space Flight Center, Greenbelt, MD 20771. Available on-line from
`http://dao.gsfc.nasa.gov/subpages/office-notes.html`.

da Silva, A. M., C. Redder, and D. P. Dee, 1996: Modeling retrieval error covariances for atmospheric data assimilation. Presented at the *Eighth Conference on Satellite Meteorology,* Atlanta, GA, 28 January–2 February, 1996. Available on-line as
`ftp://dao.gsfc.nasa.gov/pub/papers/dasilva/atlanta96/tuning.ps.Z`.

Shapiro, R., 1970: Smoothing, filtering and boundary effects. *Rev. Geophys. Space Phys.*, **8**, 359-387.

Slutz, R. J., S. J. Lubker, J. D. Hiscox, S. D. Woodruff, R. L. Jenne, D. H. Joseph, P. M. Steuer, and J. D. Elms, 1985: Comprehensive Ocean-Atmosphere Data Set: Release 1. NOAA Environmental Research Laboratory, Boulder, CO, 268 pp.

Suarez, M. J., and L. L. Takacs, 1996: Documentation of the Aries/GEOS Dynamical Core Version 2. *NASA Technical Memorandum 104606*, Volume **5**, NASA Goddard Space Flight Center, Greenbelt, MD 20771. Available on-line from
`http://dao.gsfc.nasa.gov/subpages/tech-reports.html`.

Sud, Y. C., and A. Molod, 1988: The roles of dry convection, cloud-radiation feedback processes and the influence of recent improvements in the parameterization of convection in the GLA GCM. *Mon. Wea. Rev.*, **116**, 2366-2387.

Sud, Y. C., P. J. Sellers, Y. Mintz, M. D. Chou, G. K. Walker, and W. E. Smith, 1990: Influence of the Biosphere on the Global Circulation and Hydrological Cycle - A GCM Simulation Experiment. *Agric. and Forest Meteo.*, **52**, 113-180.

Takacs, L. L. , A. Molod, and T. Wang, 1994: Documentation of the Goddard Earth Observing System (GEOS) General Circulation Model-Version 1. *NASA Technical Memorandum 104606*, Volume **1**, NASA Goddard Space Flight Center, Greenbelt, MD 20771. Available on-line from
`http://dao.gsfc.nasa.gov/subpages/tech-reports.html`.

Takacs, L.L., and M.J. Suarez, 1996: Dynamical aspects of climate simulations Using the GEOS General Circulation Model. *NASA Technical Memorandum 104606*, Volume **10**, NASA Goddard Space Flight Center, Greenbelt, MD 20771. Available on-line from
`http://dao.gsfc.nasa.gov/subpages/tech-reports.html`.

Thépaut, J.-N., P. Courtier, G. Belaud and G. Lemaitre, 1996: Dynamical structure functions in a four-dimensional variational assimilation: A case study. *Q. J. R. Meteorol. Soc.*, **122**, 535–561.

Tibaldi, S., and F. Molteni, 1990: On the operational predictability of blocking. *Tellus*, **42A**, 343–365.

Todling, R., N.S. Sivakumaran, and S.E. Cohn, 1996: Some strategies for retrospective data assimilation: Approximate fixed-lag Kalman smoothers. *Preprint volume, 11th Conf. on Numerical Weather Prediction*, August 19-23, 1996, Norfolk, VA, pp. 238–240.

Woodruff, S. D., S. J. Lubker, K. Wolter, S. J. Worley, and J. D. Elms, 1993: Comprehensive Ocean-Atmosphere Data Set (COADS) Release 1a: 1980-1992. Earth System Monitor, Vol. 4, No. 1, September 1993, NOAA.

Yaglom, A. M., and B. A. Kader, 1974: Heat and mass transfer between a rough wall and turbulent fluid flow at high Reynolds and Peclet numbers. *J. Fluid Mech.*, **62**, 601-623.

Yamada, T., 1977: A numerical experiment on pollutant dispersion in a hor izontally-homogenious atmospheric boudnary layer. *Atmos. Environ.*, **11**, 1015-1024.

Zhou, J., Y.C. Sud, and K.-M. Lau, 1995: Impact of Orographically Induced Gravity Wave Drag in the GLA GCM, *Quart. J. Roy. Meteor. Soc.*, **122**, 903-927.

5.6 Acronyms

5.6.1 General acronyms

DAO	Data Assimilation Office
GEOS	Goddard Earth Observing System (The name of the DAO data assimilation system)
GCM	General Circulation Model
DAS	Data Assimilation System
QC	Quality Control
NWP	Numerical Weather Prediction
CARD	Consistent Assimilation of Retrieved Data
PSAS	Physical-space Statistical Analysis System
NASA	National Aeronautics and Space Administration
GSFC	Goddard Space Flight Center
MTPE	Mission to Planet Earth
EOS	Earth Observing System
EOSDIS	Earth Observing System Data and Information System
NOAA	National Oceanic and Atmospheric Administration
NCEP	National Centers for Environmental Prediction (formerly, NMC)
NMC	National Meteorological Center
NESDIS	National Environmental Satellite Data and Information Service
ECMWF	European Center for Medium-range Weather Forecasts
UKMO	United Kingdom Meteorological Office

5.6.2 Instruments

ADEOS	Advanced Earth Observting Satellite (Mid-late 1996)
AIRS	Atmospheric Infrared Sounder (EOS PM)
AMSU A-B	Advanced Microwave Sounding Unit (POES, EOS PM)
AVHRR	Advanced Very High-Resolution Radiometer
ASTER	Advanced Spaceborne Thermal Emission and Reflection Radiometer (EOS AM)
ATOVS	Advanced TOVS; HIRS3/AMSU (POES)
CERES	Clouds and Earth's Radiation Energy System (TRMM, EOS AM)
CLAES	Cryogenic Limb Array Etalon Spectrometer (UARS)
DMSP	Defense Meteorological Satellite Program (currently operational)
EOS AM1	Earth Observting Satellite AM (June 98 launch)
EPS	EUMETSAT (European Meteorology Satellite) Polar System
ERBE	Earth Radiation Budget Experiment (ERBS)
ERBS	Earth Radiation Budget Satellite
ERS-1,2	European Remote Sensing Satellite (Scatterometer, 6 channel, IR-Visible radiometer)

GOES	Geostationary Observational Environmental Satellite (Imager and 18 channel visible and infrared sounder, currently operational)
GOME	Global Ozone Monitoring Experiment (ERS-2)
GPS	Global Positioning System
HALOE	Halogen Occultation Experiment (UARS)
HIRS2/3	High-Resolution InfraRed Sounder (POES)
HRDI	High Resolution Doppler Imager
IASI	Infrared Atmospheric Sounding Interferometer (EPS)
ILAS	Improved Limb Atmospheric Spectrometer (ADEOS)
IMG	Interferometric Monitor for Greenhouse Gases (ADEOS)
ISCCP	International Satellite Cloud Climatology Project (several IR and visible instruments aboard different satellite)
LIMS	Limb Infrared Monitor of the Stratosphere (Nimbus 7)
MAPS	Measurement of Atmospheric Pollution from Satellites
MHS	Microwave Humidity Sounder (EOS-PM)
MLS	Microwave Limb Sounder (UARS)
MODIS	Moderate-Resolution Imaging Spectrometer (EOS AM)
MSU	Microwave Sounding Unit
MOPITT	Measurement of Pollution in the Troposphere (EOS AM)
NSCAT	NASA Scatterometer (ADEOS)
POES	Polar Orbiting Environmental Satellite (Currently Operational)
PR	Precipitation Radar (TRMM)
SBUV	Satellite Backscatter Ultraviolet radiometer (Nimbus 7, POES)
SAGE	Stratospheric Aerosol and Gas Experiment (ERBS)
SMMR	Scanning Multispectral Microwave Radiometer (?)
SSM/I	Special Sensor Microwave/Imager (DMSP)
SSM/T	Special Sensor Microwave (Temperature sounder, DMSP)
SSM/T2	Special Sensor Microwave (Water vapor sounder) (DMSP)
SSU	Stratospheric Sounding Unit (POES)
TMI	TRMM Microwave Imager (TRMM)
TOMS	Total Ozone Mapping Spectrometer (ADEOS, Meteor, Earth Probe, Nimbus 7)
TOVS	TIROS Operational Vertical Sounder; HIRS2/MSU/SSU (POES)
TRMM	Tropical Rainfall Measuring Mission (summer '97 launch)
UARS	Upper Atmospheric Research Satellite (some instruments in operation)
WINDII	Wind Imaging Interferometer (UARS)

Chapter 6

Quality Control of Input Data Sets

Contents

6.1 Quality Control in the GEOS Data Assimilation System

One of the major components of any assimilation system is the quality control of input data stream. Originally (see Section 2.4.3), the DAO relied on existing quality control algorithms, with the strategy of importing more modern algorithms from NCEP. While the NCEP algorithms can provide the basis for improved DAO quality control, experience with GEOS-1 requires the DAO to pay more attention to developing quality control algorithms. This is due both to analysis sensitivity to quality control decisions and the requirement for the DAO to accommodate many new data types which are not used by, or of little interest to, the numerical weather prediction community.

Quality control (QC) refers to the process by which observational data and their attributes are analyzed in order to

- identify data items which are likely to contain gross errors
- attempt to correct such errors

Gross errors, also known as rough errors in papers by Collins and Gandin (1990–1996), are any inaccuracies that cannot be explained in terms of

- detection noise of the observing instrument under normal operating conditions
- small-scale variability
- approximations inherent to the observation operator

Clearly QC for any single observation must involve information other than the observational datum itself, such as:

- attributes of the observation (units, time, location, etc.)
- observation error statistics (for non-gross errors)
- operating conditions of the instrument (e.g. scan angle)
- gross error statistics
- probable causes of gross errors
- other nearby observations
- known spatial and/or temporal relationships between geophysical parameters
- climatological information
- a model forecast valid in the vicinity of the observation location
- forecast error statistics

The QC process consists of a set of algorithms which examine each data item, singly or jointly, in the context of this additional information. Their primary purpose is to determine which of the data are likely to contain unknown (incorrigible) gross errors, and which are not. The algorithms can be categorized as follows:

QC1: A testing algorithm produces a quality mark for each data item it processes. Each test can be regarded as a hypothesis test on the actual error associated with the data item in view of some of the additional information listed above.

QC2: A correction algorithm produces an estimate of the actual gross error, which may (or may not) be subsequently used to modify a data item. Correction algorithms analyze the probable cause of the gross error, and produce an estimate of the gross error if the cause can be determined with a sufficient degree of confidence.

QC3: A decision making algorithm (DMA) produces the final decision regarding the disposition of each data item, which is one of the following: *accept* or *reject*. This decision is made at the very end of the QC process, based on the cumulative results of the testing and correction algorithms (TCA) to which the data have been subjected.

It might seem natural to include bias correction algorithms in the domain of quality control as well. However, bias is not a manifestation of gross error. Bias is, by definition, systematic whereas gross errors tend to be erratic. Conceptually, therefore, bias correction must be separated from the quality control process.

In addition to these requirements there are other quality control functions required for the input data stream. These are categorized as pre-processing functions which synchronize and reformat the observations. This process also tests for completeness of the observations and performs some basic consistency checks.

6.2 Pre-processing and Quality Control in GEOS-1 Data Assimilation System

One of the major accomplishments of the GEOS-1 project was pre-processing fifteen years of data from rawinsondes, dropwindsondes, aircraft winds, cloud drift winds, and NOAA NESDIS TOVS retrievals. Acquisition of the data, and filling in data gaps was a major bottleneck in the production stream, and required at times going through boxes of tapes stored at federal warehouses or seeking data from other institutions. One benefit is that the DAO was able to provide some of their mined data to NCEP for the NCEP re-analysis. This effort produced an archive of information about the historical data record that provides a relative indicator of analysis quality based on the input data stream. The DAO archive also provides the basis for future DAO re-analyses.

6.2.1 Pre-processing: Completeness, Synchronization, Sorting

The GEOS-1 DAS ingests the global conventional observations and the temperature retrievals from the HIRS2/MSU/SSU sounders on the NOAA satellites. Either the NESDIS retrieved temperature profiles or those created by the Goddard Laboratory for Atmospheres (Susskind 1993) physical retrieval system are used.

In the first step conventional data in (NMC Office Note 29, Keyser, 1994), format as well as the NESDIS format retrieval data are unpacked and put into common format data sets of one day each. A day corresponds to the four analysis times: 0, 6, 12 and 18 UTC. Thus, the observations in one file will be from 2100 UTC of the previous day to 2059 UTC of the current day. All data that appear in the original data sets are kept, except those that do not have a realistic time stamp. Reports that are obviously in the wrong synoptic time (late arriving data, for example) are moved to the correct file. These data sets form a complete set of historical observations that are easily manageable on the computer system.

The second step standardizes the observations for ingest into the objective analysis. Only observations of quantities to be analyzed are extracted for these data sets: sea level pressure and wind, upper-air height, wind and moisture. The satellite temperature retrievals are converted into thicknesses. The observations are stratified by type (e.g., surface land, surface ship) and in some instances by location. This is necessary to assign the proper observation errors to the data.

Once the observations to be analyzed are extracted, the next step:

- eliminates observations marked as bad by the provider
- keeps observations marked as suspicious by the provider and maintains provider's quality flag.
- eliminates observations with grossly bad values.
- performs a hydrostatic check on rawinsonde data.
- checks satellite profiles for completeness

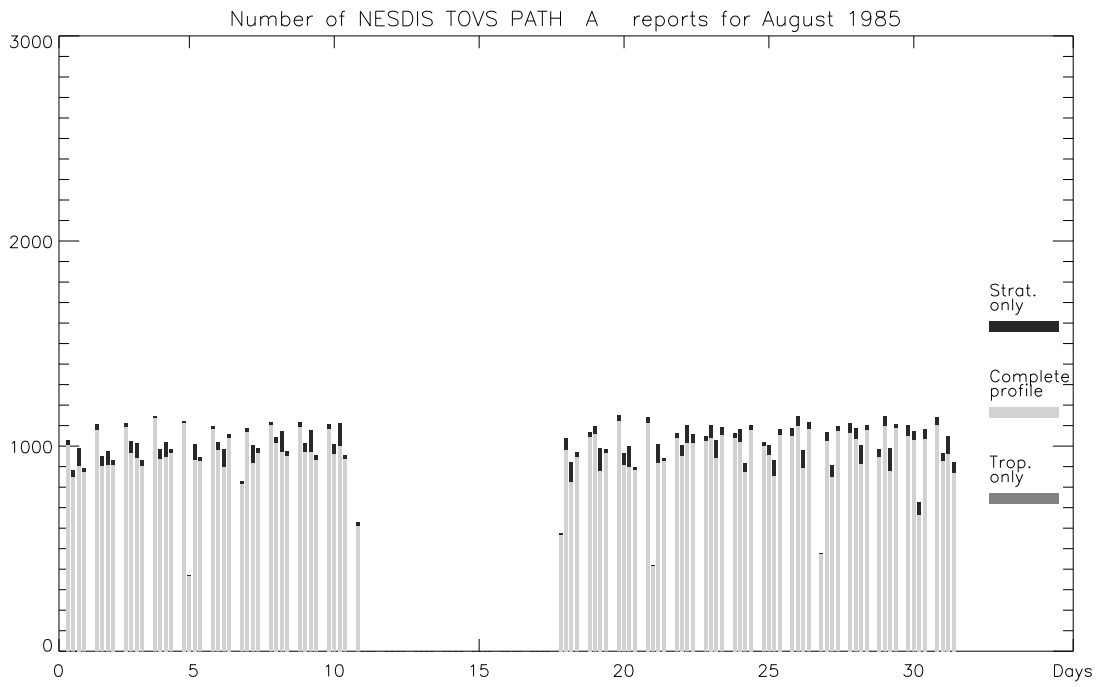

Figure 6.1: Number of NESDIS TOVS retrievals for August 1985. Number of NESDIS TOVS path A (clear column) temperature retrievals for each synoptic time in the month of August 1985. Stratospheric retrieval profiles are those that only have levels above 100 hPa; tropospheric retrieval profiles are those that only have levels below 100 hPa. Complete profiles report at all levels.

The observation data sets are checked for completeness. A program is run to detect gaps in the observation time series. This program also categorizes each observation by type, synoptic time and in the case of retrieved satellite temperature profiles, by the vertical extent of the profile stratospheric and tropospheric profiles in the case of NESDIS TOVS data). These counts are then graphically displayed as a series of bar charts as in Figure 6.1. In this figure, the number of NESDIS TOVS path A (clear column) temperature retrievals for each synoptic time in the month of August 1985 is shown. The program has identified a significant gap in the TOVS data record from 11 to 17 August. If possible, attempts are made to fill these data gaps. If not, the normal procedure is to forecast through the data gap, counting on the other data in the assimilation to maintain credible accuracy on the analysis. These charts provide a record of the observational data that are available to the analysis at a particular time and are made available to the users. They provide a relative measure of analysis quality.

6.2.2 Quality Control during Objective Analysis

The data quality control is an important part of any data analysis scheme, as demonstrated in Shaw et al. (1986). More recent studies performed with the GEOS-1 DAS confirm that changes in quality control and subsequent data selection can have a significant impact on

the assimilation. Park and Schubert (1996) identified quality control decisions as one of the source of differences between the NCEP re-analyses and GEOS-1.

The quality control technique during the analysis cycle employed in the GEOS-1 DAS consists of two major steps: a gross error check and a buddy check (Seablom 1990). The gross error check is defined to be:

$$\Delta \geq \left(\sigma_o^2 + \sigma_f^2\right) \tau, \tag{6.1}$$

where Δ is the difference between an observation and the interpolated background first-guess value, σ_o and σ_f are the observation and forecast error variances, respectively, and τ is a subjectively defined tolerance value which varies with quantity, latitude and height.

The tolerance value is somewhat reduced for all quantities in the tropics and increased slightly for the winds near jet level in the middle latitudes. Those data that fail to satisfy the gross error check are marked as suspect. The buddy check involves performing a single pass successive-correction analysis of the data that passed the gross check to the locations of the suspect data. The difference between the interpolated value and the suspect value is then compared to the error statistics as in the gross error check and a decision is then made to re-accept the observation or to reject it. Typical rejection rates are between 5 and 10%.

6.3 Pre-processing and Quality Control for GEOS-2 Data Assimilation System

The effort to improve quality control for the GEOS-DAS is just getting underway. The lessons learned from GEOS-1 are helping to define the future directions. The quality control for GEOS-2 will remain virtually the same as that for GEOS-1. Intentions for incremental quality control development are outlined in Chapter 9.

6.4 References

Collins, W. G., 1991: Complex Quality Control of Rawinsonde Heights and Temperatures at the National Meteorological Center, Preprints, Ninth Conference on Numerical Weather Prediction, Denver, CO, American Meteorological Society, 15-18.

Collins, W. G., and L. S. Gandin, 1996: Complex Quality Control for Observation Errors of Rawinsonde Temperatures and Heights, Office Note 413, U. S. Department of Commerce, National Oceanographic and Atmospheric Administration, National Weather Service, Environmental Modeling Center.

Collins, W. G., and L. S. Gandin, 1995: Complex Quality Control of Rawinsonde Heights and Temperatures – Principles and Application at the National Meteorological Center, Office Note 408, U. S. Department of Commerce, National Oceanographic and Atmospheric Administration, National Weather Service, National Meteorological Center.

Collins, W. G., and L. S. Gandin, 1992: Complex Quality Control of Rawinsonde Heights and Temperatures (CQCHT) at the National Meteorological Center, Office Note 390, U. S. Department of Commerce, National Oceanographic and Atmospheric Administration, National Weather Service, National Meteorological Center.

Collins, W. G. and L. S. Gandin, 1990: Comprehensive hydrostatic quality control at the National Meteorological Center, Mon. Wea. Rev., 18, 2754–2767.

Gandin, L. S., 1991: Two Years of Operational Comprehensive Hydrostatic Quality Control at the NMC, Preprints, Ninth Conference on Numerical Weather Prediction, Denver, CO, American Meteorological Society, 11-14.

Keyser, D., 1994: NMC Format for Observational Data (Upper-air, Single-level, Cloud Cover, Additional Reports), Office Note 29, U. S. Department of Commerce, National Oceanographic and Atmospheric Administration, National Weather Service, National Meteorological Center, Revised version of original 1973 edition.

Seablom, M. S., 1990: Experiments with new quality control techniques in the NASA optimum interpolation analysis system, Preprints, International Symposium on Assimilation of Observations in Meteorology and Oceanography, Clermont-Ferrand, France, World Meteorological Organization, 628-630.

Shaw, D. B., P. Lonnberg, A. Hollingsworth, and P. Unden, 1986: Data assimilation 1984/1985 revisions of the ECMWF mass and wind analysis, Q. J. Roy. Meteor. Soc., 113, 553-566.

Susskind, J. 1993: Water vapor and temperature, in Atlas of Satellite Observations Related to Global Change, Edited by R. J. Gurney, J. L. Foster. and C. L. Parkinson. Cambridge University Press, Cambridge England, 89-128.

6.5 Acronyms

6.5.1 General acronyms

DAO	Data Assimilation Office
GEOS	Goddard Earth Observing System (The name of the DAO data assimilation system)
GCM	General Circulation Model
DAS	Data Assimilation System
QC	Quality Control
NWP	Numerical Weather Prediction
CARD	Consistent Assimilation of Retrieved Data
PSAS	Physical-space Statistical Analysis System
NASA	National Aeronautics and Space Administration
GSFC	Goddard Space Flight Center
MTPE	Mission to Planet Earth
EOS	Earth Observing System
EOSDIS	Earth Observing System Data and Information System
NOAA	National Oceanic and Atmospheric Administration
NCEP	National Centers for Environmental Prediction (formerly, NMC)
NMC	National Meteorological Center
NESDIS	National Environmental Satellite Data and Information Service
ECMWF	European Center for Medium-range Weather Forecasts
UKMO	United Kingdom Meteorological Office

6.5.2 Instruments

ADEOS	Advanced Earth Observting Satellite (Mid-late 1996)
AIRS	Atmospheric Infrared Sounder (EOS PM)
AMSU A-B	Advanced Microwave Sounding Unit (POES, EOS PM)
AVHRR	Advanced Very High-Resolution Radiometer
ASTER	Advanced Spaceborne Thermal Emission and Reflection Radiometer (EOS AM)
ATOVS	Advanced TOVS; HIRS3/AMSU (POES)
CERES	Clouds and Earth's Radiation Energy System (TRMM, EOS AM)
CLAES	Cryogenic Limb Array Etalon Spectrometer (UARS)
DMSP	Defense Meteorological Satellite Program (currently operational)
EOS AM1	Earth Observting Satellite AM (June 98 launch)
EPS	EUMETSAT (European Meteorology Satellite) Polar System
ERBE	Earth Radiation Budget Experiment (ERBS)
ERBS	Earth Radiation Budget Satellite
ERS-1,2	European Remote Sensing Satellite (Scatterometer, 6 channel, IR-Visible radiometer)

GOES	Geostationary Observational Environmental Satellite (Imager and 18 channel visible and infrared sounder, currently operational)
GOME	Global Ozone Monitoring Experiment (ERS-2)
GPS	Global Positioning System
HALOE	Halogen Occultation Experiment (UARS)
HIRS2/3	High-Resolution InfraRed Sounder (POES)
HRDI	High Resolution Doppler Imager
IASI	Infrared Atmospheric Sounding Interferometer (EPS)
ILAS	Improved Limb Atmospheric Spectrometer (ADEOS)
IMG	Interferometric Monitor for Greenhouse Gases (ADEOS)
ISCCP	International Satellite Cloud Climatology Project (several IR and visible instruments aboard different satellite)
LIMS	Limb Infrared Monitor of the Stratosphere (Nimbus 7)
MAPS	Measurement of Atmospheric Pollution from Satellites
MHS	Microwave Humidity Sounder (EOS-PM)
MLS	Microwave Limb Sounder (UARS)
MODIS	Moderate-Resolution Imaging Spectrometer (EOS AM)
MSU	Microwave Sounding Unit
MOPITT	Measurement of Pollution in the Troposphere (EOS AM)
NSCAT	NASA Scatterometer (ADEOS)
POES	Polar Orbiting Environmental Satellite (Currently Operational)
PR	Precipitation Radar (TRMM)
SBUV	Satellite Backscatter Ultraviolet radiometer (Nimbus 7, POES)
SAGE	Stratospheric Aerosol and Gas Experiment (ERBS)
SMMR	Scanning Multispectral Microwave Radiometer (?)
SSM/I	Special Sensor Microwave/Imager (DMSP)
SSM/T	Special Sensor Microwave (Temperature sounder, DMSP)
SSM/T2	Special Sensor Microwave (Water vapor sounder) (DMSP)
SSU	Stratospheric Sounding Unit (POES)
TMI	TRMM Microwave Imager (TRMM)
TOMS	Total Ozone Mapping Spectrometer (ADEOS, Meteor, Earth Probe, Nimbus 7)
TOVS	TIROS Operational Vertical Sounder; HIRS2/MSU/SSU (POES)
TRMM	Tropical Rainfall Measuring Mission (summer '97 launch)
UARS	Upper Atmospheric Research Satellite (some instruments in operation)
WINDII	Wind Imaging Interferometer (UARS)

Chapter 7

New Data Types

Contents

7.1 The Incorporation of New Data Types into the GEOS DAS

Perhaps the most important part of the DAO mission is the assimilation of new data types from current and future instruments. Emphasis is given to instruments that will fly as part of NASA's Mission to Planet Earth (MTPE) program, particularly those on board the Advanced Earth Observing System (ADEOS), the Tropical Rainfall Measuring Mission (TRMM), and the Earth Observing System AM-1 (EOS AM-1) scheduled for launches in 1996, 1997, and 1998, respectively (currently, this document only addresses satellites through EOS AM-1). The instruments aboard these satellites are designed to measure quantities related to atmospheric and surface parameters of particular relevance to Earth Systems study.

Much of the algorithm development discussed in Chapter 5 for GEOS-2 is building the infrastructure for new data types. The Physical–space Statistical Analysis System (PSAS) is designed to allow arbitrary specification of observation operators and error statistics. Much of the modeling development discussed in Chapter9 for GEOS-3 is to provide physically–based links to new types of observations. This includes cloud water parameterizations and a land-surface model.

Even with this infrastructure, the effort required to assimilate new data types is non-trivial. For example, at operational NWP centers, the effort to incorporate new data types has required approximately 5-10 person-years per new data type (and is an ongoing effort). New data types currently being considered for assimilation at the DAO may be classified into two categories:

1. Data types from instruments with an assimilation heritage at the DAO and other centers (*e.g.,* TOVS radiances, Scatterometer measurements, etc.)
2. Data types that do not have a long-term operational heritage (*e.g.,* precipitation, surface wetness, etc.).

Data types in (2) are considered to be a higher risk than those in (1).

The DAO effort to assimilate new data types includes:

- developing advanced assimilation methodologies to handle the large volume of data from future instruments
- monitoring new data types to assess data quality and develop error statistics
- interacting with instrument teams to assist with covariance tuning, systematic error correction (bias), quality control, operations, and development

This chapter defines and prioritizes the DAO approach to using new data types. The approach will evolve and achieve higher levels of definition as experience is gained with new data types. It will also provide instrument teams with information about what will be required from them in order to effectively incorporate observations into the GEOS DAS.

The outline of the document is as follows: Section 7.2 integrates the Earth-science fields introduced in section 2.6.2 with the effort to incorporate new data types into the GEOS DAS. This section begins with an overview and follows with subsections devoted to ES1-ES6 from section 2.6.2: the hydrological cycle, land-surface/atmosphere interaction, ocean-surface/atmosphere interaction, radiation (clouds, aerosols, greenhouse gases), atmospheric circulation, and constituents. For each scientific driver, examples of relevant data types are given. Section 7.3 discusses traditional and advanced methodologies for assimilating data and provides examples of relevant data types for each method. Section 7.4 describes several topics related to implementation: computational issues, data flow, and instrument team interaction. Finally, new and existing data types are prioritized in section 7.5. Cross-references of instrument to data type, scientific driver, and use in the GEOS DAS are provided.

7.2 Integration of Science Requirements with Sources of New Data

7.2.1 Overview

The NASA Mission to Planet Earth (MTPE) is a program designed to make use of ground, aircraft, and satellite-based measurements in order to better understand the systems that govern the Earth's climate, their interactions, and their variations. NASA's Earth Observing System (EOS) and several other satellite systems are key components of this program. Driving the selection of new data types in the GEOS DAS are the scientific objectives outlined by the MTPE program (see section 2.6.2). The link between new data types, data assimilation, and the Earth-science fields targeted by the DAO follow.

7.2.2 Hydrological Cycle

Water substance plays an integral role in many of the processes operating within the Earth System. In the atmosphere, latent heat release through condensation of water vapor, producing clouds, is a major source of energy that regulates atmospheric circulation. A large fraction of the energy transferred from the surface to the atmosphere is in the form of latent heat due to evaporation which itself depends on the moisture gradient between the surface and atmosphere. In addition, the presence of clouds and precipitation determines the availability of solar radiation and water at the surface. Water vapor is also the predominant greenhouse gas and plays a crucial radiative role in the global climate system.

Clearly, an accurate depiction of the global atmospheric moisture field, its vertical and horizontal transport, and the transfer of water across its boundaries, is critical to understanding the hydrologic cycle and its impact on climate. As discussed in Chapters 4 and 8 many of the deficiencies of the GEOS DAS (and, in fact, all data assimilation systems) are related to the representation of atmospheric water and clouds.

Currently most of the moisture information used in the GEOS DAS comes from rawinsonde ascents. Satellite moisture estimates offer a significant improvement over the spatial and temporal sampling problems of the existing rawinsonde network, but they also have

limitations. Polar orbiting satellites such as those in the Defense Meteorological Satellite Program (DMSP) carry microwave instruments which are sensitive to atmospheric moisture. The Special Sensor Microwave/Imager (SSM/I) for instance, gives an accurate estimate of the integrated water vapor in an atmospheric column (referred to as Total Precipitable Water, TPW) but contains little information about the vertical distribution of moisture which is critical to understanding many of the physical processes mentioned above. The SSM/I observations are also limited by the fact that they are only available over the oceans in regions free of precipitation and sea ice. SSM/T2 provides similar coverage, but contains additional channels that provide information about the vertical structure of moisture. However, SSM/T2 has virtually no heritage in data assimilation and its error characteristics are not well known. Other satellites, such as TIROS Operational Vertical Sounder (TOVS) which carries the High-resolution Infrared Sounder (HIRS) and the Microwave Sounding Unit (MSU), have better geographical coverage (over land as well as ocean) and can resolve the integrated water in approximately two thick slabs. Future microwave and infrared (IR) instruments, such as MHS (AMSU-B), AIRS, and IASI, will have improved vertical resolution for moisture sounding. Although still fairly crude, the moisture estimates that are/will be available from these satellites are valuable both for assimilation, validation, and bias estimation. For example, information about global moisture derived from SSM/I and TOVS has been assimilated at DAO and other centers (*e.g.,* Ledvina and Pfaendtner 1995, Derber *private communication*, Andersson et al. 1994) and has significantly impacted global analyses.

Significant discrepancies have been found between precipitation estimates from analysis systems and those derived from satellite measurements (*e.g.,* Adler et al. 1996). Systematic differences in both the intensity and spatial distribution of monthly mean precipitation are especially large in the tropics. Current research at the DAO is directed towards assimilating precipitation data. Improving the hydrological cycle in analyses in both the tropics and extra-tropics will ultimately aid in the understanding of climate sensitivity, climate variability, the role of dynamical feedback, and other physical processes. Improving the hydrological cycle in data assimilation systems will also benefit studies in which precipitation estimates from a DAS are used to drive surface hydrological models.

7.2.3 Land-Surface/Atmosphere Interaction

The land-surface is an important component in the Earth System affecting energy balance, the hydrological cycle, and chemical cycles. Latent heat, sensible heat, and momentum fluxes at the land-surface modulate near-surface turbulence and boundary layer convection on diurnal and longer time-scales. The land-surface plays an important role in the hydrological cycle receiving water from the atmosphere in the form of rain or snow with the soil and vegetation acting as reservoirs. Precipitation that does not infiltrate the soil forms surface runoff. The biosphere over the land surface also affects the carbon cycle through photosynthesis to produce the greenhouse gas CO_2.

Although still in its infancy, land surface data assimilation has generated interest in both environmental and meteorological communities. Over the past decade, state-of-art land surface models (LSM) have been coupled with general circulation models. Remote sounding instruments that infer land surface quantities will play an integral role in land-surface modeling and data assimilation in the future. Many new data types can be inferred

remotely from satellite instruments that provide superior geographic coverage of the land-surface as compared with conventional surface station observations. These satellite-derived data types include surface (skin) temperature from infrared instruments such as TOVS, AVHRR (MODIS predecessor), and MODIS, as well as snow water equivalent content and soil moisture information from passive microwave instruments such as SSM/I and in the future TMI. In addition to measurements that can be assimilated, satellite-derived quantities such as vegetation indices from AVHRR and MODIS can also be used to specify or estimate model parameters in some LSMs. Use of these data should improve both short-term forecasts and analyses of climate events such as El Niño.

7.2.4 Ocean-Surface/Atmosphere Interaction

The ocean surface (including regions immediately above and below) is an interface between two of the great subsystems involved in the Earth System: the ocean and the atmosphere. Considerable Earth Systems Science research will be devoted to the interplay of dynamics and features between these two subsystems. There is a considerable disparity in the nature of our understanding of these subsystems and their interaction. A better understanding of the workings of the Earth System, especially for long time scales, will entail a detailed knowledge of the behavior of the coupled atmosphere-ocean system. El Niño and its global effects is certainly an example of this, and these are key objects of study in the MTPE Initiative, *Seasonal to Interannual Climate Variability Research*. Thus it is important to have improved ocean surface data to better delineate the mechanisms that govern the atmosphere-ocean interaction.

Past observations of ocean surface variables have largely been obtained from *in situ* platforms: ships, buoys and island data. These observing systems provide information on sea level pressure, winds, humidity and sea surface temperature. Such observations have suffered from a variety of problems, ranging from unrepresentative sampling to inherently poor quality. The most serious problem with these historical data sources lies in their poor sampling of the Tropics and the southern oceans.

There are currently in place satellite-based sensing systems which provide information related to sea surface temperature and sea level winds. For example, one source of information concerning winds in the lower atmosphere, cloud-tracked winds (CTW), has been available for a number of years. Research using data from the current space-based ocean surface wind sensors, SSM/I and Scatterometer, has found potential benefits and difficulties in using these data. The benefits are clear; the satellite sensors provide a tremendously improved sampling, in both space and time, of the ocean surface wind. The difficulties with using data from these sensors lie in drawing the proper inferences from the information provided by the sensors. For example, the SSM/I provides information related to the wind speed near the ocean surface - provided a number of assumptions pertaining to the wind-sea state relation and the nature of the boundary layer near the sea surface are valid. Similar problems arise in the consideration of Scatterometer data.

Improvements in the sensing of winds near the ocean surface will benefit a number of Earth Science research enterprises. More accurate surface winds will lead to improved estimates of momentum fluxes, and will have a potentially positive impact on the fluxes of sensible heat and moisture for use in atmospheric modeling. Similarly improved esti-

mates of momentum, heat, and fresh water fluxes will be used for ocean models. Such wind data will provide important forcing, or boundary conditions, for research in coupled atmosphere-ocean modeling. Ultimately, the assimilation of surface wind data into a coupled atmosphere-ocean system will be used to correct the state of such a system. Another area of interest for these wind data is in ocean wave modeling; accurate high-resolution winds will improve the process of data assimilation of surface winds into ocean wave models. Finally, improved surface wind datasets, obtained from the global assimilation of these new surface wind data, will provide more useful forcing for offline model studies, such as sea-ice transport studies.

7.2.5 Radiation (Clouds, Aerosols, and Greenhouse Gases)

The transfer of electromagnetic radiation in the atmosphere, *i.e.,* absorption, emission, scattering, and refraction of energy by particles (clouds and aerosols) and molecules, is the most important process affecting energy transfer. Radiative transfer in the atmosphere is generally separated into two regions: (1) Solar or shortwave radiation that peaks near 0.5 μm in the visible part of the electromagnetic spectrum (2) Terrestrial or longwave radiation that peaks in the infrared part of the spectrum near 10μm. One consequence of molecular absorption is the so-called greenhouse effect in which a gas is virtually transparent to incoming shortwave radiation while absorbing and re-emitting longwave radiation. The major greenhouse gases are CO_2, H_2O, and O_3 with CO, CH_4, N_2O and others playing a smaller role. The CO_2 concentration remains relatively homogeneous in both space and time, although observations show a seasonal variation and long-term increase. In contrast, concentrations of H_2O, O_3, and some of the minor greenhouse gases exhibit relatively large spatial and temporal variations. Climate changes resulting from variations in greenhouse gas abundances are difficult to predict because of complex radiative-convective feedbacks and remain a controversial issue.

Cloud properties have a large impact on energy balance at the top of the atmosphere and the surface. In the shortwave, suspended liquid water in clouds reflects incoming solar radiation back to space. In the longwave, liquid water drops absorb and re-emit radiation. Molod et al. (1995) have shown that systematic errors in the GEOS-1 GCM linked to physical parameterizations of clouds, convection, and rainfall result in latitudinally-dependent systematic differences between observed and GEOS-1 derived long and shortwave flux at both the upper and lower boundaries of the atmosphere. As discussed in Chapters 4 and 8 many of the deficiencies of the GEOS DAS (and, in fact, all data assimilation systems) are related to the representation of atmospheric water and clouds.

Aerosols, like cloud particles, can significantly affect the heat balance of the Earth-atmosphere system by scattering and absorbing incoming solar radiation. Aerosols, or suspended particles in the atmosphere, include volcanic dust, sea spray, dust generated from wind, smoke from forest fires and biomass burning, particles produced during combustion, chemical reactions involving naturally occurring gases or gases formed during combustion, and cataclysmic impacts between the Earth and other solar system bodies. Temporal and spatial variations in aerosol distributions have not been given much attention in current data assimilation systems.

There currently exists an abundance of radiation-related data inferred from satellite

and ground-based instruments, such as cloud-top temperature and cloud fraction in the ISCCP data base (derived from combined infrared and visible observations) and cloud-liquid water derived from passive microwave instruments such as SSM/I. Future instruments such as MODIS and the TRMM microwave imager will provide additional estimates of these quantities. Ground-based aerosol observations date back to the early 1900's. Aerosol parameters have also been measured with satellite instruments such as SAGE, HALOE, and CLAES, primarily in the stratosphere. Advanced instruments such as MISR have been designed for improved observations of aerosol properties. Ground-based monitoring of greenhouse gas concentration has been taking place over the last several decades. In the future, more complete global monitoring of greenhouse gases will be accomplished with instruments such as MOPITT. These data types related to radiation have not yet been used in operational data assimilation systems. Research at the DAO is currently ongoing to more fully exploit these new data types in a DAS. This should lead to a better understanding of the role of radiation and dynamical feedback processes in regulating the climate system.

7.2.6 Atmospheric Circulation

Accurate, consistent, long-period measurements of global mass (height and temperature) and momentum (wind) fields are important for Earth System studies. The ability to calculate budgets of constituents, heat, mass, and momentum require accurate representation of the atmospheric circulation. The study of climate variability focuses in part on inter-annual differences and on anomaly fields (differences from climatological means), including changes in large-scale flows such as the Hadley circulation, which transports mass, energy and moisture from the tropics to the mid-latitudes. Another important long time-scale circulation is the El Nino-Southern Oscillation (ENSO), which has been linked to changes in the extra-tropical circulation resulting in floods and droughts. The stratospheric quasi-biennial oscillation (QBO) is a major component of the inter-annual variability in the stratosphere. Several documented deficiencies in GEOS-1, such as a weak Hadley cell and warm-biased tropopause temperatures in the tropics (see Chapters 4 and 8), can potentially be addressed with new data types (including improved use of current observations).

7.2.6.1 Tropospheric circulation and temperature

In the troposphere (and lower stratosphere), both winds and temperatures are observed with a network of conventional rawinsondes. This network is dense in the Northern Hemisphere over land. However, observation density and quality in the tropics, Southern Hemisphere, and over oceans, is much poorer. In these areas satellite observations provide excellent geographic coverage. Advances in global weather models and data assimilation have led to better global analyses and forecasts of these fields, but there is room for improvement, both in the observations themselves as well as the way in which they are used in assimilation systems. Advanced instruments for temperature sounding, such as AIRS and IASI, will provide measurements with higher information content about the mass field than the current NOAA polar-orbiting satellites. Yet, even with improved sounding capabilities, there are still both technical and scientific issues to be addressed when considering how best to assimilate remote satellite observations. These issues will be addressed in more detail in section 7.3.

7.2.6.2 Stratospheric circulation and temperature

The need for improved knowledge of stratospheric winds and temperatures is most strongly driven by efforts to understand stratospheric ozone variability and predict anthropogenic changes in the ozone distribution. Recently, there has been increased interest in role of the stratosphere in climate change, especially changes associated with upper tropospheric and lower stratospheric water vapor and ozone. Both chemistry and climate initiatives require better quantification of stratosphere-troposphere exchange.

Winds and temperature from data assimilation systems have been central in increasing the quanititive level of stratospheric chemistry. In the lower stratosphere, middle latitudes the winds are already of sufficient quality that transport calculations can be used to unify constituent measurements from different observing platforms. The chemical studies have also revealed places where the winds and temperatures remain of low enough quality that uncertainties in chemical assessments are still strongly tied to meteorological conditions.

Within the current GEOS system the most notable problems with the winds lie in the tropics and the subtropical middle latitude boundary. The transport between the subtropics and middle latitudes is an especially important topic because mixing of middle latitude pollutants into the tropics can strongly perturb the ozone sources. With regard to temperature, field scientists in the aircraft missions have noted a warm bias of GEOS temperatures in the lower stratosphere when the extreme cold events occur. Improvements in the temperature representation are needed because heterogeneous chemical processes become more important at extremely low tempertures. Long-term transport experiments show that recent versions of GEOS have extensive improvements in the representation of the seasonal, zonal-mean meridional circulation (see section 4.3.2.3). However, misrepresentations of the equatorial upwelling and polar downwelling remain large enough that it is difficult to represent interannual variability in long-lived tracers.

Much of the projected improvement in stratospheric meteorological fields is expected to come from advances in modeling, analysis, and specification of improved error statistics. New data sources are limited primarily to improved temperature sounders, such as MLS and GPS, that have increased vertical resolution and accuracy. Indirect improvements to meteorological fields may also be derived from the assimilation of long-lived tracers. Stratospheric wind measurements from the Upper Atmosphere Research Satellite (UARS) have proven difficult to utilize and the DAO will follow the progress on impact studies being carried at at the UKMO.

7.2.7 Constituents

Building the capability of assimilating constituent observations is one of the long-term goals of the DAO. In such an assimilation scheme the constituent data are allowed to influence both the estimate of the tracer itself and - by the coupling of the fields through the linear transport equation - the estimate of the flow field (Daley 1995, Riishøjgaard 1996). Constituent assimilation in the present context means assimilation of observations of the minor constituents of the atmosphere, such as water vapor, N_2O, CO, CH_4, etc. However, one of the main motivations for recent development in methodologies for constituent assimilation is the availability of ozone derived from satellite-based instruments. Assimilation of these

data would be useful for the atmospheric chemistry community since it would allow us to build a multi-year sequence of three-dimensional ozone fields consistent with atmospheric dynamics, available for each analysis time.

From a meteorological point of view the ozone data is of interest because the flow patterns around the tropopause level generates a very strong signal in total ozone observations. Conversely, this implies that the total ozone measurements carry information about the winds at these level, information that over large parts of the globe is not readily available from alternative sources. There are a number of different strategies that one can follow in order to retrieve this information, depending on the model underlying the data assimilation procedure. The basic ideas involved in constituent assimilation are intuitively appealing and conceptually simple. However, the actual design and implementation of a multivariate scheme in a general circulation model is technically a major effort, and there remain a number of scientific issues to be resolved. Thus it is far from clear at the present time which assimilation method (extended Kalman filter, 4D-VAR, Fixed-interval smoothing, assimilation through a transport model or through a potential vorticity model, etc.) will be best suited for the purpose. Theorems of non-Gaussian statistics need to be developed. Also, even though some of these methods theoretically should be insensitive to the initial specification of the forecast error covariances, this may not be true for a particular numerical implementation. Since the partitioning of the information present in the data will be determined by the error specified, work towards improving our understanding of the errors both of the observations and of the background model estimate is clearly needed and will be an integral part of constituent assimilation at the DAO.

7.3 Assimilation of New Data Types into the GEOS DAS

Several approaches have been proposed and used to incorporate both conventional and satellite observations in data assimilation systems. These methods will be reviewed in subsequent sections following a brief review of statistical analysis and description of the DAO's Physical-space Statistical Analysis System (PSAS). We will focus here on assimilation of remotely sensed data from satellites in PSAS, although the concepts also apply to conventional data as well as other assimilation methods such as the Kalman filter. Because of the need to accommodate new data with enormous data volumes, new ways of assimilation must also be considered.

7.3.1 Statistical Analysis

The objective of statistical interpolation is to produce an optimal estimate of the atmospheric state, given a set of observations and a first guess usually in the form of a short-term forecast. In the variational framework (*i.e.,* 3D-VAR), this can be accomplished by minimizing the likelihood functional

$$J(w) = (w - w^f)^T (P^f)^{-1}(w - w^f) + (w^o - h(w))^T (R^o)^{-1}(w^o - h(w)), \tag{7.1}$$

where $w \in I\!R^n$ is a vector representing the 3D state of the atmosphere, $w^f \in I\!R^n$ is the forecast, $w^o \in I\!R^p$ is the observation vector, and $h(w)$ is an observation operator that maps

the 3D atmospheric state into observables. The first term on the RHS of (7.1) is weighted by the inverse of the forecast error covariance matrix $P^f \in I\!R^n \times I\!R^n$, while the second term is weighted by the inverse of the observation error covariance matrix $R^o \in I\!R^p \times I\!R^p$. Provided these covariances are specified correctly, the analysis state obtained by minimizing $J(w)$ is the mode of the conditional probability density function $p(w|w^f \bigcup w^o)$ and is derived from a maximum-likelihood principle assuming that forecast and observation errors are unbiased, normally distributed, and uncorrelated with each other.

Because the observation operator, $h(w)$, is in general nonlinear, the minimum of $J(w)$ can be obtained by a quasi-Newton iteration of the form

$$w_{i+1} = w^f + P^f H_i^T \left(H_i P^f H_i^T + R^o \right)^{-1} \left[w^o - h(w_i) + H_i(w_i - w^f) \right], \tag{7.2}$$

where

$$H_i = \left. \frac{\partial h(w)}{\partial w} \right|_{w=w_i}. \tag{7.3}$$

The analysis vector, w^a, that minimizes $J(w)$ is given by

$$w^a = \lim_{i \to \infty} w_i. \tag{7.4}$$

In PSAS, a $p \times p$ system of equations is first solved at observation locations

$$\left(H_i P^f H_i^T + R^o \right) x_i = w^o - h(w_i) + H_i \left(w_i - w^f \right) \tag{7.5}$$

for the vector $x_i \in I\!R^p$ using a conjugate gradient algorithm (da Silva et al. 1995, Guo and da Silva 1995). The first term on the LHS of (7.5) is called the innovation covariance. The state at iteration $(i+1)$ is updated by an additional matrix-vector multiply, viz.

$$w_{i+1} = w^f + P^f H_i^T x_i. \tag{7.6}$$

The computation required for the solution of the linear system (7.5) is approximately $\mathcal{O}(N_{cg} p^2)$, where N_{cg} is the number of iterations of the conjugate gradient algorithm. N_{cg} depends on the conditioning of the innovation covariance matrix. The matrix-vector multiply in (7.6) requires $\mathcal{O}(np)$ floating point operations. The total operation count to solve (7.5)-(7.6) is approximately $\mathcal{O}[N_o(N_{cg} p^2 + np)]$, where N_o is the number of outer (quasi-Newton) iterations performed. It is evident any type of data compression that reduces the number of observables will significantly reduce computation in PSAS. At the DAO, development of improved methodology to assimilate new data types with very high spatial- or spectral-resolution has been driven largely by consideration of computational costs.

It is the availability or development of observation operators, $h(w)$, that is key to versatile and efficient incorporation of new data. Development of observation operators is best done with the partnership with instrument teams. The instrument teams have the expertise. Without such partnerships the resources needed in the DAO to utilize new data types balloons. This is one area where overguiding direction from the EOS project could help defining priorities.

7.3.2 Direct radiance assimilation

In this document, radiance is a general term meaning a directly measured quantity (as opposed to a retrieved quantity). For example, radiance could refer to refractivity measured by Global Positioning System (GPS) receivers, backscatter from a scatterometer, or thermal/reflected radiation measured by a passive infrared or microwave sounder. The term radiance also applies to pre-processed raw radiance (*e.g.,* cloud-cleared radiance). Assimilation of radiances involves utilizing radiance measurements from a remote sounding instrument as the observable and specifying the radiance error covariance as the observation error covariance in (7.1). In addition the observation operator h in (7.1) that maps the state variables to the radiances must be specified.

For remote measurements, h is an approximate radiative transfer or empirical model relating the atmospheric state in grid space to the radiance at the observation location using a set of parameters such as spectral line data and/or calibration parameters. To assimilate radiances correctly, an appropriate radiance error covariance must be specified that incorporates both detector noise and observation operator error. Practical implementation at the DAO will use statistical modeling from innovation sequences or some form of online parameter estimation such as discussed in Dee (1995) to estimate radiance errors. Observation operator parameter errors are usually systematic and may be estimated and corrected for in part by utilizing independent observations and/or forecasts (*e.g.,* Eyre 1992, Susskind and Pfaendtner 1989).

Radiance assimilation is computationally feasible with current instruments and analysis schemes. However the cost of this approach may be prohibitive for future high-spectral resolution sounding instruments, such as AIRS and IASI, with large numbers of channels. More efficient approaches are currently being examined as an alternative to radiance assimilation for such instruments.

7.3.3 Traditional retrieval assimilation

Remotely sensed data have been traditionally assimilated in the form of physical-space retrievals. In this approach, radiances are processed off-line by data producers, and *familiar* data types such as temperature/moisture profiles or wind vectors are used in the assimilation system. Specifying the retrieval z as the observable w^o in (7.1), the observation operator h is a linear interpolation operator so that the iterated form of (7.2) can be reduced to

$$w^a = w^f + \left(P^f \mathcal{I}^T\right)\left(\mathcal{I} P^f \mathcal{I}^T + R^z\right)^{-1} \ (z - \mathcal{I} w^f), \tag{7.7}$$

where $z \in I\!R^p$ denotes the retrieved data, $R^z = \left\langle \epsilon^z (\epsilon^z)^T \right\rangle$ is the retrieval error covariance, and $\mathcal{I} \in I\!R^n \times I\!R^p$ is the interpolation operator used above. A more general form of (7.7) that includes the retrieval-forecast error cross-covariance, denoted $X = \left\langle \epsilon^z (\epsilon^f)^T \right\rangle$, is given by

$$w^a = w^f + \left(P^f \mathcal{I}^T - X^T\right)\left(\mathcal{I} P^f \mathcal{I}^T + R^z - \mathcal{I} X^T - X \mathcal{I}^T\right)^{-1} \ (z - \mathcal{I} w^f). \tag{7.8}$$

The assimilation of retrievals requires the specification of the retrieval error covariance matrix R^z and the retrieval-forecast error cross-covariance X. Operational implementations of retrieval assimilation are often based on statistically modeled retrieval error covariances under the assumption of stationarity and isotropy. In addition, the retrieval-forecast error cross-covariance matrix X is often neglected as a result of the difficulty associated with modeling it and accounting for it in a DAS. At the DAO, TOVS retrieval errors have been estimated using a tuning algorithm that separates horizontally-correlated components of the error from uncorrelated components as described in da Silva et al. (1996a).

7.3.4 Consistent Assimilation of Retrieved Data (CARD)

Ménard (1995) proposed a potentially less expensive alternative to radiance assimilation that has a more theoretically sound basis than traditional retrieval assimilation. This method combines Rodgers' (1990) characterization of retrieval errors with Kalman filter theory leading to the consistent assimilation of retrieved data (CARD). The implementation of CARD may be considerably less expensive than radiance assimilation for advanced instruments where the number of radiance measurements is much greater than the number of retrieved products (*i.e.,* the retrieval is a form of data compression). The retrieval of geophysical parameters is a nonlinear estimation process. Often the problem is ill-posed and in this case requires the use of prior information. For example, nadir-viewing infrared and microwave profiling instruments use forecasts as prior information for interactive physical retrievals. Prior information could also come from climatology or a representative ensemble of profiles used to create a regression, pattern recognition, or neural net retrieval algorithm. The general CARD approach requires the specification of error characteristics for the radiances as well as the prior information. Because the statistical characteristics of the prior information are often not known and/or difficult to model and account for in a DAS, some modification to the retrieval may be necessary in order to eliminate the effects of prior information. In the following two subsections, examples of different CARD implementations are given.

7.3.4.1 Physical Space

If little or no prior information is used in the retrieval, the retrieval errors may be computed by propagation of instrument error (including detector noise and transfer modeling errors) as described in Rodgers (1990). In this way, the state dependence of the retrieval error is accounted for. If the state dependence is to be properly accounted for, instrument error must be specified (as in the case of radiance assimilation). Once the retrieval error is estimated, the retrievals can then be assimilated in a consistent manner. This approach has been used by Ménard et al. (1995) to assimilate constituent data from the Cryogenic Limb Array Etalon Spectrometer (CLAES) using a Kalman filter algorithm where retrieval errors were reported by the instrument team.

7.3.4.2 Phase Space

If a significant amount of prior information is incorporated into the retrieval, the implementation becomes more difficult as a result of the cross-correlation between the prior

information and forecast errors X in (7.8). Joiner and da Silva (1996) describe several ways to modify retrievals in order to remove the effect of the prior information thereby effectively removing X. These approaches involve (1) filtering the portion of the retrieval affected by the use of prior information (*i.e.,* null-space filtering or NSF) or (2) performing a partial eigendecomposition (PED) retrieval in which prior information is not incorporated into the retrieval. These approaches compress radiance observations in a single sounding to a small number of orthogonal functions that will impact the data assimilation system. For example, Joiner and da Silva (1996) showed that over 500 radiances observations from the AIRS instrument could be compressed into approximately 10 pieces of relevant information about the temperature profile. Similarly, radiances from other spectral bands provide information about the water vapor profile, surface temperature, and emissivity of clouds. Once radiances from individual soundings have been compressed, the compressed retrievals may then be combined horizontally (*i.e.,* combined into a super-observation or super-ob) provided the retrievals are defined in terms of a consistent set of basis functions. The approaches described here have been demonstrated with simulated data in 1-D thus far. Full implementation of both direct radiance assimilation and the CARD/PED approach using TOVS data in PSAS is underway at the DAO so that these methods can be compared both in terms of cost and analysis quality.

7.4 Implementation

7.4.1 Data flow and Computational Issues

One important consideration for incorporating new data types an appropriate data assimilation method is the bandwidth required to accommodate data flow between the site where the raw data is pre-processed and the site where the data is assimilated. For future high-spatial and high-spectral resolution instruments, such as MODIS and AIRS, the required bandwidths (assuming no data compression) can be quite large. Using level 3 products when possible, super-obbing, and/or the CARD methodologies described in section 7.3.4 that allow for data compression, a significant reduction in data flow as well as computation in PSAS can be achieved. To achieve this reduction in data flow, the preprocessing required to produce appropriate retrievals and to perform super-obbing must take place at the site where the data resides. Furthermore, quality control (and in some cases covariance tuning) will have to be performed at the data site in conjunction with data compression. Data pre-processing and transfer strongly impact DAO computing resources and have yet to be well defined.

7.4.2 Instrument Team Interaction

Members of instrument teams are familiar with the intricate and unique problems associated with a particular instrument (*e.g.,* calibration and other sources of systematic error in the observations and operators). In many cases, instrument teams have developed the tools that are necessary to effectively use the data in a DAS (*e.g.,* observation operators). In the past, interaction between instrument teams and data assimilation teams has been weak. The DAO needs to foster stronger interaction with instrument teams. For this interaction

to succeed, strong commitment by both the DAO and instrument teams is required. A prototype for this interaction is planned with the MLS team.

The current plan for instrument team interaction is that at least one representative from an instrument team will work closely with the DAO for an extended period of time (of the order of a few months to a year). The time required to integrate the new data type into the DAS will depend on several factors including the amount of previous experience with a similar data type, the readiness of tools to assimilate the new data type (*i.e.,* observation operators), the quality of the data type (including the ability to remove bias), and the amount of pre-processing needed prior to assimilation. In most cases, instrument teams will be expected to provide the DAO with the tools needed to properly assimilate the data, such as observation operators and their derivatives. The instrument team member will interact with DAO staff specializing in covariance tuning, quality control, and the PSAS interface. The instrument team member is expected to provide baseline models for systematic error correction and covariance modeling and will assist with quality control and monitoring.

Another aspect of instrument team interaction involves teams utilizing the data assimilation system to diagnose and correct problems with the instrument (*i.e.,* calibration error) and observation operators (*e.g.,* tuning the forward model). An example of this is the work done with the ERS-1 scatterometer by Stoffelen and Anderson (1995). This interaction will be part of the monitoring activity for any new data type to be used in the GEOS system (see discussion in section 7.4.3).

As part of the DAO commitment to bring together instrument teams and data assimilation teams, the DAO has agreed to host and help organize a satellite assimilation workshop headed by Ron Errico and George Ohring in September 1997. Also numerous speakers have been invited to help evaluate instrument capabilities and applications. Table 7.1 lists speakers to date that have given seminars at the DAO. Table 7.2 lists other visitors, collaborators, and consultants in contact with the DAO.

7.4.3 Passive Data Types/Observing System Monitoring

Prior to the assimilation of any new data type the quality of data must be determined. This includes sanity checks of the geophysical realism of the observation

- does it look like other observations of the same type?
- does it make sense with theoretical expectations?

After initial sanity checks the candidate data set needs to be monitored in order to develop the statistics necessary for assimilation. This is accomplished by monitoring, but not assimilating, the observation data stream.

One of the essential ingredients for the Physical-space Statistical Analysis System (Chapter 5) is the specification of covariance models for the forecast and observation errors, along with effective bias removal procedures. Current error covariance modeling methodology (Dee et al. 1996) requires the availability of innovations (O-F residuals) for statistically deriving such models and for physically-based bias removal. Therefore, before an observation can be used for assimilation O-F residuals need to be available. One possibility is to have

this data type go through GEOS DAS as a *passive* data type. A passive data is not used in the analysis, but is included in the assimilation *Observation Data Stream* (ODS) output (da Silva and Redder 1995). For historical data types, ODS files can be created by using pre-existing 6 hour forecasts and observational data. In any event, bias corrections and random error characterization are generally developed off-line based on ODS files.

Once error covariance models and bias correction schemes are developed and the new-data type is assimilated into the GEOS DAS, post-analysis ODS files need to be constantly monitored to assess the goodness-of-fit of the assumed statistical models, and to adaptively re-tune model parameters. As instruments are replaced, or calibration characteristics change over time, an automated system capable of detecting and correcting such problems is an essential requirement. This is a crucial step for the overall stability of the data assimilation system.

At a minimum, the Observation System Monitoring sub-system shall include:

Innovations (O-F): time-mean, standard deviations and time evolution. The goal is to detect abrupt changes, assess the realism of the statistical models in PSAS, and the effectiveness of the bias correction procedures.

Observation minus Analysis (O-A) residuals: time-mean, standard deviations and time evolution. The goal is to detect abrupt changes, and the existence of time-mean biases in the analysis. O-A residuals are also useful to diagnose the performance of the analysis, in particular whether the observations are being used efficiently by the analysis system (Hollingsworth and Lönnberg 1989).

QC statistics: recent history of data counts, rejects and re-acceptance. An outline of the Quality Control procedures currently used at DAO and planned for 1998 is given in Chapters 6 and 9.

The above statistics shall be monitored for each major instrument, with observations spatially averaged over key regions (*e.g.*, North America, Europe, etc.). For real-time/near real-time systems, a global map of QC decisions shall be produced. Global maps of O-F and O-A at key levels shall also be produced (on a synoptic time basis for real-time systems, on a monthly mean basis otherwise).

A detailed plan for goodness-of-fit assessment and re-tuning of error covariance and bias correction parameters will be described elsewhere.

7.5 Priorities

Prioritization of which new data types to assimilate is influenced by many factors. These include:

- baseline credibility of the GEOS DAS
- Earth-science priorities
- programmatic mandate

Table 7.1: Seminar Speakers for New Data Types Group

Speaker	affiliation	Topic
Steve Bloom	NASA	Ocean-surface Wind Retrievals
Al Chang	NASA	Snow Water Equivalent Retrieval
John Derber	NMC/NCEP	Radiance Assimilation at NMC
Anne Douglass	NASA	Ozone 3D Chemistry-Transport Model
Gregory Gurevich	USRA/UMd	Satellite Tomography
Paul Houser	U Arizona	Remote Sensing of Soil Moisture
Randy Koster	NASA	Mosaic Land Surface Model
Chris Kummerow	NASA	Precipitation Retrievals (SSM/I and TRMM)
Venkataraman Lakshmi	NASA	Soil Moisture from SSM/I
Andrea Molod	NASA	Coupling of Land Surface Model at DAO
Howard Motteler	UMBC	Neural Net Retrievals (SSM/T2 and AIRS)
Bill Seegar	Aberdeen	Bird-based meteorological measurements
Larrabee Strow	UMBC	Fast and hyperfast IR radiative transfer modeling
David Tobin	UMBC	Infrared spectral lineshapes

Table 7.2: Visitors, Consultants, and Collaborators

Contact	Affiliation	Subject
P.K. Bhartia	NASA	TOMS/SBUV retrievals
Moustafa Chahine	JPL	AIRS retrievals
Jean Dickey	JPL	GPS ground-based H_2O retrievals
Steve Engman	NASA	Soil moisture from passive microwave
Evan Fishbein	JPL	MLS retrievals
Larry Gordley	GATS	CLAES retrievals, limb sounding radiative transfer
Christian Keppenne	JPL	GPS ground-based H_2O retrievals
Arlin Krueger	NASA	TOMS retrievals
Steven Marcus	JPL	GPS ground-based H_2O retrievals
Piers Sellers	NASA	Sib2 Land-Surface Model
Max Suarez	NASA	Mosaic Land Surface Model, etc.
Joel Susskind	NASA	TOVS/AIRS retrievals
Joe Waters	JPL	MLS retrievals

- ease of assimilation
- specifically directed funding
- instrument team resources
- it might just be fun to try

Instruments on past, present, and future platforms were reviewed in order to prioritize their usage in the GEOS DAS. Data types were selected to be used either for assimilation, analysis (non-cycled), or validation. When two or more instruments provided redundant information, generally one was selected for assimilation, allowing for the other to be used as independent validation (or perhaps bias estimation). An initial selection of a data type for validation may change to assimilation after monitoring if

- the data appear to be of higher quality than data currently used for assimilation
- a commitment is made by an instrument team
- priority of the data type is increased

Each data type was initially assigned a score on a four point scale based on an estimate of the cost-to-benefit ratio, where benefit is defined primarily in terms of meeting the scientific goals described in section 7.2 and cost is estimated primarily in terms of person labor and to a lesser extent computational cost (off-line and on-line computation, data storage and transfer). Factored into the *benefit* are the spatial and temporal coverage (*e.g.,* time-period and coverage for which data type is available). The *cost* estimate includes factors such as

- instrument team commitment
- previous experience with a similar data type
- estimate of how much work is needed to produce the observation operator
- known difficulties with calibration and systematic error
- an estimate of the amount of preprocessing needed prior to assimilation

The initial scores were translated into either a ranking of either high or low priority. These rankings are listed in following subsections along with relevant information about each data type considered. The prioritization is to be used as a guide for allocating resources and does not necessarily indicate a commitment by the DAO to assimilate or use a particular data type. The actual use of a data type in the GEOS system will depend on resources available (including instrument team commitments).

7.5.1 Priorities grouped by science topic

New data types are first grouped roughly by science topic. The groupings below are not listed in order of priority. For a given topic, all data types considered are listed. For each data type, the expected use in the GEOS system is also listed, *i.e.,* whether the data type will be used in the first look analysis, final platform, reanalysis only, pocket analysis, etc. (see Section 2.6.3 for definitions). Although we found some data types to be strong candidates for assimilation, they may have been selected for validation on the basis of personnel considerations.

If available, a specific product name is listed. Data volumes are also listed. These were estimated from W. Bass (*private communication*, EOSDIS most recent estimate) when available or from values reported in NASA (1994). These are given in gigabytes/day for level 2 products unless otherwise noted. Caution should be exercised in extrapolating from the figures listed here for data flow calculations. In some cases super-obbing will be performed to reduce data flow (see section 7.4.1 and section 7.3.4). For example, the data volume from super-obbed or level 3 MODIS data types will be more than a factor of 100 less than the data volume of the level 2 products. In some cases, data types are produced less than once per assimilation period (*e.g.,* land-surface products from MODIS to be used as boundary conditions produced once every 6, 15, or 30 days) and need not be re-transmitted every assimilation cycle. Estimates for data volume for level 3 products are not yet available.

The notations used in the tables are defined as follows:

1L: First Look Analysis (performed 12-24 hours after data time, used by EOS instrument teams for retrieval algorithms, etc.)

FP: Final Platform including reanalysis of final platform (runs several months after data time, includes data from first look as well as data from the EOS platform)

RA: Reanalysis (multi-year reprocessing of pre-EOS era and EOS-era using frozen system)

V: Validation

OA: Offline Analysis

B: Boundary Condition

PA: Pocket Analysis (similar to reanalysis, but for a limited time-period)

H: High priority

L: Low priority

S: Candidate for super-obbing/pre-processing at data site

E: Estimate

*past

‡future

†past, present, future

7.5.1.1 Temperature

There is an abundance of temperature data available for assimilation and validation. For both the first look system and final platform, TOVS was given the highest priority. The other measurements, with the exception of MLS, were selected for validation. Currently, in addition to conventional data, retrieved temperature (height) profiles from TOVS (from NESDIS and Susskind 1993) are assimilated in the traditional manner. This approach has been implemented with covariance tuning as described in da Silva et al. (1996a) in GEOS-1 and GEOS-2.

The advanced methodologies (radiance assimilation and phase-space retrieval assimilation) described in section 7.3 are currently being implemented and evaluated with TOVS Pathfinder data in anticipation of future sounders such as AIRS and IASI. For the first look system as well as final platform and reanalysis with GEOS-3 and beyond, the most appropriate method will be selected on the basis of cost and quality of the analysis.

The strategy for implementing new methodologies with TOVS is as follows:

1. A 1-D simulation of the PED approach using TOVS and AIRS radiances was completed in early 1996. The results showed that the data compression for both AIRS and TOVS should significantly reduce computation in PSAS. Based on the 1-D results, the theoretical foundation for this approach appears sound.

2. A fast forward radiative transfer model was extracted from the TOVS Pathfinder code (Susskind et al. 1983) and an analytic Jacobian (can be used as tangent linear model and adjoint) was added. This model, called GLATOVS, is described in Sienkiewicz (1996a). This model is currently being compared with RTTOVS, the standard fast radiative transfer model used for TOVS data (see Sienkiewicz, 1996b).

3. Systematic error correction to account for errors in the forward model and instrument calibration is an integral part of assimilating data from any microwave/IR sounder. In early 1996 a simulation of forward model error was completed. The results showed that, as expected, systematic error can be as large or larger detector noise. In the first part of 1996, several systematic error correction schemes have been compared in a simulation environment. Currently, a physically-based correction scheme is being implemented with TOVS Pathfinder data. After the algorithm has been tested, validated, and frozen, the results will be documented.

Table 7.3: Priorities for assimilating temperature data

Instrument	Satellite	Observable	Use/Priority	Vol (GB/day)
†Conventional	N/A	Trop/Strat	1L **H**	0.010
†TOVS, ATOVS	POES (NESDIS)	Trop/Strat	1L **H**	0.030
†TOVS, ATOVS	POES (GLA)	Trop/Strat	RA **H**	0.2
†MLS	UARS	Strat	RA **H**	0.02
†GPS	GPSMET	Trop/Strat	V **H**	0.0E
†SSM/T	DMSP	Trop/Strat	V **H**	?
†GOES sounder	GOES	Trop	V **L**	?S
*LIMS	Nimbus 7	Strat	PA **H**	?
*CLAES	UARS	Strat	V **H**	0.02
‡MODIS	EOS AM	Trop (MOD30)	V **H**	11.2S
‡IMG	ADEOS	Trop/Strat	V **L**	?S

4. After the systematic error correction scheme has been implemented, the radiance error covariance will be estimated using the approach described in da Silva et al. (1996a).

5. When observation operators have been implemented in PSAS, a comparison of the PED and the direct radiance assimilation approaches will be completed using TOVS Pathfinder data for one season. The results will also be compared with the current method of tuned retrieval assimilation. One approach will be selected on the basis of cost and analysis quality for use in GEOS-3.

Stratospheric temperature measurements from MLS were also given a high priority for assimilation as a result of a commitment from the MLS team. The availability of MLS temporal coverage makes it a candidate for pocket analysis. The first meeting with the MLS team took place in summer of 1996.

7.5.1.2 Moisture Assimilation

Conventional data has been the primary source of moisture data in the GEOS DAS to date. Experiments with assimilating total precipitable water (TPW) from SSM/I at the DAO (Ledvina and Pfaendtner, 1995) have shown positive impact especially in the tropics where the GCM is known to have a dry bias. Both TOVS and SSM/I (and TMI) provide information about TPW. In addition, TOVS provides some additional information about the profile and has coverage over both land and water. The capability to assimilate moisture information from both TOVS (as described above) and SSM/I will be in place for GEOS-3 and beyond. The final decision on which data type or combination thereof will be made on the basis of computational cost and analysis quality.

A collaborative effort is underway with scientists at JPL and DAO to use ground-based GPS data in the GEOS system. The actual assimilation of GPS data into the GEOS system will begin in approximately two years after initial studies have been completed. The

Table 7.4: Priorities for assimilating water vapor data

Instr.	Satellite	Observable	Use/Priority	Vol (GB/day)
†Conven.	N/A	RDSONDS	1L **H**	0.01
†TOVS, ATOVS	POES (NESDIS)	TOVS_RETS	1L **H**	0.030
†TOVS	POES (GLA)	Trop	RA **H**	0.2
†SSM/I	DMSP	SMI_PRCP_WATER	1L **H**	0.050
†GPS	Ground	TPW	RA **H**	0.0
†SAGE	ERBS, etc.	Strat	V **H**	0.0
†MLS	UARS	Strat	V **H**	0.02
†SSM/T2	DMSP	Trop	V **H**	?
†GOES	GOES	Trop (prof)	V **L**	?S
*HALOE	UARS	Strat	V **H**	0.0
‡TMI	TRMM	TPW	FP **H**	?
‡MODIS	EOS AM	Trop (MOD30_L2)	V **H**	7.192S
‡IMG	ADEOS	Trop	V **L**	?S

Note: Volumes in GB/day

number of GPS ground-based measurement systems is expected to increase dramatically in the future and initial studies show the TPW from these systems to be of high quality.

Several other instruments received high priority for validation. Although several of these data types are strong candidates for assimilation in the GEOS system (*e.g.*, MLS and SSM/T2), resources in addition to those currently in place would be required for this as these data types have little heritage in data assimilation systems.

7.5.1.3 Convective/Precip. Retrieval Assimilation

Developing the capability to assimilate convective data, including precipitation, is an ongoing research project at DAO. The goal is to have this capability ready in fall of 1996, and to compare this approach with the physical initialization approach used by Krishnamurti et al. (1991) in winter of 1996. The basic approach is to use a physical model (GCM convective parameterization) as an observation operator to perform a 1-D retrieval of water vapor, which is then assimilated in PSAS in the context of the CARD/PED approach described above. Currently, a simplified version of this algorithm has been coded and is undergoing tests. This approach does not assume that either the data or the model are perfect. The first implementation will use data inferred from SSM/I. TRMM data will be used when it becomes available. In the future, other data types including inferred cloud top temperature and outgoing longwave radiation, will be assessed for assimilation in a similar manner. A summary of convective data types is given in table 7.5.

Table 7.5: Priorities for assimilating convective retrievals

Instrument	Satellite	Observable	Use/Priority	Vol (GB/day)
†SSM/I	DMSP	Prec rate, surf	FP **H**	0.04
†SSM/I	DMSP	Cloud liq H_2O	V **H**	0.04
†ISCCP	(POES)	Cloud Top, frac	V **H**	0.01
†Conven.	N/A	Cloud base	V **H**	0.0
†TOVS	POES (GLA)	Cloud top	V **H**	0.2
†Conven.	N/A	Radar Precip	V **H**	0.03
†MSU	POES (Path)	Precip ocean	V **L**	0.01
*ERBE	ERBS	TOA flux	V **H**	0.0
‡TMI	TRMM	(M69) TMI_PROF_L2A-12	FP **H**	1.314S
‡TMI,PR	TRMM	TRMM_COMB_L2B-31(M73)	V **H**	0.848S
‡PR	TRMM	PR Prof (M72)	V **H**	1.8S
‡MODIS	EOS AM	Cloud (MOD06)	V **H**	1.13S
‡CERES	TRMM	TOA, cloud (CER07)	V **H**	0.26S
‡CERES	EOS AM	TOA, cloud (CER07)	V **H**	0.26S
‡AMSU	POES	Cloud liq H_2O	V **L**	TBD

7.5.1.4 Land Surface

The DAO is currently developing the capability to assimilate land-surface data. At the present time, the Mosaic (Koster and Suarez, 1992) land-surface model (LSM) has just been coupled with the GEOS GCM and is undergoing validation. Off-line assimilation tests with the Mosaic LSM are also being performed. The current version of the Mosaic LSM does not have the ability to accept satellite data in order to specify boundary conditions. It is planned that part of the Sib2 (*e.g.,* Sellers et al. 1986) LSM that accepts satellite data will be integrated with the Mosaic model in GEOS. When this is accomplished, satellite derived products such as the Normalized Differential Vegetation Index (NDVI) and others listed in Table 7.6 from AVHRR and MODIS will be ingested. In addition to surface station observations (temperature T_a and humidity q_a), we are investigating the feasibility of assimilating surface (skin) temperature (T_s) derived from IR instruments, as well as snow water equivalent (SWE) and surface wetness inferred from passive microwave instruments. It is expected that some combination of these data types will be used in the final platform system.

7.5.1.5 Ocean Surface

Ocean wind data from both passive microwave (SSM/I and SMMR) and scatterometers (ERS-1 and NSCAT) were identified as high priority data types for the 1998 system (both first look and final platform). Table 7.7 lists the details of ocean surface data types considered. For the 1998 system, the capability of assimilating data from both passive microwave and scatterometers will be in place. However, before one or more of these data types are

Table 7.6: Priorities for assimilating land-surface data

Instrum.	Satellite	Observable	Use/Priority	Vol (GB/day)
†Conven.	N/A	T_a, q_a ANC_NOAA_SFC_OBS	FP, RA **H**	0.05
†TOVS	POES (GLA)	T_s	FP, RA **H**	0.2
†SSM/I	DMSP	Snow Wat.Eq. (SWE)	FP, RA **H**	0.01
†SSM/I	DMSP	Surface Wetness	FP, RA **H**	0.01
†AVHRR	POES	ANC_NESDIS_NDVI	B, RA **H**	0.069S
*SMMR	Nimbus7	SWE	RA **H**	0.00
‡MODIS	EOS AM	T_s (MOD11_L2)	V (FP) **H**	6.376
‡MODIS	EOS AM	NDVI (MOD34_L3_10DY)	B, FP **H**	93.558GB/10day-S
‡MODIS	EOS AM	LAI, FPAR (MOD15_L4_10DY)	B, FP **H**	1.502GB/10day-S
‡MODIS	EOS AM	Evaptrans (MOD16_L3_10DY)	B, FP **H**	22.537GB/10day-S
‡MODIS	EOS AM	(MOD09_BRDF_L3_16DY)	B, FP **H**	108.16GB/16day-S
‡MODIS	EOS AM	Land type (MOD12_L3_32DY)	B, FP **H**	0.417/32day-S
‡MODIS	EOS AM	LS res (MOD41_L2)	B, FP **H**	23.652/day???
‡ASTER	EOS AM	T_s (on demand only)	V **L**	?S

used, the data will have been monitored and corrected if necessary for systematic errors (including observation operator error). The specific plans for use of NSCAT data are outlined below.

Starting in December 1996, the Synoptic Evaluation Group will start receiving NSCAT science products, which includes backscatter measurements, (Level 1.7 data), retrieved ranked wind ambiguities (Level 2.0 data), as well as gridded wind fields (Level 3.0 data). The operational release of the data is scheduled to start about March 1997, although the data format will change. The initial plan is to assimilate NSCAT retrieved wind velocity and possibly employ an ambiguity removal algorithm.

The process of assimilating surface wind data includes the following steps:

1. A process, known as MOVEZ, is used to create a suitable first guess wind field by a reduction process of the lowest model level wind field to 10m, consistent with the GEOS PBL. The multivariate wind and sea level pressure analysis is performed. Subsequently, the analyzed wind field is extended up to the lowest vertical model level and the analysis increments are computed. The analysis increments of the upper air wind field at 850 hPa and the lowest model level are then interpolated linearly in log (P) to the vertical model levels in between. This work will begin approximately 4 weeks after the GEOS-2 (with PSAS) is frozen.

2. In order to maximize the influence of the surface wind field in the GEOS DAS, the NSCAT wind vectors are also extended by a process analogous to MOVEZ to the model lowest vertical level. The observation innovations are computed and used by the multivariate mass - wind analysis. A check is made of the atmospheric stability, and only the observations under the unstable or neutral conditions are used. The

Table 7.7: Priorities for assimilating ocean-surface data

Instrument	Satellite	Observable	Use/Priority	Vol (GB/day)
†Conventional	N/A	u, v, T_{air}, q_s	1L **H**	0.0
†SSM/I	DMSP	Wind speed	1L, RA **H**	0.01
†ERS-1,2	ERS-1,2	speed, dir, σ^o	1L, FP **H**	0.20E
*SMMR	Nimbus-7	speed	V **L**	0.01
‡NSCAT	ADEOS	ANC_NESDIS_NSCAT_WNDPDT	1L **H**	0.046
‡NSCAT	ADEOS	ANC_JPL_NSCAT_WNDPDT	FP **H**	0.046

3-D global analysis that makes use of the data and propagates the information in the vertical according to the background error vertical correlation function. This particular process has experimentally been applied to ERS-1 scatterometer data within the GEOS-1 DAS environment and presented in Tokyo in 1995. It resulted in modest improvement of the resultant forecast experiments. Within the framework of PSAS it is expected to result in a more significant impact of scatterometer data due to a truly global three dimentional design of PSAS. This step will begin approximately 4 weeks after step (1).

3. A simple surface wind ambiguity removal algorithm is in place in GEOS-1 DAS. It will be tested with the new GEOS DAS. The algorithm compares the directions of available ambiguous wind vectors with the background field and chooses the one closest to it. In the future an interactive procedure or a 2D Variational ambiguity removal algorithm might replace the current one. If done, this work would begin in Jan or Feb of 1997.

7.5.1.6 Constituents

The plans for constituent assimilation are being developed. Currently long-lived tracers from UARS are being assimilated in prototype experiments. A joint project with University of Maryland and the Interdisciplinary Study led by M. Schoeberl focusing on lower stratospheric and tropospheric ozone is being designed. In addition we are looking to make better use of TOMS and SBUV observations. The data types considered for ozone assimilation are given in table 7.8. Recently a new Interdisciplinary Study has been funded (P. Kasibhatla) to look at CO assimilation, and there is joint work with NCAR on CO retrievals. The data types considered for CO assimilation are given in table 7.9. All of the current approaches are with off-line analyses.

Table 7.8: Priorities for assimilating ozone data

Instrument	Satellite	Observable	Use/Priority	Vol (GB/day)
†TOMS	N7/Meteor/ADEOS	total	OA **H**	0.01
†SBUV	N7/POES	prof	V (OA) **H**	0.001
†Conven.	N/A	prof	V **H**	0.0
†SAGE	ERBS, etc.	strat prof	V **H**	0.0
†MLS	UARS	upper strat prof	V **H**	0.02
†GOME	ERS-2	total, prof	V **L**	?
†TOVS	POES (GLA)	lower strat	V **L**	0.2
*CLAES	UARS	upper strat prof	V **L**	0.02
*HALOE	UARS	upper strat prof	V **L**	0.02
‡ILAS	ADEOS	upper strat prof	V **L**	?
‡IMG	ADEOS	lower strat prof	V **L**	?

Table 7.9: Priorities for assimilating CO data

Instrument	Satellite	Observable	Use/Priority	Vol (GB/day)
*MAPS	Shuttle	prof	OA **H**	0.0
‡MOPITT	EOS AM	prof	OA **H**	TBD
†Conven.	N/A	prof	V **H**	0.0

7.5.1.7 Wind profile

Currently, wind profile data used in GEOS are obtained from radiosondes and derived cloud track winds. Several of the data types listed in table 7.10 appear to be strong candidates for assimilation (*e.g.*, water vapor winds similar to cloud track winds). Water vapor winds will soon become available through the current operational data link. These new data types can enhance the coverage of current wind profile data. However, because there is little heritage for assimilating these data types, they are presently selected for validation. As resources permit, some of these data types may eventually be assimilated.

7.5.1.8 Aerosols

Although consideration has been given to aerosol assimilation (Ménard, personal notes), this topic has been given an overall low priority at present. Therefore, all data types listed in table 7.11 were selected for validation.

7.5.2 Priorities grouped by satellite

This section categorizes high priority items by satellite. The priorities for the POES, UARS, TRMM, ADEOS, and EOS AM-1 satellites are listed in tables 7.12-7.16, respectively.

Table 7.10: Priorities for assimilating wind profiles

Instrument	Satellite	Observable	Use/Priority	Vol (GB/day)
†Conventional	N/A	ANC_NOAA_RDSONDS_OBS	1L **H**	0.01
†Conventional	N/A	ACARS_ANC_NOAA_ARCFT_OBS	1L **H**	0.01
†cloud track	GOES	ANC_NESDIS_GOES_WIND_MOTION	1L **H**	0.008
†RADAR	N/A	trop/strat/mes	V**H**	?
water vapor	GOES/other	trop	V **H**	?
*HRDI	UARS	strat/mes	V **L**	0.003
*WINDII	UARS	mes	V **L**	0.03
*MODE	Shuttle		V **L**	?
‡SWIPE	TBD			

Table 7.11: Priorities for use of aerosol data

Instrument	Satellite	Observable	Use/Priority	Vol (GB/day)
†SAGE	ERBS, etc.	Strat	V **L**	0.0
†TOMS	Nimbus 7	Strat/Trop	V **L**	0.01
*CLAES	UARS	Strat	V **L**	0.02
*HALOE	UARS	Strat	V **L**	0.02
‡MISR	EOS-AM	properties	V **L**	?
‡ILAS	ADEOS	Strat	V **L**	?

Table 7.12: High-priority data types from POES satellite

Instrument	Observable	Use
†TOVS	Temp. Prof/rad	1L
†TOVS	H_2O Prof/rad	1L
†TOVS	T_s	FP, RA
†AVHRR	ANC_NESDIS_NDVI	B, RA

Table 7.13: High-priority data types from UARS satellite

Instrument	Observable	Use
†MLS	Strat T	RA
†MLS	Upper Trop/Strat H_2O	V
†MLS	upper strat O_3	V
*CLAES	Strat T	V
*HALOE	Strat H_2O	V
*HALOE	upper strat prof O_3	V

Table 7.14: High-priority data types from TRMM satellite

Instrument	Observable	Use
‡TMI	PR Prof (M69)	FP
‡TMI,PR	PR Prof (M73)	V
‡PR	PR Prof (M72)	V
‡CERES	cloud (CER07)	V

Table 7.15: High-priority data types from the ADEOS satellite

Instrument	Observable	Use
‡NSCAT	wind speed, dir, σ^o	FP
†TOMS	total O_3	OA

7.5.3 Priorities grouped by use in GEOS

This section categorizes high priority items according to use in GEOS. Data types are grouped as either used for first look, final platform (data types in addition to those used for the first look), or reanalysis/pocket analysis (may include data types used in the first look and final platform) in tables 7.17-7.19, respectively. Some of the high-risk data types (such as land-surface data) have not been included here. Data types used for validation are not listed here.

Table 7.16: High-priority data types from EOS AM1 satellite

Instrument	Observable	Use
‡MODIS	NDVI	B, FP
‡MODIS	LAI, FPAR	B, FP
‡MODIS	Evaptrans	B, FP
‡MODIS	BidirRefl	B, FP
‡MODIS	Land type	B, FP
‡MODIS	LS res	B, FP
‡MODIS	Cloud	V
‡MODIS	T_s	V
‡MODIS	T,q Prof (MOD30)	V
‡MOPITT	CO Prof	OA
‡CERES	TOA, cloud (CER07)	V

Table 7.17: High-priority data types for first look system

Instrument	Platform	Observable	Volume
†Conventional	N/A	ANC_NOAA_RDSONDS_OBS	0.010
†TOVS, ATOVS	POES (NESDIS)	ANC_NESDIS_TOVS_THKN_RETS (T, q, radiance)	0.030
†Conventional	ship, buoy	u, v, T_{air}, q_s	0.0
†SSM/I	DMSP	ANC_MSFC_SSMI_PRCP_WATER	0.050
†SSM/I	DMSP	Wind speed	0.01
†ERS-1	ERS-1	speed, dir	0.20E
‡NSCAT	ADEOS	ANC_NESDIS_NSCAT_WNDPDT	0.046
†Conventional	N/A	ACARS_ANC_NOAA_ARCFT_OBS	0.01
†cloud track	GOES	ANC_NESDIS_GOES_WIND_MOTION	0.008

Table 7.18: High-priority data types for final platform.

Instrument	Platform	Observable	Volume
†SSM/I	DMSP	Prec rate, surf	0.04
‡TMI	TRMM	(M69) TMI_PROF_L2A-12	1.314S
‡NSCAT	ADEOS	ANC_JPL_NSCAT_WNDPDT	0.046
‡MODIS	EOS AM	NDVI (MOD34_L3_10DY)	93.558GB/10day-S
‡MODIS	EOS AM	LAI, FPAR (MOD15_L4_10DY)	1.502GB/10day-S
‡MODIS	EOS AM	Evaptrans (MOD16_L3_10DY)	22.537GB/10day-S
‡MODIS	EOS AM	(MOD09_BRDF_L3_16DY)	108.16GB/16day-S
‡MODIS	EOS AM	Land type (MOD12_L3_32DY)	0.417/32day-S
‡MODIS	EOS AM	LS res (MOD41_L2)	23.652/day???

Table 7.19: High-priority data types for reanalysis and/or pocket analysis.

Instrument	Platform	Observable	Volume
†MLS	UARS	Strat T	0.02
†TOVS	POES (GLA)	T, q	0.2

7.6 References

Adler, R., C. Kidd, M. Goodman, A. Ritchie, R. Schudalla, G. Petty, M. Morrissey, and S. Greene, 1996: On the relation between ozone and potential vorticity, *PIP-3 Intercomparison Results*, PIP-3 Workshop, 18-20 November 1996, College Park, MD.

Andersson, E., Pailleux, J., Thépaut, J. N., Eyre, J. R., McNally, A. P., Kelly, G. A., and P. Courtier, 1994: Use of cloud-cleared radiances in three/four-dimensional variational data assimilation. *Q. J. R. Meteorol. Soc.*, **120**, 627-653.

Daley, R., 1995: Estimating the wind field from chemical constituent observations: Experiments with a one-dimensional extended Kalman filter. *Mon. Wea. Rev.*, **123**, 181-198.

Dee, D. P., 1995: On-line estimation of error covariance parameters for atmospheric data assimilation. *Mon. Wea. Rev.*, **123**, 1128-1145.

Dee, D. P., and A. Trenholme, 1996: DAO QC Strategy Document, *DAO Office Note* 96-15. Data Assimilation Office, Goddard Space Flight Center, Greenbelt, MD 20771. Available on-line from
`http://dao.gsfc.nasa.gov/subpages/office-notes.html`.

Dee, D., C. Redder and A. da Silva, 1996: Off-line tuning of forecast and observation error covariance parameters. *DAO Office Note, in preparation.* Data Assimilation Office, Goddard Space Flight Center, Greenbelt, MD 20771. This Office Note will be available on-line from
`http://dao.gsfc.nasa.gov/subpages/office-notes.html`.

Eyre, J. R., 1992: A bias correction scheme for simulated TOVS brightness temperatures. ECMWF Tech. Memo 176.

Guo, J. and A. M. da Silva, 1995: Computational Aspects of Goddard's Physical-space Statistical Analysis System (PSAS). *Preprints, Second UNAM-CRAY Supercomputing Conf. on Numerical Simulations in the Environmental and Earth Sciences.* Mexico City, Mexico, 6pp.

Hollingsworth, A. and P. Lönnberg, 1989: The verification of objective analyses: diagnostics of analysis system performance, *Meteorol. Atmos. Phys.*, **40**, 3–27.

Joiner, J. and A. M. da Silva, 1996: Efficient methods to Assimilate Satellite Retrievals Based on Information Content. *DAO Office Note 96-06.* Data Assimilation Office, Goddard Space Flight Center, Greenbelt, MD 20771. Available on-line from
`http://dao.gsfc.nasa.gov/subpages/office-notes.html`.

Koster, R. D., and M. J. Suarez, 1992: Modeling the land surface boundary in climate models as a composite of independent vegetation stands, *J. Geophys. Res.*, **97**, 2697-2715.

Krishnamurti, T. N., Xue, J., Bedi, H.S., K. Ingles, and D. Oosterhof, 1991: Physical initialization for numerical weather prediction over the tropics. *Tellus*, **43AB**, 53-81.

Ledvina, D. V., and J. Pfaendtner, 1995: Inclusion of Special Sensor Microwave/Imager (SSM/I) total precipitable water estimates into the GEOS-1 Data Assimilation System, *Mon. Weath. Rev.*, **123**, 3003-3015.

Ménard, R., 1995: Middle atmosphere assimilation of UARS constituent data using Kalman filtering: Preliminary results. *International symposium on assimilation of observations in meteorology and oceanography*, Tokyo, Japan, 273-278.

Ménard, R., 1996: Consistent assimilation of retrieved data (CARD), private notes and manuscript in preparation.

Molod, A., H. M. Helfand, and L. L. Takacs, 1995: The climatology of parameterized physical processes in the GEOS-1 GCM and their impact on the GEOS-1 Data Assimilation System, *J. Climate*.

NASA/Goddard Space Flight Center, 1994; *Science Data Plan for the EOS Data and Information System covering EOSDIS Version 0 and Beyond*, Document version 4, Ed. M. Schwaller and B. Krupp.

Riishøjgaard, L. P., 1996: On four-dimensional variational assimilation of ozone data in weather prediction models. *(accepted for publication in the Q. J. R. Meteorol. Soc.)*

Rodgers, C. D., 1990: Characterization and error analysis of profiles retrieved from remote sounding measurements. *J. Geophys. Res.*, **95**, 5587-5595.

Pfaendtner, J., S. Bloom, D. Lamich, M. Seablom, M. Sienkiewicz, J. Stobie, A. da Silva, 1995: Documentation of the Goddard Earth Observing System (GEOS) Data Assimilation System–Version 1. *NASA Tech. Memo. No. 104606*, Vol. **4**, Goddard Space Flight Center, Greenbelt, MD 20771. Available on-line from `http://dao.gsfc.nasa.gov/subpages/tech-reports.html`.

Schubert, S.D., R. B. Rood, and J. Pfaendtner, 1993: An assimilated data set for earth science applications. *Bul. Amer. Meteor. Soc.*, **74**, 2331-2342.

Schubert, S., C.-K. Park, Chung-Yu Wu, W. Higgins, Y. Kondratyeva, A. Molod, L. Tkacs, M. Seablom, and R. Rood, 1995: A Multiyear Assimilation with the GEOS-1 System: Overview and Results. *NASA Tech. Memo. 104606*, Vol. **6.** Goddard Space Flight Center, Greenbelt, MD 20771. Available on-line from `http://dao.gsfc.nasa.gov/subpages/tech-reports.html`.

Schubert, S. D., 1996: DAO's Quality Assessment Team: Definition and Planing Document. *DAO Office.*. Data Assimilation Office, Goddard Space Flight Center, Greenbelt, MD 20771. *In preparation.* This Office Note will be available from `http://dao.gsfc.nasa.gov/subpages/office-notes.html`.

Schubert, S. D. and R. Rood, 1995: Proceedings of the Workshop on the GEOS-1 Five-Year Assimilation. *NASA Tech. Memo. 104606*, Vol. **7**, Goddard Space Flight Center, Greenbelt, MD 20771. Available on-line from `http://dao.gsfc.nasa.gov/subpages/tech-reports.html`.

Sellers, P. J., Y. Mintz, Y. C. Sud, and A. Dalcher, 1986: A simple boisphere model (SiB) for use within general circulation models, *J. Atmos. Sci.*, **43**, 505-531.

Sienkiewicz, M., 1996a: The GLA TOVS rapid algorithm forward radiance modules and Jacobian version 1.0, *DAO Office Note 96-08.* Data Assimilation Office, Goddard Space Flight Center, Greenbelt, MD 20771. Available on-line from `http://dao.gsfc.nasa.gov/subpages/office-notes.html`.

Sienkiewicz, M., 1996b: Evaluation of RTTOV and GLA TOVS forward model and Jacobian, *DAO Office Note 96-20.* Data Assimilation Office, Goddard Space Flight Center, Greenbelt, MD 20771. Available on-line from `http://dao.gsfc.nasa.gov/subpages/office-notes.html`.

da Silva, A. M., Pfaendtner, J., Guo, J., Sienkiewicz, M., and S. E. Cohn, 1995: Assessing the effects of data selection with DAO's Physical-space Statistical Analysis System. *International symposium on assimilation of observations in meteorology and oceanography*, Tokyo, Japan, 273-278.

da Silva, A. and C. Redder, 1995: Documentation of the GEOS/DAS Observation Data Stream (ODS) Version 1.0. *DAO Office Note 95-01.* Data Assimilation Office, Goddard Space Flight Center, Greenbelt, MD 20771. Available on-line from `http://dao.gsfc.nasa.gov/subpages/office-notes.html`.

da Silva, A., and J. Guo, 1996: Documentation of the Physical-Space Statistical Analysis System (PSAS) Part I: The Conjugate Gradiant Solver version PSAS-1.00 *DAO Office Note 96-02.* Data Assimilation Office, Goddard Space Flight Center, Greenbelt, MD 20771. Available on-line from `http://dao.gsfc.nasa.gov/subpages/office-notes.html`.

da Silva, A. M., C. Redder, and D. P. Dee, 1996: Modeling retrieval error covariances for atmospheric data assimilation. Presented at the *Eighth Conference on Satellite Meteorology,* Atlanta, GA, 28 January–2 February, 1996. Available on-line as `ftp://dao.gsfc.nasa.gov/pub/papers/dasilva/atlanta96/tuning.ps.Z`.

da Silva, A., Ekers, K., and A. Conaty, 1996b: Requirements for DAO's On-Line Monitoring System ($\mathcal{DOLMS}$) version 1.00, *DAO Office Note 96-14.* Data Assimilation Office, Goddard Space Flight Center, Greenbelt, MD 20771. Available on-line from `http://dao.gsfc.nasa.gov/subpages/office-notes.html`.

Stobie, J, 1996: Data Assimilation Computing and Mass Storage Requirements for 1998. *DAO Office Note 96-16.* Data Assimilation Office, Goddard Space Flight Center, Greenbelt, MD 20771. Available on-line from `http://dao.gsfc.nasa.gov/subpages/office-notes.html`.

Stoffelen A., and D. Anderson, 1995: The ECMWF contribution to the characterisation, interpretation, calibration, and validation of ERS-1 scatterometer backscatter measurements and winds, and their use in numerical weather prediction models, *European Space Agency Contract Report.*

Susskind, J., Rosenfield, J., and D. Reuter, 1983: An accurate radiative transfer model for use in the direct physical inversion of HIRS and MSU temperature sounding data. *J. Geophys. Res.* **88**, 8550-8568.

Susskind, J., and J. Pfaendtner, 1989: Impact of iterative physical retrievals on NWP. Report on the Joint ECMWF/EUETSAT Workshop on the Use of Satellite Data in operational weather prediction: 1989-1993. Vol. 1, 245-270. T. Hollingsworth, Ed.

Susskind, J. 1993: Water vapor and temperature. *Atlas of Satellite Observations Related to Global Change*, Edited by R. J. Gurney, J. L. Foster. and C. L. Parkinson. Cambridge University Press, Cambridge England, 89-128.

Takacs, L.L., A. Molod, and T. Wang, 1994: Documentation of the Goddard Earth Observing System (GEOS) General Circulation Model–Version 1. *NASA Tech. Memo. No. 104606*, Vol. **1**, Goddard Space Flight Center, Greenbelt, MD 20771. Available on-line from `http://dao.gsfc.nasa.gov/subpages/tech-reports.html`.

7.7 Acronyms

7.7.1 General acronyms

DAO	Data Assimilation Office
GEOS	Goddard Earth Observing System (The name of the DAO data assimilation system)
GCM	General Circulation Model
DAS	Data Assimilation System
QC	Quality Control
NWP	Numerical Weather Prediction
CARD	Consistent Assimilation of Retrieved Data
PSAS	Physical-space Statistical Analysis System
NASA	National Aeronautics and Space Administration
GSFC	Goddard Space Flight Center
MTPE	Mission to Planet Earth
EOS	Earth Observing System
EOSDIS	Earth Observing System Data and Information System
NOAA	National Oceanic and Atmospheric Administration
NCEP	National Centers for Environmental Prediction (formerly, NMC)
NMC	National Meteorological Center
NESDIS	National Environmental Satellite Data and Information Service
ECMWF	European Center for Medium-range Weather Forecasts
UKMO	United Kingdom Meteorological Office

7.7.2 Instruments

ADEOS	Advanced Earth Observting Satellite (Mid-late 1996)
AIRS	Atmospheric Infrared Sounder (EOS PM)
AMSU A-B	Advanced Microwave Sounding Unit (POES, EOS PM)
AVHRR	Advanced Very High-Resolution Radiometer
ASTER	Advanced Spaceborne Thermal Emission and Reflection Radiometer (EOS AM)
ATOVS	Advanced TOVS; HIRS3/AMSU (POES)
CERES	Clouds and Earth's Radiation Energy System (TRMM, EOS AM)
CLAES	Cryogenic Limb Array Etalon Spectrometer (UARS)
DMSP	Defense Meteorological Satellite Program (currently operational)
EOS AM1	Earth Observting Satellite AM (June 98 launch)
EPS	EUMETSAT (European Meteorology Satellite) Polar System
ERBE	Earth Radiation Budget Experiment (ERBS)
ERBS	Earth Radiation Budget Satellite
ERS-1,2	European Remote Sensing Satellite (Scatterometer, 6 channel, IR-Visible radiometer)

GOES	Geostationary Observational Environmental Satellite (Imager and 18 channel visible and infrared sounder, currently operational)
GOME	Global Ozone Monitoring Experiment (ERS-2)
GPS	Global Positioning System
HALOE	Halogen Occultation Experiment (UARS)
HIRS2/3	High-Resolution InfraRed Sounder (POES)
HRDI	High Resolution Doppler Imager
IASI	Infrared Atmospheric Sounding Interferometer (EPS)
ILAS	Improved Limb Atmospheric Spectrometer (ADEOS)
IMG	Interferometric Monitor for Greenhouse Gases (ADEOS)
ISCCP	International Satellite Cloud Climatology Project (several IR and visible instruments aboard different satellite)
LIMS	Limb Infrared Monitor of the Stratosphere (Nimbus 7)
MAPS	Measurement of Atmospheric Pollution from Satellites
MHS	Microwave Humidity Sounder (EOS-PM)
MLS	Microwave Limb Sounder (UARS)
MODIS	Moderate-Resolution Imaging Spectrometer (EOS AM)
MSU	Microwave Sounding Unit
MOPITT	Measurement of Pollution in the Troposphere (EOS AM)
NSCAT	NASA Scatterometer (ADEOS)
POES	Polar Orbiting Environmental Satellite (Currently Operational)
PR	Precipitation Radar (TRMM)
SBUV	Satellite Backscatter Ultraviolet radiometer (Nimbus 7, POES)
SAGE	Stratospheric Aerosol and Gas Experiment (ERBS)
SMMR	Scanning Multispectral Microwave Radiometer (?)
SSM/I	Special Sensor Microwave/Imager (DMSP)
SSM/T	Special Sensor Microwave (Temperature sounder, DMSP)
SSM/T2	Special Sensor Microwave (Water vapor sounder) (DMSP)
SSU	Stratospheric Sounding Unit (POES)
TMI	TRMM Microwave Imager (TRMM)
TOMS	Total Ozone Mapping Spectrometer (ADEOS, Meteor, Earth Probe, Nimbus 7)
TOVS	TIROS Operational Vertical Sounder; HIRS2/MSU/SSU (POES)
TRMM	Tropical Rainfall Measuring Mission (summer '97 launch)
UARS	Upper Atmospheric Research Satellite (some instruments in operation)
WINDII	Wind Imaging Interferometer (UARS)

Chapter 8

Quality Assessment/Validation of the GEOS Data Assimilation System

Contents

8.1 Validation for Earth-science Data Assimilation

Since the inception of the DAO validation of system performance and improvement has been an open question. In the early reports of the DAO Science Advisory Panel, questions were raised about how to validate in ways other than forecast skill. The DAO has always worked from the premise that short and medium range forecast skill is not the absolute

measure of analysis quality. In fact, it is possible to improve forecast skill at the expense of analysis accuracy. This situation arises because there are compensating errors in the model-analysis-data system. Furthermore, many of the problems of interest to customers of the DAO are so far removed from weather forecasting that the weather forecast is insensitive to their representation. Therefore, more general methods of validation must be developed.

If the assimilation system is focused at generalized applications then the number of possible problems to provide metrics to measure improvement becomes very large. Often conflicts develop because efforts to improve performance in one area degrade performance in another area. The temptation to fix a problem with an ad hoc specification of a system parameter is high. Inevitably fixes haunt future development, because fixes, almost by definition, are short circuiting some feedback loop that is not well understood.

The DAO has grappled with the validation problem from the beginning. We maintain an internal group focused on scientific applications of GEOS data sets in order to assure that basic climate processes are evaluated. We continually seek and organize independent validation data sets (see http://dao.gsfc.nasa.gov/ for the current archive). We maintain a series of collaborations within GSFC to evaluate problems of atmospheric chemistry and climate parameters. We maintain a collaboration with NCEP to intercompare NCEP and DAO products. We have built a community of several hundred scientists who have looked at the GEOS data sets with varying degrees of scrutiny. This section details the current status of the DAO validation effort. More information can be found in Schubert et al. (1996).

One of the major goals of the GEOS-1 project (Chapter 4) was to develop a suite of problems to serve as baseline metrics to evaluate future performance. The number of problems identified from GEOS-1 is too large for all of them to be treated as equal metrics. Many are related to each other. Some are clearly beyond the near-term ability of any assimilation system. There are resource issues as conflicts development, for instance, between the need to improve ozone transport and the need to improve the surface energy balance.

Therefore, the DAO is faced with the problem of defining priorities to the different problems. These priorities are prescribed based on the science priorities of the MTPE (see Section 2.6), customer base, specifically focused funding, projected ability to impact a particular problem, performance relative to other available products, and initiatives in the broad science community. With so many different pulls on the process, validation is made even more difficult. There can be focus and improvement on one aspect of the system, and inattention to other aspects. In order to damp some of this volatility we have tried to focus on two broad disciplines which are at the basis of many aspects of Earth science:

- global hydrological and energy cycles, including interaction between the atmosphere ocean and land surfaces and storage in the soil
- transport processes in the atmosphere in order to calculate quantitatively dynamic variability of tropospheric and stratospheric trace constituents

One conclusion of our efforts has been the realization that assessment of the quality of the data assimilation system extends beyond traditional validation. With multi-year assimilated data sets and parallel experiments with identical models techniques are being developed that bridge the gap between traditional space and time averaged climate diagnostics and

process-oriented modeling. We are discovering fundamental research questions that must be answered in order to develop soundly based validation criteria. This chapter will focus on the quality assessment plans for GEOS systems. At the time of this writing the validation for GEOS-2 is in progress and much is being learned about system integration and validation. GEOS-2 validation is, therefore, the focus of the chapter. Status of the GEOS-2 validation can be found at

`http://zymurgy.gsfc.nasa.gov/lamich/geos2.0/closure/CM/status.html`

In an attempt to manage the quality assessment process we have identified three major components:

1. System validation
2. Scientific evaluation
3. Monitoring

These major components will be described below.

8.2 Overview of GEOS-2 Quality Assessment/Validation

The validation of data assimilation systems has traditionally focused on measuring the improvement in the accuracy of the forecast of the state variables of the atmosphere. This reflects the development of data assimilation as a method for improving numerical weather forecasts. Therefore, forecast skill is, culturally, the current fundamental measure of the quality of the assimilated product.

Over the past 15 years the scientific community has come to realize that assimilated atmospheric data provide a unique resource for studying the dynamics of the atmosphere. In fact, the analyses being routinely generated by the operational numerical weather prediction (NWP) community have become indispensable tools for studying a wide array of atmospheric science problems. Traditionally, the NWP products suffer from inhomogeneities resulting from system changes (*e.g.*, Trenberth and Olson 1988; Arpe 1990), which have made them inappropriate for many studies focused on longer term weather and climate variations. The NWP products also have, historically, not included many of the diagnostic quantities (*e.g.*, precipitation, heat rates, radiative fluxes, etc.) needed for studying climate processes. This likely reflects a lack of confidence in the quality of these quantities, the secondary importance these have received in the validation of NWP analyses, as well as the substantial expense of their generation and storage.

Recently, to address the problem of spurious signals from system changes, a number of centers have generated re-analyses of historical observations (Schubert et al. 1993; Gibson et al. 1994; Kalnay et al. 1996). For the DAO effort, the re-analysis (employing GEOS-1, Chapter 4) provided a unique opportunity to both produce a benchmark for further development and to provide a timely product to the science community. While the GEOS-1 DAS has a strong NWP heritage, the primary goal of this effort was to seek feedback from a wide as possible range of users to help guide the development of future versions of the GEOS system (Schubert and Rood 1995, TM Volume 7). One of the key lessons learned from this effort is that validation of assimilation products is in its infancy - there is no simple measure of quality that is appropriate for the entire array of potential applications.

The quality assessment effort within the DAO (Schubert et al. 1996) is attempting to address this broader role of validation by employing an integrated approach closely coupled with the development and production process, involving system validation, scientific evaluation, and monitoring.

8.2.1 System Validation

System validation is the process by which major modifications to the system are evaluated and judged suitable for incorporation into the next production system. This effort is perhaps the most demanding in terms of coordination with other activities. In particular, it must determine how to best coordinate with, complement, and take advantage of the ongoing validation activities inherent in the development process. In addition, it must bring to bear the results of the relevant scientific investigations, new verification data, and the diagnostic tools which are best suited for evaluating the system modifications at hand. It must also tackle the daunting task of quantifying the quality of the assimilated products for climate and other Earth Science applications. Without this link to representative Earth- science

problems the validation can lose relevance.

The process of system validation is an evolving one; we have yet to learn how to best ensure that the validation process is directly linked to the requirements of our customers. These requirements (Chapter 9) may be conflicting and as such the validation effort must be given guidance on priorities which may be based on other than scientific justifications. There are, for example, special production requirements on accuracy and timeliness imposed by the EOS instrument teams.

8.2.2 Scientific Evaluation

The centerpiece of the DAO quality assessment effort is the scientific evaluation of the assimilated products. This requires multi-year data sets to assess the ability of the assimilation system to faithfully reproduce the mean climate, its variations and the associated physical processes. While a considerable amount of work is done within the DAO and other Goddard Laboratories (*e.g.*, codes 913 and 916) , the broad range of potential applications necessitate that much of the assessment of the quality of the GEOS DAS products be carried out by outside investigators. To ensure this takes place it is imperative that the DAO periodically produce and make available useful long term assimilated data sets to the general science community.

The in-house scientific assessment has been divided into four areas of research consisting of

IH1: climate variability and sensitivity

IH2: stratospheric meteorology and transport

IH3: regional climate, weather and the hydrological cycle

IH4: tropospheric chemistry.

There is significant in-house experience in these four areas, and a history of applications define the necessary improvements needed to address specific scientific projects. The usefulness of the assimilated data for addressing science issues in each of these areas, generally depends on the internal (physical and dynamical) consistency of the assimilated data, which in turn depends on the veracity of the physical processes represented in the geophysical model and their consistency with the observations. Furthermore, the degree to which the assimilated data track nature depends on the availability and quality of observations, and the ability of the analysis scheme to extract and optimally combine the relevant information from the observations and model-generated first guess fields.

8.2.3 Monitoring

The real-time monitoring of on-going data assimilation experiments is crucial to a successful production effort. The general goal of monitoring is to ensure that any errors in the processing are detected (and possibly corrected) at an early stage before substantial resources are wasted. This includes the monitoring of both the input observations and output assimilated

data and ancillary information (such as quality control information) which characterize the quality of the assimilated product.

A requirements document for monitoring the output from an assimilation (da Silva et al., 1996) provides the framework for the initial implementation of the DAO On-line Monitoring System (DOLMS). The requirements are tailored to the specific modes of operation of the GEOS DAS involving the first-look analysis, the final platform analysis, multi-year reanalyses, and system validation experiments (see Section 2.6.3). As outlined in the DOLMS document, the monitoring system for the first-look analysis must provide on- line access to recent analyses, forecasts, quality control information and selected climate diagnostics. The monitoring system for the final platform analysis will be similar but with the addition of statistics for monitoring new (both active and passive) data types. For multi-year reanalyses the monitoring system will focus on time series at key locations or regional averages and on a comprehensive collection of climate diagnostics. If forecasts are issued these will be monitored in a way similar to the first look system. The monitoring system for system validation will focus on monthly time series and climate diagnostics with the additional capability to simultaneously depict the performance of the new system compared to the control system.

DOLMS can be reviewed at

`http://dao.gsfc.nasa.gov/monitoring`

DOLMS capabilities are being continually upgraded. The DOLMS page and some of the experiments represented there are volatile and contain errors that are being addressed in validation projects. Therefore none of the results on the DOLMS page should be used for scientific applications without first contacting the DAO.

8.2.4 Infrastructure

In order to support the validation effort a substantial infrastructure is needed. Beaudoin and Schubert (1996) describe the visualization and user interface that plays a vital role in managing and integrating validation and development resources. These resources consist of verification data, subsets of assimilated data, visualization and other scientific tools, and documentation.

8.3 GEOS-2 Validation Process

8.3.1 The GEOS-1 Baseline

The process of evolving the data assimilation system from one version to the next is volatile, often driven by discoveries made during the process. During development, modifications are built upon an existing frozen, validated system. The experience from the frozen system defines the baseline on which to validate the next system. Documentation of both known deficiencies and validated features of the frozen system is needed.

The GEOS-1 experiment (Chapter 4) provided the baseline for improvement of GEOS-2. In this section we review the GEOS-1 system. The validated features (successes) and identified shortcomings of the GEOS-1 system are summarized here. Schubert and Rood (1995, TM Volume 7) provide a more detailed exposition of both successes and failures of GEOS-1. Deficiencies that have been discovered since the publication of Schubert and Rood are also included here.

8.3.1.1 Validated Features (Successes) of the GEOS-1 DAS

The relative validation described in Section 8.3.3.1 involves the comparison of features in the system being considered with those from the latest frozen or control system. This requires a documented list of validated features which will be updated at each system validation step. Since the GEOS-2 validation is the first major system validation exercise, we present below (in lieu of officially validated features for GEOS-1) a list of features that have been documented as being well captured by the DAS.

8.3.1.1.1 Low Frequency Variability. The primary strength of the GEOS-1 assimilation system lies in its ability to capture many of the key patterns of climate variations associated with El Nino and La Nina events, monsoons, droughts and other low frequency variations. These consist of the following:

- The global signature of low frequency variations in the atmospheric moisture field compare favorably with SSM/I data. (Chen et al. 1995).
- The tropical zonal winds and pressure fields have realistic variations associated with the Madden-Julian Oscillation and westerly wind bursts. (Lau et al. 1995) The large scale tropical divergent wind field captures the evolution of the Madden-Julian Oscillation (Schubert et al. 1995, Mo and Higgins 1996).
- The large cloud forcing anomaly in the central equatorial Pacific associated with 1986/87 El Nino compares favorably with ERBE data (Chen and Bates 1995). The tropical Pacific outgoing longwave radiation (OLR) anomalies associated with the 1987/88 El Nino/La Nina event compare favorably with OLR observations (Schubert et al. 1995). The monsoon precipitation anomalies associated with the 1987/88 El Nino/La Nina event are consistent with the OLR observations (Schubert et al. 1995).

- The reduced precipitation during the 1988 (June) drought and the much enhanced precipitation during the 1993 (July) wet conditions over the United States compare favorably with station observations (Schubert et al. 1995).

- GEOS-1 captures the seasonal placement of upper tropospheric moisture patterns quite well (Salathe and Chesters 1995)

8.3.1.1.2 Short Term Variability. A number of shorter term fluctuations are well represented in the assimilation. These are primarily associated with fluctuations in the zonal wind and/or the boundary layer winds and surface stresses. These consist of:

- The GEOS-1 equatorial winds appear to successfully capture the sub-daily atmospheric tidal variations (Salstein and Rosen 1995).

- GEOS-1 winds compared with length of day measurements suggest that the momentum variations are well captured for periods as short as 8-9 days. Comparisons between NCEP and GEOS-1 re-analyses shows coherence on all time scales longer than 3 days, which is shorter (better) than has been typically obtained from operational analyses. This suggests the re-analyses are in closer agreement than operational series have been in the past for this quantity (Salstein and Rosen 1995).

- The horizontal winds, convective cloud mass flux, detrainment, and planetary boundary layer depth are of sufficient quality to be used with significant success as input to tropospheric chemistry transport models for Freon-11, Rn-222, and CO. Middle latitude synoptic variability is well captured; however, interhemispheric gradients are not well simulated. Convective transport suggests that the cloud mass fluxes are of the right magnitude (Allen et al. 1995; Pickering et al. 1995).

- GEOS-1 wind stress provides good estimates of ocean transport through the Florida Straits. The GEOS wind stress generally provides improvements over the operational ECMWF results, but tends to overestimate amplitudes beyond about 10 days (Greatbatch and da Silva 1995).

- Variations in the low level winds over the Great Plains are quite realistic despite the lack of observations going into the GEOS-1 DAS below 850 hPa (Helfand et al. 1995).

8.3.1.1.3 Climate Mean. The following climate mean quantities are generally consistent with available verifying observations, and/or are consistent or better than found in other analyses:

- The climate mean and seasonal evolution of the tropospheric zonal wind appears to be well captured (Schubert et al. 1995).

- The clear sky longwave flux and albedo are in good agreement with ERBE measurements. See, however, below comment concerning a cancellation of errors (Charlock and Rose 1995; Chen and Bates 1995; Wu et al. 1995; Arking 1995).

- The general patterns of tropical convection and their seasonal evolution are consistent with available observations, but details of local maxima and amplitudes are not (Robertson et al. 1995).
- The wind stress fields have been employed to force an ocean model in the North Pacific with some success in producing the sub-polar circulation (Rienecker 1995).

8.3.1.1.4 Stratosphere The stratospheric version of GEOS-1 DAS has the following validated features:

- Forecasts from the GEOS system have been used with general success in planning and directing flights of the high-altitude NASA ER-2 aircraft to potential vorticity, and hence chemical, targets in middle and high latitudes (Newman et al. 1995).
- Lagrangian tracking techniques have been successful in mapping tracer structures that are much finer than the resolution of the assimilating model. Tracking of the Pinatubo eruption cloud with GEOS winds has been more successful than similar experiments with NCEP winds.
- GEOS winds have been successfully used to model ozone chemistry and transport for integrations longer than one year. Prior experiments that did not use the IAU were not useful for more than a three month integration. Synoptic and planetary-scale variability are well simulated (Douglass et al. 1995, Douglass et al. 1996).
- The rotated pole model effectively eliminates spurious noise that was noted at the pole in earlier versions of the GEOS analysis. The location of the computational pole at low latitudes does not appear to cause a problem; this is likely because the Coriolis term is small (T.-C. Chen, Takacs, Min, unpublished results).
- The tropical quasi-biennial wind oscillation is present in the analyses. Though details of the quasi-biennial oscillation are not well represented, the variability is far better than has ever been achieved in GCM calculations.

8.3.1.2 Deficiencies of the GEOS-1 DAS

It is from the identification and confrontation of our weaknesses that future strengths are built.

The primary deficiencies in the GEOS-1 DAS products are tied to errors in the water vapor and cloud fields. This is not unique to GEOS-1 as all analyses continue to have problems with these parameters. The humidity bias, in particular, has been linked to a number of problems with the GEOS-1 assimilation system. One of the most disturbing deficiencies is an apparent feedback between the analysis increments and the model first guess fields which generates spurious tropical cloudiness and precipitation intensities which are unrealistic (particularly during boreal summer) and, in fact, in some cases less accurate than that simulated by the model (Molod et al. 1996, and see section 4.3.1.2). Another is a strong sensitivity of the assimilated climate to moisture observations (Park et al. 1996) which leads to artificial climate signals tied to inhomogeneities in the input observations.

Another place where the data insertion reduces the quality obtained by the model simulation is in the representation of the surface energy balance. In particular, the GEOS-1 DAS has excessively cold surface temperatures over land during winter (Schubert et al. 1995). In this case, the insertion of observed moisture and temperature profiles lead to a reduction in large-scale cloudiness generated by the model, which in turn produces excessive radiative cooling to space. These instances where the assimilation of data degrades the performance of the model in simulation mode require the highest attention.

In general, the differences between the behavior of the system in simulation and assimilation mode have presented unforeseen difficulties with both tuning and overall validation efforts. Not surprisingly, tuning (or cancellation of errors in general) can lead to misleading conclusions on the quality of the system. An example, is the excessive water vapor in the upper tropospheric and stratospheric water vapor (Starr et al. 1995; Charlock and Rose 1995). This occurs despite a very good match between the GEOS-1 DAS and ERBE clear sky outgoing long wave radiation (OLR). This rather misleading result appears to be the result of a cancellation of errors (Takacs, personal communication) with excessive upper level moisture and too little moisture in the lower troposphere (Molod et al. 1996). The close match between the ERBE and DAS clear sky OLR in GEOS-1 is also suspect in view of the missing contribution from trace gases in the current radiation code (Suarez, personal communication).

Below we summarize the known deficiencies in the GEOS-1 DAS products.

D1: Moisture and clouds

- A much too wet upper troposphere (300 hPa) over the Pacific Ocean compared with available observations and other analyses (Starr et al. 1995; Charlock and Rose 1995).
- The horizontal moisture gradients between very moist and very dry regions of the upper troposphere are too weak (Salathe and Chesters 1995).
- The tropics and subtropics over the oceans are too dry compared with the vertically integrated moisture from SSM/I (Molod et al. 1996; Ledvina and Pfaendtner 1995).
- Longwave and shortwave cloud radiative forcing are overestimated over regions of deep convection in the intertropical convergence zone (ITCZ) especially during Northern summer (Molod et al. 1996; Wu et al. 1995; Charlock and Rose 1995; Chen and Bates 1995; Ledvina and Hou 1996; Arking 1995).
- Middle-latitude longwave and shortwave cloud radiative forcing are weaker than ERBE especially over the storm tracks of both hemispheres (Molod et al. 1996; Chen and Bates 1995). The vertical distribution of diabatic heating and vertical heat transport may also be too shallow in these regions (especially the North Atlantic, Straus and Paolino 1995).
- High clouds in the tropics are excessive. Middle and low clouds in extratropics are deficient (Joseph and Geller 1995).
- Low level coastal stratiform clouds are underestimated (Wu et al. 1995).

- Cloud mass flux associated with June squall line over Kansas and Oklahoma is too shallow (Pickering et al. 1995)
- Cloud mass flux does not entrain and detrain mass over a deep enough layer. Therefore, the boundary layer and upper troposphere are linked too strongly. Consequently the middle troposphere is too isolated from convective processes. (Pickering et al. 1995; Allen et al. 1995)
- Deficient tropospheric interhemispheric exchange (Allen et al. 1995)

D2: Precipitation, evaporation and near surface fields

- Precipitation over eastern Pacific ITCZ is underestimated (Ledvina and Pfaendtner, 1995).
- Summertime precipitation over eastern North America is overestimated (Schubert et al. 1995; Higgins et al. 1996; Arpe and Stendel 1995).
- Springtime evaporation over central and eastern United States is too large (Schubert and Chang 1996; Higgins et al. 1996).
- The amplitude of the diurnal cycle of the precipitation over the southeast US is too large with little evidence of a nocturnal maximum over the Great Plains (Higgins et al. 1996; Min and Schubert 1996a, b).
- The amplitude of the annual cycle of tropical precipitation/OLR is too large (Kondragunta and Gruber 1996; Yang and Schubert 1996).
- Interannual variability in precipitation is too weak (Kondragunta and Gruber 1996; Yang and Schubert 1996).
- Wintertime precipitation is too low over the Northern Rockies and along the southern coast of the United States (Arpe and Stendel 1995).
- The gap in precipitation between the western Ghats and the Bay of Bengal is missing (Arpe and Stendel 1995).
- Rain over continental Europe and northern Asia in July is excessive. Rain over the Mediterranean during January is weak (Arpe and Stendel 1995).
- Precipitation over Caribbean and Gulf of Mexico during summer is excessive (Adler et al. 1996).
- Days with small rain amounts are too frequent. Days with no rain are too few. Days with intense rain amounts are underestimated (Wood et al. 1995; Higgins et al. 1996; Min and Schubert 1996a,b)
- The 1988 drought over the United States extends too long into the summer with warmer and drier conditions than were observed in July (Schubert et al. 1995).
- The near surface temperature is too cold over the northern United States and Canada during winter (Schubert et al. 1995).

- The implied oceanic heat transport based on the net heat flux into the ocean is unrealistically large (da Silva and White 1995).
- Subtropical deserts are less reflective than in ERBE. The diurnal cycle of out- going longwave radiation over land shows significant phase shifts with respect to ERBE (Joseph and Geller 1995).
- Subtropical/middle latitude (*e.g.* in region of Kuroshio current) wind stress is too weak (Rienecker 1995; Rienecker et al. 1996).

D3: Wind, temperature and pressure fields

- The Hadley cell is too weak during Northern winter (Arpe and Stendel 1995; Hou, personal communication; Schubert et al. 1995; DeWeaver and Nigam 1996).
- Zonal mean sea level pressure and zonal wind are biased (Arpe and Stendel 1995; Takacs and Suarez 1996).
- Transport (heat, momentum, and moisture) by NH transient waves is too strong and by stationary waves too weak (Min et al. 1996; Takacs and Suarez 1996).
- Baroclinic energy conversions in synoptic and smaller scales are weak (Straus and Paolino 1996).
- The northward component of the summertime low level wind over the southern Great Plains and Gulf Coast appears to be underestimated (Higgins et al. 1996).
- Various quantities including the temperature, wind and sea level pressure show evidence of noise near the poles (Takacs and Suarez 1996).
- Small scale noise in stratosphere tropics is excessive (Douglass et al. 1996)
- "barrier" between tropics and middle latitudes is too weak in lower stratosphere (Douglass et al. 1996).
- Stratospheric tropical upward motion is too strong. Polar winter descent is too weak (Newman et al. 1995; Douglass et al. 1995; 1996)
- There is a warm bias at the stratospheric wintertime pole for the most extreme cold events. (Newman et al. 1995)
- Tropical Kelvin waves are not well represented.
- Five-day tropospheric forecast skill is not competitive (Atlas et al. 1996)
- Tropical stratospheric forecasts are poor (Newman et al. 1995).

8.3.2 Distillation of the GEOS-1 Baseline

As part of the Quality Assessment the four teams (IH1-IH4 in Section 8.2.2) plus representatives from the DAO modeling and analysis groups have distilled the above deficiencies into groups of Science Issues which represented integrated views of many of the individual deficiencies. This process is directed by the head of the system validation group. The process evaluates on-going validation activities inherent in the development process, results of the relevant scientific investigations, new verification data, and the diagnostic tools which are best suited for evaluating the system modifications at hand. The distillation of above deficiencies are presented in Table 8.1.

Table 8.1: Distillation of GEOS-1 Deficiencies for GEOS-2 Validation

Science Issue	*GEOS-1*	*GEOS-2 (expected)*	*Verification Data Sets*	*Unacceptable*
Cloud Forcing	too much, tropical	improved	ERBE, NOAA OLR	no improvement
	too little, storm track	improved	ERBE	no improvement
	too little stratus	no worse	ERBE, ISCCP	worse
Moisture	too dry integral	improved	SSM/I	worse
	too wet upper trop	improved	MLS, TOVS	worse
	large increments	improved	vertical budget	worse
Precipitation (ocean)	poor E Pacific ITCZ	no worse	GPCP, OLR, etc	
	too much Gulf Mexico	no worse	GPCP, OLR, etc	
Precipitation (land (US))	summer mean	no worse	station data	worse
	diurnal much too strong			
Stratosphere:				
• residual circ	poor (inconsistent)	credible	UARS, TOMS	worse
• zonal-mean U,T	fair	improved	ER-2	worse
• Pot. Vorticity	noisy	improved	ER-2, UARS	worse
• 3-D fields	fair/good	improved	UARS, TOMS	worse
Sfc wind stress	good/weak	improved	COADS, ERS-1, NSCAT, SSM/I	worse
Net flux ocean	poor	improved	COADS	no improvement
Sfc temp land	much too cold winter	improved	station data	worse
Hadley Cell	weak	improved	radiosonde, consensus	worse
Low Level Jet	good/weak	no worse	station data	worse
48 hr Forecast	not competitive	improved		no improvement
O-F Statistics		improved	radiosondes	no improvement

The first two columns contain a summary of the main deficiencies that GEOS-2 is designed to directly or indirectly impact. This provides guidance for which diagnostics to compute. The third column shows the expected impact, the fourth column lists the various verification data to be employed, and the final column indicates "show stoppers",

i.e. a result that would bring the validation to a halt and require immediate attention of the validation committee. The teams are monitoring the performance of these parameters as GEOS-2 experiments are run. New capabilities of GEOS-2 and GEOS-3, such as soil moisture, will be validated in component models during the development stage, but ultimate validation will depend upon the results from applications.

8.3.3 GEOS-2 Validation

Prior to the actual implementation of the validation process, a detailed validation plan is written (Schubert et al. 1996). The plan ensures that all aspects of validation are carried out and finally, to decide (based on the results of the validation diagnostics), whether or not the system modifications have lead to an acceptable new production version of the DAS.

System validation is constrained by time and resources to a limited set of experiments. This complicates the determination of climate variability and sensitivity characteristics which require comparisons between different years. As such, the validation outlined here can only be preliminary, trying to catch egregious errors and anticipate performance when longer data sets are available. Re-analyses carried out with validated systems become an integral part of the overall scientific evaluation. Results from long assimilations with GEOS-2 will form the basis for further development and provide input for the system validation of future systems.

Hence, a major early decision is what experiments to run for validation. The choice is not easy. Many of the deficiencies identified by users are for specific time periods. While they might represent general process deficiencies, often the user only has quantitative information on a small number of case studies. Also, some of the validation data sets are only available for a particular time. It is impossible to produce multi-year data sets in a timely fashion for system validation.

The validation steps carried out as part of the development process must also be reconciled with the final system validation. This module testing of individual system components must be carried out in a controlled fashion and documented for evaluation by the full validation committee. The decision as to what constitutes a major modification (or group of modifications) and requires system integration and a full system validation step is as yet unclear, though it is certainly clear that the GEOS-2 validation process is hampered by an abundance of modifications that are all coming on-line simultaneously. (Currently a process is being defined to use the Scientific Steering Board of the DAO. The Scientific Steering Board is an internal group, reporting to the Head, of DAO, comprised of individuals who represent all key aspects of the GEOS system and MTPE mission requirements.)

For the current validation of GEOS-2.0, we are generating assimilations from three periods for comparisons to the control (GEOS, STRAT, the configuration of GEOS-1 that fully resolves the stratosphere); these assimilations will begin in mid May of 1987 and 1988 and mid December of 1991. Each run will consist of one and one half months of assimilation with a one half month period of spin-up time. Numerous repeats are performed as problems are identified and corrected. A one year GEOS-2.0 model simulation will be carried out in parallel to help assess the causes of deficiencies found in the assimilation.

System validation of GEOS-2 will pursue two strategies: relative validation and absolute

validation. Relative validation compares the behavior of the current (candidate) system with that of a previous system (control). The control's performance has been baselined. Where the control system has had previously acceptable (i.e validated) performance, it is reasonable to require the candidate system to perform at a similar level.

Absolute validation evaluates the products of a candidate system by comparing them to products obtained from independent data. An absolute validation criterion is satisfied when the candidate system value agrees with the independent validation standard within the uncertainties inherent in both the candidate and validation standard values. The uncertainties (i.e. error bars) in the validation data will be complicated combinations of instrument, sampling and even modeling errors. Thus, while absolute validation is generally the most desirable approach to follow in order to address scientific issues, it is also a more challenging approach to perform correctly.

Note: the summary in Table 8.1 contains issues pertaining to both validation strategies. In the following we expand on the relative and absolute validation approaches to be used for the GEOS-2 system validation.

8.3.3.1 Relative Validation

There are a number of objective measures available for comparing the behavior of GEOS-2 against a control system. In relative validation short-term forecasting plays a substantial role. This addresses some of the lessons learned from the GEOS-1 project listed in Chapter 4. The following list is a descriptive summary of those that will be used for the system validation of GEOS-2.

8.3.3.1.1 O-F statistics. How well does the candidate system forecast future data? O-F statistics are the mean variance, for pre-defined regions and selected data types at various levels of the atmosphere, of differences of observations from 6-hour model forecast fields. Although the variance of O-F should not be zero (since there are observational errors), the general guiding principle is that an improved system should show decreases in O-F variances.

8.3.3.1.2 QC statistics. QC (quality control) statistics are an accounting of the number of data which fail the quality control checks within a particular system. The tropics, mid-latitudes and polar regions will be examined separately. A large number of observations failing the QC generally indicates a drift in the assimilation system away from observations. This, along with growing O-F's, is usually a sign of defect in an assimilation system.

8.3.3.1.3 A-F spectra, time means. A-F spectra are the Fourier spectra of analysis minus forecast (analysis increments) around latitude circles. Power at high wave numbers is generally indicative of noise in the analysis. Does the candidate system have reduced A-F spectra at high wave numbers?

Time means of analysis increments can be revealing of possible biases in the assimilation system (especially in the GCM component). A non-zero time mean A-F indicates that the

analysis (and, by inference, data) is constantly fighting changes introduced by the GCM integration since a previous analysis.

8.3.3.1.4 O-A statistics O-A statistics (observation minus analysis residuals) are a measure of how well an analysis extracts information from data (Hollingsworth and Lönneberg 1989). Here O-A statistic refers to the covariance between analyses and some specific observation type (*e.g.* rawinsonde heights); in particular, this diagnostic focuses on the (extrapolated) intercept of the O-A covariance at zero distance. An intercept of zero or a negative value indicates that the analysis is extracting the maximum available information from that observation type.

8.3.3.1.5 Forecast skill - Anomaly Correlations Anomaly correlations will be generated from the suite of forecasts made from initial conditions taken from the assimilation runs. Our interest is on the short-term (1-3, up to 5 days) anomaly correlation behavior, as that reflects to a greater degree on the nature of the assimilation system's handling of data and to a lesser degree on strictly performance of the forecast model. The higher the anomaly correlation, the better the result.

In Chapter 5 are numerous examples of relative validation. They show a measure of new system performance relative to old system performance. O-F statistics are shown in Figure 5.27 to show that in both January and July the system with the incremental analysis update draws forecasts to the background state with greater accuracy. Figures 5.2 through 5.4 show spectra of analysis increments which reveal that the Physical-space Statistical Analysis System reduces the spurious noise at high wavenumbers relative to the old optimal interpolation.

8.3.4 Absolute Validation

Absolute validation is the foundation of system validation. It is the part of the validation activity that is most directly tied to specific science and/or operational objectives. It forms the basis for judging whether the GEOS system meets the various customer requirements (see Chapter 9) and thus measures the success of the overall GEOS DAS development effort.

Absolute validation requires that measures of product quality be formulated to reflect the impact on specific science and/or operational requirements. It is only within such a context that meaningful measures of "accuracy" and pre-defined criteria for designating a particular product feature to be of acceptable quality can be made. This, in turn, requires that uncertainties in the estimates of the DAS product and the verification data be considered.

Since absolute validation requires independent data sets, the DAO continually seeks and organizes independent validation data sets (see http://dao.gsfc.nasa.gov/ for the current archive). While there are a few consensus data sets accepted by the community as standards, for many primary parameters (e. g. precipitation) there is not general consensus. In most of these more uncertain parameters there is wide spread in the range of the independent validation data sets.

It is worth noting that the most widely accepted standard for accuracy of temperature and wind measurements are rawinsondes. Therefore, rawinsonde data are at the very basis

of absolute validation. It is often biases and root mean square (rms) differences with rawinsondes that are the first line of validation. An absolute standard is also at the very basis of bias correction techniques (See Chapter 9).

The fourth column in Table 8.1 lists some of the key independent verification data that will be used for the GEOS-2 absolute validation. These range from the relatively accurate rawinsonde reports of winds to the much less certain cloud information from the ISCCP data. How these data are used also impacts the accuracy of the comparison. For example, the use of N_2O transport calculations to assess the quality of the GEOS winds must take into account not only the accuracy of the UARS N_2O data but also the uncertainties inherent in the off-line transport calculations.

Requirements to provide ancillary data for instrument retrievals are sometimes the easiest to deal with in terms of formulating specific measures of quality. For example, the CERES instrument team requires moisture and temperature profiles with specific (rms) accuracies and bias tolerances. The GEOS-2 products will be compared with rawinsonde reports of these quantities where available, and with other satellite observations of these quantities to determine whether the GEOS-2 products meets these requirements.

Science requirements are more difficult to formulate and can often only be addressed indirectly. For example, the outgoing longwave radiation (OLR) must meet certain bias and rms tolerances (compared with ERBE data) which are linked to the accuracy of the upper level moisture field, the cloud distribution and cloud optical properties. These tolerances must be set to allow climate sensitivity studies of sea-surface temperature and upper level moisture as well as to provide accurate surface energy balances at the ocean surface to produce reasonable implied ocean heat transports.

Those items in Table 8.1 having specific entries in the column labeled "Verification" will be the subjects of absolute validation activities for GEOS-2. The detailed absolute validation plans for each of these, including the specific links to science/customer requirements are currently being formulated. The end result of the absolute validation activity is a list of validated features of the GEOS-2 DAS that will be updated with each new validation activity.

8.4 New Approaches to Validation

The pursuit of generalized data assimilation opens up a whole range of new questions. Many of these questions have never been addressed, and are fundamental research issues.

For instance, the production of re-analyses removed the spurious signals from multi-year data sets caused by analysis systems that were continually changing to improve weather forecasts. The re-analyses have been successful in providing information about interseasonal and interannual variability. New questions are now raised about the variability of the input data stream. Concerns about the variability of the input data stream include

ID1: a new type of data becomes available

ID2: a different instrument makes the same type of measurement

ID3: The same instrument degrades in time

ID4: a different data handling process is applied to data provided by outside sources

Clearly, for instance, given the tremendous shortcomings in the cloud and precipitation fields, data from a MTPE platform such as the Tropical Rainfall Measurement Mission (TRMM) will have a dramatic change on data set quality. This will leave a spurious signal in the long-term data set. There are many open questions in how to best address the impact of the changing input data stream.

But there are many more subtle problems with the input data stream than the availability of a completely new data type. One of the most important lessons learned from the re- analysis projects is the impact of quality control decisions. Park et al. (1996) show, for example, that Indian monsoon rainfall fluctuations are at least in part associated with fluctuations in the number of radiosonde moisture observations that were ingested in the GEOS-1 DAS. The impact of observations, in particular, the extent to which they constrain the assimilation, and the extent to which they are optimally utilized by the assimilation system are key validation issues that are just beginning to be addressed.

Sienkiewicz and Pfaendtner (1996) showed, for example, that differences in the initial conditions for an assimilation can be traced for several weeks, depending on the data distribution, on the model formulation, and on the parameter that is being studied. One consequence of this research is to define how much overlap is required and what is the impact on long-term variability from piecing together short data sets to create long data sets?

Other new validation techniques focus on physical and dynamical consistency, one of the most important expectations of assimilated data sets. The lack of consistency between the state variables and parameterized diagnostic or forcing quantities substantially reduces the value of the DAS products for many applications. The lack of consistency typical manifests itself as a mean artificial source/sink term in budget equations that, in current assimilated data, are comparable in magnitude to the physical forcing. In this respect data assimilation is itself an important validation exercise, since the mismatch between the observations and first guess fields can form the basis for judging the quality of the system.

Schubert and Chang (1996) embraced this idea to address the physical and dynamical consistency of the U.S. hydrological cycle within the GEOS-DAS. A methodology was developed (Restricted Statistical Correction or RSC) that allows output from DAS runs to be used directly to infer the sources of the model errors. The RSC approach, in fact, suggests more general validation criteria that measure the extent to which the observations systematically (and thus improperly) influence the assimilated climate.

The consistency question brings attention to model parameterizations and how they impact estimates of poorly constrained parameters. Chang and Schubert (unpublished) have conducted sensitivity studies where a subtle change to the convective parameterization leads to uncertainties in the assimilated tropical wind field of up to 30the climate variance.

Finally, understanding the climate generated by a data assimilation requires that we understand the climate of the geophysical model employed in the assimilation system. Such long simulations employing the same model used in the assimilation have previously been unavailable. Mismatches between the simulate and assimilate climates can provide new insights into the deficiencies of the assimilation system (Molod et al. 1996). Such simulations can also be used to look more carefully at the constraints imposed on the climate system. The extent to which these constraints are not satisfied in climate simulations should help to address model deficiencies and help quantify science requirements (*e.g.*, Johnson 1996, MIT 1996).

8.5 GEOS-2 Validation Tasks

In consideration of the constraints on time and computing resources, the validation runs will be limited to two boreal summer and one boreal winter assimilations. The tentative schedule is outlined below:

Development and integration of the proposed GEOS-2.0 system will be completed on a pre-specified date (PD). At this time the new system will be set to run three 2 1/2 assimilations; two will begin in mid May 1987, 1988 while the other will begin in mid December 1991. These three years have been chosen for a number of reasons, though ultimately the choice was based on the availability of some of the key verification data sets (particularly ERBE data for 1987, 1988 and UARS data for 1991/92). The comparison of 1987 and 1988 allows an assessment of interannual variability associated with ENSO.

A control employing GEOS-1.2 has already produced results for these time periods. Two business days (2D) will be allotted for preparation of a restart file for each assimilation and for the preparation time needed to set-up each assimilation run (*e.g.* scripts and directories). Thus, beginning on PD + 2D the three assimilations will begin running in parallel (on separate computers) in support of the validation effort.

Each run will undergo a one half month assimilation check to verify the model and the analysis are operating as expected. Extensive use will be made of the DOLMS to ensure there are no obvious errors. When running an assimilation it takes about one half of a month for spin-up time so this check is based on the results of the spin-up. During the assimilation runs, five-day forecasts will automatically be generated every 6th day (limited to June/July 1988 and Jan/Feb 1992). This is not expected to add to the amount of time to complete the assimilation since both the assimilation and forecasts can run simultaneously.

Based on the current resources provided, it should take about four days to run one half month of assimilation for GEOS 2.0 and two days to run a thorough check of the spin-up. Sixteen days is the expected time to run the remainder of the two and one half month assimilations. Allowing an additional week for contingencies, this phase of the work should be completed on PD + 2D + 27D.

Responsibilities for each area of validation (see Table 8.1) are assigned in advance as part of the initial meetings of the Validation Panel. After the two and one half months of assimilation for the three periods and the suite of forecasts are complete, epvaluation of the diagnostics will commence. A complete package of all results will be completed in 15 days (15D).

The Validation Panel will be assembled and given the results of the validation tests. Based on the results, each panel member will decide how the system performed in each of the areas shown in Table 8.1 It is expected that the system will meet most of the expectations and have none of the show stoppers listed in Table 8.1. A written evaluation by each panel member must be completed and submitted to the chair of the Validation Panel within seven days followed by a final meeting of the Validation Panel to vote on whether the proposed system is acceptable. A final summary report documenting the decision of the Panel will be made within one week.

8.6 References

Adler, R., C. Kidd, M. Goodman, A. Ritchie, R. Schudalla, G. Petty, M. Morrissey and S. Greene: PIP-3 Intercomparison Results, Oct 1996, prepared for PIP-3 Workshop 18-20 November 1996, College Park, MD.

Allen, D., R. Hudson, R. Rood, and A. Thompson, 1995: F-11 and Rn-222 calculations using a 3-D CTM and assimilated data, proceedings of the Workshop on the GEOS-1 Five- Year Assimilation, NASA Tech. Memo. No. 104606, Volume 7, Goddard Space Flight Center, Greenbelt, MD 20771.

Arkin, A., 1995: Shortwave Radiation Absorption in Clear and Cloudy Atmospheres. Proceedings of the Workshop on the GEOS-1 Five-Year Assimilation, NASA Tech. Memo. No. 104606, Volume 7, Goddard Space Flight Center, Greenbelt, MD 20771.

Arpe, K. 1990: Impact of changes in the ECMWF analysis-forecasting scheme on the systematic error of the model, Ten years of medium-range weather forecasting, Volume 1, 4-8 September 1989, June 1990, ECMWF, Shinfield Park, Reading RG2 9AX, U.K.

Arpe, K. and M. Stendel 1995: Comparison of GEOS-1 data with analysis and short-range forecast data from ECMWF and other estimates of truth. Proceedings of the Workshop on the GEOS-1 Five-Year Assimilation, NASA Tech. Memo. No. 104606, Volume 7, Goddard Space Flight Center, Greenbelt, MD 20771.

Atlas, R., R. N. Hoffman, E. Brin, S. Bloom and P. M. Woiceshyn 1996: The impact of ERS-1 scatterometer data on GEOS and NCEP model forecasts, 11th Conference on Numerical Weather Prediction, 99-101, August 19-23, 1996, Norfolk, Va.

Beaudoin, P. and S. Schubert, 1996: Visualization and user interface: requirements documentation, to appear as DAO Office Note.

Charlock, T. P. and F. G. Rose, 1995: Comparison of Pre-CERES, Satellite-Based Calculations of Atmospheric Longwave Radiation Budget with GEOS-1. Proceedings of the Workshop on the GEOS-1 Five-Year Assimilation, NASA Tech. Memo. No. 104606, Volume 7, Goddard Space Flight Center, Greenbelt, MD 20771.

Chen, T.-C., J. Pfaendtner, J.-M. Chen, and C. K. Wikle, 1995: Variability of the Global Precipitable Water with a Time-Scale of 90-150 Days. Proceedings of the Workshop on the GEOS-1 Five-Year Assimilation, NASA Tech. Memo. No. 104606, volume 7, Goddard Space Flight Center, Greenbelt, MD 20771.

Chen, M. and J. R. Bates, 1995: Cloud Radiative Forcing: GEOS-1 Assimilation Versus ERBE Observation, proceedings of the Workshop on the GEOS-1 Five-Year Assimilation, NASA Tech. Memo. No. 104606, volume 7, Goddard Space Flight Center, Greenbelt, MD 20771.

DeWeaver, E. and S. Nigam, 1996: Differences between NASA/GEOS assimilated and ECMWF analyzed divergent circulatations: causes and dynamical implications for El Nino wintertime anomalies, submitted to J. Atmos. Sci.

Douglass, A. R., C. J. Weaver, R. B. Rood, and L. Coy, 1995: A Three Dimensional Simulation of the Ozone Annual Cycle Using winds from a Data Assimilation System, proceedings of the Workshop on the GEOS-1 Five-Year Assimilation, NASA Tech. Memo. No. 104606, volume 7, Goddard Space Flight Center, Greenbelt, MD 20771.

Douglass, A. R., C. J. Weaver, R. B. Rood, and L. Coy, 1996: A three-dimensional simulation of the ozone annual cycle using winds from a data assimilation system, J. Geophys. Res., 101, 1463-1474.

Gibson, J. K., P. Kallberg, A. Nomura and S. Uppala, 1994: The ECMWF re-analysis (ERA) project-plans and current status, Tenth International Conference on Interactive Information and Processing Systems for Meteorology, Oceanography and Hydrology, American Meteorological Society, Nashville, Tennessee.

Greatbatch, R. J. and A. M. da Silva, 1995: Using GEOS-1 Wind Stress to Model the Variation of Transport Through the STraits of Florida. Proceedings of the Workshop on the GEOS-1 Five-Year Assimilation, NASA Tech. Memo. No. 104606, volume 7, Goddard Space Flight Center, Greenbelt, MD 20771.

Helfand, H. M., S. D. Schubert and C.-Y. Wu, 1995: Characteristics of the Simulated and Assimilated Great Plains Low Level Jet. Proceedings of the Workshop on the GEOS-1 Five-Year Assimilation, NASA Tech. Memo. No. 104606, volume 7, Goddard Space Flight Center, Greenbelt, MD 20771.

Higgins, R. W., K. C. Mo and S. D. Schubert, 1996: The moisture budget of the central United States in spring as evaluated in the NMC/NCAR and the NASA/DAO reanalyses, Mon. Wea. Rev.,124, 939-963.

Hollingsworth, A. and P. Lönnberg, 1989: The verification of objective analyses: diagnostics of analysis system performance, *Meteorol. Atmos. Phys.*, **40**, 3-27.

Johnson, D. R. 1996: On the 'General Coldness of Climate Models' and the second law: implications for modeling the Earth System, to be submitted.

Joseph, R. R., and M. A. Geller, 1995: Comparison of the Diabatic Fields in the GEOS DAS with those in the Atmosphere. Proceedings of the Workshop on the GEOS-1 Five- Year Assimilation, NASA Tech. Memo. No. 104606, volume 7, Goddard Space Flight Center, Greenbelt, MD 20771.

Kalnay, E., M. Kanamitsu, R. Kistler, W. Collins, D. Deaven, J. Derber, L. Gandin, S. Sara, G. White, J. Woollen, Y. Zhu, M. Chelliah, W. Ebisuzaki, W. Higgins, J. Janowiak, K. C. Mo, C. Ropelewski, J. Wang, A Leetma, R. Renolds, R Jenne, 1995: The NMC/NCAR Reanalysis Project, Bulletin of the American Meteorological Society, 77, 437 - 471.

Kondragunta, C. R. and A. Gruber, 1996: Intercomparison of spatial and temporal variability of precipitation products, Advances in Space Research, to appear.

Lau, K.-M., P. J. Sheu , S. Schubert, D. Ledvina, and H. Weng, 1995: Evolution of Large Scale Circulation During TOGA-COARE: Model Intercomparison and Basic Features, Proceedings of the Workshop on the GEOS-1 Five-Year Assimilation, NASA Tech. Memo. No. 104606, volume 7, Goddard Space Flight Center, Greenbelt, MD 20771.

Ledvina, D. V. and J. Pfaendtner, 1995: Inclusion of Special Microwave/Imager (SSM/I) total precipitable water estimates into the GEOS-1 data assimilation system, Mon. Wea. Rev., 123, 3003-3015.

Ledvina, D. V. and A. Hou, 1996: Data impact studies using the GEOS-1 DAS during TOGA COARE: Inclusion of SSM/I total precipitable water and surface wind estimates, WMO TOGA 95, in press.

MIT Climate Sensitivity Workshop, 1996: Estimating climate variability and sensitivity from satellite observations-Summary Report from the MIT Climate Sensitivity Workshop, April 21-22, 1996, Cambridge, MA

Min W. and S. Schubert, 1996a: A summary of precipitation statistics over the United States. *DAO Office Note 96-17.* Data Assimilation Office, Goddard Space Flight Center, Greenbelt, MD 20771. Available on-line from
`http://dao.gsfc.nasa.gov/subpages/office-notes.html`.

Min W. and S. Schubert, 1996b: The climate signal in regional moisture fluxes: A comparison of three global assimilation products, J. Climate, submitted.

Min W., S. Schubert and C.-K. Park, 1996: Am intercomparison of assimilated and simulated atmospheric variance/covariance statistics, NASA Tech. Memo. No. 104606, in preparation, Goddard Space Flight Center, Greenbelt, MD 20771.

Mo, K. C. and R. W. Higgins, 1996: Large Scale Atmospheric Water Vapor Transport as Evaluated from the NCEP/NCAR and NASA/DAO Reanalyses. J. Climate, in press.

Molod, A., H. M. Helfand, and L. L. Takacs, 1996: The climate of the GEOS-1 GCM and its impact on the GEOS-1 data assimilation system, J. Climate, 9, 764-785.

Newman, P., L. Lait, M. Schoeberl, M. Seablom, L. Coy, D. Lamich, R. Rood, R. Stimpfle and K. R. Chan, 1995: The use of GEOS-1 data for the Airborne Southern Hemisphere Ozone Experiment (ASHOE) and the Measurements for Assessing the Effects of Stratospheric Aircraft (MAESA) mission, proceedings of the Workshop on the GEOS-1 Five-Year Assimilation, NASA Tech. Memo. No. 104606, volume 7, Goddard Space Flight Center, Greenbelt, MD 20771.

Park, C.-K., S.-D. Schubert, D. J. Lamich, and Y. Kondratyeva, 1996: Monsoon Rainfall in the GEOS-1 Assimilation: Sensitivity to Input Data. *DAO Office Note 96-24.* Data Assimilation Office, Goddard Space Flight Center, Greenbelt, MD 20771. Available on-line from
`http://dao.gsfc.nasa.gov/subpages/office-notes.html`.

Pickering, K. E. , W.-K. Tao, Y. Wang, J. R. Scala, A. M. Thompson, D. P. McNamara, S.- J. Lin, A. M. Molod, and R. B. Rood, 1995: Transport Investigations Using the GEOS-1 Convective Fluxes, proceedings of the Workshop on the GEOS-1 Five-Year Assimilation, NASA Tech. Memo. No. 104606, volume 7, Goddard Space Flight Center, Greenbelt, MD 20771.

Rienecker, M., 1995: A comparison of surface wind products over the North Pacific Ocean, proceedings of the Workshop on the GEOS-1 Five-Year Assimilation, NASA Tech. Memo. No. 104606, volume 7, Goddard Space Flight Center, Greenbelt, MD 20771.

Rienecker, M. M., R. Atlas, S. D. Schubert, and C. A. Scholz, 1995: A comparison of surface wind products over the North Pacific Ocean, J. Geophys. Res.-Oceans, 101, 1011- 1023.

Robertson, F., W. Lapenta, D. Samuelson, J. Srikishen, and E. McCaul, 1995: Divergent Circulations and Deep Convective Processess in the GEOS-1 Assimilated Fields as Compared to Remotely Sensed Data. Proceedings of the Workshop on the GEOS-1 Five-Year Assimilation, NASA Tech. Memo. No. 104606, volume 7, Goddard Space Flight Center, Greenbelt, MD 20771.

Salathe, E. P. Jr. and D. Chesters, 1995: Evaluation of Upper-Tropospheric Moisture in the GEOS Assimilation Using TOVS Radiance Observations. Proceedings of the Workshop on the GEOS-1 Five-Year Assimilation, NASA Tech. Memo. No. 104606, volume 7, Goddard Space Flight Center, Greenbelt, MD 20771.

Salstein, D. A. and R. Rosen, 1995: Global Momentum and Energy Diagnostics from the GEOS-1 Assimilation. Proceedings of the Workshop on the GEOS-1 Five-Year Assimilation, NASA Tech. Memo. No. 104606, volume 7, Goddard Space Flight Center, Greenbelt, MD 20771.

Schubert, S. D., R. B. Rood, J. W. Pfaendtner, 1993: An assimilated data set for earth science applications, Bull. Amer. Meteor. Soc., 74, 2331-2342.

Schubert, S., C.-K, Park, C.-Y. Wu, W. Higgins, Y. Kondratyeva, A. Molod, L. Takacs, M. Seablom. R. Rood, 1995: A multiyear assimilation with the GEOS-1 system: overview and results, NASA Tech. Memo. No. 104606, volume 6, Goddard Space Flight Center, Greenbelt, MD 20771.

Schubert, S. D. and R. B. Rood, 1995: Proceedings of the Workshop on the GEOS-1 five-year assimilation, NASA Tech. Memo. No. 104606, volume 7, Goddard Space Flight Center, Greenbelt, MD 20771.

Schubert, S. D. and Y. Chang, 1996: An objective method for inferring sources of model error, Mon. Wea. Rev., 124, 325-340.

Schubert, S. D., S. C. Bloom, K. Ekers, 1996: Validation Plan for Version 2.0 of the Goddard Earth Observing System (GEOS) Data Assimilation System, Office Note xx-96 (to appear), Data Assimilation Office.

Sienkiewicz, M. E., and J. Pfaendtner, 1996: Assimilation Variability in the GEOS-1 DAS, to appear Mon. Wea. Rev.

da Silva, A., and G. White, 1995: A Comparison of Surface Marine Fluxes from GEOS-1/DAS and NMC Reanalyses. Proceedings of the Workshop on the GEOS-1 Five-Year Assimilation, NASA Tech. Memo. No. 104606, volume 7, Goddard Space Flight Center, Greenbelt, MD 20771.

da Silva, A., K. Ekers, and A. Conaty, 1996: Requirements for DAO's On-Line Monitoring System (DOLMS) Version 1.00, DAO Office Note 96-13. Data Assimilation Office, Goddard Space Flight Center, Greenbelt, MD 20771.

Starr, D., B. Diehl, A. Lare and B. Soden, 1995: Upper Tropospheric Humidity in the 5- Year GEOS Assimilation, proceedings of the Workshop on the GEOS-1 Five-Year Assimilation, NASA Tech. Memo. No. 104606, volume 7, Goddard Space Flight Center, Greenbelt, MD 20771.

Straus, D. M. and D. Paolino, 1995: Diabatic Heating in the NASA DAO Re-analyses: Interactions with dynamics, proceedings of the Workshop on the GEOS-1 Five-Year Assimilation, NASA Tech. Memo. No. 104606, volume 7, Goddard Space Flight Center, Greenbelt, MD 20771.

Straus, D. M. and D. Paolino, 1996: Diagnosis of the mid-latitude baroclinic regime in the NASA DAO reanalyses and ECMWF operational analyses, Center for Ocean-Land-Atmosphere Studies, Report No. 25, March 1996.

Takacs, L. L., and, M. J. Suarez, 1996: Evaluation of the climate of the GEOS-1 GCM: Dynamical processes, NASA Tech. Memo. No. 104606, volume 10, Goddard Space Flight Center, Greenbelt, MD 20771.

Trenberth, K. E., and J. G. Olson, 1988: ECMWF global analyses 1979-1986: Circulation statistics and data evaluation, NCAR Technical Note, NCAR/TN-300+STR, Boulder, CO.

Wood, E. F., T. Stevens, and R. Koster, 1995: Analysis of GEOS-1 Rainfall Data for Hydrological Modeling, proceedings of the Workshop on the GEOS-1 Five-Year Assimilation, NASA Tech. Memo. No. 104606, volume 7, Goddard Space Flight Center, Greenbelt, MD 20771.

Wu, M.-L. C., K. M. Lau, P. Beaudoin and W. Smith, 1995: Studies of the radiation budget at the top of the atmosphere and surface energy budget from the 5-Year Assimilation with the Goddard Earth Observation System, proceedings of the Workshop on the GEOS-1 Five-Year Assimilation, NASA Tech. Memo. No. 104606, volume 7, Goddard Space Flight Center, Greenbelt, MD 20771.

Yang, R. and S. Schubert, 1996: Variability of tropical precipitation as inferred from a nine-year GEOS-1 Assimilation, J. Climate, to be submitted.

8.7 Acronyms

8.7.1 General acronyms

DAO	Data Assimilation Office
GEOS	Goddard Earth Observing System (The name of the DAO data assimilation system)
GCM	General Circulation Model
DAS	Data Assimilation System
QC	Quality Control
NWP	Numerical Weather Prediction
CARD	Consistent Assimilation of Retrieved Data
PSAS	Physical-space Statistical Analysis System
NASA	National Aeronautics and Space Administration
GSFC	Goddard Space Flight Center
MTPE	Mission to Planet Earth
EOS	Earth Observing System
EOSDIS	Earth Observing System Data and Information System
NOAA	National Oceanic and Atmospheric Administration
NCEP	National Centers for Environmental Prediction (formerly, NMC)
NMC	National Meteorological Center
NESDIS	National Environmental Satellite Data and Information Service
ECMWF	European Center for Medium-range Weather Forecasts
UKMO	United Kingdom Meteorological Office

8.7.2 Instruments

ADEOS	Advanced Earth Observting Satellite (Mid-late 1996)
AIRS	Atmospheric Infrared Sounder (EOS PM)
AMSU A-B	Advanced Microwave Sounding Unit (POES, EOS PM)
AVHRR	Advanced Very High-Resolution Radiometer
ASTER	Advanced Spaceborne Thermal Emission and Reflection Radiometer (EOS AM)
ATOVS	Advanced TOVS; HIRS3/AMSU (POES)
CERES	Clouds and Earth's Radiation Energy System (TRMM, EOS AM)
CLAES	Cryogenic Limb Array Etalon Spectrometer (UARS)
DMSP	Defense Meteorological Satellite Program (currently operational)
EOS AM1	Earth Observting Satellite AM (June 98 launch)
EPS	EUMETSAT (European Meteorology Satellite) Polar System
ERBE	Earth Radiation Budget Experiment (ERBS)
ERBS	Earth Radiation Budget Satellite
ERS-1,2	European Remote Sensing Satellite (Scatterometer, 6 channel, IR-Visible radiometer)

GOES	Geostationary Observational Environmental Satellite (Imager and 18 channel visible and infrared sounder, currently operational)
GOME	Global Ozone Monitoring Experiment (ERS-2)
GPS	Global Positioning System
HALOE	Halogen Occultation Experiment (UARS)
HIRS2/3	High-Resolution InfraRed Sounder (POES)
HRDI	High Resolution Doppler Imager
IASI	Infrared Atmospheric Sounding Interferometer (EPS)
ILAS	Improved Limb Atmospheric Spectrometer (ADEOS)
IMG	Interferometric Monitor for Greenhouse Gases (ADEOS)
ISCCP	International Satellite Cloud Climatology Project (several IR and visible instruments aboard different satellite)
LIMS	Limb Infrared Monitor of the Stratosphere (Nimbus 7)
MAPS	Measurement of Atmospheric Pollution from Satellites
MHS	Microwave Humidity Sounder (EOS-PM)
MLS	Microwave Limb Sounder (UARS)
MODIS	Moderate-Resolution Imaging Spectrometer (EOS AM)
MSU	Microwave Sounding Unit
MOPITT	Measurement of Pollution in the Troposphere (EOS AM)
NSCAT	NASA Scatterometer (ADEOS)
POES	Polar Orbiting Environmental Satellite (Currently Operational)
PR	Precipitation Radar (TRMM)
SBUV	Satellite Backscatter Ultraviolet radiometer (Nimbus 7, POES)
SAGE	Stratospheric Aerosol and Gas Experiment (ERBS)
SMMR	Scanning Multispectral Microwave Radiometer (?)
SSM/I	Special Sensor Microwave/Imager (DMSP)
SSM/T	Special Sensor Microwave (Temperature sounder, DMSP)
SSM/T2	Special Sensor Microwave (Water vapor sounder) (DMSP)
SSU	Stratospheric Sounding Unit (POES)
TMI	TRMM Microwave Imager (TRMM)
TOMS	Total Ozone Mapping Spectrometer (ADEOS, Meteor, Earth Probe, Nimbus 7)
TOVS	TIROS Operational Vertical Sounder; HIRS2/MSU/SSU (POES)
TRMM	Tropical Rainfall Measuring Mission (summer '97 launch)
UARS	Upper Atmospheric Research Satellite (some instruments in operation)
WINDII	Wind Imaging Interferometer (UARS)

Chapter 9

Evolution from GEOS-2 DAS to GEOS-3 DAS

Contents

9.1 The Path from 1996 to 1998/GEOS-2 to GEOS-3

The core of the GEOS DAS algorithm is described in Chapters 5 through 7. This will be the core of GEOS-3, which will be the operational algorithm to support MTPE science at the launch of AM-1 in Summer 1998. Both the analysis and model development presented in Chapter 5 included the building of a scientific infrastruture to allow the GEOS DAS to expand to meet its broader mission in the future. Much of the GEOS-2 development was aimed at the ability to accommodate new data types. In the progression to GEOS-3 there are two major forces that must be reconciled.

1. The changing computing environment (See Chapter 2) requires that the GEOS-3 software scale to a relatively large number of processors (64-256) in order to meet production requirements. Since high performance tools for large scientific applications will not be easily available in 1998, much of the software development falls on the DAO staff. In order to mitigate the risk of the volatility of the computer industry, code that meets the standards of the message passing interface will be required. This is a major task. It is a task that requires much higher adherence to software engineering standards than is common for scientific code. Much of the effort between GEOS-2 and GEOS-3 will be developing a controlled software environment to support the message passing conversion. At the same time the code will be designed to better support collaborations with scientists both inside and outside of the DAO and NASA.

2. Continued scientific development of the GEOS-2 code is required. GEOS-2 provides the infrastructure. In order to take advantage of the infrastructure scientific development of applications algorithms is required. This includes

   - improvement of statistical models to represent observational and model errors to take advantage of the capabilities of PSAS
   - improvement of the physics parameterizations of the GEOS-2 GCM, especially with regard to hydrological and surface processes
   - actual incorporation of new data types or improved treatment of historical data sets

Because of the overhead involved in the software effort, the scientific and software development are often in direct conflict. With the drive to achieve scientific milestones, extreme diligence is required to maintain attention on the software problem. Success in the software engineering is essential for the long-term viability of the GEOS software.

This Chapter first lists the requirements for the GEOS-3 system. These have been derived from the process described in Chapter 2. Then, in parallel with earlier chapters, development plans for the analysis, the model, quality control, and new data types are outlined. No specific plans beyond Chapter 8 are given for validation. We are relying on the experience from the process outlined in Chapter 8 to lead to improved validation procedures. Finally, some of the research in the DAO which might contribute to advanced features in the 1998 time frame are described.

9.2 Primary System Requirements for GEOS-3

This section summarizes the primary system requirements for the *Goddard EOS Data Assimilation System, Version 3* (GEOS-3). GEOS-3 will be the operational data assimilation system at the time of the AM1 launch (June 1998). A priority customer for GEOS-3 will be the AM1 instrument teams, providing ancillary information for their retrieval algorithms. GEOS-3 will also be used for a wide variety of climate applications including multi-year reanalyses and assimilations using AM1 data.

The requirements listed in this document are only the highest system-level requirements. Lower level derived requirements are not described. Also, only a very brief description of each requirement is given along with its justification. A more complete requirements document, including original source documents, is maintained by the DAO. This document is available as an Office Note 96-96 (Stobie 1996) on

`http://dao.gsfc.nasa.gov/subpages/office-notes.html`.

The requirements listing represents substantial work to balance the expectations and customer desires listed in Chapter 2 with resources and computer technology. It contains information from feedback during workshops and through informal channels. The requirements reflect the results of validation exercises. As they are reviewed, the requirements are being refined and examined for completeness. Viewing the GEOS DAS as an MTPE resource, a more robust process needs to be put into place to assure that MTPE requirements are being met. This requires more active participation from the scientists in the MTPE Enterprise and this is an area that needs Project Attention.

9.2.1 Output Data

9.2.1.1 Fields

Description: Will output all fields listed in Requirements Office Note on

`http://dao.gsfc.nasa.gov/subpages/office-notes.html`.

This list is similar to that in Schubert et al. (1995) with addition of ozone, CO, and some other trace gas fields.

Comment: The prototype version of the GEOS DAS, GEOS-1 output these same variables, all of which have proved valuable for climate studies. Additionally, new variables have been introduced to meet specific request from the scientific community.

9.2.1.2 Resolution (space)

Description: $2^\circ \times 2.5^\circ$ latitude$\times$longitude horizontal, 70 sigma and 36 pressure vertical levels.

Comment: While there is a demand for $1^\circ \times 1^\circ$ horizontal resolution, the GEOS DAS will not be scientifically ready for this at the time of the AM1 launch. Physical parameterizations will require work beyond this date to make this conversion. It is hoped that $1^\circ \times 1^\circ$ horizontal resolution can be achieved in 1999. In the mean

time, very high vertical resolution (70 sigma and 36 pressure levels) has already been achieved.

9.2.1.3 Resolution (time)

Description: As listed in Requirements Office Note on
`http://dao.gsfc.nasa.gov/subpages/office-notes.html`.
Nominally, surface fields are archived every 3 hours and upper air fields every 6 hours. There are also more frequent archives of some fields at the request of instrument teams.

Comment: Since the AM1 instrument teams are a priority customers for GEOS-3, the temporal resolutions have been tailored to their needs.

9.2.1.4 Format

Description: EOS-HDF Grid.

Comment: GEOS-3 produces standard products like the other AM1 instrument teams. It will therefore, use the standard EOS format for AM1 data. This will enable GEOS-3 data to be accessed and manipulated with all the HDF-EOS tools being developed by EOSDIS. EOSDIS would not provide full functionality for other formats.

9.2.1.5 Delivery Time

Description: First-look fields must be available from the DAAC within 24 hours of data time, except during field experiments when they must be available within 12 hours.

Comment: Based on communications with the EOS instrument teams, the earliest they require assimilation products is 24 hours after data time. However, GEOS-3 will also be used to support NASA field experiments which occasionally involve flight operations. In these cases, the assimilated products must be available within 12 hours of data time.

9.2.1.6 Delivery Rate

Description: GEOS-3 must be capable of assimilating approximately 30 days of historical data in one day when run in re-analysis configuration.

Comment: Allows timely production of multi-year data sets to support interannual variability research and validation and release schedule.

9.2.1.7 Scientific Quality

Description: Scientific quality must be better than GEOS-2 with respect to science metrics determined by the DAO Scientific Steering Board (SSB).

Comment: The GEOS DAS is an evolving system that must show continuous improvement. The DAO has established an SSB to determined to evaluate the scientific quality of GEOS-3.

9.2.2 Input Data

9.2.2.1 Assimilated Data

Description: GEOS-3 will assimilate all currently used data plus new data listed in Table 17 of DAO Office Note 96-13 (see also Chapter 7).

Comment: The incorporation of new data types into the GEOS DAS is one of the primary responsibilities of the DAO. The incorporation of new data types was discussed in Chapter 7. The selections were based on a cost-benefit analysis where the expected product improvement was weighed against the cost of developing an algorithm to include a given data type.

9.2.2.2 Boundary Conditions

Description: GEOS-3 will include more flexible algorithms for using various types of time varying boundary conditions. It must be able to (1) adjust to varying grid resolutions, (2) use other sources of data, and (3) use EOS instrument data

Comment: Current versions of the GEOS DAS use long-term averages for certain boundary conditions, like sea-surface temperature, when the system is run in near real-time. This doesn't allow for important inter-annual variability in these boundary conditions to inter into the assimilation. To bring these variations into the system, more flexible algorithms must be developed to take advantage of the very best boundary conditions available at run time.

9.2.3 Objective Analysis Attributes

9.2.3.1 Data Pre-processing QC Software

Description: Receive raw NCEP data before their QC and implement DAO version of NCEP QC. Plan is to bring NCEP pre-process software to the DAO and modify it.

Comment: Currently, data received by the DAO from NCEP have been pre-processed through their quality control algorithms. These algorithms are closely tied to their assimilation system. As their algorithms evolve there is a distinct possibility that incompatibilities could arise between the GEOS DAS and the QC'd NCEP data. Therefore, to ensure appropriate data continue to flow into GEOS-3, the DAO must port the current NCEP QC software to the GEOS DAS and modify it to meet their specific needs.

9.2.3.2 ADEOS, ERS-1, and DMSP Pre-processing

Description: Develop pre-processing systems to accept and QC ADEOS, ERS-1, and DMSP (SSM/I) data.

Comment: These new data types are part of the basic input requirements for GEOS-3 (para 2.1).

9.2.3.3 Assimilate Non-state Variables (Observation Operator)

Description: Make system capable of assimilating observables which are not state variables (e.g. radiances).

Comment: This algorithm will allow GEOS-3 to use new observation types that are not state variables.

9.2.3.4 Non-separable forecast error correlations

Description: Allow forecast error correlation length to depend on vertical level.

Comment: This capability has been installed in GEOS-2 and is currently being validated. Assuming successful validation, the requirement will be met with GEOS-2.

9.2.3.5 State Dependent Vertical Correlations

Description: Include correlations between surface error fields and upper air error fields that reflect stability of the PBL.

Comment: This is expected to improve the way data in and near the boundary layer are treated within the analysis. This will enable GEOS-3 to make better use of NSCAT data.

9.2.3.6 Anisotropic Horizontal Forecast Error Correlations

Description: Incorporate a univariate forecast error correlation model in which correlation between the error at two points does not depend solely on the distance between them (*i.e.*, depends on direction as well).

Comment: This is a step in relaxing the assumptions that have traditionally been used to describe error characteristics. The impact of these assumptions are more important in PSAS due to increased sensitivity to error statistics.

9.2.3.7 On-line Continuous Forecast Error Variance Estimation

Description: Update of forecast error variance based on recent observation minus forecast (O-F) statistics.

Comment: This capability has been installed in GEOS-2 and is currently being validated. Assuming successful validation, the requirement will be met with GEOS-2.

9.2.4 Model Attributes

9.2.4.1 Koster/Suarez Land Surface Parameterization

Description: GEOS-3 must include a plug-compatible version of the Koster/Suarez land-surface parameterization.

Comment: The Koster/Suarez land surface parameterization is expected to:

- Improve upward fluxes of solar and longwave radiation at the surface
- Improve turbulent heat and moisture fluxes
- Improve clouds and precipitation
- Provide a more accurate representation of the near- surface environment and ground hydrology
- Improve the ability to assimilate near-surface quantities (temperature and moisture)
- Provide for the potential for assimilating ground wetness paramenters
- Provide for the potential for assimilating snow parameters

9.2.4.2 Hybridized Koster/Suarez/Sellers Land Surface Parameterization

Description: Incorporate attributes from Sellers scheme with those of Koster/Suarez.

Comment: This will enable the land-surface parameterization to interface with satellite observations and enhance performance of the baseline scheme.

9.2.4.3 Lin–Rood Tracer Advection Scheme

Description: Include conservative monotonic tracer advection scheme developed by Lin and Rood for cloud liquid water and specific humidity.

Comment: This will allow for more accurate simulation of moisture and clouds and provides for implementation of a cloud liquid water scheme. This will also enhance the ability to assimilate water vapor, cloud water, and ozone.

9.2.4.4 Improved Gravity Wave Drag Parameterization

Description: Improve gravity wave drag parameterization for stratospheric circulation

Comment: This will strengthen the stratospheric residual circulation which is too weak in the current GEOS DAS.

9.2.4.5 RAS-2 Cloud Scheme With Downdrafts

Description: Incorporate RAS-2 scheme developed by Moorthi at NCEP which includes downdrafts.

Comment: This is expected to correct boundary layer and upper tropospheric moisture problems identified in the prototype GEOS DAS. It is also expected to enable the assimilation of TRMM data and SSM/I precipitation data. It may also improve CO specification and distribution of clouds.

9.2.4.6 Cloud Liquid Water

Description: Include cloud liquid water as a prognostic variable to improve cloud radiative forcing.

Comment: Cloud radiation processes are a known weakness of the current GEOS DAS. This is expected to improve them.

9.2.4.7 Moist Turbulence

Description: Include moist processes (latent heat) in boundary layer turbulence scheme.

Comment: Boundary layer clouds are not correctly specified in the current system. This is expected to help correct this problem.

9.2.4.8 Variable Cloud Base

Description: Allow convective cloud bases to vary.

Comment: The current system always puts convective cloud bases at 50 hPa above ground level. This needs to be corrected so convective cloud bases can vary as they do in nature.

9.2.4.9 On-line Tracer Advection of O3, N2O, and CO

Description: Allow for tracer advection of O_3, N_2O, and CO within the model.

Comment: Initial studies using earlier versions of the GEOS DAS for off-line tracer advection have been very promising. There is significant scientific demand for such a capability for O_3, N_2O, and CO. The products will be used for both diagnostic studies and as ancillary information for instrument teams.

9.2.5 Computing

9.2.5.1 Cost

Description: Costs for product generation system hardware cannot exceed $23,926K from FY95 to FY02.

Comment: This is the amount currently allotted by NASA for DAO computing during this period. This requires extremely aggressive use of commodity hardware to achieve supercomputing capabilities.

9.2.5.2 Hardware

Description: Hardware must be purchased and developed that is sufficient to meet the requirements described above.

Comment: The DAO must make the most economical hardware selections to meet the performance requirements in this document.

9.2.5.3 Software

Description: Software must be purchased and developed that is sufficient to meet the requirements described above.

Comment: The DAO must develop and/or purchase software to meet the other requirements in this document.

9.2.5.4 Network

Description: Must connect to EOS network as described in DAO/ESDISP Memo of Understanding (MOU), 21 Jun 96. Also must be able to to meet the requirements described above.

Comment: GEOS-3 must be able to obtain the input data in a timely manner and provide output data in a timely manner as well.

9.2.5.5 Performance

Description: The operational performance is a derived requirement. That is, performance must be sufficient to achieve hardware, software and network attributes described above. There is an additional high performance requirement that must be achieved by an optimized core data assimilation system.

Comment: The additional high performance requirement comes from NASA's High Performance Computing and Communications (HPCC) program.

9.2.6 Validation/Monitoring

9.2.6.1 Scientific Evaluation

Description: Must carry out scientific analyses of GEOS-3 with respect to hydrological cycle, climate variability, stratospheric meteorology and transport, regional climate and weather, and tropospheric chemistry to verify it is better, or at least no worse than the baseline system (GEOS-2.x).

9.2.6.2 Validation Testing

Description: Must use a set of objective measures to evaluate the modifications made between GEOS-3 and GEOS-2.x.

Comment: Objective measures must be established to determine scientific quality. Otherwise, quality cannot be determined.

9.2.6.3 Monitoring

Description: Must provide on-line monitoring capability to assess product quality as validation experiments progress.

Comment: This is needed to make sure resources are not wasted during testing and operations. An effective monitoring system is needed to identify problems early so they can be corrected as soon as possible.

9.2.7 Interfaces

9.2.7.1 With EOSDIS

Description: DAO must provide interface with EOSDIS in accordance with DAO/ESDISP MOU, 21 June 96.

Comment: This is an EOSDISP requirement.

9.2.8 Documentation

9.2.8.1 Algorithm Theoretical Basis Document (ATBD)

Description: Must provide ATBD to EOS Project Office by 15 November 96.

Comment: This is an EOS requirement.

9.2.8.2 Interface Control Document

Description: Must provide an interface control document in accordance with DAO/ESDISP MOU, 21 June 96.

Comment: This is an EOSDISP requirement.

9.2.8.3 Normal Life-cycle Documents

Description: Must provide normal life cycle documents associated with an evolutionary software development lifecycle

Comment: This will keep the project on track and allow for efficient evolution of future versions of the GEOS DAS.

9.2.9 Schedule

9.2.9.1 Operational

Description: GEOS-3 must be operational at time of AM1 launch (June 98)

Comment: AM1 instrument teams will require DAO products at launch.

9.2.9.2 Frozen

Description: GEOS-3 must be frozen 4 months after launch of AM1.

Comment: MISR has requested this date.

9.3 Development of Objective Analysis (PSAS)

The development and validation of the Physical-space Statistical Analysis System (PSAS) was a major development in GEOS-2. When compared with GEOS-1, PSAS is a completely new analysis system. PSAS is designed to be sensitive to error statistics and to flexibly ingest new data types. The primary developments of the analysis system include improvement of statistical representation of errors and expansion of capabilities to utilize non-conventional data. Confronting another assumption that lies at the basis of most historical data assimilation efforts, significant effort will be directed towards reducing the impact of biases between different data types and the assimilating model. These major efforts are described here. Other developments of the analysis system are implied by the requirements listed above (subsection 9.2.3).

9.3.1 Assimilation of observables which are not state variables

Although not required by the statistical analysis formalism of Chapter 5, an implicit assumption in the GEOS-1 and GEOS-2 assimilation systems described earlier is that there is a one-to-one correspondence between observables and state variables. These systems can only handle observations of geopotential heights, winds, sea level pressure and specific humidity. For example, in the case of satellite retrieved layer mean virtual temperatures, a pre-processing step is necessary to translate these observations into geopotential height by means of the hydrostatic assumption and sea level pressure/forecast information at the lowest level. By contaminating the observations with forecast information this procedure violates an assumption built into the system, which says that observations and first guess errors are uncorrerlated.

The power of modern data asimilation systems stems from their ability to assimilate observables which are related but not identical to state variables. A typical example is satellite measured radiances which are related to moisture and temperature profiles through a non-linear radiative transfer model. These systems also provide a simpler framework to assimilate observables linearly related to state variables such as layer mean virtual temperature and total precipitable water. In order to fulfill the data assimilation requirements imposed by EOS instruments, GEOS-3 DAS must be capable of assimilating a broad range observables which are not necessarily state variables. To achieve this goal, a straightforward generalization of the PSAS algorithm described in section 5.2.2 is necessary.

Non-linear PSAS

When observables are non-linearly related to state variables (*e.g.* radiances), the analysis equations (5.7)—(5.8) need to be generalized. In this case, the analysis state w^a can be found by minimizing the maximum likelihood functional:

$$J(w) = \left(w - w^f\right)^T (P^f)^{-1} \left(w - w^f\right) + (h(w) - w^o)^T R^{-1} (h(w) - w^o) \tag{9.1}$$

where $h : I\!R^n \rightarrow I\!R^p$ is a non-linear observation operator which maps the gridded state variables w into observables w^o. Provided the error covariances P^f and R are specified

correctly, the analysis state obtained by minimizing $J(w)$ is the mode of the conditional probability density function $p(w|w^f \bigcup w^o)$ (Jazwinski 1970) and is derived from a maximum-likelihood principle assuming that forecast and observation errors are unbiased, normally distributed, and uncorrelated with each other.

Algorithms for the minimization of (9.1) have been described in Courtier *et al.* (1993) and Parrish and Derber (1992). One minimization strategy is by means of the quasi-Newton iteration:

$$w_{i+1} = w^f + \underbrace{P^f H_i^T \left[H_i P^f H_i^T + R \right]^{-1} \left[w^o - h(w_i) + H_i(w_i - w^f) \right]}_{\text{Linear PSAS}}, \tag{9.2}$$

where w_i is an approximation for the analysis state at the i^{th} iteration, and H_i is the linearized observation operator given by

$$H_i = \left. \frac{\partial h(w)}{\partial w} \right|_{w=w_i} . \tag{9.3}$$

The analysis state is defined as the limit of this iteration,

$$w_a = \lim_{i \to \infty} w_i$$

Notice that each iteration relies on a *linear PSAS* solve involving the linearized observation operator H_i. The core of the software development effort is to extend the current PSAS implementation to handle general linearized observation operators.

9.3.2 Account of forecast error bias in the statistical analysis equation

A large portion of the research pertaining to the specification of error statistics in data assimilation systems has been concerned with *covariance modeling*, that is, methods for representing and estimating forecast and observation error covariances. Error statistics required for statistical interpolation are usually estimated from time series of *observed-minus-forecast residuals* (section 5.2.7.1). Advanced statistical data assimilation techniques aim to improve the accuracy of forecast error statistics by taking into account the effect of model dynamics on the evolution of forecast errors (Ghil et al. 1981; Cohn 1996; Cohn and Todling 1996).

The point of departure in covariance modeling is complete knowledge of the means. Most often it is simply assumed that the forecast model as well as the observing instruments are unbiased; that is, the mean errors are zero or have been removed. Identification and correction of observational bias is an important component of operational data assimilation systems. Examples include radiation correction procedures for radiosonde observations (Julian 1991), and bias removal schemes for cloud-cleared radiances (Eyre 1992). Some centers use 6-hour model forecasts to provide a reference for removing bias from the observations (Baker 1991), at the risk of perpetuating any existing biases in the forecast itself.

The term *forecast bias* is synonymous with *non-zero mean forecast error;* if present, the forecast model is a biased estimator of the actual atmosphere. Forecast bias is associated

with the presence of systematic errors in the forecast model, such as caused by incorrect physical parameterizations, numerical dispersion, or faulty boundary conditions. Although it is well known that systematic errors contribute significantly to forecast errors (see, for example, Reynolds et al. 1996), the problem of estimating and correcting forecast bias has received little attention so far.

A practical algorithm for estimation of forecast error bias is described in Dee and da Silva (1996); a summary of the main results of this paper is presented next.

9.3.2.1 A framework for forecast bias estimation.

The only way to estimate forecast bias from data is by comparing forecasts with observations, i.e. from the observed-minus-forecast residuals

$$v_k = w_k^o - H_k w_k^f. \tag{9.4}$$

It is generally not possible to separate forecast bias from observation bias unless additional information is available. There are two ways in which to incorporate such information. The first has to do with the nature of the observations, while the second is closely related to the notion of forecast bias one chooses to adopt in practice.

Starting with the observations, we introduce as a basic assumption that there exists a set of observations which are unbiased, or, rather, for which

$$|b_k^o| \ll |H_k b_k^f| \tag{9.5}$$

in some meaningful sense. This amounts to the requirement that systematic errors, if any, have been effectively removed from these observations. In that case, it can be shown that

$$v_k = -H_k b_k^f + \widetilde{\eta}_k, \tag{9.6}$$

where $\widetilde{\eta}_k$ is a zero-mean noise term.

Equation (9.6) can be regarded as a *measurement model* for the forecast bias b_k^f. It expresses the relationship between the observations, the forecast, and the actual forecast bias under the assumption (9.5). If observations alone are insufficient to completely determine forecast bias, they must be supplemented with additional information. We therefore introduce a *state model* for b_k^f which describes its evolution in time. Formulation of the state model in fact amounts to an explicit definition of the quantity we wish to estimate, i.e., of what we actually mean by forecast bias.

Our practical goal is to estimate the time-mean forecast error, averaged over a time period which exceeds synoptic time scales. By definition, this quantity is approximately constant in time, so that a reasonable state model for b_k^f is *the persistence model*

$$b_k^f = b_{k-1}^f. \tag{9.7}$$

This model will serve to predict forecast bias at time t_k based on an estimate at time t_{k-1}.

Forecast bias is likely to be state-dependent, and its evolution in time is almost certainly more complex than the persistence model (9.7) suggests. For example, the presence of a systematic error in the convective parameterization of a forecast model will result in short-term forecast bias in convectively active regions only. Tibaldi and Molteni (1990) and Miyakoda and Sirutis (1990) discuss the relatively low forecast skills during the onset of blocking and the impact on systematic forecast errors. It will be a challenge to express this type of information explicitly in terms of a bias evolution model of a more general form, say,

$$b_k^f = b_{k-1}^f + g(w_{k-1}^t), \tag{9.8}$$

where g is a nonlinear operator which possibly includes stochastic components and other parameters.

9.3.2.2 Sequential bias estimation.

Equations (9.6,9.7) or (9.6,9.8) together constitute a *state-space description* (Anderson & Moore 1979) of the forecast bias b_k^f. Based on such a description, forecast bias estimation can be phrased as a standard problem in estimation theory. Specifically, one would like to obtain the optimal bias estimate given all unbiased observations available at a given time, and update this estimate whenever new observations become available. Therefore it is natural to view bias estimation as a *filtering problem*. The optimal solution of this problem, in case of a linear stochastic-dynamic bias model (9.8), is given by the Kalman filter. For a deterministic bias model such as (9.7), the Kalman filter simply reduces to a recursive weighted least-squares algorithm (Jazwinski 1970).

These ideas have been used in Dee and da Silva (1996) to derive a sequential bias estimation algorithm consisting of the following components:

1. A prediction step based on the bias evolution model (analogous to the forecast step in the analysis cycle).
2. Solution of a global linear system of equations at observation locations (analogous to the PSAS equation (5.7).
3. An update equation for the bias estimate (analogous to the PSAS equation (5.8)).

Due to this analogy with the analysis cycle, sequential bias estimation algorithms can be designed to utilize existing components of an operational statistical data assimilation system. Further details are given in Dee and da Silva (1996).

9.3.3 Improvement of error correlation models

A fundamental design objective for PSAS has been that it should not impose artificial constraints on the types of covariance models that it can handle. The underlying idea is

that there is a great potential gain in analysis accuracy to be obtained by improving the specification of forecast and observation error covariances. All currently operational global atmospheric data assimilation systems are inherently limited in this respect; these systems contain implementation constraints on covariance models which are unrealistic in view of what is actually known from observational data.

In the next decade an increasing volume of high-quality data will become available that should enable us to study in greater detail the statistical properties of forecast and observation error characteristics. In order to be able to benefit from any substantial new knowledge of these properties, we need to develop a class of theoretically sound (i.e., positive definite on the global domain) covariance models involving an appropriate degree of generality. That is, the models should be sufficiently general to allow an adequate expression of that which is actually known about error characteristics. At the same time, implementation of these models in a data assimilation system should not require the specification of parameters that are not in fact identifiable from the data.

9.3.3.1 Anisotropic correlation models

One of the most obvious and generally acknowledged shortcomings of current forecast error covariance models is that they are based on the assumption that height error correlations are isotropic at fixed pressure levels. This means that the correlation between errors in (fixed-level) height forecasts at two locations is assumed to be a function only of the distance between the two locations. Clearly this is an oversimplification; we know that actual forecast errors are state-dependent and their correlations can therefore not be a function of distance alone. Currently available observational data do not contain sufficient information to quantify the true anisotropic forecast error correlations in much detail, yet they do indicate that correlations tend to decrease more slowly with distance in the tropics than in the extratropics. In fact it is possible to obtain rough estimates of the (time-averaged) decorrelation length scales associated with height forecast errors at various latitudes.

Anisotropic correlation models can be obtained by applying a coordinate transformation to each of the arguments of an isotropic correlation model. If $\mathbf{x}, \mathbf{y}$ are any two points in R^3, $c_0(\mathbf{x}, \mathbf{y})$ is a correlation model, and $g : R^3 \rightarrow R^3$, then

$$c(\mathbf{x}, \mathbf{y}) = \mathbf{c_0}(\mathbf{g}(\mathbf{x}), \mathbf{g}(\mathbf{y})) \tag{9.9}$$

is a correlation model as well. That is, $c(\mathbf{x}, \mathbf{y})$ is positive semidefinite if $c_0(\mathbf{x}, \mathbf{y})$ is positive semidefinite. In particular, if $c_0(\mathbf{x}, \mathbf{y})$ is isotropic:

$$c_0(\mathbf{x}, \mathbf{y}) = \rho(||\mathbf{x} - \mathbf{y})||) \tag{9.10}$$

then

$$c(\mathbf{x}, \mathbf{y}) = \rho(||\mathbf{g}(\mathbf{x}) - \mathbf{g}(\mathbf{y}))||) \tag{9.11}$$

is generally anisotropic. The transformation g can be constructed in such a way that the local length scales associated with $c(\mathbf{x}, \mathbf{y})$ vary as a function of space in a prescribed manner.

An example of an anisotropic correlation model with a prescribed latitude-dependent length scale (Dee and Gaspari 1996) is shown in figure 9.1. The left panel shows the length-scale as a function of latitude; in this example the function was parameterized in terms of Legendre polynomials, and the (five) parameters were estimated from a global time series of 48h-24h forecast residuals (the so-called *NMC method*). The contour plots show the one-point correlation maps at various latitudes which are obtained by evaluating the resulting global anisotropic model.

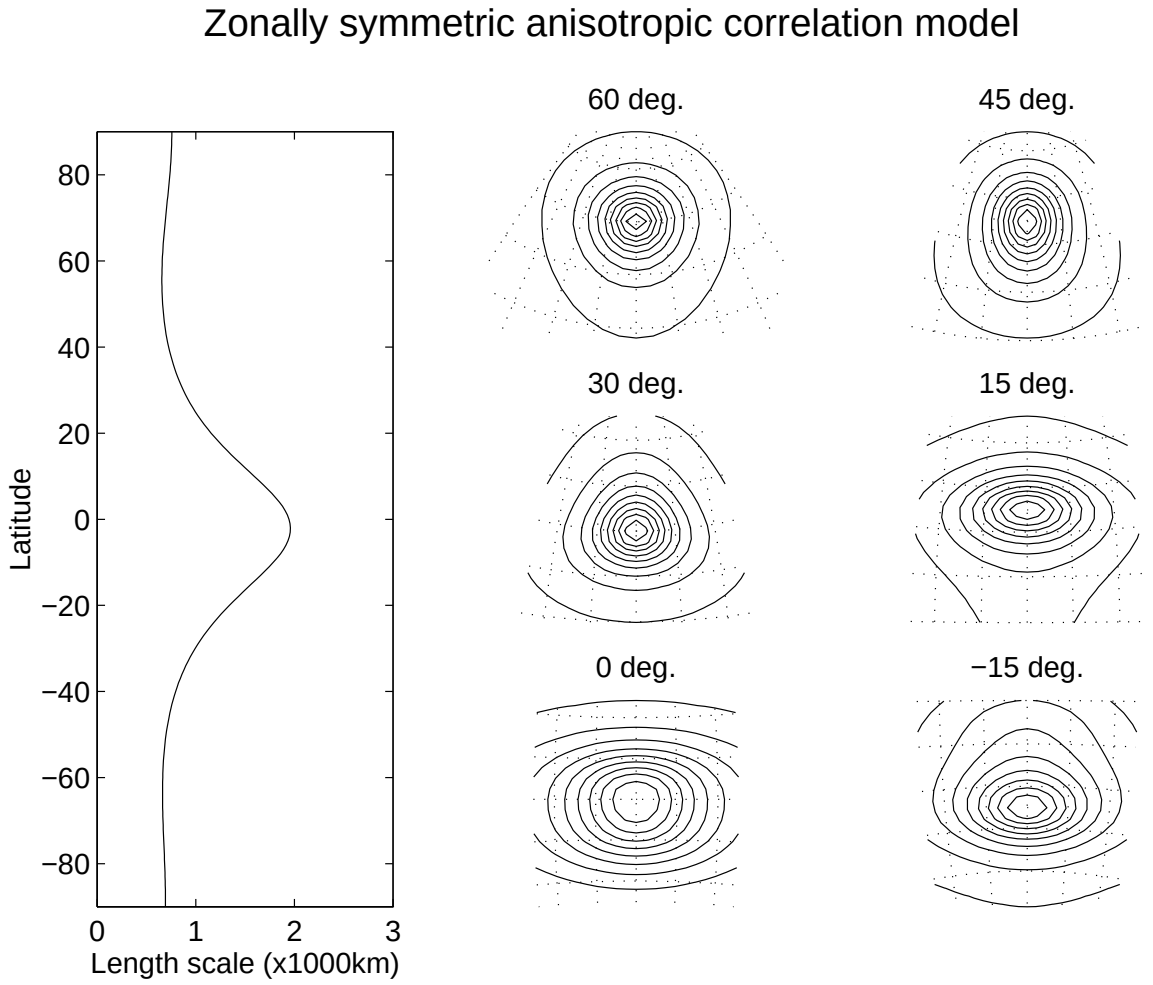

Figure 9.1: Example of an anisotropic univariate correlation model with a spatially varying length scale. The left panel shows the prescribed length-scale as a function of latitude. The shaded contour plots are one-point correlation maps at various latitudes. The contour interval is 0.1.

9.4 Development of GEOS GCM

The progression of the GEOS general circulation model (GCM) from GEOS-2 to GEOS-3 will involve implementation of several new algorithms to improve the representation of physical processes in the model. Most of these improvements focus on the representation of atmospheric water and near-surface processes. To address these hydrological processes requires several parallel efforts. The inclusion of the cloud water scheme demands that tracer advection capabilities be more physical and that the radiation scheme has suitable characteristics for cloud radiative interactions. Similarly, the land-surface model requires the capability to calculate photosynthetically active radiation. The land-surface model is aimed at providing a soil moisture storage mechanism and possibly a data-constrained soil moisture product. At the very least, the interactive land surface is expected to improved some of the shortcomings of the current precipitation products.

GEOS products of unobserved parameters come directly from the model. As discussed in Chapter 4, there are instances when the data insertion process degrades the model simulation. Because of the existence of these destructive interactions, in the GEOS-2 and GEOS-3 development there has been less tuning of the model in simulation studies and closer links between the assimilation process and model definition. The GEOS-2 GCM has already achieved some significant improvements. Figure 9.2 shows some climate parameters from a seasonal integration of GEOS-2. The bottom left panel of the figure is directly compared with the bottom panel of Figure 4.3. Compared with the GEOS-1 simulation, GEOS-2 compares much better with the ERBE observations. This is especially true in middle latitudes where GEOS-1 simulations were deficient in middle latitude clouds. Since middle latitude clouds were not very sensitive to the data insertion, we anticipate that the GEOS-2 model will provide substantial improvement in some climate parameters. GEOS-3 should provide more robust physical consistency, which should yield even more improvements.

Perhaps the most controversial decision about the GEOS-3 GCM is the decision to have the first delivery at $2^\circ \times 2.5^\circ$ latitude$\times$longitude horizontal resolution. The DAO had planned to deliver the first system at $1^\circ \times 1^\circ$ latitude$\times$longitude horizontal resolution. However, this is not possible without sacrificing many fundamental developments, which we feel is short-sighted. After consultation with the original customers who had given the one degree requirement, it was decided that an improved product at lower resolution was better than a tuned production simply for the sake of resolution. There are numerous scientific sacrifices in this decision, especially associated with near-surface processes and possible regional applications. As soon as possible GEOS-3 will be extended to the one degree resolution.

The inability to go to one degree resolution at launch is mostly resource related. There are significant personnel resources needed to adapt the parameterizations to a new resolution. Given the development of new physical paramaterizations, to start a one degree conversion prior to the validation of the parameterizations is not judicious. Computer resources are also not available. To acquire enough computer resources to develop and validate a one degree model in 1996 would consume the bulk of the computer budget through the year 2000. In 1998 such an expenditure up-front on, then obsolete, computing would look foolish and compromise the ability to support MTPE science. The move to one degree is dependent on the message passing conversion (see Chapter 2) in order to allow commodity-based computer systems.

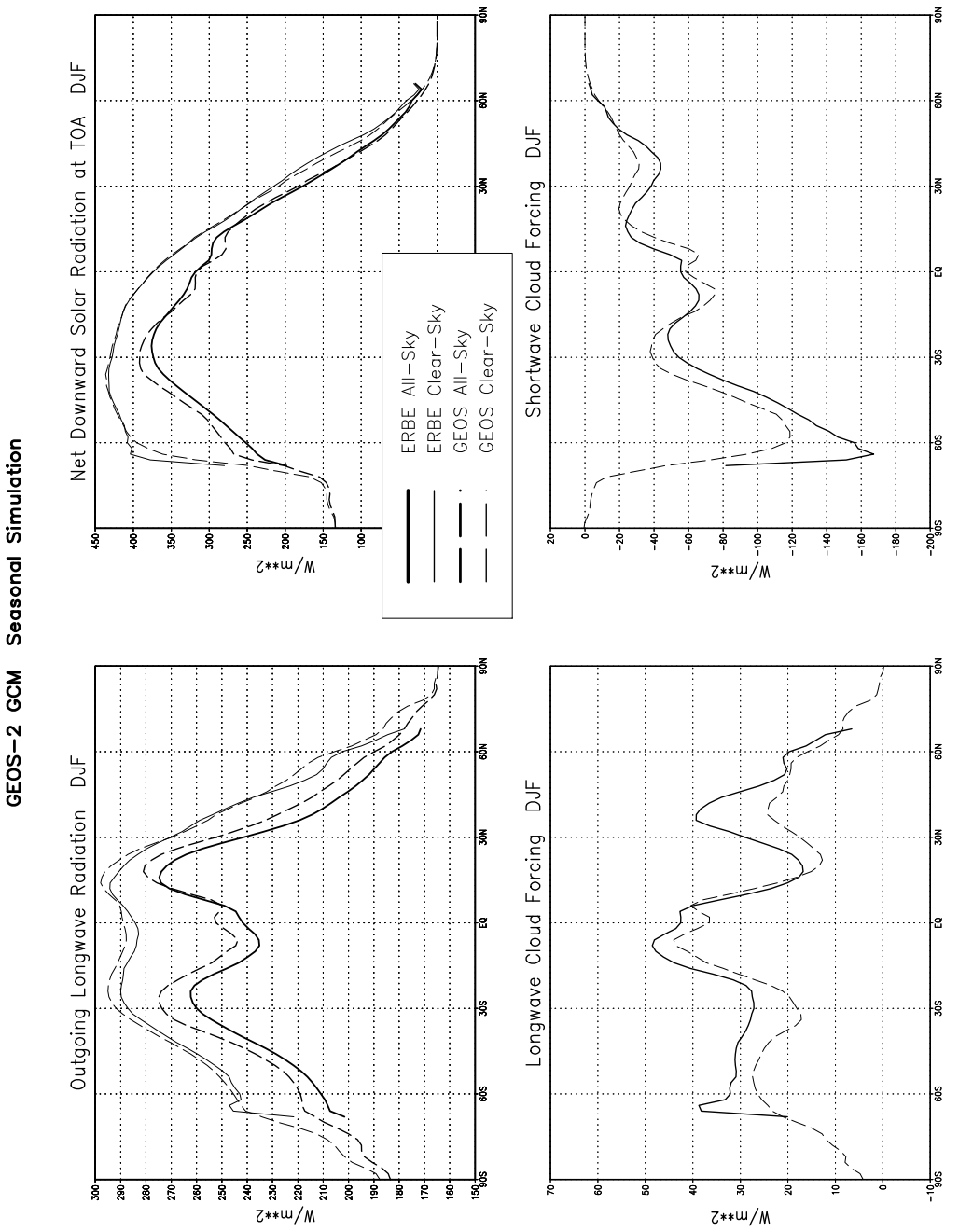

Figure 9.2: Zonal mean climate radiative diagnostics from GEOS-2 model simulation. Compared with the GEOS-2 results shown in Chapter 4 and in Molod et al. (1996) there are first order improvements in these quantities. Note in particular the longwave cloud forcing in middle latitudes which show a substantial increase compared with the earlier simulations.

The subsections below describe major model developments from GEOS-2 to GEOS-3. Numerous other activities are implied in the requirements list presented earlier in this chapter (section 9.2).

9.4.1 Monotonic, Uptream Tracer Advection

The advection algorithm developed at DAO and currently used in GSFC 2D and 3D chemistry transport modeling is the Flux- Form Semi-Lagrangian (FFSL) scheme of Lin and Rood (1996a). The FFSL algorithm is a mass-conserving, multi-dimensional, and semi- Lagrangian extension of 1D Eulerian finite-volume advection schemes. It contains physically-based monotonicity constraints that emulate the subgrid mixing processes occurring in the real atmosphere and eliminate the need for the commonly used numerical smoothing (e.g., the Shapiro filter) and filling techniques. The FFSL algorithm has been proven to be both accurate and computationally efficient.

Motivated initially by the need to better simulate the transport of chemistry species in the stratosphere (ozone in particular), the FFSL advection algorithm has recently been adopted in a wider range of applications. A transport module based on the FFSL algorithm for the transport of water vapor as well as cloud liquid water is in place for the GEOS-DAS. Within the context of climate simulations, Rasch and Williamson (1991) and Lin et al. (1994) have demonstrated the importance of a transport algorithm's ability to preserve positivity of the water vapor and to prevent the numerically generated large- scale super saturation. The water vapor mixing ratio profile in the troposhere is strongly correlated to the temperature profile. These two fields are physically constrained, at least in part, by the Clausius-Clapeyron equation and the threshold for the moist convective instability. The filling algorithm commonly used in GCMs to fix the negatives in the water vapor field not only disrupts the correlation but also interacts with physical parameterizations (cumulus parameterization in particular), which could then falsely induce heating as well as precipitation. The monotonicity- preserving characteristics of the FFSL advection algorithm would be even more important for the simulation and assimilation of the cloud liquid water within the GEOS-DAS. The original center differencing algorithm will be inadequate for the transport of scalars with large spatial gradients such as the cloud liquid water.

9.4.2 Prognostic Cloud Water

9.4.2.1 General description of Development

The Del Genio et al. (1996) prognostic cloud water scheme was chosen to take advantage of the expertise within the NASA program on parameterizing cloud water. The implementation of the Del Genio et al. (1996) cloud water scheme into the GEOS-3 GCM is based on two prognostic equations for the cloud water content (i.e., the mixing ratio of the mass of cloud water to that of air) and for the relative humidity of the grid box; a consideration of the most recent history of ice water in the layer; and a consideration of cloud-top-entrainment-instability (CTEI). Based on empirically determined parameters, the scheme diagnoses the effective cloud droplet radius, liquid water path, and fractional cloudiness as a function of the cloud water content associated with stratiform clouds.

9.4.2.2 Motivation for the development

General problem in modeling: Up until mid-1980s, the atmospheric global climate models (GCM) were based on prognostic equations for the horizontal components of the wind, the surface pressure, the temperature and the mass of water vapor. Given the available computing resources of the times, for low spatial resolution, the set of five prognostic variables seemed sufficient to study temporal variations in some climate related quantities. However, as our needs for a better and more comprehensive understanding of the climate system grew, and as the precision, resolution and coverage of available measured parameters improved, the opportunity for a more complete physical description of the atmosphere in AGCMs improved, as well.

The treatment of atmospheric water in terms of water vapor alone is incomplete. Water vapor is input to the atmosphere at the lower boundary, and then, is transported vertically (i.e., by means of convection, turbulent diffusion and vertical advection) and horizontally (mostly advection) by the motion of air masses, including those induced by latent heat exchanges in water phase transitions. As a result, in the real atmosphere several phases of water may coexist suspended in air. Although the suspended liquid and ice phases are a small portion of the total water substance in the column, an accurate knowledge of their mass distribution is important to ascertain the radiative balance of the atmosphere, since the albedo of the earth and the infrared absorption are greatly affected by clouds. Previous GCMs tried to compensate for this by diagnosing fractional cloudiness and optical thickness of clouds in terms of empirically derived functions of temperature, pressure and relative humidity. This approach cannot be used to build a cloud water mass history consistently representing growth and decay of clouds, and their life- time. Furthermore, even if the life time of cloud water were to be much smaller than that of vapor, the water in clouds can have a lasting effect over certain regions of the globe, particularly where its formation is strongly linked to the diurnal cycle, or even longer time scales phenomena. Lastly, an accurate representation of cloud water would help in the proper determination of buoyancy effects that are relevant to the shorter convective time scales in AGCMs.

GEOS problem: In the newer versions of GEOS an increase in the spatial resolution is accompanied by an increase in the time resolution, and by the explicit consideration of formerly parameterized phenomena. As an example, the improvement of the vertical resolution allows to resolve better the planetary boundary layer moisture and temperature gradients, and the top of the troposphere moisture concentrations. The first one may allow a better description of the formation of stratocumuli off the western mid-latitude continental boundaries, if the proper moist physics are included. The second one may help in physically based studies of the life span of thin cirrus clouds over tropical oceans. The consideration of temperature inversion layers and vertical gradients of the turbulent fluxes are important physics to the former, while cloud water and cloud ice evolution are to the second.

For all the reasons mentioned above, which certainly apply to GEOS-2, it is necessary to include better cloud physics in GEOS-3. A first step in that direction is to parameterize the life cycles of stratiform clouds.

9.4.2.3 Interface with new observational data types

The cloud water parameterization will allow the GEOS DAS to interface with some of the new data types discussed in Chapter 7. While there is the possibility of assimilating cloud liquid water and cloud ice in the future, we anticipate that much of the early work with new data types will be monitoring the quality of the ingested data and of the model parameterizations. At the present time there are some estimates of the asynoptic distribution of cloud water in rather thick layers (for example, see Weng and Grody 1994) which may be useful in devising test cases in cloud water assimilation. Therefore the availability of new data will advance the discovery stage of this still immature parameterization.

9.4.2.4 Description of the algorithm

As in Del Genio et al. (1996), the equation for the local tendency in cloud water content is given by,

$$\frac{\partial m}{\partial t} = \frac{Q + (1-b)E_r}{L} - P - S_e$$

where the condensation function, Q, in energy units is defined as,

$$Q = \frac{M - Lq_s \partial u/\partial t}{1 + u\epsilon L^2 q_s/(Rc_p T^2)}$$

the moisture convergence function is,

$$M = L\frac{\partial q}{\partial t} - uS_q c_p \frac{\partial T}{\partial t} + \frac{Lq}{p}\frac{\partial p}{\partial t}$$

and

$$S_q = \frac{\epsilon L^2 q_s}{Rc_p T^2}$$

Here, m, q, q_s, u, T, p refer to the cloud water mixing ratio, the specific and the saturation humidities, the relative humidity, the temperature and the pressure, respectively; and R, c_p, L are the gas constant, the specific heat constant, and the appropiate latent heat constant, respectively. E_r is the evaporation rate for raindrops falling off an anvil cloud into the clear sky environment beneath; P is the precipitation flux rate out of the layer; S_e is the sink of cloud water due to CTEI; b is the fractional cloudiness of the grid box. Similarly, the equation for the relative humidity tendency is,

$$\frac{\partial u}{\partial t} = \frac{2(1-b)^2(1-U_{00})(M + E_c + E_r)}{L(2q_s(1-b)(1-U_{00}) + m/b)}$$

where E_c refers to the evaporation rate of cloud droplets into the clear sky part of the grid box, and U_{00} is an adjustable threshold relative humidity for the clear sky portion of the layer.

The equations mentioned above are the essentials of the scheme, but the parameterization estimates some of the terms as follows. The convectively generated condensate updates the existing cloud water content, which, in conjunction with the knowledge about the phase of the cloud water in the previous time step, allows a determination of whether

Bergeron-Findeisen processes will take place in the layer. This glaciation process affects the precipitation efficiency (*i.e.*, the fraction of the suspended cloud water that precipitates out of the layer), in a larger or lesser manner, depending upon whether the precipitation will fall over land, over oceanic areas, or over land areas covered by ice. The precipitation efficiency depends also on temperature factors and on the vertical velocity of the air in which the droplets fall. The last one is an attempt to represent slower droplet growth by sedimentation in uprising convective plumes (Del Genio et al. 1996). Both condensate types, cloud water and rain droplets, can evaporate into the environment, in a process that degrades for a saturated environment.

The relative humidity of the layer can change due to advection of water vapor, or because of local pressure and temperature changes. The moisture convergence function is defined as in Sundqvist (1988), and the collective effect of evaporation, convergence and precipitation will determine the tendencies for the relative humidity and the cloud water content.

Supersaturation of a given layer is removed by increasing the condensate in an iterative procedure that looks for the balanced set of temperature and specific humidity at saturation.

For any cloud top layer that is unstable (*i.e.*, CTEI defined in the sense of Randall 1980 and of MacVean and Mason 1990) mixing of horizontal momentum, static energy, water vapor and cloud water will occur between contiguous layers until stability is achieved. This affects mostly the bottom of the cloud layer.

The fractional cloudiness is estimated as a function of the relative humidity of the environment and of the grid box, and the effective cloud droplet radius from the in-cloud water density, and a specification of a critical density that is a function of surface type.

The Del Genio et al. (1996) stratiform cloud water parameterization has been implemented on a early version of the GEOS-2 GCM having 46 levels in the vertical. Several short term runs (typically 65 days of Northern Winter simulations) produced reasonable prognostic and diagnostic fields. Currently, we are calibrating the parameterization by means of semi-prognostic tests with observational datasets, and with synthetic datasets from the Goddard Cumulus Ensemble Model. We are evaluating the schemes impact on the simulated cloud-radiation interactions by comparing with known satellite derived products.

9.4.2.5 Strengths and Weaknesses of Prognostic Cloud Water Algorithm

Strengths:

- Provides a history of cloud water in either of two phases: liquid or ice.
- Provides physical estimates of cloud-radiation interface parameters: fractional cloud cover and geometrical optical thickness.
- The dissipation of cloudiness (specially in the lower troposphere) for unstable environments is considered.
- The cloud water parameterization described above will also allow for the consideration of chemical tracer studies, particularly of those dependent on the water droplets for chemical deposition.

Weaknesses:

- May not be an adequate representation of low level or boundary layer clouds.
- The physics of cirrus clouds evolution is not well known (Starr and Wylie 1990), and the current efforts to represent them simply as clouds of frozen particles (anvils?) may not be adequate.
- The mixed phase cloud (i.e., cloud water and cloud ice in the same layer) is treated in terms of a statistical procedure and some empirically determined functions to solve in favor of only one of the phases. The effects of such treatment or its replacement in terms of more detailed cloud physics are not quite well known at this time.

9.4.3 Land-Surface Model

The GEOS-3 GCM will be coupled to the Koster-Suarez Land Surface Model (LSM), (Koster and Suarez 1992) referred to as 'Mosaic'. This decision was made in concert with several modeling groups at GSFC and the rationale is provided in the Model Requirements for Data Assimilation at Launch Report which can be seen on `http://dao.gsfc.nasa.gov/`.

Mosaic is a Soil-Vegetation- Atmosphere-Transfer model (SVAT) which was developed based on the Simple Biosphere (SiB) model of Sellers et al (1986). The predicted quantities are deep soil temperature and canopy temperature, three soil moisture layers, a canopy interception reservoir, a canopy air specific humidity, and a snow pack. Mosaic links the physical descriptions of canopy processes with detailed descriptions of soil moisture and temperature transfers, and solves moisture and energy balance equations at each level. The energy and water transfers are modeled using an electrical resistance network analog, where the resistance to the flow of heat or moisture in the ground or to and from the vegetation canopy are functions of specified soil and vegetation parameters. The vegetation canopy essentially determines the surface roughness, which impacts the intensity of turbulence in the canopy and surface layer, controls the surface reflectance through the leaf areal coverage and fraction of live vegetation, and dictates the effective canopy resistance to the flow of heat or moisture. The sub-grid scale variability of the surface is modeled by viewing each GCM grid cell as a Mosaic of independent vegetation stands, using linear aggregation/disaggregation formulae for links to the GCM grid. The vegetation stands, or 'tiles', interact only through the coupling to the GCM atmosphere. The coupling between the GCM and Mosaic involves issues of numerical stability and energy conservation. Fluxes of heat, moisture, and momentum at the land-surface interface calculated by the SVAT must be consistent with those calculated by the GCM surface layer scheme (Helfand and Schubert 1995).

The additional physical description of the climate system that is included in an SVAT has many advantages over the existing formulation. The GEOS-2 GCM uses a specified soil moisture, calculated monthly using observed ground temperature and precipitation from Schemm et al. (1992). The soil moisture is then used, along with a constant, specified ratio of evaporation to potential evapotranspiration, (beta-function) to calculate the latent heat flux. This, in turn, through the surface energy balance constraint, determines the energy available for sensible heat flux as well. Although such a technique acts to inhibit any model

drift in beta or in soil moisture, and has been used extensively in GCM's until recently, the smaller scale temporal variability cannot be captured, and much of the highly nonlinear feedback between the atmosphere and the land surface is inhibited. The soil surface, for example, cannot respond to an extreme precipitation event by absorbing water, thereby causing errors in the surface energy budget and resultant ground temperature. Even a simple so-called 'bucket' type of land surface model must specify the beta function (usually constant) and cannot properly capture the variety of influences that the atmosphere exerts over surface processes. The impact of the errors in temporal variability on the resultant climate simulation is shown clearly in Koster and Suarez (1994), and Betts et al. (1993) demonstrate the impact of an inaccurately simulated diurnal cycle on the climate bias. GEOS-1 and GEOS-2 GCM simulations, and GEOS-1 DAS, all show striking errors in the diurnal cycle of ground temperature as compared to station observations, the diurnal variability of precipitation over the United States in springtime (Min and Schubert 1996), and the diurnal cycle of the ratio of latent to sensible heat flux as compared to FIFE-1987 data.

These errors described above can be related to an inaccurate depiction of the physics at the land-surface interface, and the presence of these errors in the GEOS-1 DAS emphasizes the lack of near surface data during assimilation. The need to incorporate the new types of relevant surface or near-surface data that will be available in the EOS era into the assimilation system is essential to the accuracy of any climate assimilation, and the ability of the GCM to properly absorb and utilize the analysed ground temperature, for instance, depends on the physics included in the land surface model.

The Mosaic SVAT in particular offers some features which are particularly suited to the needs of a climate data assimilation system. The computational efficiency, due in part to some approximations and simplifications to the SiB algorithms, makes long assimilations viable. The method of handling sub-grid scale variability, that is, the 'tiles' philosophy, makes possible a reasonable comparison with, and eventual assimilation of, surface station observations of ground temperature. The ability of the GCM to associate the station observations with their particular surface type within a grid cell partly ameliorates the substantial problem of representativeness of highly localized measurements. In addition, the history of Mosaic as an element of the ARIES GCM (Suarez *et al.* 1996),which has many similarities with the GEOS GCM, eases many of the implementation and tuning issues during the process of incorporation into the GEOS-3 GCM, and makes possible the smooth transition to future versions of Mosaic.

9.5 Development of Quality Control of Input Data Sets

The algorithms and basic functionality of the GEOS-2 QC system has been described in Chapter 6. This section presents the strategy for developing and implementing quality control (QC) for GEOS-3 DAS. For additional details consult Dee and Trenholme (1996) and Trenholme (1996).

Much of the GEOS-3 capability is directed at the current operational data stream, with emphasis on rawinsonde observations and infrared sounder (TOVS). Beyond basic QC capabilities, the development of sophisticated QC for specific EOS instruments calls for in-depth knowledge of each data type, and undoubtly will require a close partnership with EOS instrument teams. The core of this new data type QC effort must take place after launch when the EOS data streams become available.

The GEOS-3 QC strategy is driven by the following two fundamental system requirements:

1. GEOS DAS QC must be state-of-the-art, both from a scientific and from a software-engineering point of view.
    - The GEOS analysis system is premised on the ability to characterize observation errors and to quantify them statistically, which obviously cannot be done well unless gross errors can be identified and effectively removed. The converse is true as well.
    - Operational experience confirms that QC has as much impact on analysis accuracy as any other major component of an assimilation system.
2. GEOS DAS QC must be self-contained and logistically independent of QC systems in place at other operational centers.
    - DAO cannot afford to be subject to operational decisions at other centers which are beyond our control.
    - DAO needs to have intellectual control over the QC system (both in terms of algorithm and software design and code) in order to be able to incorporate QC components for new data types.

The concepts and general approach described here are strongly influenced by the quality control system that has evolved at the National Centers for Environmental Prediction as documented in Ballish (1991), Collins (1991) Collins and Gandin (1990, 1992, 1995, 1996), Gandin (1991), Kalnay et al. (1996), Morone (1991), and Woolen (1991).

The GEOS-2 quality control procedure discussed in Chapter 6 is targeted at raw input data that the DAO acquired through an extensive data mining project. For the quasi-operational products currently produced by the DAO in support of the stratospheric chemistry missions (see section 2.6.3) there exists an implicit link to NCEP quality control. For this near-real time product the DAO acquires data through a direct data link to NCEP. This data has already been through the NCEP quality control, and the GEOS quality control uses the NCEP data flags. If any inconsistency exists between the QC requirements for NCEP and for the DAO, then the DAO is in no position to account for this inconsistency.

Furthermore, as the NCEP QC algorithm changes, the characteristics of the GEOS input data stream changes.

Simply counting on import of the quality control system from NCEP to the DAO does not solve all of the needs to upgrade the GEOS QC system. Aside from potentially diverging requirements for QC, the DAO must develop methods to use a wide variety of new data types. The strategy for moving from the current situation to the long-term objective starts with the following broad requirements for the GEOS QC system:

1. A self-contained QC system should be operational at DAO as soon as possible, because:
   - We will not be assured of system stability, since the QC system at NCEP is in a state of flux.
   - We need to get hands-on experience before we can actually begin to improve QC.
   - We need the ability for new data types to flow through the system as soon as possible. This includes data that is not being assimilated, which are defined as passive data types, in order to monitor and develop statistics for new data types.
2. The technology for the first operational GEOS QC system should be imported from NCEP.
   - NCEP QC contains the technology with which we are most familiar. The NCEP QC system is reasonably portable, and some of its components have been ported to different environments in the past.
   - DAO has a formal agreement with NCEP which should greatly facilitate this transfer of technology.
3. The GEOS QC system should roughly reproduce the NCEP QC marks and corrections.
   - This requirement allows us to introduce incremental changes with respect to the present system, and to investigate the effect of such changes.

Incremental implementation of the QC for versions of the GEOS-DAS that follow GEOS-2 requires significant re-engineering of existing GEOS algorithms and porting of a major portion of the NCEP system. The re-engineering of the GEOS algorithms is to accommodate both increased flexibility to address new data types as well as differing DAO products (see section 2.6.3) and a distributed software environment. The requirements for the first incremental development of GEOS QC include:

- conform to the requirements of the DAO Observation Data Stream (ODS) described in da Silva and Redder (1995)
- allow passive data types (un-assimilated) to pass through the system
- roughly reproduce the QC decisions of the previous version of the algorithm

A major motivation for using the NCEP QC is to take advantage of their Complex Quality Control (CQC) capabilities. The Complex Quality Control has the capability, amongst others, of fixing radiosonde data that has been erroneously entered in the global weather data stream. This is done by a sophisticated system of scientific and logistical checking. Figures 9.3–9.4. show a data flow diagram of the Quality Control aspects of the proposed NCEP Global Assimilation System[1]. The intent is to port all of the relevant algorithms up through the Complex Quality Control. The figure also reveals another problem the DAO must account for data formats. While EOS has its own standards of data format, the operational data stream has its own formats as well. Since the operational data is at the very core of a credible assimilation, the DAO must also develop algorithms to use the formats of the broad weather forecasting community.

A key component of the GEOS-3 QC system is the implementation of a radiosonde temperature correction. It has been well documented that solar radiation and infrared cooling effects can contaminate the temperature reported by radiosondes, causing large biases in the lower and upper stratosphere. The NCEP radiation correction system developed by Julian (1991) has been tested at DAO with mixed results. For some regions of the world (*e.g.*, North America), NCEP's radiation correction scheme is effective removing the temperature bias. However, for other regions (*e.g.*, Europe), appears to introduce a temperature bias to otherwise unbiased temperature reports. A sucessful radiation correction effort will require rather complete metadata information, such as intrument types and whether radiation correction has already bee applied by the data producer. In the past, NASA has made a significant investment in radiation correction algorithms (F. Schmidlin, *personal communication*), and DAO plans to develop a close collaboration with NASA and other external groups with expertise in this area.

The schematic for the first increment of the GEOS QC is given in Figure 9.5. Raw data ingested by the system will be synchronized and reformatted as necessary. Most data will be ingested in WMO BUFR format from NCEP and will proceed directly to preprocessing testing and correction algorithms (TCA) using the NCEP routine PREPDATA. Other data will be preprocessed using DAO routines. The pre-processed radiosonde and conventional aircraft data, still written in BUFR format, will be passed to the NCEP routines CQCHT or ACQC, where they will be checked against a background and written out to an ODS format; other data will be written directly to ODS format after preprocessing. All data will then undergo the GEOS/DAS Gross and Buddy Check procedures, where they are checked against a background and compared to their neighbors. A decision making algorithm (DMA) will make a final pass/fail decision for each datum based on the results of all tests it has

[1]In the diagram, all references to BUFR are to data files written in WMO BUFR format. Files marked BUFR 1 and BUFR 2 are files containing data which has not passed through any NCEP preprocessing. Files marked sequentially as PREPBUFR 1 through 6 are BUFR files of data which have passed through the various NCEP preprocessors. The DAO will import routines PREPDATA, PREVENTS, PREPACQC, and CQC from NCEP. Thus we anticipate receiving data at the stage of the BUFR 2 file in this diagram. It will then be passed through PREPDATA, which performs basic *sanity checks*, and funneled to PREVENTS, which interpolates a gridded background to observation locations. (PREVENTS must be re-engineered to utilize a background in the DAO format and so cannot be entirely "blackboxed" from NCEP.) Radiosonde data will then be passed to NCEP's Complex Quality Control Routine CQC (actually CQCHT in its latest naming), where it is subjected to a variety of checks, some using background, before a final decision is made whether to accept the data, change it, or reject it. Conventional aircraft data is passed to the NCEP routine PREPACQC, which performs specialized checks such as track checking. At the end of the DAO's utilization of NCEP routines, data will be output approximately at the stage indicated as PREPBUFR (4) on the diagram.

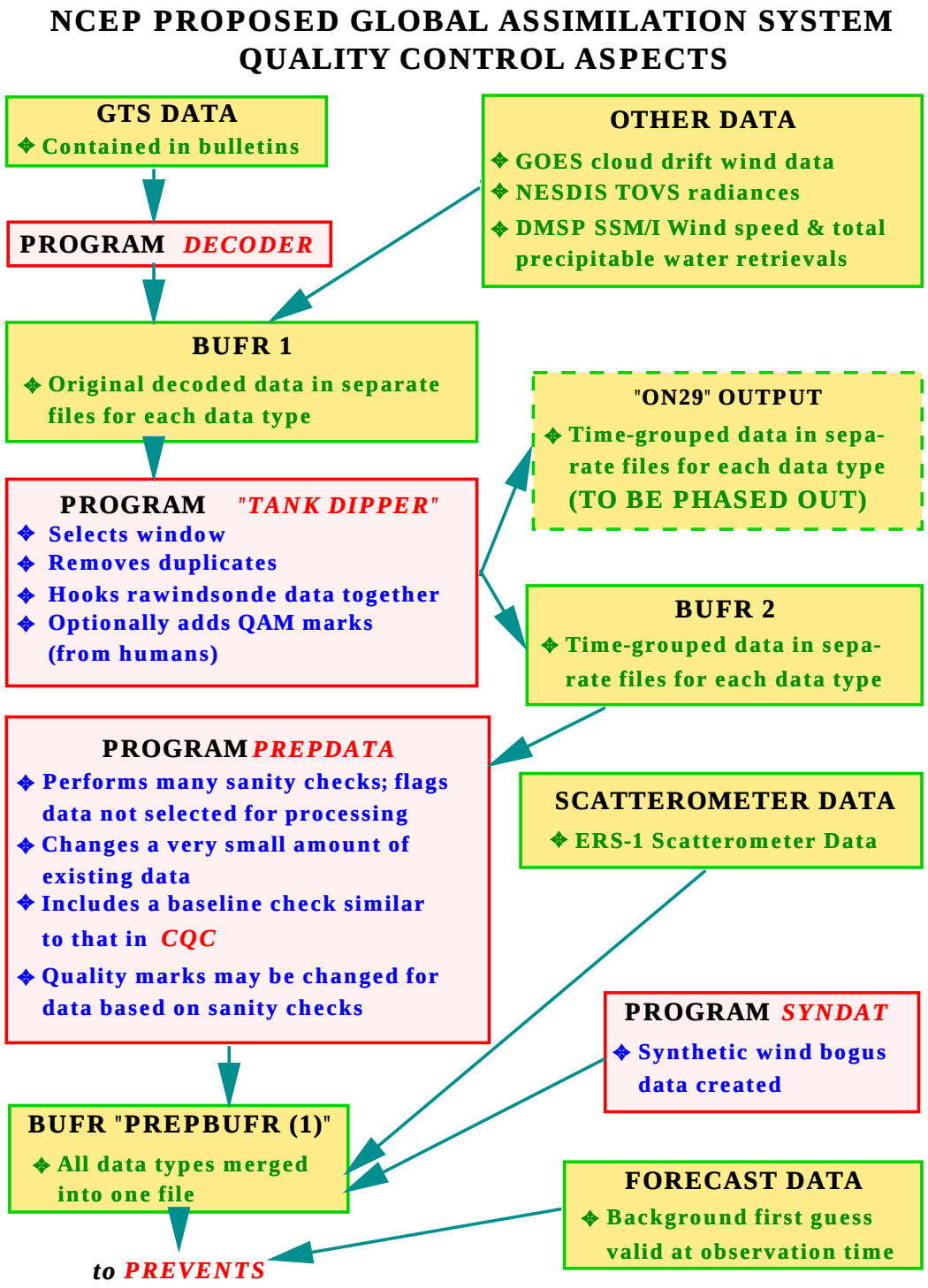

Figure 9.3: Data flow diagram of the Quality Control aspects of the proposed NCEP Global Assimilation System (PART I). See text for details.

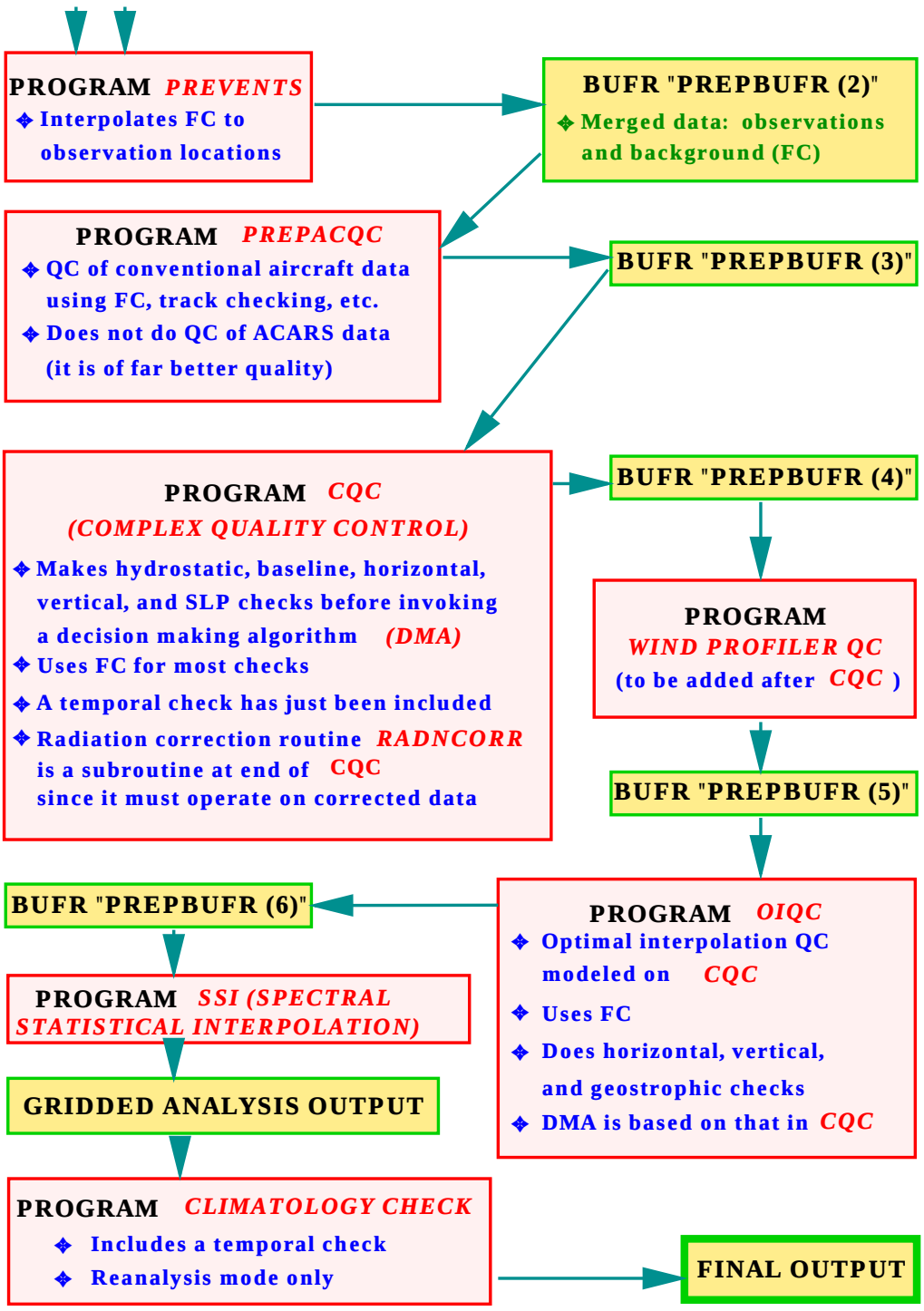

Figure 9.4: Data flow diagram of the Quality Control aspects of the proposed NCEP Global Assimilation System (PART II). See text for details.

undergone. Finally, passing data are ingested by the analysis process.

The primary development from this system to the system for GEOS-3 includes implementation of the MPI system for fully distributed computing. Initial work which identifies the problems of QC in a a distributed computing environment are discussed in Laszewski et al. (1995). In addition if resources allow, additional capabilities of the NCEP system which use post-forecast data will be implemented.

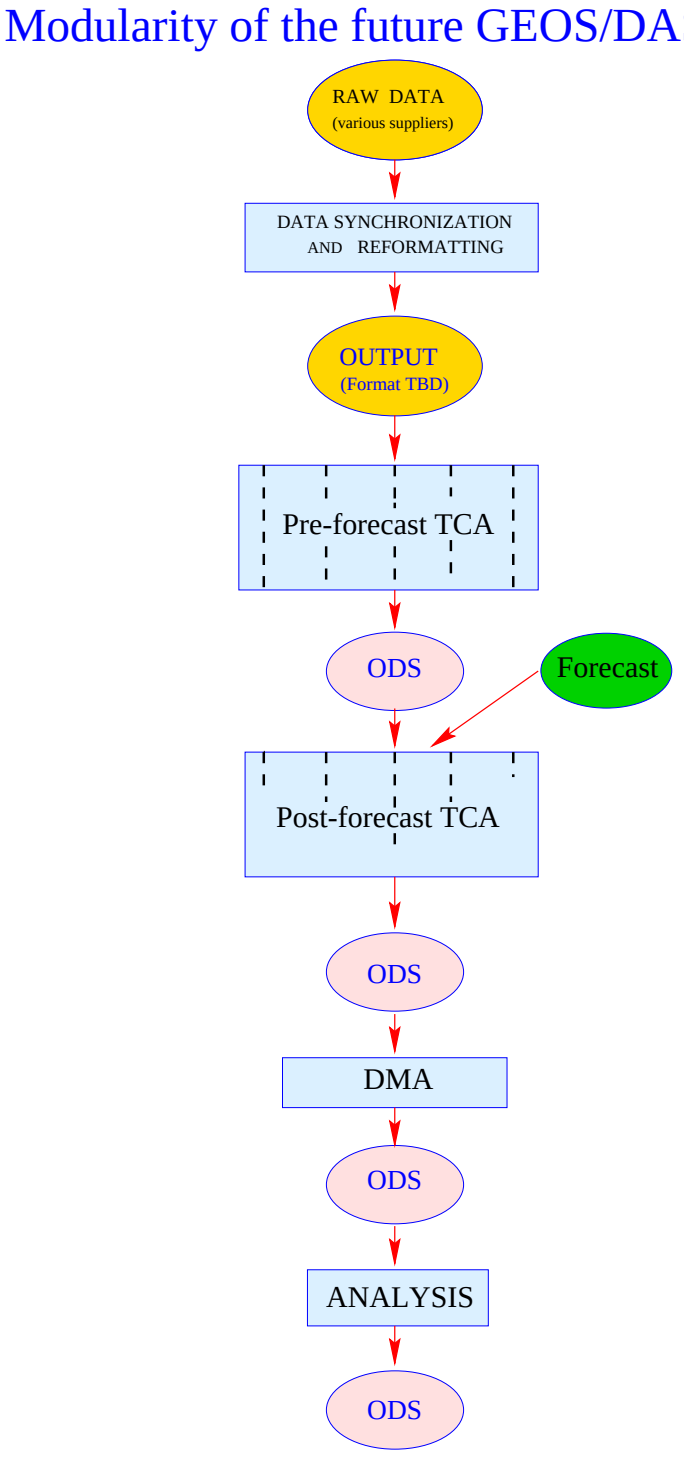

Figure 9.5: Data flow diagram for the GEOS-3 quality control system.

9.6 Incorporation of New Input Data Sets

The incorporation of new data types into the GEOS DAS is central to the mission of the DAO. As discussed in Chapter 7, it is also a potentially all-consuming task. In order to address the task, the strategy laid out in Chapter 7 relies on instrument team participation to expedite the inclusion of any particular data type. We have tried to build the infrastructure in the GEOS-DAS to make the use of new data types as straightforward as possible.

We have also identified in Chapter 7 that the monitoring process as an essential first step in assimilating a new data type. This is necessary for both qualitative and quantitative evaluation of data quality. In order to assimilate data properly, it is necessary to know bias characteristics and more general error statistics. Monitoring candidate data sets for a year allows collection of statistics in all seasons.

Because of the requirement to monitor new data types, instruments from AM-1 will not be directly assimilated immediately at launch. Amongst other things, this allows delay of computer purchases required to use some of the large data sets of the AM-1 platform. The new data types effort between GEOS-2 and GEOS-3 will focus on improvement of use of temperature and moisture information from operational weather satellites, NSCAT observations from ADEOS, and TMI and PR observations from TRMM. Much of the experience for these new data types has been gained from already existing instruments such as SSM/I and the scatterometer on ERS-1.

In addition, there is a nascent effort in constituent assimilation that shows great promise. With the possible exception of carbon dioxide measurements from MOPITT, the constituent effort will not directly support the AM-1 platform. The constituent effort currently focuses on UARS data, but success with long-lived tracers from HALOE on UARS motivates accelerated development of techniques to use SAGE data to develop long-term global data sets. The development of constituent assimilation techniques is very challenging because tracers are described by different statistics from traditional meteorological parameters.

9.6.1 Improved Treatment of Operational Temperature Sounders: TOVS, IASI and AIRS

The temperature sounding from the operational satellites are one of the fundamental data sets needed for a credible assimilation system. Tremendous efforts have been made at the operational NWP centers to utilize the TOVS data, and only recently is the potential of the TOVS data being realized. In the future the operational instruments will be changing their instrumentation. In addition the United States will become more dependent on foreign partners for operational data. It is at the core of the assimilation system to improve the use of operational temperature data. This section highlights our efforts.

1. A 1-D simulation of the PED approach using TOVS and AIRS radiances was completed in early 1996. The results showed that the data compression for both AIRS and TOVS should significantly reduce computation in PSAS. Based on the 1-D results, the theoretical foundation for this approach appears sound.

2. A fast forward radiative transfer model was extracted from the TOVS Pathfinder code (Susskind *et al.* 1983) and an analytic Jacobian (can be used as tangent linear model

and adjoint) was added. This model, called GLATOVS, is described in Sienkiewicz (1996a). This model is currently being compared with RTTOVS, the standard fast radiative transfer model used for TOVS data (see Sienkiewicz 1996b).

3. Systematic error correction to account for errors in the forward model and instrument calibration is an integral part of assimilating data from any microwave/IR sounder. In early 1996 a simulation of forward model error was completed. The results showed that, as expected, systematic error can be as large or larger than detector noise. In the first part of 1996, several systematic error correction schemes have been compared in a simulation environment. Currently, a physically-based correction scheme is being implemented with TOVS Pathfinder data. After the algorithm has been tested, validated, and frozen, the results will be documented.

4. After the systematic error correction scheme has been implemented, the radiance error covariance will be estimated using the approach described in da Silva *et al.*(1996a).

5. When observation operators have been implemented in PSAS, a comparison of the PED and the direct radiance assimilation approaches will be completed using TOVS Pathfinder data for one season. The results will also be compared with the current method of tuned retrieval assimilation. One approach will be selected on the basis of cost and analysis quality for use in GEOS-3.

9.6.2 Assimilation of surface marine winds

The assimilation of satellite-observed surface marine wind speeds and direction have a great impact on the quality of global analyses. The satellite provides coverage where there are no conventional observations. There is an especially large impact on the representation of synoptic scales with are often underobserved, if not completely missed, by surface and other satellite methods. Atlas et al. (1996) and Chapter 7 (subsection 7.2.4) both describe the motivation for surface marine wind assimilation and algorithms to address the problem. For AM-1 MODIS team members have prescribed a high priority to have excellent surface wind fields to improve the quality of MODIS surface marine products.

The detailed plans for the use of NSCAT data are described in section 7.5.1.5 and will not be repeated here. Figure 9.6 shows the first results from use of NSCAT (launched August 1996) data in the DAO. The figure focuses on a portion of the North Atlantic where previous studies have shown that the GEOS analysis generally performs well. The GEOS wind fields are used to help solve the directional ambuiguity problem inherent in the scatterometry observations. Then a variational analysis of the NSCAT observations with the directional ambiguity removed is performed. The NSCAT observations are capable of fully resolving a small cyclone that was not indicated in the original analysis from GEOS.

This example clearly shows the ability of the new observations and the assimilation analysis to function together and provide a combined product superior to each individual component. In the near future the NSCAT data will be directly incorporated into the GEOS analysis. Research to communicate the impact of the surface observations upward into atmosphere is underway, and some of the requirements listed at the beginning of this Chapter are aimed at improving the linkage between the surface and free atmosphere.

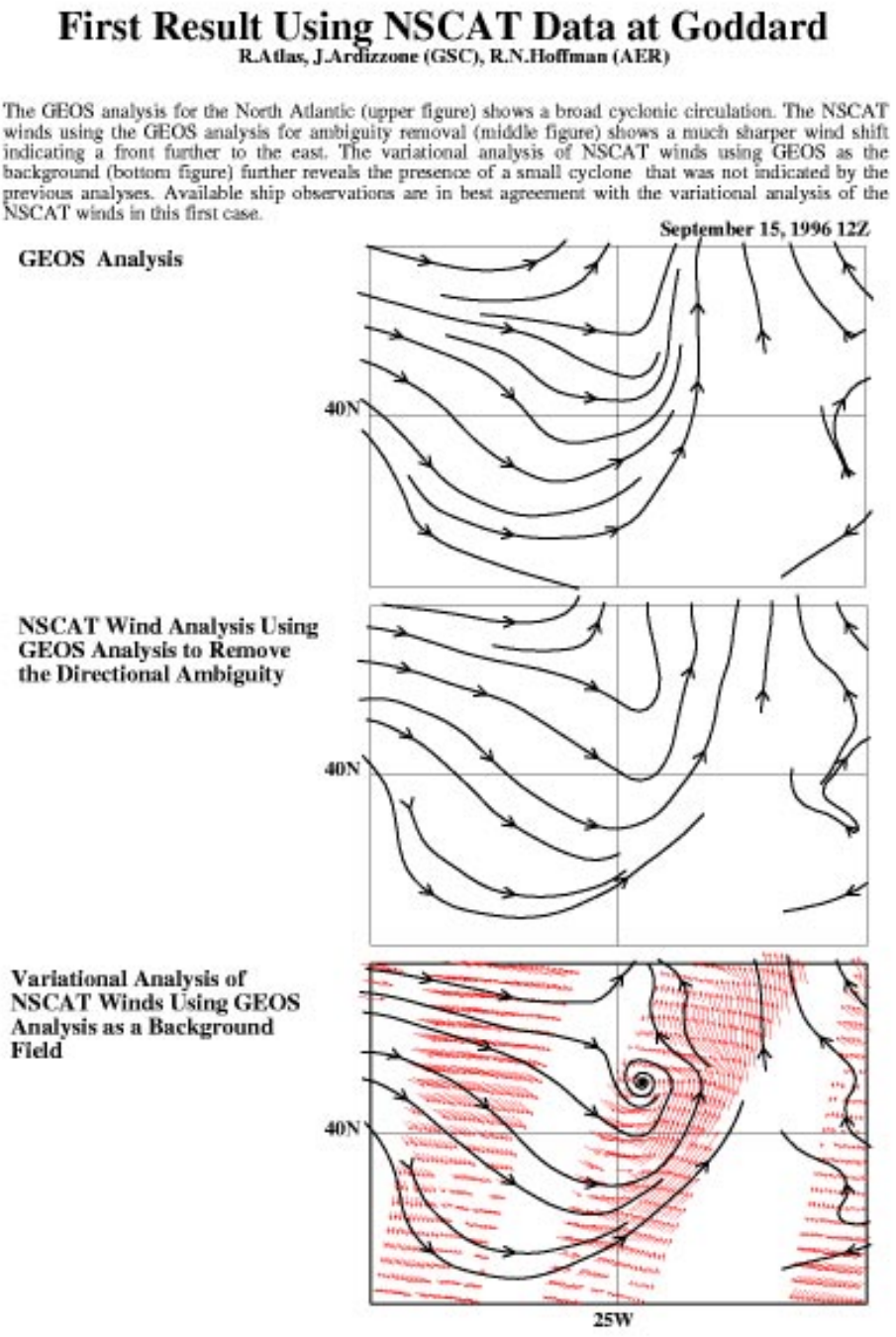

Figure 9.6: First tests of NSCAT data with the GEOS assimilation system.

9.6.3 Assimilation of Satellite Retrievals of Total Precipitable Water and Surface Precipitation/TRMM

The global-mean atmospheric response to climate perturbations (*e.g.*, changes in the sea surface temperature or greenhouse gases) depends upon dynamical redistributions of heat and potential vorticity, which are sensitive to the westerly acceleration of the subtropical jet by the divergent circulation associated with latent heat release in the tropics (Hou 1993, 1996). Small errors in the temporal or spatial structure in tropical latent heating could therefore have a significant impact on atmospheric energetics. A major discrepancy that exists between the analyses produced by different assimilation systems is the estimate of the tropical divergent wind (Molod et al. 1996), which is significantly influenced by the model's convective parameterization due to sparse wind observations (Rind and Rossow 1984, Trenberth and Olson 1988). Studies have shown that physical initialization or diabatic dynamic initialization using surface rainfall as a constraint on the vertically-integrated latent heat release can reduce model spin-up and improve short-range forecasts, which could, in turn, have a positive impact on analyzed data through improved first-guess fields (*e.g.*, Turpeinen *et al.* 1990, Puri and Miller 1990, Heckley et al. 1990, Krishnamurti et al. 1991, Kasahara et al. 1992, Manobianco *et al.* 1994, Treadon 1995, Peng and Chang 1996). Alternatively, rainfall data may be used to directly constrain the precipitation produced by a 4D variational data assimilation schemes (e.g. Zupanski and Mesinger 1995, Tsuyuki 1995).

The use of high-quality satellite precipitation data to constrain precipitation in GEOS DAS can directly improve the representation of latent heating and indirectly influence the circulation and clouds in the tropics. In the near future, apart from surface wind estimates from NSCAT (NASA Scatterometer), there will be little direct wind observations available for improving the analysis, making it crucial to utilize rainfall data as a way to improve the divergent wind in the tropics. This would have a significant impact on atmospheric energetics since the clear-sky outgoing longwave radiation is dominated by humidity in the upper troposphere (Soden et al. 1994, Bates et al. 1996), which is sensitive to the vertical motion field directly related to the horizontally divergent flow. Given that the ratio of the area-averaged net downward shortwave-plus-longwave radiation at the top of the atmosphere to the averaged sea surface temperature is one useful indicator of climate sensitivity (Lindzen 1990, Chou 1994), it is crucial that the 4D structure of tropical rainfall be accurately represented in GEOS DAS for the assimilation to provide useful diagnostics of atmospheric energetics. Rainfall assimilation allows us to address our needs in this critical area through the use of increasingly more accurate satellite-based rainfall estimates to upgrade the quality of the GEOS analysis. A physically- consistent global analysis with the observed tropical rainfall is requisite for analyzing regional and global climate variations associated with tropical rainfall variability. It also provides estimates of the tropical latent heating as realized through physical parameterizations in the global model, which may be compared with physically-retrieved heating profiles from TRMM or special field campaigns such as South China Sea Monsoon Experiment (SCSMEX) to improve model parameterizations.

9.6.3.1 Assimilation methodology

A Multivariate one-dimensional variational (1D-VAR) technique is being developed to assimilate satellite-retrieved total precipitable water (TPW) and surface rainfall estimates. The procedure minimizes the cost functional (9.1) in one-dimension, having temperature and moisture increments as state variables. This 1D-VAR scheme differs from the work of Fillion and Errico (1996) by using grid-box, 6-hour time averaged rainfall estimates as observables, instead of instantaneous values. By having constant IAU increments (section 5.4) as control variables, this procedure has the potential to at least partially account for model error bias (Derber 1989).

In principle, the assimilation of time-mean precipitation could be formulated as in the standard 4D-VAR framework (*e.g.*, Zupanski and Mesinger 1995). However, the computational cost of an operational implementation of 4D-VAR is beyond DAO's computational resources. Our 1D-VAR scheme can be regarded as an interactive retrieval system which translates TPW and rainfall estimates (or microwave radiances in future implementations) into increments of familiar temperature and moisture data types. The information content of these *retrieved profiles* can be extracted using a partial eigenvector decomposition method (Joiner and da Silva 1996) before being assimilated along with other data in PSAS (Chapter 5).

Issues concerning the balance between the convective heating and divergent wind fields will be addressed within the PSAS framework. Initial results from a simplified version of this procedure showed that rainfall assimilation does not cause noticeable spin-up problems within the Incremental Analysis Update (IAU) framework (Hou et al. 1996). If needed, the *Balanced IAU* procedure based on the iterative diabatic dynamic initialization scheme of Fox-Rabinovitz (1996) is available for the GEOS DAS.

9.6.3.2 Data Source

The primary data source currently available for this effort is the 6- hour gridded Goddard Profiling (GPROF) physical retrieval of surface rainfall based on two Special Sensor Microwave/Imager (SSM/I) instruments aboard the Defense Meteorological Satellite Program satellites produced by the Mesoscale Atmospheric Processes Branch (MAPD) at GSFC (Kummerow et al. 1996, Olson et al. 1996). During the Tropical Rainfall Measuring Mission (TRMM) this data base will be further augmented by observations from the TRMM Microwave Imager (TMI) and Precipitation Radar (PR). In anticipation of this, currently only rainfall data between 30°S and 30°N are assimilated in the GEOS-DAS. Since the total surface precipitation produced by the GEOS-DAS comprises rainfall due to penetrative convection as generated by the relaxed Arakawa-Schubert (RAS) parameterization (Moorthi and Suarez 1992) coupled with a Kessler-type of re- evaporation of falling rain, and large-scale precipitation from super- saturation (Sud and Molod 1988), for TRMM applications the precipitation term in the cost function may be further divided into rainfall due to penetrative convection and stratiform rain since each has its own forward model in the GEOS-DAS. The inclusion of cloud ice/water content in the cost function is straightforward using a corresponding forward model when hydrometeor data become available from TRMM.

Satellite rainfall retrievals are useful for improving assimilated data products only if observations errors over a GCM gridbox are small relative to forecast errors. For the TMI, Bell et al. (1990) estimated an overpass frequency of approximately 1-2 day-1 near the equator and 3-4 day^{-1} at a latitude of 30°. During TRMM, this would be augmented by two SSM/I instruments, each of which would, on average, add another 1 day-1 per gridbox near the equator. Altogether, the footprints of approximately 1 per 56 km^2 from TMI and 1 per 156 km^2 from SSM/I will yield 1100 and 394 samples, respectively, per overpass, over a $2° \times 2.5°$ grid-box. Given these large samples per gridbox, the instantaneous, gridbox-average parameters have relatively low random error. Following the analysis of Bell *et al.* (1990), the typical error of a gridbox surface rainfall rate derived from TMI would be 12% of the GATE mean rainfall rate (this estimate assumes an expected error of 50% in individual rain rate retrievals going into the gridbox average; see Kummerow et al. 1996). Raingauge comparisons have shown that bias errors in GPROF retrieved rainfall rates are on the order of 20%.

Time-averaged retrieved parameters are subject to additional error arising from the infrequent sampling of the microwave sensors. The additional sampling error in a 6 hour average rain rate over a $2° \times 2.5°$ grid-box deduced from one or two satellite overpasses within the averaging period may be in the range of 50 -100%, based upon GATE rainfall statistics (Bell, personal communication). In an independent study, sampling errors of 30% in estimates of 6 hour rain depth were obtained by Kummerow (personal communication), based upon sampling of radar rain rates over the TOGA/COARE Intensive Flux Array at SSM/I overpass times.

Although sampling errors in time-average rain estimates from TMI or SSM/I may be relatively large, errors in the model-generated precipitation in 4DDA are often even larger, especially in terms of its spatial distribution. Sampling errors can be reduced by combining the microwave data with more frequent infrared observations from geostationary satellites. Using the variable infrared threshold technique of Kummerow and Giglio (1995) to calibrate the infrared observations with SSM/I estimates, Kummerow found that errors in 6 hour rain depths were reduced from 30% to 10% using hourly infrared measurements calibrated by radar data sampled at the SSM/I overpass times (personal communication). This work is currently underway at the MAPB at Goddard to produce merged microwave/infrared 6-hour averaged rainfall estimates based on calibrated geostationary infrared data using TMI and/or SSM/I observations during TRMM.

9.6.4 Constituent Assimilation

Most of the constiuent assimilation effort is focused on stratospheric constituents and not of direct relevance to the GEOS-2 and GEOS-3 algorithms, at least with regard to the support of the AM-1 platform. Constituent assimilation plans are being actively developed, with an increased focus on both stratospheric and tropospheric ozone.

The successes indicated in the results described in Section 4.3.2.3 have motivated several new instrument initiatives (i.e. ESSP satellite program) to incorporate some assimilation capabilities in their proposals. The carbon monoxide results shown in Figure 4.5 suggest that the model will be able to provide useful information for carbon monoxide retrievals. Recently, P. Kasibhatla (Duke University) received EOS funding to work collaboratively

with the DAO on carbon monoxide assimilation.

9.7 Advanced Research Topics

There are numerous research projects in the DAO focused on special and advanced aspects of the data assimilation problem. Most of these efforts are supported by individual peer-reviewed proposals. This section provides a brief description on these projects.

One project, to study retrospective analysis is detailed at a much higher level. Retrospective analysis is one of the obvious algorithms that become viable once data assimilation is broken from its operational mission. Retrospective analysis refers to the use of observations taken after the analysis time in the analysis. This has the impact to potentially improve analysis quality, and recent progress in the DAO has revealed computationally viable strategies.

9.7.1 Retrospective Data Assimilation

Fixed–lag smoothing techniques will provide GEOS DAS with the capability to perform retrospective data assimilation. This capability allows for improvement of analyses beyond the accuracy provided by purely three-dimensional filtering techniques, such as PSAS, by incorporating data past each analysis time into each analysis. Retrospective data assimilation is distinct from current efforts on re-analysis (e.g., Burridge 1996, Kalnay *et al.* 1996, Schubert and Rood 1995). As pointed out by Cohn *et al.* (1994), retrospective data assimilation should be an ultimate goal of re-analysis. Although retrospective data assimilation has been introduced for analysis purposes, it is foreseeable that this procedure could also be adopted in numerical weather prediction to produce improved mid– to long–range forecasts, starting from a given retrospective analysis. Once the DAO retrospective data assimilation system (RDAS) is operational, our re-analysis will automatically benefit from the fixed–lag smoothing development.

Our RDAS is based on the fixed–lag Kalman smoother (FLKS) of Cohn et al. (1994), following the extension to nonlinear dynamics and observing systems of Todling and Cohn (1996). The algorithm, referred to as the *extended* fixed-lag Kalman smoother, is based on the extended Kalman filter (EKF; Jazwinski 1970, p. 278). As a consequence, the filter portion of the extended FLKS is just the EKF. Brute–force implementation of the extended FLKS to construct an operational RDAS is not possible for the same reasons that a brute–force EKF–based data assimilation system would be impractical: computational requirements are excessive, and knowledge of the requisite error statistics is lacking. Therefore, approximations not only must be employed but cannot be escaped from. In the initial phase of our studies, we developed and evaluated the performance of potentially useful approximate schemes. Todling *et al.* (1996) chose a linear shallow–water model as a test–bed for this investigation, since in this context exact performance evaluation is possible. All of the approximate schemes evaluated in that work have relatively simple nonlinear equivalents.

Among the many schemes developed by Todling et al. (1996), the adaptive constant error covariance (CEC) scheme is the simplest to implement in an operational environment. This scheme approximates the filter only, and calculates the smoother equations exactly. It replaces the forecast error covariance matrix calculation as dictated by the Kalman filter by a constant forecast error covariance matrix multiplied by a parameter that is adaptively

tuned on the basis of innovations, following the algorithm of Dee (1995). This constant forecast error covariance matrix can be thought of as a climatological error covariance. In essence, with regard to the specification of the forecast error statistics, this scheme resembles operational analysis schemes currently in place at the DAO, ECMWF and NCEP, except for the adaptive tuning.

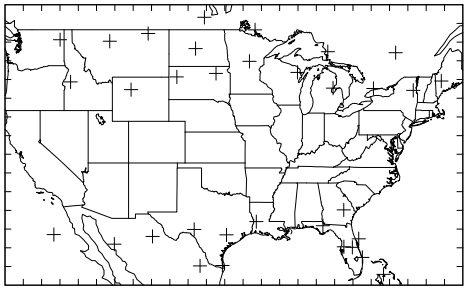

Figure 9.7: Radiosonde network composed of 33 stations observing winds and heights every 12 hours (same as Fig. 2 of Cohn and Todling 1996).

We briefly discuss here the performance of the adaptive CEC as an RDAS in the context a barotropically unstable shallow–water model linearized about a meridionally–dependent square–hyperbolic secant jet. We refer the reader to Fig. 1 of Cohn and Todling (1996) for the shape, extent and strength of the jet. The model domain and the 33–station network of radiosondes observing wind and heights every 12 hours are displayed in Fig. 9.7.

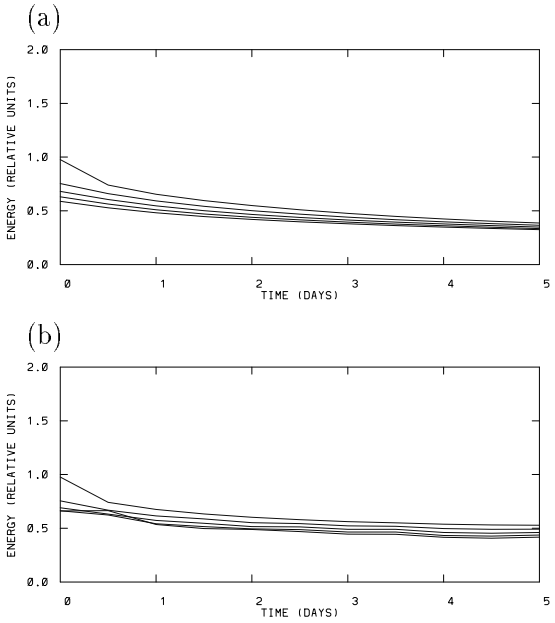

Figure 9.8: ERMS analysis error in total energy for (a) the Kalman filter (upper curve) and fixed-lag Kalman smoother (lower curves); and (b) the adaptive CEC filter and corresponding fixed–lag smoother.

In Fig. 9.8 we show results for the optimal RDAS experiment [panel (a)], obtained with the FLKS, and for the approximate RDAS utilizing the adaptive CEC scheme [panel (b)]. The curves are for the domain–averaged expected root–mean–square (ERMS) analysis

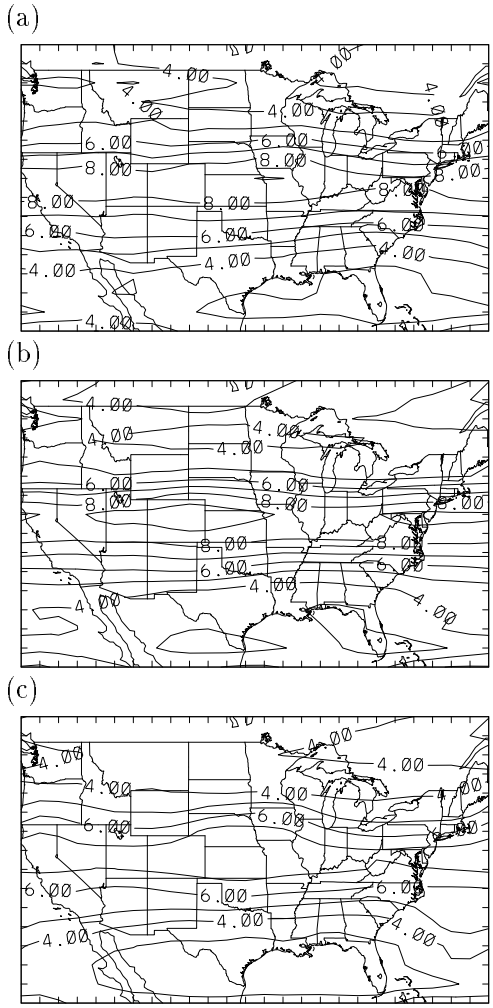

Figure 9.9: Analysis error standard deviation in the height field at time $t = 2$ days. Panel (a) is for the Kalman filter analysis; panels (b) and (c) are for the smoother analysis with lags $\ell = 1$ and 4, respectively, when the RDAS utilizes the adaptive CEC filter.

error in the total energy. The top curve in each panel corresponds to the filter result, while successive retrospective analysis results are given by successively lower curves in each panel, and refer to analyses including data 12, 24, 36 and 48 hours ahead of a given time, that is, lags $\ell = 1, 2, 3$, and 4, respectively. The most relevant results are those for the transient part of the assimilation period, before the filter (top curve) begins tending toward a steady state. From the optimal result in panel (a) we see that incorporating new data into past analyses reduces the corresponding past analysis errors considerably. The performance of the adaptive CEC filter [top curve, panel (b)] is, of course, worse than seen in panel (a) for the Kalman filter. As a consequence, the performance of the retrospective analysis in panel (b) is not as good as that in panel (a).

However, a comparison between panels (a) and (b) of Fig. 9.8 indicates that retrospective analysis based on a suboptimal filter can be viewed as a way of improving suboptimal filter performance toward optimal filter performance. Specifically, notice that by day 2 the lag–1 suboptimal retrospective analysis of Fig. 9.8b has about the same error level as the

optimal filter analysis of Fig. 9.8a, and the lag–4 analysis has better performance than the optimal filter analysis. This is further illustrated in Fig. 9.9, where maps for the analysis error standard deviation in the height field are shown at time $t = 2$ days for the Kalman filter, panel (a), and the approximate RDAS using the adaptive CEC filter: panels (b) and (c) correspond to lags $\ell = 1$ and 4, respectively. We see here that the retrospective result for lag $\ell = 1$ has about the same spatial error distribution as that obtained using the Kalman filter, except along the central part of the domain where the jet is strongest; the Kalman filter analysis still performs better there. Furthermore, with lag $\ell = 4$, when data 2 days ahead of the analysis time have been incorporated with the retrospective algorithm, the retrospective analysis presents smaller error levels than those obtained with the Kalman filter, even when a suboptimal filter is driving the RDAS [compare panels (a) and (c)].

We are currently implementing a version of the CEC scheme in the GEOS DAS. This experimental RDAS is based on the PSAS formulation, which includes adaptive tuning of forecast error variances as explained in Chapter 5. The algorithm can be written as follows:

for $k = 1, 2, \ldots$
  PSAS Solve: $\left(\mathbf{H}_k \mathbf{P}^f \mathbf{H}_k^T + \mathbf{R}_k\right) \mathbf{y} = \mathbf{w}_k^o - \mathbf{h}(\mathbf{w}_{k|k-1}^f)$
  $\mathbf{x}^0 = \mathbf{H}_k^T \mathbf{y}$
  for $\ell = 1, 2, \ldots, \mathbf{min}(k, L)$
    Adjoint Integration: $\mathbf{x}^\ell = \mathbf{F}_{k-\ell|k-\ell}^T \mathbf{x}^{\ell-1}$
    PSAS Solve: $(\mathbf{H}_{k-\ell} \mathbf{P}^f \mathbf{H}_{k-\ell}^T + \mathbf{R}_{k-\ell})\, \mathbf{y} = \mathbf{H}_{k-\ell} \mathbf{P}^f \mathbf{x}^\ell$
    $\mathbf{x}^\ell := \mathbf{x}^\ell - \mathbf{H}_{k-\ell}^T \mathbf{y}$
    Retrospective Increment: $\delta \mathbf{w}_{k-\ell|k}^a = \mathbf{P}^f \mathbf{x}^\ell$
  endfor
endfor

Here the loop on k corresponds to the current analysis cycle, and the loop on ℓ corresponds to the retrospective cycle for a total of L lags. After the solution vector $\mathbf{y}$ from the PSAS equation (5.7), reproduced in the algorithm above, has been computed, we interpolate and convert it to the model grid and variables to obtain the increment $\mathbf{x}^0$. This is done with the transpose of the tangent linear observation operator $\mathbf{H}_k$. For each lag of the RDAS, an integration with the adjoint model of the GCM, represented by the operator $\mathbf{F}_{k-\ell|k-\ell}^T$, is required. This operator is the transpose of the Jacobian operator $\mathbf{F}_{k-\ell|k-\ell}$ defined as:

$$\mathbf{F}_{k-\ell|k-\ell} \equiv \left. \frac{\partial \mathbf{f}(\mathbf{w})}{\partial \mathbf{w}} \right|_{\mathbf{w}=\mathbf{w}_{k-\ell|k-\ell}^a} \tag{9.12}$$

where $\mathbf{f}$ represents the GCM, and $\mathbf{w}_{k-\ell|k-\ell}^a$ is the retrospective analysis at time $t_{k-\ell}$ obtained using data up to and including time $t_{k-\ell}$, i.e., the filter analysis (see Todling and Cohn 1996, for details). The evolved increment $\mathbf{x}^\ell$, weighted by $\mathbf{H}_{k-\ell} \mathbf{P}^f$, serves now as the right–hand–side of the PSAS solver, which utilizes observation operators corresponding to time $t_{k-\ell}$. The result provided by the PSAS solver is the new vector $\mathbf{y}$, which is used to compute the retrospective increments $\delta \mathbf{w}_{k-\ell|k}^a$, for each lag ℓ. The retrospective analysis at time $t_{k-\ell}$,

using data up to and including time t_k, is then obtained by

$$\mathbf{w}^a_{k-\ell|k} \;=\; \mathbf{w}^a_{k-\ell|k-1} \;+\; \delta\mathbf{w}^a_{k-\ell|k} \tag{9.13}$$

which is a correction to the analysis $\mathbf{w}^a_{k-\ell|k-1}$ at time $t_{k-\ell}$ that used data up to and including time t_{k-1}.

In our experimental RDAS, only the lag–1 retrospective algorithm is being implemented. This means that each analysis will be retrospectively corrected by introducing data 6 hours ahead of each analysis time, since this is the time interval between two consecutive analyses in the GEOS DAS. This preliminary implementation uses the adjoint of the GEOS-1 GCM dynamics (Takacs *et al.* 1994) constructed by Yang and Navon (1995), together with the adjoint of part of the physics, namely the relaxed Arakawa-Schubert moisture parameterization scheme (Yang and Navon 1996). The RDAS utilizes the GEOS-2 version of PSAS, but should be readily upgraded to use the GEOS-3 version of PSAS. Our plan is to make extensive studies of lag–1 retrospective analysis results to assess performance and reliability of the algorithm. It will also be interesting to compare with the 6–hour 4D–Var results of Rabier *et al.* (1996).

A variety of issues will be addressed with the experimental RDAS, including the following:

- The role of frequency of the trajectory update used in the adjoint model integration.
- The impact on the retrospective analysis results due to utilization of simplified physics in the adjoint model.
- The role of IAU in the trajectory used as the basic state for the adjoint model.
- The impact of improved forecast error statistics, as the GEOS-2 version of PSAS matures into the GEOS-3 version.
- The development and implementation of statistical tools to monitor retrospective innovations, to serve as diagnostics for the RDAS.

Further issues to be addressed as we go beyond lag–1 are: the impact of higher lags, the question of number of lags versus computational cost, and the impact of performing certain calculations at reduced resolution following Todling *et al.* (1996).

As the adaptive tuning methodology, forecast bias estimation, and anisotropic correlation modeling efforts mature in PSAS, the "PSAS filter" on which the RDAS is based becomes closer to optimal. These improvements, along with improvements in the GCM, should translate immediately into improvements in RDAS analysis accuracy. In particular, as we learn more about statistics of model error and incorporate this knowledge into PSAS, the retrospective analysis algorithm will inherit the benefit automatically.

9.7.2 Diabatic Dynamic Initialization

M. Fox-Rabinovitz has secured funding from NASA to study diabatic dynamical initialization. Despite the properties of the IAU the GEOS DAS still has some noise problems,

especially in the stratosphere. The initialization has been implemented in GEOS and integrated with the IAU. The method does control stratospheric noise, and if the underlying cause of the noise cannot be eliminated then the initialization will be used. In addition, diabatic initialization might be necessary for precipitation assimilation.

9.7.3 Vertical Structure of Model

A short-term research project has been initiated with personnel from the Mesoscale Atmospheric Processes Branch to investigate vertical finite differencing and grid structure in the GEOS GCM. This research is motivated by a continued need to improve noise characteristics in the stratosphere. Hybrid pressure and sigma coordinates are being considered. The use of an isentropic coordinate is a longer term research project which is currently unfunded.

In another project the finite-volume integration method proposed by Lin (1996) for the computation of the pressure gradient forces in a terrain following vertical coordinate is being investigated. This physically-based approach to vertical differencing reduces the deformational error in the horizontal pressure gradient caused by topography in the sigma coordinates by more than an order of magnitude. This research is led by S. J. Lin.

9.7.4 Potential Vorticity Based Model

This is a funded research project headed by Y. Li to develop an atmospheric GCM based on the semi-Lagrangian advection of potential vorticity (PV), i.e., PV is a direct model prognostic variable. Additional features of this GCM will include a hybrid vertical coordinate which becomes isentropic away from the Earth's surface. The motivation of this model is manifold. One is to take advantage of the advective nature of potential vorticity. There is evidence from initial experiments that assimilation into the potential vorticity model may have some advantages over conventional models. A major motivation for the development is the need to assimilate constituent data, and the strong relationship between PV and constituents, at least in the stratosphere. The constituents might serve as a surrogate for PV measurements, and it may be possible to extract wind information from the constituent observations.

9.7.5 Regional Applications of the Global Assimilation System

In order to address the MTPE priority of regionally-oriented science prototype funding has been secured by M. Fox-Rabinovitz to investigate a stretched grid model. The stretched grid model allows high resolution telescoping to a particular area of interest. The numerical noise control technique for the stretched grid GEOS dynamical core and GCM has been developed and implemented. A successful benchmark of long-term and medium-range dynamical core integrations has been completed. The results show that the method has real potential of representing regional processes in a global model with a high level of consistency between regional and global dynamics. Since the PSAS algorithm makes no assumption about the nature of the grid (subsection 5.2.1), the development of a stretched grid data assimilation system is straightforward.

9.7.6 Advanced Advection Modeling

In order to investigate the potential advantage of the monotonicity-preserving FFSL advection scheme (Lin and Rood, 1996a), Lin and Rood (1996b) developed a two-step two-grid algorithm for applying the FFSL scheme to the shallow water equations. Although potential vorticity is not explicitly a prognostic variable, it is implicitly advected by the FFSL scheme using a novel reverse engineering procedure. The computational advantage of the reverse engineering procedure is that there is no need to solve an elliptic equation. Comparisons against standard tests are given in Lin and Rood (1996b). In general the scheme provides stable non-deforming solutions to the test problems better than the high resolution standards proposed in the test problems. Ultimately advanced advection methods might be important for improving the representation of subgrid processes, covariance propagation, and constituent modeling.

9.7.7 Data Assimilation with the IASI Instrument

This research is focused at preparation for use of future operational data. J. Joiner has secured funding in a European Space Agency proposal funded by NASA. The research involves development of state-of-the-art spectroscopic models and data bases for computing monochromatic and band transmittances and validation with laboratory measurements and aircraft data. There will also be comparison of data assimilation methodologies, including direct assimilation of radiances and assimilation of PED (partial eigendecomposition) retrievals, in a limited 3-D DAS using simulated IASI radiances.

9.7.8 Constituent Data Assimilation

Advanced data assimilation methodologies are being formulated and implemented to provide global maps of stratospheric constituents using measurements from instruments aboard the Upper Atmosphere Research Satellite (UARS). These methodologies are based on a dynamical Kalman filter, which uses a transport model to evolve both the state and its associated error covariance matrix. Lagrangian dynamics are being employed to increase effective spatial resolution and to both simplify and make more accurate the covariance evolution. The standard Kalman filter assumption of Gaussian-distributed errors has been generalized to lognormally-distributed errors, a more appropriate assumption for predicted and observed constituent mixing ratios. Funding for this work has been obtained from NASA by S. Cohn.

9.7.9 New Methods to Study Carbon Monoxide Chemistry

In a proposal led by P. Kasibhatla of Duke University the assimilation of carbon monoxide will be studied. The goal of this project will be to improve and use the newly developed DAO Chemical Transport Model (CTM), in conjunction with space-based, airborne, and ground-based measurements to synthesize a comprehensive picture of the global CO distribution and its seasonal variation. This will then form the basis for elucidating the various factors that shape the CO distribution, and in delineating key areas of uncertainty which can then be targets of future studies. It is anticipated that the techniques developed as part of this

activity will be particularly useful in terms of analyzing measurements from the MOPITT and TES instruments scheduled to fly on the EOS space platforms.

9.8 References

Atlas, R., R. N. Hoffman, S. C. Bloom, J. C. Jusem, and J. Ardizzone, 1996: A multiyear global surface wind velocity data set using SSM/I observations. *Bull. Amer. Meteor. Soc.*, **77**, 869-882.

Baker, N. L., 1991: An adaptive correction procedure for radiosonde geopotential height biases. *Preprints, Ninth Conference on Numerical Weather Prediction,* Denver CO, 192–194.

Ballish, B. A., 1991: Quality Control Case Studies with the NMC Global Analysis System. *Preprints, Ninth Conference on Numerical Weather Prediction*, Denver, CO, American Meteorological Society, 143-146.

Bates, J. J. X, Wu, D. L. Jackson, 1996: Interannual variability of upper-troposphere water vapor band brightness temperature. *J. Climate*, **9**, 427-438.

Bell, T. L., A. Abdullah, R. L. Martin, and G. R. North, 1990: Sampling errors for satellite- derived tropical rainfall: Monte Carlo study using a space-time stochastic model. *J. Geophys. Res.*, **95**, 2195-2205.

Betts, A. K., John H. Ball and Anton C. M. Beljaars, 1993: Comparison Between the Land Surface Response of the ECMWF Model and the FIFE-1987 Data. *Q. J. Roy. Meteor. Soc.*, **119**, 975-1001.

Burridge, D., 1996: The ECMWF re–analysis: data for research. *Proc. ECMWF Seminar on Data Assimilation*, in press.

Chou, M. D., 1994: Coolness in the tropical Pacific during an El Nino episode. *J. Climate*, **7**, 1684-1692.

Cohn, S. E., 1996: Introduction to estimation theory. *J. Met. Soc. Japan*, in press.

Cohn, S. E., and R. Todling, 1996: Approximate data assimilation schemes for stable and unstable dynamics. *J. Met. Soc. Japan*, **74**, 63–75.

Cohn, S.E., N. S. Sivakumaran, and R. Todling, 1994: A fixed-lag Kalman smoother for retrospective data assimilation. *Mon. Wea. Rev.,* **122**, 2838–2867.

Collins, W. G. and L. S. Gandin, 1990: Comprehensive hydrostatic quality control at the National Meteorological Center. *Mon. Wea. Rev.*, **18**, 2754–2767.

Collins, W. G., 1991: Complex Quality Control of Rawinsonde Heights and Temperatures at the National Meteorological Center. *Preprints, Ninth Conference on Numerical Weather Prediction*, Denver, CO, American Meteorological Society, 15-18.

Collins, W. G., and L. S. Gandin, 1992: Complex Quality Control of Rawinsonde Heights and Temperatures (CQCHT) at the National Meteorological Center. *Office Note 390,* U. S. Department of Commerce, National Oceanographic and Atmospheric Administration, National Weather Service, National Meteorological Center.

Collins, W. G., and L. S. Gandin, 1995: Complex Quality Control of Rawinsonde Heights and Temperatures – Principles and Application at the National Meteorological Center. *Office Note 408,* U. S. Department of Commerce, National Oceanographic and Atmospheric Administration, National Weather Service, National Meteorological Center.

Collins, W. G., and L. S. Gandin, 1996: Complex Quality Control for Observation Errors of Rawinsonde Temperatures and Heights. *NMC Office Note xxx,* U. S. Department of Commerce, National Oceanographic and Atmospheric Administration, National Weather Service, Environmental Modeling Center.

Courtier, P., E. Andersson, W. Heckley, G. Kelly, J. Pailleux, F. Rabier, J.-N. Thepaut, P. Unden, D. Vasiljevic, C. Cardinali, J. Eyre, M. Hamrud, J. Haseler, A. Hollingsworth, A. Mc Nally, and A. Stoffelen, 1993: Variational Assimilation at ECMWF. *ECMWF Technical Memorandum*, No. 194. Reading, England, 84pp.

Dee, D. P. and G. Gaspari, 1996: Development of anisotropic correlation models for atmospheric data assimilation. *Preprint volume, 11th Conf. on Numerical Weather Prediction,* August 19–23, 1996, Norfolk, VA, pp 249–251.

Dee, D. P., 1995: On-line estimation of error covariance parameters for atmospheric data assimilation. *Mon. Wea. Rev.*, **123**, 1128–1145.

Dee, D. P., and A. Trenholme, 1996: DAO QC Strategy Document, *Office Note*96-15, *Data Assimilation Office.*

DelGenio, A. D., M.-S. Yao, W. Kovari, and K. K.-W. Lo, 1996: A prognostic cloud water parameterization for global climate models. *J. of Climate*, **9**, 270-304.

Derber, J., 1989: A variational continuous data assimilation technique. *Mon. Wea. Rev.*, **117**, 2437-2448.

Fillion, L., and R. Errico, 1996: Variational assimilation of precipitation data using moist-convective parameterization schemes: a 1DVAR study. *Mon. Wea. Rev.*, Submitted.

Fox-Rabinovitz, M. S., 1996: Diabatic dynamic initialization with an iterative time integration scheme as a filter. *Mon. Wea. Rev.*, **124**, 1544-1557.

Gandin, L. S., 1991: Two Years of Operational Comprehensive Hydrostatic Quality Control at the NMC. *Preprints, Ninth Conference on Numerical Weather Prediction,* Denver, CO, American Meteorological Society, 11-14.

Ghil, M., S. Cohn, J. Tavantzis, K. Bube, and E. Isaacson, 1981: Applications of estimation theory to numerical weather prediction. Pp. 139–225 in: Bengtsson, L., M. Ghil, and E. Källén, *Dynamic Meteorology: Data Assimilation Methods*, Springer-Verlag, New York, 330pp.

Heckley, W. A., G. Kelley, M. Tiedtke, 1990: On the use of satellite- derived heating rates for data assimilation within the tropics. *Mon. Wea. Rev.*, **118**, 1743-1757.

Helfand, H. M., M. and S. D. Schubert, 1995: Climatology of the Simulated Great Plains Low-Level Jet and Its contribution to the Continental Moisture Budget of the United States. *J. Climate*, **8**, 784-806.

Hou, A. Y., 1993: The influence of tropical heating displacements on the extratropical climate. *J. Atmos. Sci.*, **50**, 3553-3570.

Hou, A. Y., 1996: Hadley circulation as a modulator of the extratropical climate. *J. Atmos. Sci.* Submitted.

Hou, A. Y., A. da Silva, D. V. Ledvina, G. Huffman, R. Adler, C. Kummerow, 1996: Assimilation of TRMM rainfall retrievals in the GEOS-DAS for climate research. *TRMM Science Team Meeting.* Greenbelt, MD, July 9-12.

Jazwinski, A. H., 1970: *Stochastic Processes and Filtering Theory*, Academic Press, New York, 376pp.

Joiner, J., and A. da Silva, 1996: Efficient methods to assimilate satellite retrievals based on information content. *DAO Office Note 96-06.* Data Assimilation Office, Goddard Space Flight Center, Greenbelt, MD 20771. Available on-line from `http://dao.gsfc.nasa.gov/subpages/office-notes.html`.

Julian, P. R., 1991: RADCOR91 - The new radiosonde radiation error correction procedure. NMC Office Note 374.

Kalnay, E., M. Kanamitsu, R. Kistler, W. Collins, D. Deaven, L. Gandin, M. Iredell, S. Saha, G. White, J. Woollen, Y. Zhu, M. Chelliah, W. Ebisuzaki, W. Higgins, J. Janowiak, K. C.. Mo, C. Ropelwski, J. Wang, A. Leetmaa, R. Reynolds, R. Jenne, and D. Joseph, 1996: The NCEP/NCAR 40-Year Reanalysis Project. *Bulletin of the American Meteorological Society* **77-3**, 437 - 471.

Kasahara, A., A. P. Mizzi, and L. J. Donner, 1992: Impact of cumulus initialization on the spinup of precipitation forecasts in the tropics. *Mon. Wea. Rev.*, **120**, 1360-1380.

Koster, Randal D. and Max J. Suarez, 1992: Modeling the Land Surface Boundary in Climate Models as a Composite of Independent Vegetation Stands. *J. Geophys. Res.* **97**, D3, 2697-2715.

Koster, Randal D., and Max J. Suarez, 1994: The Components of a 'SVAT' Scheme and their effects on a GCM's hydrological cycle. *Adv. in Water Resources*, **17**, 61-78.

Krishnamurti, T. N., J. Xue, H. S. Bedi, K. Ingles, and O. Oosterhof, 1991: Physical initialization for numerical weather prediction over the tropics. *Tellus*, **43AB**, 53-81.

Kummerow, C., W. S. Olson, and L. Giglio, 1996: A simplified scheme for obtaining precipitation and vertical hydrometeor profiles from passive microwave sensors. *IEEE Trans. Geosci. Remote Sensing*, **34**, 1213-1232.

Kummerow, C., and L. Giglio, 1995: A method for combining passive microwave and infrared rainfall observations. *J. Atmos. Oceanic Tech.*, **12**, 33-45.

von Laszewski, G., M. Seablom, M. Makivic, P. M. Lyster, S. Ranka: Design issues for the parallelization of an Optimal Interpolation Algorithm. *Coming of Age: Proceedings of Sixth ECMWF Workshop on the Use of Parallel Processors in Meteorology*, Eds. G-R. Hoffmann and N. Kreitz, 290-302, (World Scientific, 1995).

Lin, S.-J., 1996: A finite-volume integration method for computing pressure gradient forces in general vertical coordinates. *Q. J. Roy. Met. Soc.*, In press.

Lin, S.-J., W. C. Chao, Y. C. Sud, and G. K. Walker, 1994: A class of the van Leer-type transport schemes and its applications to the moisture transport in a general circulation model. *Mon. Wea. Rev.*, **122**, 1575-1593.

Lin, S.-J., and R. B. Rood, 1996a: Multidimensional flux-form semi- Lagrangian transport schemes. *Mon. Wea. Rev.*, **124**, 2046-2070.

Lin, S.-J., and R. B. Rood, 1996b: An explicit flux-form semi- Lagrangian shallow water model on the sphere. *Quart. J. Roy. Met. Soc.*, In press.

Lindzen, R. S., 1990: Some coolness concerning global warming. Bulletin. *Atmos. Meteor. Soc.*, **71**, 288-299.

MacVean, M. K. and P. J. Mason, 1990: Cloud-top entrainment instability through small-scale mixing and its parameterization in numerical models. *J. Atmos. Sci.*, **47**, 1012-30.

Manobianco, J., S. Koch, V. M. Karyampudi, and A. J. Negri, 1993: The impact of assimilating satellite-derived precipitation rates on numerical simulations of the ERICA IOP 4 cyclone. *Mon. Wea. Rev.*, **122**, 341-365.

Moorthi, S., and M. J. Suarez, 1992: Relaxed Arakawa-Schubert: A parameterization of moist convection for general circulation models. *Mon. Wea. Rev.*, **120**, 978-1002.

Morone, L. L., 1991: Near Real-Time Monitoring of Automatic Quality Control Decisions at the National Meteorological Center. *Preprints, Ninth Conference on Numerical Weather Prediction,* Denver, CO, American Meteorological Society, 139-142.

Olson, W. S., C. D. Kummerow, G. M. Heymsfield, and L. Giglio, 1996: A method for combined passive-active microwave retrievals of cloud and precipitation profiles. *J. Appl. Meteor.*, **35**, 1763-1789.

Parrish, D.F. and J.C. Derber, 1992: The National Meteorlogical Center's statistical spectral interpolation analysis system. *Mon. Wea. Rev.*, **109**, 1747-1763.

Peng, M. S., and S. W. Chang, 1996: Impacts of SSM/I retrieved rainfall rates on numerical prediction of a tropical cyclone. *Mon. Wea. Rev.*, **124**, 1181-1198.

Puri, K., and M. J. Miller, 1990: The use of satellite data in the specification of convective heating for diabatic initialization and moisture adjustment in numerical weather prediction models. *Mon. Wea. Rev.*, **118**, 67-93.

Rabier, F., J.–N. Thépaut, and P. Courtier, 1996: Four–dimensional variational assimilation at ECMWF. *Proc. ECMWF Seminar on Data Assimilation*, in press.

Randall, D. A., 1980: Conditional instability of the first kind upside-down. *J. Atmos. Sci.*, **37**, 125-30.

Rasch, P. J., and D. L. Williamson, 1991: The sensivity of a general circulation model climate to the moisture transport formulation. *J. Geophys. Res.*, **96**, 13, 123-137.

Rind, D., and W. B. Rossow, 1984: The effects of physical processes on the Hadley circulation. *J. Atmos. Sci.*, **41**, 479-507.

Schubert, S., C.-K. Park, Chung-Yu Wu, W. Higgins, Y. Kondratyeva, A. Molod, L. Tkacs, M. Seablom, and R. Rood, 1995: A Multiyear Assimilation with the GEOS-1 System: Overview and Results. *NASA Tech. Memo. 104606*, Vol. **6.** Goddard Space Flight Center, Greenbelt, MD 20771. Available on-line from `http://dao.gsfc.nasa.gov/subpages/tech-reports.html`.

Schubert, S.D., and R.B. Rood, 1995: Proceedings of the Workshop on the GEOS–1 five–year assimilation. NASA Tech. Memo. 104606, Vol. 7, 201 pp. Available on-line from `http://dao.gsfc.nasa.gov/subpages/tech-reports.html`.

Sellers, P. J., Y. Mintz, Y. C. Sud and A. Dalcher, 1986: A Simple Biosphere Model (SiB) for Use within General Circulation Models. *J. Atmos. Sci.*, **43**, 505-531.

Sienkiewicz, M., 1996a: The GLA TOVS rapid algorithm forward radiance modules and Jacobian version 1.0, *DAO Office Note 96-08*, Data Assimilation Office, Goddard Space Flight Center, Greenbelt, MD 20771. Available on-line from `http://dao.gsfc.nasa.gov/subpages/office-notes.html`.

Sienkiewicz, M., 1996b: Evaluation of RTTOV and GLA TOVS forward model and Jacobian, *DAO Office Note 96-20*, Data Assimilation Office, Goddard Space Flight Center, Greenbelt, MD 20771. Available on-line from `http://dao.gsfc.nasa.gov/subpages/office-notes.html`.

da Silva, A. and C. Redder, 1995: Documentation of the GEOS/DAS Observation Data Stream (ODS) Version 1.0. *DAO Office Note 95-01.* Data Assimilation Office, Goddard Space Flight Center, Greenbelt, MD 20771. Available on-line from `http://dao.gsfc.nasa.gov/subpages/office-notes.html`.

da Silva, A., J. Pfaendtner, J. Guo, M. Sienkiewicz and S. E. Cohn, 1995: Assessing the Effects of Data Selection with DAO's Physical-space Statistical Analysis System. *International Symposium on Assimilation of Observations*, Tokyo, Japan, 133-17 March 1995, 273–278.

da Silva, A. M., Redder, C., and D. P. Dee, 1996: Modeling retrieval error covariances for global data assimilation. *Proc. 8^{th} Conf. Satell. Meteor.*, Atlanta, GA., in press. Available on-line as `ftp://dao.gsfc.nasa.gov/pub/papers/dasilva/atlanta96/tuning.ps.Z`.

Soden, B. J., S. A. Ackerman, D. O'C. Starr, S. H. Melfi, and R. A. Ferrare, 1994: Comparison of upper tropospheric water vapor from GOES, Raman lidar, and cross-chain loran atmospheric sounding system measurements. *J. Geophys. Res.*, **99**, 21,005-21,016.

Starr, D. O. and D. P. Wylie, 1990: The 27-28 October 1986 FIRE cirrus case study: meteorology and clouds. *Mon. Wea. Rev.*, **118**, 2259-87

Stobie, J., 1996: Primary Requirements for the GEOS-3 Data Assimilation System. *DAO Office Note 96–21.* Data Assimilation Office, Goddard Space Flight Center, Greenbelt, MD 20771. Available on-line from
`http://dao.gsfc.nasa.gov/subpages/office-notes.html`.

Suarez, M. J., and L. L. Takacs, 1996: Documentation of the Aries/GEOS Dynamical Core Version 2, NASA Technical Memorandum 104606 Volume 5, NASA, Goddard Space Flight Center, Greenbelt, MD. Available on-line from
`http://dao.gsfc.nasa.gov/subpages/tech-reports.html`.

Sud, Y. C., and A. Molod, 1988: The roles of dry convection, cloud- radiation feedback processes and the influence of recent improvements in the parameterization of convection in the GLA GCM. *Mon. Wea. Rev.*, **123**, 1112-1127.

Sundqvist, H., 1988: Parameterization of condensation and associated clouds in models for weather prediction and general circulation simulation. Physically-based modelling and simulation of climate and climate change, Part 1. Schlesinger, ed. *Kluwer Acad. Publ.*, 433-61.

Todling, R., N.S. Sivakumaran, and S.E. Cohn, 1996: Some strategies for retrospective data assimilation: approximate fixed–lag Kalman smoothers. *Proc. 11th Conf. on Numerical Weather Prediction*, Norfolk, VA, Amer. Meterol. Soc., 238–240.

Todling, R., and S.E. Cohn, 1996: Some strategies for Kalman filtering and smoothing. *Proc. ECMWF Seminar on Data Assimilation*, in press. Available from
`http://dao.gsfc.nasa.gov/DAO_people/todling.`

Treadon, R. E., 1995: Physical initialization in the NMC global data assimilation system. Dept. Meteorology, Florida State University, Tallahasse, Florida. 68 pp.

Trenberth, K., and J. G. Olson, 1988: ECMWF global analyses 1976-1986: Circulation statistics and data evaluation. *Tech. Note NCAR/TN-300+STR*, 117 pp.

Trenholme, A., 1996: GEOS-3/DAS Quality Control Requirements, Document Version 1. *DAO Office Note 96-19.* Data Assimilation Office, Goddard Space Flight Center, Greenbelt, MD 20771. Available on-line from
`http://dao.gsfc.nasa.gov/subpages/office-notes.html`.

Tsuyuki, T., 1995: Variational data assimilation in the tropics using precipitation data. Part II: 3-d model. Dept. Meteorology, Florida State University, Tallahasse, Florida. 41 pp.

Turpeinen, O. M., L. Garand, R. Benoit, and M. Roch, 1990: Diabatic initialization of the Canadian regional finite-element (RFE) model using satellite data. Part I: methodology and application to a winter storm. *Mon. Wea. Rev.*, **118**, 1381- 1395.

Weng, F. and N. C. Grody, 1994: Retrieval of cloud liquid water using the special sensor microwave imager (SSM/I). *J. of Geophys. Res.*, D12, **99**, 25,535-25,551.

Woolen, J. S., 1991: New NMC Operational OI Quality Control. *Preprints, Ninth Conference on Numerical Weather Prediction,* Denver, CO, American Meteorological Society, 24-27.

Yang, W., and M.I. Navon, 1996: Documentation of the tangent linear model and its adjoint of the adiabatic version of the NASA GEOS-1 C-Grid GCM - Version 5.2. NASA Tech. Memo. 104606, Vol. 8, 61 pp. Available on-line from
`http://dao.gsfc.nasa.gov/subpages/tech-reports.html`.

Yang, W., and M.I. Navon, 1996: Documentation of the tangent linear and adjoint models of the relaxed Arakawa–Schubert moisture parameterization package of the NASA GEOS–1 GCM (Version 5.2). NASA Tech. Memo. 104606, sub–judice. Available on-line from
`http://dao.gsfc.nasa.gov/subpages/tech-reports.html`.

Zupanski, D., and F. Mesinger, 1995: Four-dimensional variational assimilation of precipitation data. *Mon. Wea. Rev.*, **123**, 1112-1127.

9.9 Acronyms

9.9.1 General acronyms

DAO	Data Assimilation Office
GEOS	Goddard Earth Observing System (The name of the DAO data assimilation system)
GCM	General Circulation Model
DAS	Data Assimilation System
QC	Quality Control
NWP	Numerical Weather Prediction
CARD	Consistent Assimilation of Retrieved Data
PSAS	Physical-space Statistical Analysis System
NASA	National Aeronautics and Space Administration
GSFC	Goddard Space Flight Center
MTPE	Mission to Planet Earth
EOS	Earth Observing System
EOSDIS	Earth Observing System Data and Information System
NOAA	National Oceanic and Atmospheric Administration
NCEP	National Centers for Environmental Prediction (formerly, NMC)
NMC	National Meteorological Center
NESDIS	National Environmental Satellite Data and Information Service
ECMWF	European Center for Medium-range Weather Forecasts
UKMO	United Kingdom Meteorological Office

9.9.2 Instruments

ADEOS	Advanced Earth Observting Satellite (Mid-late 1996)
AIRS	Atmospheric Infrared Sounder (EOS PM)
AMSU A-B	Advanced Microwave Sounding Unit (POES, EOS PM)
AVHRR	Advanced Very High-Resolution Radiometer
ASTER	Advanced Spaceborne Thermal Emission and Reflection Radiometer (EOS AM)
ATOVS	Advanced TOVS; HIRS3/AMSU (POES)
CERES	Clouds and Earth's Radiation Energy System (TRMM, EOS AM)
CLAES	Cryogenic Limb Array Etalon Spectrometer (UARS)
DMSP	Defense Meteorological Satellite Program (currently operational)
EOS AM1	Earth Observting Satellite AM (June 98 launch)
EPS	EUMETSAT (European Meteorology Satellite) Polar System
ERBE	Earth Radiation Budget Experiment (ERBS)
ERBS	Earth Radiation Budget Satellite
ERS-1,2	European Remote Sensing Satellite (Scatterometer, 6 channel, IR-Visible radiometer)

GOES	Geostationary Observational Environmental Satellite (Imager and 18 channel visible and infrared sounder, currently operational)
GOME	Global Ozone Monitoring Experiment (ERS-2)
GPS	Global Positioning System
HALOE	Halogen Occultation Experiment (UARS)
HIRS2/3	High-Resolution InfraRed Sounder (POES)
HRDI	High Resolution Doppler Imager
IASI	Infrared Atmospheric Sounding Interferometer (EPS)
ILAS	Improved Limb Atmospheric Spectrometer (ADEOS)
IMG	Interferometric Monitor for Greenhouse Gases (ADEOS)
ISCCP	International Satellite Cloud Climatology Project (several IR and visible instruments aboard different satellite)
LIMS	Limb Infrared Monitor of the Stratosphere (Nimbus 7)
MAPS	Measurement of Atmospheric Pollution from Satellites
MHS	Microwave Humidity Sounder (EOS-PM)
MLS	Microwave Limb Sounder (UARS)
MODIS	Moderate-Resolution Imaging Spectrometer (EOS AM)
MSU	Microwave Sounding Unit
MOPITT	Measurement of Pollution in the Troposphere (EOS AM)
NSCAT	NASA Scatterometer (ADEOS)
POES	Polar Orbiting Environmental Satellite (Currently Operational)
PR	Precipitation Radar (TRMM)
SBUV	Satellite Backscatter Ultraviolet radiometer (Nimbus 7, POES)
SAGE	Stratospheric Aerosol and Gas Experiment (ERBS)
SMMR	Scanning Multispectral Microwave Radiometer (?)
SSM/I	Special Sensor Microwave/Imager (DMSP)
SSM/T	Special Sensor Microwave (Temperature sounder, DMSP)
SSM/T2	Special Sensor Microwave (Water vapor sounder) (DMSP)
SSU	Stratospheric Sounding Unit (POES)
TMI	TRMM Microwave Imager (TRMM)
TOMS	Total Ozone Mapping Spectrometer (ADEOS, Meteor, Earth Probe, Nimbus 7)
TOVS	TIROS Operational Vertical Sounder; HIRS2/MSU/SSU (POES)
TRMM	Tropical Rainfall Measuring Mission (summer '97 launch)
UARS	Upper Atmospheric Research Satellite (some instruments in operation)
WINDII	Wind Imaging Interferometer (UARS)

Chapter 10

Summary of Algorithm Theoretical Basis Document

Contents

10.1 Summary of Algorithm Theoretical Basis Document

This document presents an integrated view of the Goddard Earth Observing System Data Assimilation System (GEOS DAS) being developed by the Data Assimilation Office (DAO) at NASA's Goddard Space Flight Center. It has focused on Version 2, GEOS-2, which is being validated at the time of the writing of the document. GEOS-2 represents a major development increment over GEOS-1, and GEOS-2 contains the infrastructure for the future GEOS DAS. The plans for GEOS-3 are also discussed. GEOS-3 will be the system provided to support the 1998 launch of the EOS AM-1 platform. GEOS-2 and its incremental developments will support ADEOS and TRMM between now and the AM-1 launch, as well as continued near-real time support of stratospheric field missions. GEOS-3 requires a major re-design of the GEOS-2 software in order to accommodate the wildly volatile supercomputing market which no longer supports boutique computing for scientific applications.

With regards to the algorithm the document established the following.

Chapter 1 outlined the scope of the document.

Chapter 2 outlined the purpose and scope of the GEOS DAS in the MTPE Enterprise. The identification of customers was presented and the manner in which requirements have been divined from the different customers was outlined. These requirements have been integrated by the DAO to develop tangible requirements for GEOS-3. The requirements process has been difficult and further refinement and mapping to resources is required. The chapter highlighted the role of the DAO Advisory Panel,

including its critical guidance of DAO maturation. Chapter 2 also placed the DAO effort in context with numerical weather prediction efforts, the community in which Earth-science data assimilation has been primarily developed. Finally, the computer problem was briefly discussed in Chapter 2.

Chapter 3 listed supporting documentation produced primarily by the DAO describing both the technical aspects of the algorithms and performance of GEOS data sets. Of particular note is the development of substantial in-house documentation and planning, as well as the commitment to having all appropriate aspects of the DAO algorithms peer- reviewed.

Chapter 4 described the GEOS-1 Re-analysis Project, which produced, in fact, the first multi-year assimilated data set with a non-varying assimilation system. This data set has proven, and is proving, to be of significant scientific value. GEOS-1 met all of its original goals. From an algorithm point of view the GEOS-1 Re-analysis Project establishes

- the credibility of the basic DAO algorithms
- a baseline on which to measure future development
- a prototype for production capabilities

Chapter 5 introduces the GEOS-2 algorithms. This is core description of technical algorithms that will be at the basis of the 1998 system. It is the system that will be used to assimilate both ADEOS and TRMM data and to continue support of other NASA scientific missions. Chapter 5 discusses the two largest components of the assimilation system.

- The Physical-space Statistical Analysis System (PSAS)
- The GEOS-2 General Circulation Model (GCM)

Both of these represent significant advances over GEOS-1. PSAS is an entirely new development, and the model is an incremental development that contains many features that improve its performance for assimilation applications. Development of both components includes building of item infrastructure to accommodate new data types.

PSAS is designed to be robustly sensitive to statistical representation of errors. The design features of the PSAS development include

- a global solver to eliminate the deleterious impact of mini-volumes and data selection
- a generalized capability to utilize arbitrary model and observational error specifications

The GEOS-2 model includes relative to GEOS-1

- replacing the second-order numerics with fourth-order numerics
- a computational polar rotation to eliminate spurious noise in the assimilation
- increased vertical domain (surface to 0.01 hPa) with 70 vertical levels

- a new radiation scheme to account for the stratosphere, photosynthetically active radiation, aerosol-radiative effects, and inclusion of additional trace gases
- inclusion of a gravity wave drag scheme
- extensive work on boundary condition data sets in preparation for inclusion of an interactive land-surface model
- tuning consistent with the above changes to improve the representation of clouds

Chapter 6 describes the quality control of input data that was used in GEOS-1 and will be used in GEOS-2. This is an area that will be developed further in GEOS-3 through increased collaboration with NCEP. A major accomplishment of GEOS-1 was quality control of the historical data sets from 1979-1994. This includes production of quality control histories which document the input data stream for any time period of the GEOS-1 re-analysis as well as future re-analyses.

Chapter 7 describes the generalized approach to utilizing new data types. This is a core capability of the GEOS DAS. Of particular note in Chapter 7 are

- the recognition of a novel way to achieve the benefit of radiance assimilation using retrieved data, thereby making future assimilation of future MTPE observations computationally viable
- the requirements for a monitoring system to develop error characteristics of candidate new data types
- the prioritization of new data sets to be assimilated, and a realistic linking of this enormous task to resources

Chapter 8 engages the difficult problem of system validation in the absence of using weather forecasts as the primary metric. The validation chapter accumulates the customer feed back and defines the baseline and deficiencies from GEOS-1 on which GEOS-2 will be validated. The chapter describes system validation, scientific evaluation, and monitoring functions. Three types of validation are discussed

- relative validation where the new system is evaluated relative to the baseline system
- absolute validation where the new system is evaluated against independent data sets
- new approaches to validation where theoretical considerations are being made in light of the extended scope of the GEOS DAS

Chapter 9 highlights the development from GEOS-2 to GEOS-3, the data assimilation system for the 1998 AM-1 launch. First, the conflict between the necessary software conversion and scientific development is discussed. Then the distilled GEOS-3 requirements are listed. Then development of the key components is outlined.

- PSAS development focuses on continued development to use new data types that are not state variables of the assimilating model. In addition, there is substantial effort to improve the representation of model and observational statistics which will improve all aspects of the assimilated data product. Novel approaches to bias correction are also considered.

- Model development focuses on the incorporation of new physics packages aimed especially at improving the representation of atmosphere hydrology and near-surface processes. This includes implementation of a new tracer advection scheme, a prognostic cloud water scheme, and an interactive land-surface model.
- Quality control development is focused on importing appropriate components of the NCEP complex quality control routines and development of in-house capabilities. Of special concern is the incorporation of improved techniques to apply radiation corrections to radiosondes. The GEOS-1 project revealed significant sensitivity to quality control decisions, and for GEOS-3 the DAO needs a better and autonomous quality control capability.
- New data type development will be focused on improved use of operational data and use of ADEOS and TRMM data. On ADEOS NSCAT data is already being tested in DAO algorithms. Capabilities to assimilate TRMM TMI and PR data are being developed with SSM/I as a prototype. In addition a collaborative effort discussed in Chapter 7 with the MLS team may be undertaken. Nascent constituent efforts are being extended to carbon monoxide and occultation ozone instruments. These constituent efforts are somewhat outside the primary functionality of the GEOS-3 system. Monitoring capabilities will also be developed to evaluate candidate data types.
- Finally, some of the other activities in the DAO relevant to the core GEOS DAS are discussed. These include retrospective techniques, a unique capability of the DAO allowed by not having primary responsibility for real-time forecasts. Other modeling, analysis, and new data type initiatives were discussed as well.

Chapter 10 is a summary and then a list of perceived risks and shortcomings. Chapter 10 probably does not provide adequate information that a reviewer can read it lieu of the main document. Hopefully it will remind the reviewer of salient features of the algorithm.

10.2 Risks

The 1994 DAO Plan recognized four major risks

R1: The development of a computationally viable analysis routine that met the ambitious design goals of PSAS (see Chapter 5).

R2: A manageable approach for the incorporation of new data types.

R3: The need for a software team to bring the code up to operational standards.

R4: The access to usable high-performance computing platforms.

Significant progress has been made to address all of these risks. R1 seems well in hand. For R2, the new data task remains enormous, but we feel we have a good strategy and have culled down initial target data sets so they are not overwhelming. Future aspects of use of new data types depends on instrument team participation, and we have defined the role the instrument teams must play. R3, the development of robust software remains a major risk and source of resource conflict. Originally the DAO sought the assistance of EOSDIS, but after two long years of meetings, EOSDIS determined that such support was outside of the scope of the contract. The DAO has developed a good strategy for software development but is having trouble with implementation of the strategy. For R4, it is strongly linked to the success of R3. It does appear that there will be affordable computers of sufficient reliability and performance specifications to run the DAO algorithms. However, the message passing software conversion must be achieved if success is to be had. As little as one month ago, it was not clear there would be a viable, affordable computing platform.

Re-evaluation of these risks would still place R3 and R4 as the most significant risks to the success of the GEOS-3 DAS.

Our own evaluation of current problems yield the following areas of weakness. Only the largest ones are listed.

- need to improve the process by which model, analysis, and other components are integrated together, need more frequent integration exercises
- lack of expertise to better utilize the operational data from both satellites and non-satellite platforms
- need for observation operators for many new data types
- inadequate capabilities of adjoint modeling
- shortage of expertise in state-of-the-art physical parameterizations for the model
- general shortage of quality control expertise
- general burnout of the organization
- the lack of good Thai and Vietnamese restaurants in the immediate area

Preface

The development of the Goddard Earth Observing System (GEOS) Data Assimilation System (DAS) has been a learning process for us all. When the effort was started the scope was not well understood by any of the principal people involved. It was deemed as something important for the Earth Observing System (EOS), and the expectations were very high.

The Data Assimilation Office (DAO) was formed in February 1992 at Goddard Space Flight Center to develop a data assimilation capability for EOS and the broader NASA mission. In the following four or so years the progress has been tremendous and hard fought. The effort extends far beyond scientific and involves many logistical aspects of developing a routine production capability. In many ways, we are just getting to the starting line.

The GEOS DAS is a computing effort as large, or larger, than any in the world. An effort that is coming on line when the traditional supercomputing paradigm is, by many counts, collapsing. The computing is characterized by high levels of processor communications which eliminates any easy solution to the problem. Therefore a tremendous scientific challenge has been compounded by an immense computational challenge. A challenge to be achieved with about half the historical budget available to comparable efforts.

This document describes the algorithms proposed by the DAO to be at the basis of the 1998 system provided to coincide with the launch of the AM-1 Platform. It is intended to be an integrated document. However, the chapters are also designed to stand alone if necessary. References and acronyms for each chapter are compiled individually. Detailed contents are given at the beginning of each chapter. Occasionally there is a comment intended to address the difficulty of writing an interesting algorithm theoretical basis document. You will have to read it carefully to find them

Greenbelt, Maryland *R. Rood*
November 1996

Outline

Chapter 1
Scope of Algorithm Theoretical Basis Document

What is and is not in this document.

Chapter 2
Background

The role of data assimilation in the MTPE enterprise. The DAO Advisory Panels and their advice. How does the GEOS DAS relate to efforts at NWP centers. How are requirements defined and linked to MTPE priorities. How to confront the computer problem. What are the limitations of data assimilation.

Chapter 3
Supporting Documentation

A list of DAO publications that provide more details on the algorithm and algorithm performance.

Chapter 4
GEOS-1 Data Assimilation System

Our first data assimilation system. The baseline on which progress is measured.

Chapter 5
The Goddard Earth Observing System - Version 2
Data Assimilation System

It is the system we are validating right now. It is a major development over GEOS-1 and provides the infrastructure to address the future mission. When you think of reviewing the algorithm, this is the main course.

Chapter 6
Quality Control of Input Data Sets

This is how we manage the input data sets in the current system.

Chapter 7
New Data Types

How will new data types be incorporated into the GEOS DAS. What are the priorities, and how are these decisions made. What is the link to MTPE Earth science priorities. This chapter is at the basis of what needs to be done over the next few years.

Chapter 8
Quality Assessment/Validation of
the GEOS Data Assimilation System

How do we decide when to declare a new version of the assimilation system. It is not easy; nothing is.

Chapter 9
Evolution from GEOS-2 DAS to GEOS-3 DAS

What will be added to GEOS-2 for the 1998 mission. Improvements to all aspects of the data assimilation system.

Chapter 10
Summarizing Remarks

Wrapping it up, and what are the risks.

The People in the DAO

The list below includes visitors, part time, and administrative staff.

NAME	*TELEPHONE*	*E-MAIL ADDRESS*
Almeida, Manina (GSC)	(301) 805-7950	almeida@dao.gsfc.nasa.gov
Alpert, Pinhas (Tel Aviv U)	(301) 805-8334	pinhas@dao.gsfc.nasa.gov
Ardizzone, Joe (GSC)	(301) 286-3109	ardizone@iris611.gsfc.nasa.gov
Atlas, R. (Bob) (GSFC)	(301) 286-3604	atlas@dao.gsfc.nasa.gov
Bloom, Steve (GSC)	(301) 286-7349	bloom@dystopia.gsfc.nasa.gov
Brin, Genia (GSC)	(301) 286-5182	genia@genia.gsfc.nasa.gov
Bungato, Dennis (GSC)	(301) 286-2705	ctdrb@iris611.gsfc.nasa.gov
Chang, L. P. (GSC)	(301) 805-6998	lpchang@dao.gsfc.nasa.gov
Chang, Yehui (GSC)	(301) 286-2511	chang@dao.gsfc.nasa.gov
Chen, Minghang (ARC)	(301) 805-6997	mchen@dao.gsfc.nasa.gov
Cohn, Steve (GSFC)	(301) 805-7951	cohn@dao.gsfc.nasa.gov
Conaty, Austin (GSC)	(301) 286-3745	conaty@dao.gsfc.nasa.gov
Dee, Dick (GSC)	(301) 805-7963	dee@dao.gsfc.nasa.gov
DelSole, Timothy (NRC)	(301) 286-8128	delsole@dao.gsfc.nasa.gov
Ekers, Ken (GSC)	(301) 805-8336	ekers@dao.gsfc.nasa.gov
Elengical, George (HITC)	(301) 286-3790	elengical@dao.gsfc.nasa.gov
Fox-Rabinovitz, Michael (JCESS)	(301) 805-7953	foxrab@dao.gsfc.nasa.gov
Gaspari, Greg (USRA)	(301) 805-8754	gaspari@dao.gsfc.nasa.gov
Govindaraju, Ravi (GSC)	(301) 805-7962	ravi@dao.gsfc.nasa.gov
Guo, Jing (GSC)	(301) 805-8333	guo@dao.gsfc.nasa.gov
Hall, Monique (GSC)	(301) 805-8440	hall@dao.gsfc.nasa.gov
Helfand, Mark (GSFC)	(301) 286-7509	hmh@dao.gsfc.nasa.gov
Hou, Arthur (GSFC)	(301) 286-3594	hou@dao.gsfc.nasa.gov
Joiner, Joanna (GSFC)	(301) 805-8442	joiner@dao.gsfc.nasa.gov
Jusem, Juan Carlos (GSC)	(301) 286-4086	carlos@gmsb02.gsfc.nasa.gov
Karki, Mahendra (GSC)	(301) 805-6105	karki@dao.gsfc.nasa.gov
Kondratyeva, Yelena (GSC)	(301) 805-7952	yelena@tyler.gsfc.nasa.gov
Lamich, Dave (GSC)	(301) 805-7954	lamich@dao.gsfc.nasa.gov
Larson, Jay (JCESS)	(301) 805-8334	larson@dao.gsfc.nasa.gov
Ledvina, Dave (GSC)	(301) 805-7955	ledvina@dao.gsfc.nasa.gov
Li, Yong (GSC)	(301) 262-0191	lyong@dao.gsfc.nasa.gov
Lin, Shian-Jiann (GSC)	(301) 286-9540	lin@dao.gsfc.nasa.gov
Lou, Guang Ping (GSC)	(301) 805-6996	glou@dao.gsfc.nasa.gov
Lucchesi, Rob (GSC)	(301) 286-9084	rob@dao.gsfc.nasa.gov
Lyster, Peter (JCESS)	(301) 805-6960	lys@dao.gsfc.nasa.gov
Menard, Richard (USRA)	(301) 805-7958	menard@dao.gsfc.nasa.gov
Min, Wei (USRA)	(301) 286-4630	min@dao.gsfc.nasa.gov
Molod, Andrea (GSC)	(301) 286-3908	molod@dao.gsfc.nasa.gov

NAME	*TELEPHONE*	*E-MAIL ADDRESS*
Nebuda, Sharon (GSC)	(301) 286-6543	nebuda@dao.gsfc.nasa.gov
Omidvar, Kazem (GSFC)	(301) 805-6930	omidvar@dao.gsfc.nasa.gov
Pabon-Ortiz, Carlos (GSC)	(301) 286-8560	pabon@dao.gsfc.nasa.gov
Park, Chung-Kyu (JCESS)	(301) 286-8695	park@dao.gsfc.nasa.gov
Pharo, Merritt (GSFC)	(301) 286-3468	pharo@dao.gsfc.nasa.gov
Philpot, Q. (GSC)	(301) 286-7562	philpot@dao.gsfc.nasa.gov
Rathod, Vipool (GSC)	(301) 286-1445	vip@dao.gsfc.nasa.gov
Redder, Chris (GSC)	(301) 805-8335	redder@dao.gsfc.nasa.gov
Riishojgaard, Lars Peter (USRA)	(301) 805-0258	riishojgaard@dao.gsfc.nasa.gov
Rood, Ricky, Head, (GSFC)	(301) 286-8203	rood@dao.gsfc.nasa.gov
Rosenberg, Jean (GSC)	(301) 286-3591	jeanr@dao.gsfc.nasa.gov
Rosenberg, Robert (GSC)	(301) 286-7126	bobr@pinhead.gsfc.nasa.gov
Rukhovets, Leonid (SUNY)	(301) 805-7961	leonidr@dao.gsfc.nasa.gov
Rumburg, Laura (GSC)	(301) 286-5691	rumburg@dao.gsfc.nasa.gov
Schubert, Siegfried (GSFC)	(301) 286-3441	schubert@dao.gsfc.nasa.gov
Sienkiewicz, Meta (GSC)	(301) 805-7956	meta@dao.gsfc.nasa.gov
da Silva, Arlindo (GSFC)	(301) 805-7959	dasilva@dao.gsfc.nasa.gov
Sivakumaran, N. (Siva) (GSC)	(301) 805-7957	siva@dao.gsfc.nasa.gov
Stajner, Ivanka (USRA)	(301) 805-6999	ivanka@dao.gsfc.nasa.gov
Stobie, Jim (GSC)	(301) 805-8441	stobie@dao.gsfc.nasa.gov
Strahan, Susan (GSC)	(301) 286-1448	strahan@dao.gsfc.nasa.gov
Takacs, Larry (GSC)	(301) 286-2510	w3llt@dao.gsfc.nasa.gov
Terry, Joe (GSC)	(301) 286-2509	terry@gmsb06.gsfc.nasa.gov
Thorpe, Felicia (IDEA, Inc.)	(301) 286-2466	thorpe@dao.gsfc.nasa.gov
Todling, Ricardo (USRA)	(301) 286-9117	todling@dao.gsfc.nasa.gov
Trenholme,Alice (GSC)	(301) 805-1079	trenholme@dao.gsfc.nasa.gov
Turkelson, Bob (GSFC)	(301) 286-7600	turkelson@dao.gsfc.nasa.gov
Vick, Tonya (GSFC)	(301) 286-5210	vick@carioca.gsfc.nasa.gov
Wu, Chung-Yu (John) (GSC)	(301) 286-1539	wu@dao.gsfc.nasa.gov
Wu, Man-Li (GSFC)	(301) 286-4087	frmlw@dao.gsfc.nasa.gov
Yang, Qiulian	(301) 286-0143	qyang@daac.gsfc.nasa.gov
Yang, Runhua (GSC)	(301) 805-8443	ryang@hera.gsfc.nasa.gov
Zero, Jose (GSC)	(301) 262-2034	zero@dao.gsfc.nasa.gov

Contents

List of Figures

List of Tables